Optimization of proteolytically induced photosensitizers for fluorescence imaging and Photodynamic Therapy

Sekkat, Nawal

UNIVERSITÉ DE GENÈVE
FACULTÉ DES SCIENCES
Section des Sciences Pharmaceutiques
Professeur Norbert Lange
Technologie Pharmaceutique

Optimization of Proteolytically Induced Photosensitizers for Fluorescence Imaging and Photodynamic Therapy

THÈSE

présentée à la Faculté des Sciences de l'Université de Genève
pour obtenir le grade de Docteur ès sciences, mention sciences pharmaceutiques

par

Nawal SEKKAT
de
Rabat (MAROC)

Thèse N°: 4719

Genève
Atelier de reproduction Repromail
2014

UNIVERSITÉ
DE GENÈVE

FACULTÉ DES SCIENCES

Doctorat ès sciences
Mention sciences pharmaceutiques

Thèse de ***Madame Nawal SEKKAT***

intitulée :

"Optimization of Proteolytically Induced Photosensitizers for Fluorescence Imaging and Photodynamic Therapy"

La Faculté des sciences, sur le préavis des Messieurs N. LANGE, professeur associé et directeur de thèse (Section des sciences pharmaceutiques), Y. KALIA, professeur associé (Section des sciences pharmaceutiques), H. VAN DEN BERGH, professeur (Institut des sciences et ingénierie chimiques, Ecole polytechnique fédérale de Lausanne, Lausanne, Suisse) et de Madame O. GEDERAAS, docteure (Department of Cancer Research and Molecular, Faculty of Medicine, Norwegian University of Science and Technology, Trondheim, Norway), autorise l'impression de la présente thèse, sans exprimer d'opinion sur les propositions qui y sont énoncées.

Genève, le 30 septembre 2014

Thèse - 4719 -

Le Doyen

N.B.- La thèse doit porter la déclaration précédente et remplir les conditions énumérées dans les "Informations relatives aux thèses de doctorat à l'Université de Genève".

A ma famille

REMERCIEMENTS

J'adresse tout d'abord mes plus vifs remerciements aux membres de mon jury, le docteur Odrun Gederaas, le professeur Hubert van den Bergh ainsi que le professeur Yogeshvar Kalia, pour m'avoir fait l'honneur de lire ma thèse et d'évaluer mon travail.

J'aimerais également remercier mon directeur de thèse le professeur Norbert Lange. Cela a été un honneur et un plaisir d'avoir fait partie de ton groupe Norbert! Merci pour ta confiance et pour m'avoir permis de travailler de manière libre et indépendante sur des sujets aussi passionnants que la thérapie photodynamique et le cancer.

Un grand merci aux professeurs Robert Gurny et Eric Allémann pour m'avoir accueillie dans leurs laboratoires. Merci de m'avoir offert l'opportunité de travailler dans un environnement idéal tant technologiquement qu'humainement.

J'aimerais également exprimer ma gratitude envers tous mes collègues et ce, depuis le début de ma thèse. Merci de mettre une telle ambiance d'entraide et de partage scientifique et personnel : un bel esprit d'équipe que ce soit pour les groupes FAGAL, FATEC, FABIO et même au-delà du 4ème étage!

Un merci tout particulier à mes collègues directs du groupe PDT passés et actuels. Merci tout particulièrement à Doris pour m'avoir initié à la PDT, à Maria-Fernanda pour tous les conseils et aide fournis et à Gesine pour les fous rires. Merci à David, Andrej, Karine et Dhananjaya pour votre aide en chimie notamment, cela m'a toujours été très profitable de bénéficier de votre expérience et connaissances précieuses de post-doc. Merci également à Marino, dont le travail exceptionnel m'a permis de trouver la motivation d'avancer dans mes projets. Enfin merci aux nouveaux venus (les baby birds du labo): Viktorjia, Jordan et Imen.

J'aimerai remercier mes collègues devenus amis, Maria-Fernanda (et oui toujours toi!), Marieke, Doris, Claudia, Karine, Viktorjia, Florence M., Magali, Sarra, Lutz, Caterina, Amandine, Mohamed, Pierre, Cédric, Myrtha et Marco. Merci de rire à mes blagues et d'être béats devant mes talents d'artiste. Merci aussi pour vos conseils professionnels et privés, pour votre soutien et votre humour.

Merci aussi aux docteurs Florence Delie et Pascal Furrer de m'avoir formé et permis de transmettre mon savoir aux futures générations de pharmaciens grâce aux TPs. Merci aussi d'avoir toujours été enthousiastes et disponibles dans vos enseignements que ce soit quand j'ai été étudiante ou doctorante. Grâce à vous, la galénique est fantastique☺.

Merci aussi à mes amis qui ont toujours su me faire rire dans les moments les plus difficiles. Merci pour votre soutien et votre présence. Je sais que vous vous reconnaitrez.

Enfin, j'adresse ma pleine gratitude et mes plus sincères remerciements à ma famille, à qui je dédie cette thèse. Merci pour votre soutien inconditionnel, et ce, quelle que soit la distance.

Un merci tout particulier à mes Parents, mon père, le professeur Abdelhak Sekkat et ma mère, Amina Bennis. Merci Papa et Maman de m'avoir transmis vos valeurs, votre force de caractère, votre optimisme et de me rappeler que « quand on veut, on peut ». Merci d'avoir su nous responsabiliser en étant les parents les plus aimants et les plus ouverts d'esprit du monde. Merci aussi d'avoir eu cet esprit cartésien qui me permet d'avancer. Merci aussi à ma grande sœur Nabila. Merci pour ton soutien Nabilti, merci de m'avoir coaché, merci pour tes conseils et ta douceur. Merci à mon grand frère Omar. Merci Omari d'être mon modèle de courage, merci aussi pour ton soutien : tu as toujours su trouver les mots justes (même tout simplement LE mot juste) pour me redonner force et courage même à des milliers de kilomètres. Merci aussi aux enfants de la famille, Rania, Ilyas et Zara. Merci pour votre amour et inch Allah un bel avenir se présentera à vous.

Merci finalement à mes grand-parents, Kenza, Ahmed, Ba Bennis (Mohamed) et Mima (Batoul). Merci pour votre protection! Cette thèse et les efforts que j'ai fournis pour l'effectuer vous sont également dédiés.

Table of Contents

INTRODUCTION

1. Photodynamic Therapy

Photodynamic Therapy (PDT) is a promising and non-invasive treatment modality for cancer[1-5], microbial and viral infections[6-8], water-purification[9,10], skin conditions[11-13], age-related macular degeneration[14-16] and others[17-19].

PDT requires the combined action of three individually non-toxic elements, a photosensitizer (PS), light, and oxygen. Typically, in PDT-mediated cancer treatment, the systemic or topical administration of the PS is followed by its preferential accumulation in the diseased tissue as illustrated by Figure 1. Although today the selectivity of PS is not fully understood, it is thought to be a multifactorial process including physico-chemical properties of the PS and its binding to plasma proteins as well as the particular characteristics of tumors such as leaky vasculature and low lymphatic drainage, known as the enhanced permeability and retention effect (EPR), expression of specific enzymes, receptors, and pH variation[1,3,20-23].

Localized irradiation with light in the diseased area results in the activation of the accumulated PS into an excited state. Subsequently, PS can emit fluorescence enabling photodetection (photodiagnosis) of the tumor but can also induce reactive oxygen species (ROS) leading to cytotoxic effects and tumor destruction as depicted by Figure 1 and 2. Depending on the PS's cellular and intracellular localization/relocalization, direct and indirect cell killing, vascular occlusion, release of cytokines and the response of the immune system can be observed[3,20].

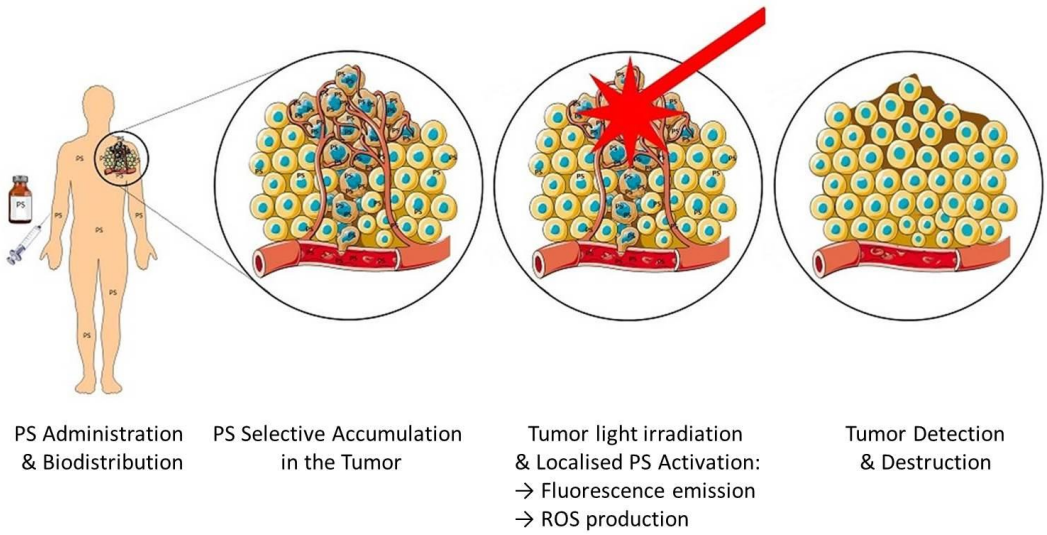

Figure 1. The principle of photodynamic therapy and fluorescence detection. After its administration, the PS will selectively accumulate in the target tissue. Localized irradiation of the diseased area with light will induce fluorescence emission and the confined production of highly toxic reactive oxygen species (ROS). These two features enable both imaging (Photodetection) and irradication (PDT) of the diseased tissue.

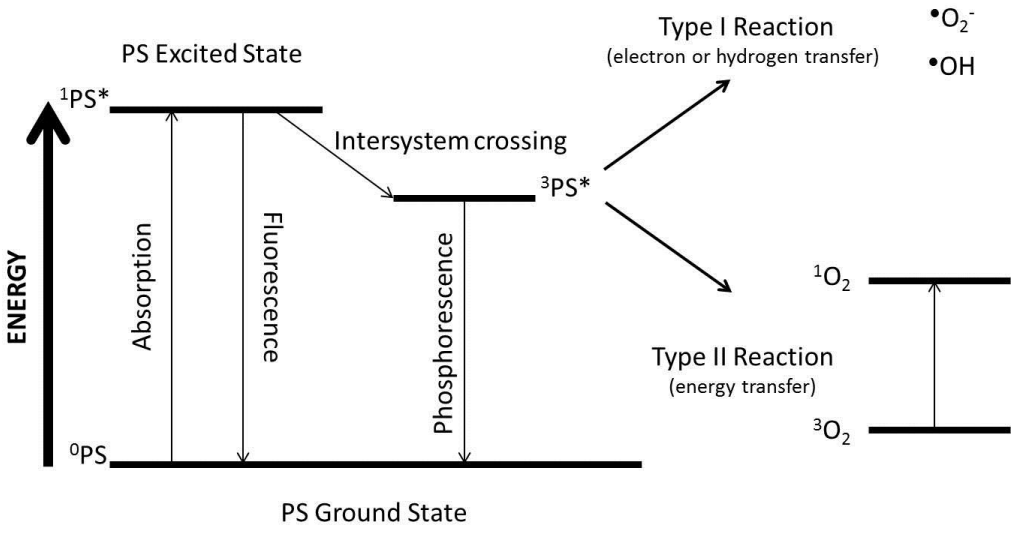

Figure 2. PDT mechanism of action illustrated by a modified Jablonski diagram. Light irradiation of the PS promotes its activation from its ground state into an excited PS singlet state. The excited PS (^{1}PS*) may return to its ground state through internal conversion, fluorescence emission, or undergo intersystem crossing to an excited triplet state (^{3}PS*). The triplet state can transfer energy to molecular oxygen ($^3O_2$) leading to the formation of the cytotoxic singlet oxygen ($^1O_2$) (**Type II reaction**) or can react directly, through electron or hydrogen transfer, with organic molecules in its direct environment leading to the oxidized cellular components and the formation of free cytotoxic radicals *i.e.* superoxide anion ($^{\bullet}O_2^-$) and hydroxyl ($HO^{\bullet}$) radicals (**Type I reaction**).

PDT as compared to conventional cancer treatment such as surgery, chemotherapy, and radiotherapy presents several advantages including being minimally invasive, have reduced systemic side effects, and a restricted range of action of the cytotoxic ROS[24]. Furthermore, it can be applied repeatedly due to reduced tumor resistance to PDT treatment[25-28].

One of the major drawbacks of PDT is the sometimes limited selectivity of the PS, resulting into side-effect such as skin photosensitivity (Figure 3).

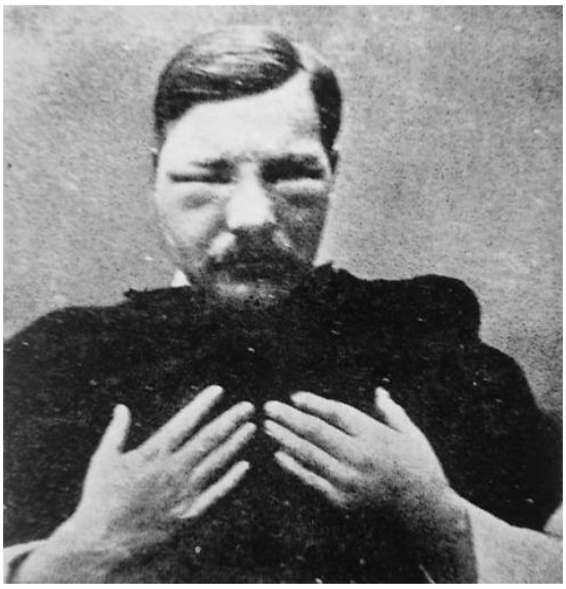

Figure 3. Skin swelling and lesion of Meyer-Betz after self-injection of 200 mg of hematoporphyrin and sun-exposure[29].

Major efforts to increase PDT therapeutic outcome have been undertaken through improvement of light delivery. Moreover, developments of 2nd generation PS and optimized pharmaceutical formulation led to improved pharmacokinetic (PK) and pharmacodynamic (PD) properties and thus, to increased interest in clinical PDT. Finally, improvement in PDT treatment settings and approaches such as the introduction of metronomic PDT or particular PDT derived treatment called Photochemical Internalisation (PCI) seem to sharpen the interest in the field of PDT treatments of cancer in clinical practice. Hence, metronomic PDT presents a great interest in brain tumor treatment and consists in the "PS and light delivery at very low doses rates over extended period of time (hours-days) which results in tumor-cell apoptosis with minimal tissue necrosis"[1,30].

PCI, on the other hand, aims at the efficient macromolecular drug delivery to target cells through disruption of endocytic vesicles by PS light activation. Hence, PCI is based on the concomitant administration of a PS and a therapeutic drug. When internalized by endocytosis, the drug can be released from this cellular compartment into the cytosol through vesicle

disruption by PS light activation and action. PCI technology enables the release of endocytosed drugs prior to lysosomal degradation thus, increasing their therapeutic efficacy within the target cells[31-33].

2. Photosensitizer

The term Photodynamic Therapy was coined by von Tappeiner and Jodlbauer more than a century ago[34] for describing a phenomenon involving oxygen for photosensitization reaction. The pioneering work of von Tappeiner's PhD student, Oscar Raab, on acridine red's toxic effect on malaria-causing protozoa when exposed to light marked the official investigation of PDT as promising modality for medical applications[35].

Among the investigated PS, hematoporphyrin held a privileged position. It was first prepared in 1841 by Scherer out of dried blood samples[36]. Then, investigated on paramecium and mice by Hausmann[37] in 1911, and on humans to assess its acute and chronic photosensitivity by Meyer-Betz[29] in 1913. The first selective tumor fluorescence localization was reported by Policard[38] in 1924. Hematoporphyrin Derivatives (HpD), a purified version of hematoporphyrin used in previous studies showed an improved tumor localization and phototoxic effect. Extensive studies and clinical trials showed the beneficial use of HpD in tumor detection and PDT-mediated treatment of cancer[3,39,40] and, although it consisted in a mixture of porphyrin oligomers, led to first approval in 1993 in Canada for bladder cancer treatment under the trade name Photofrin®.

These first generation PS are however surpassed by the considerable efforts undertaken for the development of second generation PS with more suitable properties for clinical use such as improved purity, stability and favorable PK/PD features together with high singlet oxygen quantum yield, no/low dark toxicity and strong absorbance in optical regions for optimal light penetration. [41-43]. Figure 4 represents the typical skeleton of most agents used in PDT.

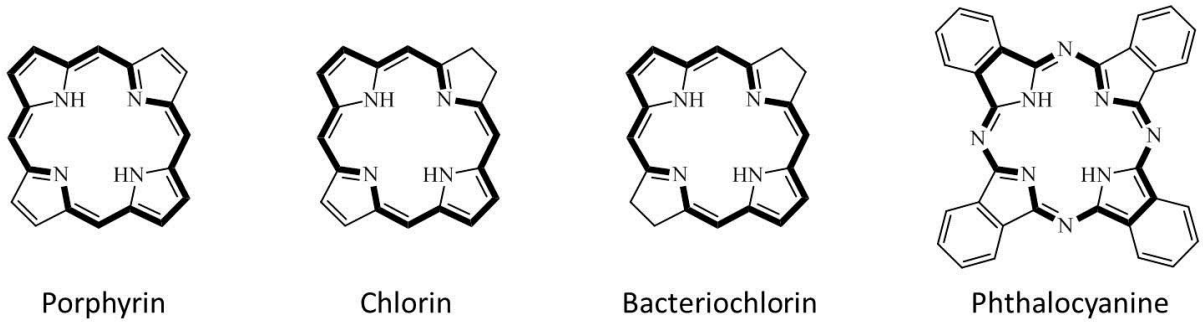

Figure 4. Structures of major PDT agents. The bold lines indicate the 18π aromatic electrons typical of these compounds.

In Table 1 some 1st and 2nd generation PS investigated in clinical trials and their potential therapeutic application in oncology are listed[2,3,44-48]

Table 1. Photosensitizers (1st and 2nd generation) used in clinical trials

Photosensitizers	Trade Name	Absorption Wavelength	Potential indications
HpD, Porfimer sodium	Photofrin	630 nm	Cervical, brain, oesophageal, breast, head and neck, lung, bladder, superficial gastric cancers, Bowen's disease, cutaneous Kaposi's sarcoma,
m-THPC, Temoporfin	Foscan	652 nm	Oesophageal, prostate and pancreatic cancer, advanced head and neck tumors
Verteporfin	Visudyne	689 nm	Basal and squamous cell carcinomas,.
HPPH*	Photochlor	665 nm	Basal cell carcinoma, Oesophageal cancers
Palladium-bacteria-pheophorbide	Tookad	763 nm	Prostate cancer
5-ALA**	Levulan	630 nm	Skin tumors, head and neck, gynaecological tumors and basal cell carcinomas
		375-400 nm	Brain, head and neck and bladder cancer photodetection
5-ALA-methylester	Metvix	635 nm	Basal cell carcinoma
5-ALA hexylester	Hexvix	375-400 nm	Photodectection of bladder cancer and colon cancer, Cervical Intraepithelial Neoplasia (CIN)
Lutetium (III)-texaphyrin	Lutex	732 nm	Prostate, cervical, breast, brain cancer, melanoma
SnET2***	Purlytin	659 nm	Kaposi's sarcoma, cutaneous metastatic adenocarcinomas, prostate, brain, lung cancers, basal cell carcinomas
NPe6, mono-L-aspartyl chlorin e6, talaporfin sodium	Talaporfin	664 nm	Solid tumors, lung cancer, cutaneous malignancies
BOPP****	BOPP	630 nm	Malignant gliomas
Zinc phthalocyanine	CGP55847	670 nm	Squamous cell carcinoma of upper aerodigestive tract
Silicon phthalocyanine	Pc 4	675 nm	Cutaneous and subcutaneous lesions from diverse solid tumor origins
Sulfonated aluminium phthalocyanine derivatives	Photosens	675 nm	Skin, breast, lung, oropharingeal, breast, larynx, head and neck cancers, Sarcoma M1, epibulbal and choroidal tumors, eyes and eyelids tumors, cervical cancer

*HPPP: 2-(1-hexyloxyethyl)-2-devinyl pyropheophorbide-alpha; ** 5-ALA: 5-aminolevulinic acid; *** SnET2: Tin (IV) ethyl etiopurpurin; **** BOPP: boronated protoporphyrin

3. Selective Drug Delivery of PS and Protease-Sensitive Prodrugs

Besides PS passively enhanced accumulation in tumors as compared to healthy tissues [21-23], selectivity of PS towards diseased tissues can be improved by taking advantage of the pathophysiological features of the tumor and its environment. Hence, pH variation, increased receptor and transporter expression as well as increased proteolytic activity have been identified as potential targets for such improvements[49,50]. The optimization of the PS delivery aiming at increasing the tumor-to-healthy tissue ratio can be achieved by improved drug delivery systems (carriers) such as micelles[51], liposomes[52,53], dendrimers[54-56], nanoparticles[57-62], polymeric drug conjugates[63-68] or oligomeric drug constructs such as regioselectively adressable functionnalized templates (RAFT) constructs[69-71] bearing both the PS and an active targeting moiety (*e.g.* carbohydrates[72-74], peptides[75,76], antibodies[77-80], ligands[81,82]).

The approach developed in this thesis is the protease-sensitive prodrug approach where clinically relevant proteases abundantly expressed in neoplastic tissue have been targeted namely urokinase-like type plasminogen activator, matrix metalloproteinase-2 and cathepsin B. This approach consists in the PS temporal inactivation through energy transfer between closely positioned PSs subsequently leading to relaxation of the PS to its ground state upon excitation with light. Upon proteolytic cleavage of the scissile protease sensitive bond, the distance between the donor and acceptor increases and results in the local activation of the prodrug with significant fluorescence signal amplification and ROS production enabling both photodetection and photodynamic therapy of the tumor.

Molecular beacons where donor and acceptor are tethered through a single protease-sensitive peptide, **polymeric prodrug** and **RAFT prodrug** approaches where multiple PS-protease-cleavable peptides are carried by the polymeric or the cyclic peptidic templates, respectively, are illustrated in Figure 5.

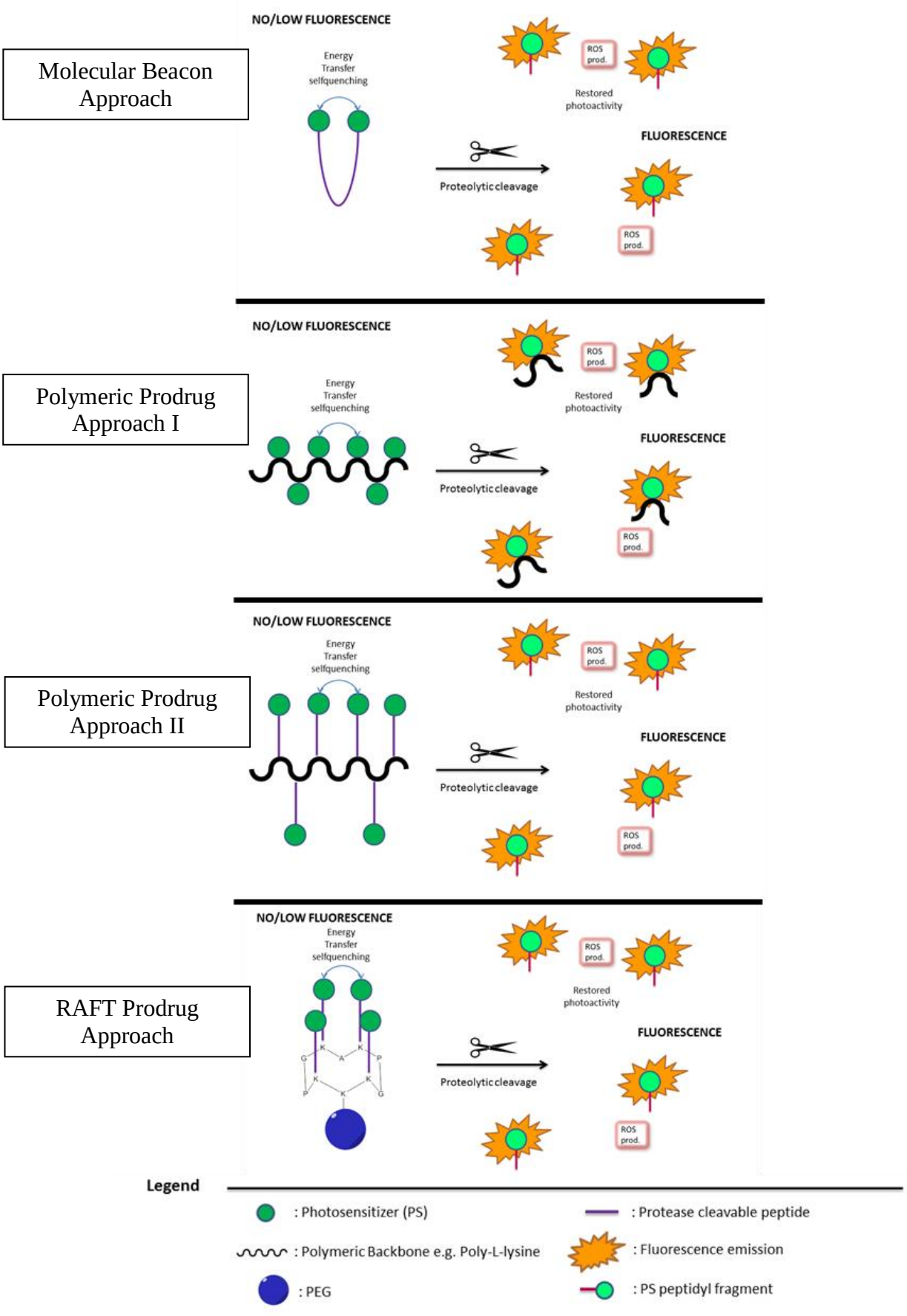

Figure 5. Schematic representation of proteolytic prodrug approaches for imaging and PDT

The identification of new PS as hit compounds as well as the pharmaceutical optimization of PS efficient and selective delivery through the molecular beacon, the protease polymeric prodrug and the RAFT prodrug approaches has been successfully investigated and achieved in the present thesis.

In **Chapter I**, a review on a promising 2nd generation PS class *i.e.* Phthalocyanines is presented with respect to chemical and pharmaceutical developments added to the field of passive and active targeting of tumors for PDT. **Chapter II**, investigates the potential phototoxic effect *in vitro* of more than 10 newly synthesized phthalocyanines (Pc) as well as improvement of their phototoxic effect through the polymeric prodrug approach. This chapter identified one hit compound and proof-of-principle is also given for phthalocyanine improved phototoxicity through the polymeric prodrug approach (PPP). Hence, phototoxic effect on cancerous cell lines PC-3, HT1080 and A549 was observed. For instance, at 4 μM of the hit compound and a light dose of 10J/cm^2, 90% of cells were destroyed. Using the same light conditions, inefficient Pcs could be rendered phototoxic through the improvement of their water-solubility, notably by the PPP approach used in this chapter and drug doses of 10 μM enabled 40 to 80% of cellular death. In the following chapters, the polymeric protease sensitive prodrug approach (PPP) (**Chapter III**), the Regioselectively Addressable Functionalized Templates (RAFT) protease sensitive approach (**Chapter IV**) and the molecular beacon approach (**Chapter V**) are investigated *in vivo* and *in vitro* with very promising results. Indeed, successful tumor ablation and mice remission *in vivo* using PPP approach was achieved in **Chapter III** while **Chapter IV** reports the successful synthesis of water-soluble PS-RAFT constructs with efficient phototoxic effect on cancerous cell lines at drug doses as low as 100 nM for a light dose of 10J/cm^2. Finally **Chapter V** gives insights into the molecular beacon approach and their potential as selective and sensitive probes for protease fluorescent imaging given their high quenching efficiencies ranging from 95 to 99% and their promising signal amplification and activation when in contact with the protease of interest *e.g.* 20 times increase in fluorescence was observed *in vitro*.

Thus, the broad spectrum of approaches investigated in this thesis as well as the results achieved in this work hold great promises for efficient PDT treatment and fluorescence imaging of tumors. This work gives an opportunity for clinical applications of such approaches in a wide range of pathologies associated with up-regulated protease levels.

References:

1. Agostinis P, Berg K, Cengel KA, et al: Photodynamic Therapy of Cancer: An Update. Ca-a Cancer Journal for Clinicians 61:250-281, 2011

2. Brown SB, Brown EA, Walker I: The present and future role of photodynamic therapy in cancer treatment. Lancet Oncol 5:497-508, 2004

3. Dolmans DE, Fukumura D, Jain RK: Photodynamic therapy for cancer. Nat Rev Cancer 3:380-7, 2003

4. Moore CM, Pendse D, Emberton M: Photodynamic therapy for prostate cancer--a review of current status and future promise. Nat Clin Pract Urol 6:18-30, 2009

5. Pass HI: Photodynamic Therapy in Oncology - Mechanisms and Clinical Use. Journal of the National Cancer Institute 85:443-456, 1993

6. Dai T, Huang YY, Hamblin MR: Photodynamic therapy for localized infections--state of the art. Photodiagnosis Photodyn Ther 6:170-88, 2009

7. Hamblin MR, Hasan T: Photodynamic therapy: a new antimicrobial approach to infectious disease? Photochem Photobiol Sci 3:436-50, 2004

8. O'Riordan K, Akilov OE, Hasan T: The potential for photodynamic therapy in the treatment of localized infections. Photodiagnosis and Photodynamic Therapy 2:247-262, 2005

9. Bonnett R, Krysteva MA, Lalov IG, et al: Water disinfection using photosensitizers immobilized on chitosan. Water Research 40:1269-1275, 2006

10. Magaraggia M, Jori G, Soncin M, et al: Porphyrin-silica microparticle conjugates as an efficient tool for the photosensitised disinfection of water contaminated by bacterial pathogens. Photochemical & Photobiological Sciences 12:2170-2176, 2013

11. Maisch T, Szeimies RM, Jori G, et al: Antibacterial photodynamic therapy in dermatology. Photochemical & Photobiological Sciences 3:907-917, 2004

12. Riddle CC, Terrell SN, Menser MB, et al: A Review of Photodynamic Therapy (PDT) for the Treatment of Acne Vulgaris. Journal of Drugs in Dermatology 8:1010-1019, 2009

13. Szeimies RM, Karrer S, Sauerwald A, et al: Photodynamic therapy with topical application of 5-aminolevulinic acid in the treatment of actinic keratoses: An initial clinical study. Dermatology 192:246-251, 1996

14. Foot B, Foy R, Chakravarthy U, et al: Introduction of photodynamic therapy for the treatment of neovascular age-related macular degeneration: tracking a moving target. Eye 17:583-586, 2003

15. Schmidt-Erfurth U, Hasan T: Mechanisms of action of photodynamic therapy with verteporfin for the treatment of age-related macular degeneration. Survey of Ophthalmology 45:195-214, 2000

16. Zuluaga MF, Mailhos C, Robinson G, et al: Synergies of VEGF inhibition and photodynamic therapy in the treatment of age-related macular degeneration. Invest Ophthalmol Vis Sci 48:1767-72, 2007

17. Azarpazhooh A, Shah PS, Tenenbaum HC, et al: The effect of photodynamic therapy for periodontitis: a systematic review and meta-analysis. J Periodontol 81:4-14, 2010

18. Fuchs SM, Fluhr JW, Bankova L, et al: Photodynamic therapy (PDT) and waterfiltered infrared A (wIRA) in patients with recalcitrant common hand and foot warts. Ger Med Sci 2:Doc08, 2004

19. Konopka K, Goslinski T: Photodynamic therapy in dentistry. Journal of Dental Research 86:694-707, 2007

20. Ackroyd R, Kelty C, Brown N, et al: The history of photodetection and photodynamic therapy. Photochem Photobiol 74:656-69, 2001

21. Maeda H, Bharate GY, Daruwalla J: Polymeric drugs for efficient tumor-targeted drug delivery based on EPR-effect. European Journal of Pharmaceutics and Biopharmaceutics 71:409-419, 2009

22. Maeda H, Takeshita J, Kanamaru R: Lipophilic Derivative of Neocarzinostatin - a Polymer Conjugation of an Anti-Tumor Protein Antibiotic. International Journal of Peptide and Protein Research 14:81-87, 1979

23. Matsumura Y, Maeda H: A New Concept for Macromolecular Therapeutics in Cancer-Chemotherapy - Mechanism of Tumoritropic Accumulation of Proteins and the Antitumor Agent Smancs. Cancer Research 46:6387-6392, 1986

24. Dysart JS, Patterson MS: Characterization of Photofrin photobleaching for singlet oxygen dose estimation during photodynamic therapy of MLL cells *in vitro*. Phys Med Biol 50:2597-616, 2005

25. Castano AP, Demidova TN, Hamblin MR: Mechanisms in photodynamic therapy: Part three- Photosensitizer pharmacokinetics, biodistribution, tumor localization and modes of tumor destruction. Photodiagnosis and Photodynamic Therapy 2:91-106, 2005

26. Robertson CA, Evans DH, Abraharnse H: Photodynamic therapy (PDT): A short review on cellular mechanisms and cancer research applications for PDT. Journal of Photochemistry and Photobiology B-Biology 96:1-8, 2009

27. Schuitmaker JJ, Bass P, vanLeengoed HLLM, et al: Photodynamic therapy: A promising new modality for the treatment of cancer. Journal of Photochemistry and Photobiology B-Biology 34:3-12, 1996

28. Sieron A, Kawczyk-Krupka A, Adamek M, et al: Photodynamic diagnosis (PDD) and photodynamic therapy (PDT) in dermatology: "How we do it". Photodiagnosis and Photodynamic Therapy 3:132-133, 2006

29. Meyer-Betz F: Untersuchungen uber die Biologische (photodynamische) Wirkung des Hamatoporphyrins und anderer Derivative des Blut- und Galenfarbstoffs. . Dtsch. Arch. Klin. Med, 112:476–503, 1913

30. Lilge L, Portnoy M, Wilson BC: Apoptosis induced *in vivo* by photodynamic therapy in normal brain and intracranial tumour tissue. Br J Cancer 83:1110-7, 2000

31. Adigbli DK, Wilson DGG, Farooqui N, et al: Photochemical internalisation of chemotherapy potentiates killing of multidrug-resistant breast and bladder cancer cells. British Journal of Cancer 97:502-512, 2007

32. Dietze A, Peng Q, Selbo PK, et al: Enhanced photodynamic destruction of a transplantable fibrosarcoma using photochemical internalisation of gelonin. British Journal of Cancer 92:2004-2009, 2005

33. Selbo PK, Sivam G, Fodstad O, et al: *In vivo* documentation of photochemical internalization, a novel approach to site specific cancer therapy. International Journal of Cancer 92:761-766, 2001

34. Von Tappeiner H, A. Jodlbauer: Die Sensibilisierende Wirkung fluorieszierender Substanzer Gesammte Untersuchungen uber die photodynamische Erscheinung. Leipzig, F. C. W. Vogel, 1907

35. Raab O: Uber die Wirkung fluoreszierender Stoffe auf Infusorien. Z. Biol 39:524–546, 1900

36. Scherer H: Chemisch-physiologische untersuchungen Ann. Chem. Pharm 40 1, 1841

37. Hausmann W: Die sensibilisierende Wirkung des Hematoporphyrins. Biochem. Z 30:276–316., 1911

38. Policard A: Etudes sur les aspects offerts par des tumeurs experimentales examinées à la lumiere de Wood. . C. R. Soc. Biol 91:1423–1428, 1924

39. Dougherty TJ, Gomer CJ, Henderson BW, et al: Photodynamic therapy. Journal of the National Cancer Institute 90:889-905, 1998

40. Ferreira J, Menezes PFC, Kurachi C, et al: Comparative study of photodegradation of three hematoporphyrin derivative: Photofrin (R), Photogem (R) and Photosan. Laser Physics Letters 4:743-748, 2007

41. Jori G: Far-Red-Absorbing Photosensitizers - Their Use in the Photodynamic Therapy of Tumors. Journal of Photochemistry and Photobiology a-Chemistry 62:371-378, 1992

42. MacDonald IJ, Dougherty TJ: Basic principles of photodynamic therapy. Journal of Porphyrins and Phthalocyanines 5:105-129, 2001

43. Stolik S, Delgado JA, Perez A, et al: Measurement of the penetration depths of red and near infrared light in human "ex vivo" tissues. Journal of Photochemistry and Photobiology B-Biology 57:90-93, 2000

44. Jori G: Tumour photosensitizers: Approaches to enhance the selectivity and efficiency of photodynamic therapy. Journal of Photochemistry and Photobiology B-Biology 36:87-93, 1996

45. Mody TD: Pharmaceutical development and medical applications of porphyrin-type macrocycles. Journal of Porphyrins and Phthalocyanines 4:362-367, 2000

46. Nyman ES, Hynninen PH: Research advances in the use of tetrapyrrolic photosensitizers for photodynamic therapy. Journal of Photochemistry and Photobiology B-Biology 73:1-28, 2004

47. Palumbo G: Photodynamic therapy and cancer: a brief sightseeing tour. Expert Opinion on Drug Delivery 4:131-148, 2007

48. Sharman WM, Allen CM, van Lier JE: Photodynamic therapeutics: basic principles and clinical applications. Drug Discovery Today 4:507-517, 1999

49. Hanahan D, Weinberg RA: The hallmarks of cancer. Cell 100:57-70, 2000

50. Hanahan D, Weinberg RA: Hallmarks of Cancer: The Next Generation. Cell 144:646-674, 2011

51. van Nostrum CF: Polymeric micelles to deliver photosensitizers for photodynamic therapy. Advanced Drug Delivery Reviews 56:9-16, 2004

52. Derycke ASL, de Witte PAM: Liposomes for photodynamic therapy. Advanced Drug Delivery Reviews 56:17-30, 2004

53. Jin CS, Zheng G: Liposomal Nanostructures for Photosensitizer Delivery. Lasers in Surgery and Medicine 43:734-748, 2011

54. Kojima C, Toi Y, Harada A, et al: Preparation of poly(ethylene glycol)-attached dendrimers encapsulating photosensitizers for application to photodynamic therapy. Bioconjugate Chemistry 18:663-670, 2007

55. Nishiyama N, Morimoto Y, Jang WD, et al: Design and development of dendrimer photosensitizer-incorporated polymeric micelles for enhanced photodynamic therapy. Advanced Drug Delivery Reviews 61:327-338, 2009

56. Zhang GD, Harada A, Nishiyama N, et al: Polyion complex micelles entrapping cationic dendrimer porphyrin: effective photosensitizer for photodynamic therapy of cancer. Journal of Controlled Release 93:141-150, 2003

57. Zeisser-Labouebe M, Lange N, Gurny R, et al: Hypericin-loaded nanoparticles for the photodynamic treatment of ovarian cancer. International Journal of Pharmaceutics 326:174-181, 2006

58. Vargas A, Pegaz B, Debefve E, et al: Improved photodynamic activity of porphyrin loaded into nanoparticles: an *in vivo* evaluation using chick embryos. International Journal of Pharmaceutics 286:131-145, 2004

59. Cheng Y, Samia AC, Meyers JD, et al: Highly efficient drug delivery with gold nanoparticle vectors for *in vivo* photodynamic therapy of cancer. Journal of the American Chemical Society 130:10643-10647, 2008

60. Eshghi H, Sazgarnia A, Rahimizadeh M, et al: Protoporphyrin IX-gold nanoparticle conjugates as an efficient photosensitizer in cervical cancer therapy. Photodiagnosis and Photodynamic Therapy 10:304-312, 2013

61. Wieder ME, Hone DC, Cook MJ, et al: Intracellular photodynamic therapy with photosensitizer-nanoparticle conjugates: cancer therapy using a 'Trojan horse'. Photochemical & Photobiological Sciences 5:727-734, 2006

62. Xiao L, Gu L, Howell SB, et al: Porous Silicon Nanoparticle Photosensitizers for Singlet Oxygen and Their Phototoxicity against Cancer Cells. Acs Nano 5:3651-3659, 2011

63. Campo MA, Gabriel D, Kucera P, et al: Polymeric photosensitizer prodrugs for photodynamic therapy. Photochemistry and Photobiology 83:958-965, 2007

64. Choi Y, Weissleder R, Tung CH: Selective antitumor effect of novel protease-mediated photodynamic agent. Cancer Research 66:7225-7229, 2006

65. Krinick NL, Sun Y, Joyner D, et al: A Polymeric Drug-Delivery System for the Simultaneous Delivery of Drugs Activatable by Enzymes and or Light. Journal of Biomaterials Science-Polymer Edition 5:303-324, 1994

66. Peterson CM, Lu JM, Sun YR, et al: Combination chemotherapy and photodynamic therapy with N-(2-hydroxypropyl)methacrylamide copolymer-bound anticancer drugs inhibit human ovarian carcinoma heterotransplanted in nude mice. Cancer Research 56:3980-3985, 1996

67. Tung CH, Bredow S, Mahmood U, et al: Preparation of a cathepsin D sensitive near-infrared fluorescence probe for imaging. Bioconjugate Chemistry 10:892-896, 1999

68. Weissleder R, Tung CH, Mahmood U, et al: *In vivo* imaging of tumors with protease-activated near-infrared fluorescent probes. Nature Biotechnology 17:375-378, 1999

69. Boturyn D, Defrancq E, Dolphin GT, et al: RAFT nano-constructs: surfing to biological applications. Journal of Peptide Science 14:224-240, 2008

70. Garanger E, Boturyn D, Jin ZH, et al: New multifunctional molecular conjugate vector for targeting, imaging, and therapy of tumors. Molecular Therapy 12:1168-1175, 2005

71. Jin ZH, Josserand V, Foillard S, et al: *In vivo* optical imaging of integrin alpha(v)-beta(3) in mice using multivalent or monovalent cRGD targeting vectors. Molecular Cancer 6, 2007

72. Pandey SK, Zheng X, Morgan J, et al: Purpurinimide carbohydrate conjugates: Effect of the position of the carbohydrate moiety in photosensitizing efficacy. Molecular Pharmaceutics 4:448-464, 2007

73. Zheng G, Graham A, Shibata M, et al: Synthesis of beta-galactose-conjugated chlorins derived by enyne metathesis as galectin-specific photosensitizers for photodynamic therapy. Journal of Organic Chemistry 66:8709-8716, 2001

74. Zheng X, Pandey RK: Porphyrin-carbohydrate conjugates: Impact of carbohydrate moieties in photodynamic therapy (PDT). Anti-Cancer Agents in Medicinal Chemistry 8:241-268, 2008

75. Choi Y, McCarthy JR, Weissleder R, et al: Conjugation of a photosensitizer to an oligoarginine-based cell-penetrating peptide increases the efficacy of photodynamic therapy. Chemmedchem 1:458-463, 2006

76. Sibrian-Vazquez M, Ortiz J, Nesterova IV, et al: Synthesis and properties of cell-targeted Zn(II)-phthalocyanine-peptide conjugates. Bioconjugate Chemistry 18:410-420, 2007

77. Carcenac M, Dorvillius M, Garambois V, et al: Internalisation enhances photo-induced cytotoxicity of monoclonal antibody-phthalocyanine conjugates. British Journal of Cancer 85:1787-1793, 2001

78. Hudson R, Carcenac M, Smith K, et al: The development and characterisation of porphyrin isothiocyanate-monoclonal antibody conjugates for photoimmunotherapy. British Journal of Cancer 92:1442-1449, 2005

79. Mew D, Lum V, Wat CK, et al: Ability of Specific Monoclonal-Antibodies and Conventional Antisera Conjugated to Hematoporphyrin to Label and Kill Selected Cell-Lines Subsequent to Light Activation. Cancer Research 45:4380-4386, 1985

80. Mew D, Wat CK, Towers GHN, et al: Photoimmunotherapy - Treatment of Animal Tumors with Tumor-Specific Monoclonal Antibody-Hematoporphyrin Conjugates. Journal of Immunology 130:1473-1477, 1983

81. Sobolev AS, Akhlynina TV, Yachmenev SV, et al: Internalizable Insulin-Bsa-Chlorin E6 Conjugate Is a More Effective Photosensitizer Than Chlorin E6 Alone. Biochemistry International 26:445-450, 1992

82. Xiao DM, Wang JN, Hampton LL, et al: The human gastrin-releasing peptide receptor gene structure, its tissue expression and promoter. Gene 264:95-103, 2001

LIKE A BOLT FROM THE BLUE: PHTHALOCYANINES IN BIOMEDICAL OPTICS

Nawal SEKKAT [1], Hubert VAN DEN BERGH [2], Tebello NYOKONG [3]

and Norbert LANGE[1,*]

[1] School of Pharmaceutical Sciences, University of Lausanne/Geneva, Geneva, 30, quai Ernest Ansermet, CH-1211 Geneva, Switzerland

[2] Laboratory of Photomedicine, Swiss Federal Institute of Technology (EPFL), Lausanne, CH-1015 Switzerland

[3] Department of Chemistry, Rhodes University, Grahamstown 6140, South Africa

*Corresponding author e-mail: norbert.lange@unige.ch

ABSTRACT

Review published in Molecules 17*(1),* 98-144*, 2011*

The purpose of this review is to compile preclinical and clinical results on phthalocyanines (Pcs) as photosensitizers (PS) for Photodynamic Therapy (PDT) and contrast agents for fluorescence imaging. Indeed, Pcs are excellent candidates in these fields due to their strong absorbance in the NIR region and high chemical and photo-stability. In particular, this is mostly relevant for their *in vivo* activation in deeper tissular regions. However, most Pcs present two major limitations, *i.e.*, a strong tendency to aggregate and a low water-solubility. In order to overcome these issues, both chemical tuning and pharmaceutical formulation combined with tumor targeting strategies were applied. These aspects will be developed in this review for the most extensively studied Pcs during the last 25 years, *i.e*., aluminium-, zinc- and silicon-based Pcs.

KEY WORDS: biomedical optics; fluorescence diagnosis; phthalocyanines; NIR dyes; photodynamic therapy

1. Introduction

The first syntheses of metal-free and copper phthalocyanines were reported in 1907 by Braun and Tcherniac at the South Metropolitan Gas Company (United Kingdom) and in 1927 by Diesbach and von der Weid at the University of Fribourg (Switzerland). A few years later, Professor Linstead in collaboration with Imperial Chemical Industries (ICI) was the first to characterize the chemical structure of the phthalocyanine molecule, using for the first time the term "phthalocyanine"[1-3].

Nowadays, phthalocyanines are widely used in the dying industry. Nearly a quarter of all pigments of organic origin are related to this class of compounds. Furthermore, they are used for the fabrication of high-speed and high resolution optical media[4], as light harvesters in photovoltaic applications[5], and as experimental catalysts in redox reactions[6]. These dyes absorb strongly in the red and near infrared (NIR) part of the visible spectrum providing them with their characteristic blue or greenish color. Pcs that absorb in the NIR are especially interesting for photomedical applications such as fluorescence imaging, Photochemical Internalisation (PCI), and Photodynamic Therapy (PDT)[7-12].

Just recently Photochemical Internalisation (PCI), a novel drug delivery process, has shed light on the importance of phthalocyanines and their applications in oncology[13-15]. The PCI technology is based on the concomitant administration of a therapeutic agent and a photosensitizer. When internalized by endocytosis and consequently colocalized in the endosomes and/or lysosomes, light activation of the PS will subsequently lead to vesicle disruption and release of the therapeutic agent. Indeed, PCI technology enables the release of endocytosed drugs prior to lysosomal degradation, thus, increasing their therapeutic efficacy within the target cells. Among the photosensitizers used in PCI, the amphiphilic disulfonated aluminium phthalocyanine $AlPcS_{2adj}$ displays all the required features and characteristics such as specific insertion of the hydrophobic part of the PS into the endocytotic membrane. Due to its amphiphilic character, $AlPcS_{2adj}$ "intrudes into the plasma cell membrane, but is unable to penetrate through the plasma membrane and will enter the cells via adsorptive endocytosis" [16]. The concomitant administration of a drug such as gelonin or bleomycin[14,17,18] will, after internalization lead to vesicle disruption and intracellular release of the drug upon light activation[14,19,20].

As mentioned previously, phthalocyanines strongly absorb in the NIR, and have been proposed for PDT of cancer as early as 1985[21,22]. Under some circumstances PDT treatment

presents several advantages over conventional cancer therapies such as chemo, radiation and surgical treatments. It enables selective destruction of malignant tissues due to specific interaction of three individually non-toxic components *i.e.*, a photosensitizer (PS), light and oxygen. PS selective accumulation in tumor combined with its controlled light activation enables selective destruction of tumors, sparing neighboring healthy tissue.

Although today the selectivity of PS is not fully understood, it is thought to be a multifactorial process including physico-chemical properties and binding to plasma proteins as well as the particular characteristics of tumors such as leaky vasculature, low lymphatic drainage, expression of specific enzymes and receptors and pH variation. Depending on its cellular and intracellular localization/relocalization, PS exhibits direct and indirect cell killing, vascular occlusion, release of cytokines and the response of the immune system[23,24].

Photofrin® (Table 1) was the first photosensitizer approved for clinical use in 1993 for the treatment of bladder cancer. Since then it gained marketing for the prophylactic treatment of several cancers such as the treatment of early-stage oesophagal, gastric, cervical and lung cancers[24,25]. However, this first generation photosensitizer has several limitations with respect to its clinical use since it[23,25-28] :

- Is composed of a undefined mixture of hematoporphyrin derivatives (HpD);
- Induces a long-lasting skin photosensitization (2 to 3 months post injection);
- Has a low extinction coefficient at wavelengths for optimal tissue penetration;
- Displays a limited selectivity for the target tissue.

Therefore, considerable efforts have been undertaken to prepare 2nd generation PS with more suitable features[29-31] such as:

- Single and chemically pure compound;
- Stability and good solubility in pharmaceutically acceptable formulations and in biological media;
- Low tendency to aggregate;
- High singlet oxygen quantum yield;
- Photostability;
- Fluorescence;
- Low phototoxicity towards healthy tissue;
- No dark toxicity;

- Fast clearance from the healthy parts of the body and specific retention in diseased tissues;
- Strong absorbance in NIR region and minimal absorbance between 400 and 600 nm.

In order to avoid skin photosensitization, the PS has to present the lowest absorbance in the spectral range where daylight intensity is the highest, *i.e.*, between 400 and 600 nm. Moreover, strong absorbance in the NIR region between 600 and 900 nm favors the optimal penetration of light into tissues, thus resulting in more efficient PDT effects when treating deeper lying lesions. However, absorption by water molecules increases for wavelengths above 800 nm and at higher wavelength energy transfer to molecular oxygen is suboptimal. Hence, the window for optimal light penetration ranges from 600 to 800 nm. These considerations are based on the assumption that healthy and diseased tissues have the same absorbance of light, which in reality is not the case. Finally, 94 kJ/mol appears to be the minimal energy required by a photon to induce singlet oxygen $^1O_2$ formation. This energy corresponds to a wavelength of approximately 1,270 nm[32-39].

In Table 1 some 1st and 2nd generation PS investigated in clinical trials and their potential therapeutic application in oncology are listed (see also Figure 1 for their chemical structures).

Table 1. Examples for PS used in clinical and preclinical trials in oncology[24,25,40-52]

Photosensitizers	Trade Name	Absorption Wavelength	Potential Indications
HpD, Porfimer sodium	Photofrin, Photogem, Photosan, Hemporfin	630 nm	Cervical, brain, oesophageal, breast, head and neck, lung, bladder, superficial gastric cancers, Bowen's disease, cutaneous Kaposi's sarcoma
m-THPC, Temoporfin	Foscan	652 nm	Oesophageal, prostate and pancreatic cancer, advanced head and neck tumors
Verteporfin	Visudyne	689 nm	Basal and squamous cell carcinomas
HPPH, 2-(1-hexyloxyethyl)-2-devinyl pyropheophorbide-alpha	Photochlor	665 nm	Basal cell carcinoma, Oesophageal cancers, Head and Neck tumors
Palladium-bacteria-pheophorbide	Tookad	763 nm	Prostate cancer

Table 1. *Cont*.

Photosensitizers	Trade Name	Absorption Wavelength	Potential Indications
5-ALA, 5-aminolevulinic acid	Levulan	630 nm	Skin tumors, head and neck, gynaecological tumors and basal cell carcinomas
		375–400 nm	Brain, head and neck and bladder cancer photodetection
5-ALA-methylester	Metvix	635 nm	Basal cell carcinoma
5-ALA benzylester	Benzvix	635 nm	Gastrointestinal tumors
5-ALA hexylester	Hexvix	375–400 nm	Photodectection of bladder cancer
Lutetium (III)-texaphyrin or Motexafin-lutetium	Lutex, Lutrin, Antrin, Optrin	732 nm	Prostate, cervical, breast, brain cancer, melanoma
SnET2, Tin (IV) ethyl etiopurpurin	Purlytin, Photrex	659 nm	Kaposi's sarcoma, cutaneous metastatic adenocarcinomas, prostate, brain, lung cancers, basal cell carcinomas
NPe6, mono-L-aspartyl chlorin e6, talaporfin sodium	Talaporfin, Laserphyrin	664 nm	Solid tumors, lung cancer, cutaneous malignancies
BOPP, boronated protoporphyrin	BOPP	630 nm	Malignant gliomas
Zinc phthalocyanine	CGP55847	670 nm	Squamous cell carcinoma of upper aerodigestive tract
Silicon phthalocyanine	Pc 4	675 nm	Cutaneous and subcutaneous lesions from diverse solid tumor origins
Mixture of sulfonated aluminium phthalocyanine derivatives	Photosens	675 nm	Skin, breast, lung, oropharingeal, breast, larynx, head and neck cancers, Sarcoma M1, epibulbal and choroidal tumors, eyes and eyelids tumors, cervical cancer
ATMPn, Acetoxy-tetrakis (β-methoxyethyl)-porphycene	NA	600–750 nm	Skin cancer
TH9402, dibromorhodamine methyl ester	NA	515 nm	Breast, myeloma, non-melanoma skin cancer

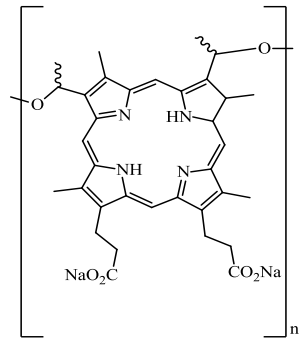

Structure of components of Photofrin n=1-9

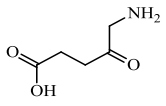

5-ALA

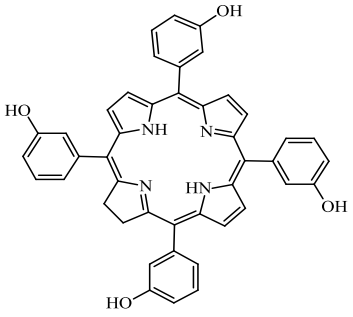

m-THPC

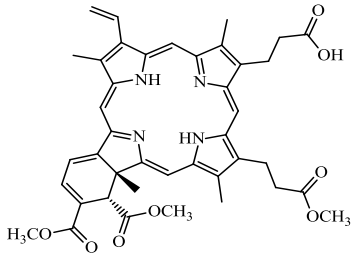

Verteporfin

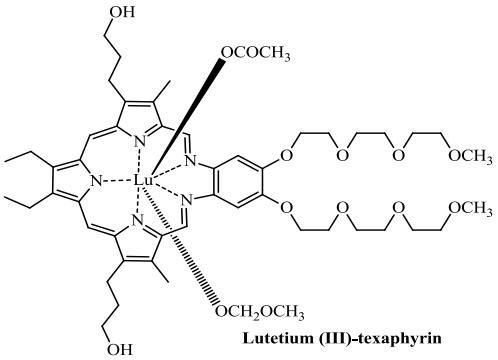

Lutetium (III)-texaphyrin

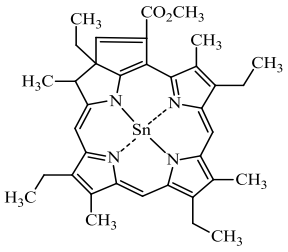

Tin Etiopurpurin

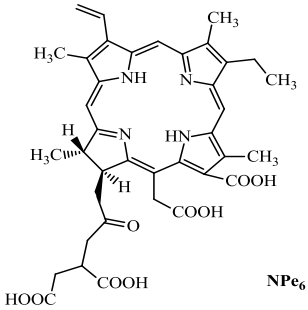

NPe_6

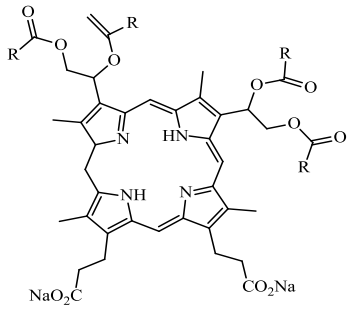

BOPP
with R = *closo*-1,2-$B_{10}C_2H_{11}$ pendant cages

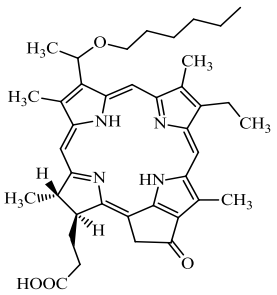

Hexylpyropheophorbide HPPH

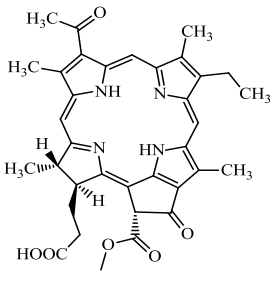

Pd-Pheophorbide a

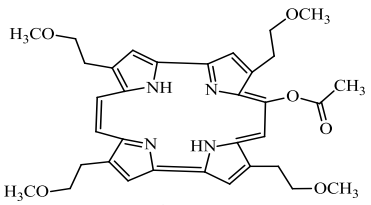

ATMPn

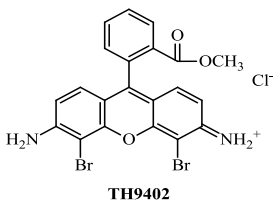

TH9402

Figure 1. Chemical structures of clinically relevant "non-phthalocyanine" photosensitizers

Another appealing feature of Pcs is the ease of the introduction of peripherial and axial substituents that can be used to fine tune absorption and emissions characteristics. Phthalocyanine dyes with absorptions bands as high as 1,000 nm with suitable fluorescence quantum yields can be prepared[11]. Therefore, Pcs are potentially interesting as fluorescence reporters for *in vitro* and *in vivo* imaging that can replace commonly used fluorophors such as fluorescein and indocyanine green. Two of such compounds, "La Jolla Blue®" and "IRD700DX®" are commercially available as labeling agents for proteins, peptides[53-55], antibodies[56-60] and oligonucleotides[61-65].

This review intends to compile preclinical and clinical data accrued with Pcs as PS for PDT. However, it has to be noted that the presented concepts can be easily translated into the use of similar compounds for the fluorescence diagnosis of disease. Thereby, we will mainly focus on the most extensively studied Pcs, *i.e.*, Pcs containing Al, Zn, and Si as central metal ion. At first we will briefly describe how chemical modulation of Pcs, alters their Structure-Activity Relationship (SAR). Then, since most Pcs are barely soluble in pharmaceutically acceptable formulations special emphasis will be placed on the impact of pharmaceutical formulation on their therapeutic efficiency. And finally, different tumor targeting strategies that have been exploited with Pcs will be discussed.

2. Phthalocyanines

Pcs belong to the group of 2nd generation PS which exhibit a high extinction coefficient around 670 and 750 nm and even up to 1,000 nm. Variation of the axial and peripheral substituents modulates the tendency for aggregation, pharmacokinetics, biodistribution, solubility, as well as fine-tuning of NIR absorbance[66]. Extinction coefficients higher than $10^5 M^{-1}cm^{-1}$ have been reported[11,66]. These compounds are porphyrin-like PS, displaying tetrapyrrolic, aromatic macrocycles with each cycle linked to the other by nitrogen atoms. Each pyrrolic ring is extended by a benzene ring resulting in the red-shift of their final absorption band[31,67,68]. Figure 2 shows the general chemical structure of Pcs and nomenclature as well as typical absorption and emission spectra.

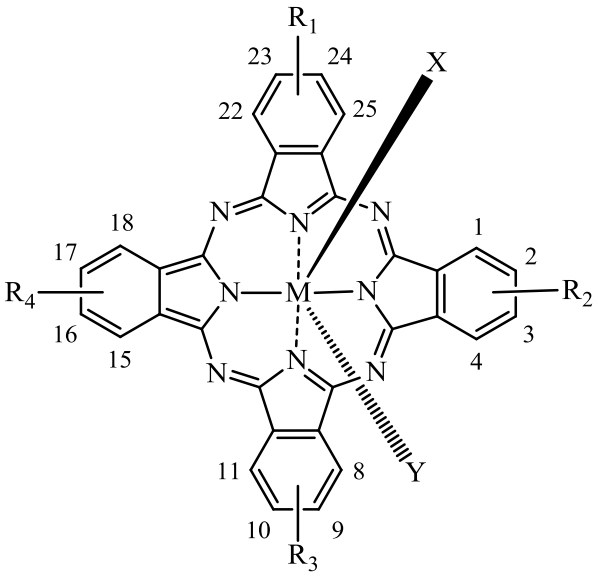

(a)

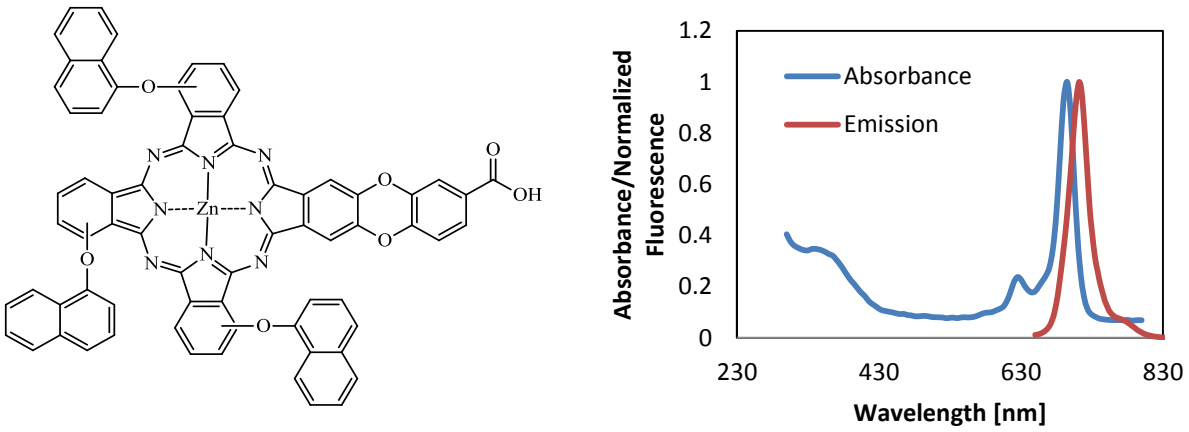

(b)

Figure 2. (a) General chemical structure of metallated phthalocyanines; **(b)** Typical absorption and emission spectra of metallated Pc (*e.g.*, zinc based phthalocyanine in DMSO).

Lowering of the symmetry of the phthalocyanine molecules results in splitting (or broadening) of the Q bands. This splitting is due to the lifting of degeneracy of the lowest unoccupied molecular orbital (LUMO) to a varying extent. It is also well established that expansion of π conjugation in phthalocyanines shifts the Q band to the red. Extension of the conjugation system is accompanied by change in colour from blue/green to colors including brown, red or purple. The location of the Q band in Pc complexes can be adjusted by attaching suitable substituents onto the peripheral and non-peripheral positions of the ring and by the change in the nature, size and number of substituents. Addition of electron donating

groups such as $–NH_2$, OR and SR at the non-peripheral (1,4,8,11,15,18,22,25) or peripheral (2,3,9,10,16,17,23,24) positions of the Pc ring results in red shift to the NIR region. Substitution at the non-peripheral position shows more red-shift than at the peripheral position[69].

Besides their strong absorption in the NIR, Pcs exhibit low absorption at wavelengths between 400 and 600 nm leading potentially to a lower skin photosensitization when exposed to sunlight[31]. Moreover, the presence of a diamagnetic central metal such as Zn^{2+} and Al^{3+} in the Pc nucleus seems to improve the triplet state life time (τ_t), as well as its yield (Φ_t) and singlet oxygen yields (Φ_Δ) compared to paramagnetic metals (*e.g.*, $\Phi_\Delta \geq 0.7$, $\Phi_t > 0.4$ and τ_t = 750 μs for $AlPcS_4$ in solution with human serum albumin)[30,48,67,70]. However, the metallation is not required for its photodynamic activity. Indeed, Feofanov *et al*.[71] and Karmakova *et al*.[72] reported efficient antitumor activity of a mixture of metal-free sulfonated phthalocyanines with an average number of sulfonated groups of 2.4 *in vitro* on human epidermoid carcinoma cells HEp2 and *in vivo* on mice bearing murine P-388 lymphoma cells, respectively.

On the other hand, Pcs with good fluorescence quantum yields up to 0.6 have been reported. This, together with their high photostability compared to commonly used labeling agents should have placed this group of compounds into the upper part of the list of NIR fluorescence reporters. As an example IR700DX® is about 20 times more stable than Cy5.5 at similar irradiation intensities and wavelengths. However, despite these photophysical and spectral characteristics the use of Pcs as labeling agents for fluorescence imaging or in PDT is still limited.

2.1. Aluminium Based Phthalocyanines

2.1.1. Aluminium Sulfonated Phthalocyanines—SAR

Sulfonated phthalocyanines bearing a central aluminium ion have been extensively studied *in vitro* as well as *in vivo*. They display potent photodynamic activity on cell lines including G361 human melanoma cells[73], pancreatic carcinoma cells (H2T)[74], and human fibrosacroma cells (HT-1080)[75], as well as *in vivo* on rat (CBH rats) bearing fibrosarcoma (HSN/TC/7)[76]. These early studies indicated a strong dependence of the photodynamic efficiency on the degree of sulfonation, later systematically assessed by Chan *et al*.[77-79].

At this point one has to keep in mind that earlier reports on aluminium sulfonated phthalocyanines can be sometimes misleading due to the designation as $AlPcS_4$ or as AlPcS of the commercially available product from Ciba-Geigy, which nevertheless consisted of a mixture of mono, di-, tri- and tetrasulfonated chloroaluminium phthalocyanines with an average degree of three sulfonated substituents. Thus, in this review, we will refer to this mixture as AlPcS, whereas $AlPcS_4$ will be used to qualify the pure tetrasulfonated Pc, keeping in mind that even these more defined compounds will be mixtures of regio- and stereoisomers. Furthermore, some early works did not disclose the identity of the axial ligands which could be chloride (Cl) as well as hydroxy (OH) groups. Since most reported studies focus on the effect of sulfonation with respect to PDT, no further distinction according to their axial ligand will be made here. Finally, the IC_{50} values reported in this review cannot be compared from a study to another since this value depends among other things on the applied light doses.

Interestingly, $AlPcS_4$ has shown promising *in vivo* results in the treatment of malignant gliomas[80,81]. Wistar rats inoculated intracranially with C6 glioma cells, responded within 5 days to intravenous injection of $AlPcS_4$ in saline solution at a dose of 5 mg/kg and irradiation 6 h post administration at a dose of 100 J/cm^2. However, upon illumination at a light dose of 200 J/cm^2, $AlPcS_4$-mediated PDT neurological symptoms (*e.g.*, brain damage and oedema) appeared, while light alone had no effect. Higher light doses lead to death in mice bearing intracerebrally implanted VMDk murine glioma cells as reported by Sandeman *et al*., presumably concomitant with hyperthermic effects in the irradiated areas[82].

2.1.2. Influence of the Degree of Sulfonation

In 1990, Chan *et al*. reported that *in vitro* monosulfonated chloroaluminium phthalocyanine ($AlPcS_1$) was taken up faster, retained to a higher degree and showed higher phototoxicity in murine colorectal carcinoma (Colo-26) cells than higher sulfonated analogues (*i.e.*, di, tri and tetrasulfonated chloroaluminum phthalocyanine; referred to as $AlPcS_2$, $AlPcS_3$ and $AlPcS_4$ respectively)[77]. Furthermore, comparison of light doses necessary for efficient PDT on WiDr cells cultured in monolayers and as spheroids revealed that spheroids were less sensitive to PDT than cells grown in monolayers[78].

In contrast to *in vitro* experiments, an inverse tendency with respect to tumor accumulation and phototoxicity was observed when PDT was perfomed with this series of sulfonated Pcs *in vivo*. In BALB/c mice inocculated with Colo-26 tumors $AlPcS_1$ had essentially no effect on

tumor regression in contrast to the higher sulfonated compounds following the order $AlPcS_4$ > $AlPcS_3$ > $AlPcS_2$ [77]. This discrepancy can be assigned to differences in pharmacokinetics and biodistribution of these compounds due to their differences in hydrophilicity[77,83]. As suggested by Chan *et al*., the fast clearance of highly sulfonated Pcs after intravenous administration can be circumvented by intraperitoneal application for these compounds[77].

Later, Chan *et al*. showed that $AlPcS_2$ was more potent than $AlPcS_3$ and $AlPcS_4$, despite its lower accumulation in tumor xenografts. This suggests different PDT mechanisms of these compounds with respect to cell killing, vasculature occlusion, and intracellular localization[78]. Interestingly, the highest *in vitro* efficiency of $AlPcS_2$ over other more hydrophilic aluminium sulfonated Pc was already demonstrated in 1988. The same tendency was later confirmed by Peng and Moan[83]. When injected intraperitoneally $AlPcS_2$ was the most efficient PS followed by $AlPcS_4$, Photofrin, and $AlPcS_1$. The best efficiency was observed with a drug dose of 10mg/kg and light exposure 2 h post-administration.

Moreover, the relative position of sulfonate group seems also to influence Pcs photoactivity. Indeed, $AlPcS_2$ bearing adjacent sulfonated side-group ($AlPcS_{2adj}$) rather than opposite side-substitution exhibited the best cell penetration and were the most phototoxic compounds amongst the sulfonated aluminium phthalocyanine serie, presumably due to their amphiphilic properties[84]. Therefore, the phototoxicity of mixed AlSPc *in vivo* should be related mostly to photoactivity of $AlPcS_{2adj}$ isomers[78,83]. In a recently reported study, Mathews *et al*. compared the phototoxic effect of $AlPcS_{2adj}$ to 5-aminolevulinic acid (5-ALA) on healthy brains in mice[85]. Based on PDT-induced and higher mortality rates, $AlPcS_{2adj}$ was considered to be a more potent photosensitizer than 5-ALA. Moreover, in a comparative study, Gupta *et al*.[86] reported that liposomal formulation of $AlPcS_2$ resulted in a higher phototoxic effect as compared to its free form on human glioma cells (BMG-1) despite its lower uptake by the cells.

Despite the higher efficiency of $AlPcS_2$ compared to other sulfonated aluminium phthalocyanines, extensive efforts and studies have been realized with the objective of further improving the pharmacokinetic properties and selectivity of the commercially available $AlPcS_4$.

Allen *et al*.[26], tested sulfonamides with an alkyl chain of 4, 8, 12 and 16 carbons to one of the sulfonated groups in AlS_4Pc (Figure 3) and compared induced photodynamic effects to $AlPcS_4$ in mice bearing EMT-6 tumors. They concluded that at doses of 0.2 μmol/kg, all

tested $AlPcS_4$-derivatives induced tumor regression and were more effective than $AlPcS_{2adj}$ or $AlPcS_4$. Moreover, with increasing alkyl chain length increased photodynamic efficacy was observed. In these experiments, $AlPcS_4$ had no effect at doses up to 5 μmol/kg, and 1 μmol/kg of $AlPcS_{2adj}$ was needed to induce 87% of tumor cure.

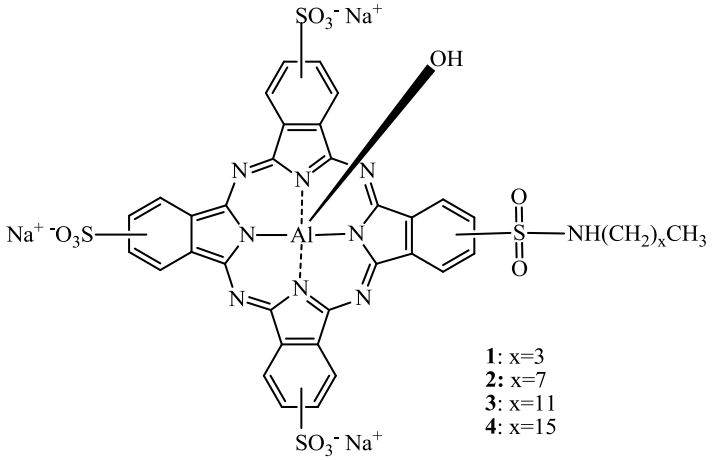

Figure 3. A homologous series of AlPc alkylsulfonamides

2.1.3. Photosens®

Photosens®, a mixture of aluminium chloride phthalocyanines with 1 to 4 sulfonated side-groups with an average sulfonated degree of 3, was developed at the General Physics Institute of the Russian Academy of Sciences. It has been evaluated *in vivo* for the treatment of sarcoma M1[87], epibulbal and choroid tumors[88], eye and eyelid related tumors[89], bladder and cervical cancer[90,91]. In a clinical trial that included 47 patients composed of 35 women presenting pre-cancerous lesions of cervix and 12 women with non-invasive cervical lesions, a Photosens® dose of 0.3 mg/kg was applied. Twenty four hours post administration, lesions were irradiated with a light dose between 150 and 200 J/cm^2 at 675 nm. No PDT-related pain was reported. Out of these two subgroups, 94.2% and 83.4% of the patients, respectively, responded fully to the treatment with complete tumor regression, with significant regression for 2.9 and 8.3% of the women. Moreover, the same percentage of women showed stabilized disease status. The remaining percentages correspond to the patients who responded only partially to the treatment. Today, Photosens® is commercialized in Russia by NIOPIK.

2.1.4. AlPcS-Conjugation to Tumor Targeting Moieties

Except for $AlPcS_1$, aluminium sulfonated Pcs are readily soluble in aqueous media. Thus, most formulation efforts were aiming at increasing Pc accumulation and uptake by the tumors through the increase of the circulation half life or cellular/subcellular targeting.

The tetraglycine derivative $Al(SO_2N_{gly})_4$ and a mono-substitued $AlPcS_4$ containing one 6-aminohexanoic acid spacer ($AlPcS_4A_1$) have been exploited for protein conjugation. The conjugation of AlS_4Pc to monoclonal antibodies (Mab) lead to an enhanced phototoxicity in different cell lines such as human colon carcinoma LoVo[92], modified human ovarian carcinoma cells SKOV3-CEA-1B9 (SKOV cells transfected with carcinoembryonic antigen (CEA) cDNA and expressing two target antigens CEA and ErbB2)[60], and various squamous carcinoma cells including UM-SCC-11B, UM-SCC-22A, UM-SCC-22B, A431, SCV-7 and OE[56,93].

Moreover, *in vivo* biodistribution studies on tumor bearing mice revealed that these conjugates presented an increased selectivity toward the malignant tissues compared to free $AlPcS_4$. Indeed, when 12 identical Pcs were conjugated to a 35A7 Mab directed against CEA (35A7 Mab-$(AlPcS_4A_1)_{12}$), a tumor-to-muscle ratio and tumor-to-skin ratio of 33 and 8, respectively, was reported in nude mice bearing a human colon carcinoma xenograft[92]. In a subsequent study, the photodyanmic efficiency was further improved using an internalizing antibody (FSP77) directed against ErbB2.

In vitro, SKOV3-CEA-1B9 showed a fast uptake of FSP77Mab-$(AlPcS_4A_1)_6$ and a higher phototoxic efficacy (*i.e.*, 96% *vs.* 68% of growth inhibition) as compared to the corresponding 35A7 Mab $(AlPcS_4A_1)_8$ [60]. These studies are in agreement with the results reported by Vrouenraets *et al*. [56,94] Pcs conjugated to internalizing Mabs, *i.e.*, SCC-Mab 425 and Mab U36, were photodynamically more effective than the corresponding non-internalizing Mab E48. Furthermore, the Mab 425-$AlPcS_4$ was 7,500 times more effective *in vitro* than free $AlPcS_4$. It has to be noted also that the loading of PS per Mab can be tuned through different conjugation methods. Indeed, by introducing a five carbon spacer chain between the Mab and $AlPcS_4$, Carcenac *et al*. [92] were able to link up to 16 $AlPcS_4A_1$ entities to the proteins whereas Vrouenraets *et al*. could only conjugate four $Al(SO_2N_{gly})_4$ without affecting its solubility.

Later, Vrouenraets *et al*. tested three different Mabs [BIWA 4 (bivatuzumab), E48 and 425] on five different SCC cell lines (22A, 22B A431, SCV-7 and OE) [93]. PS conjugation to the aforementioned Mabs resulted in a higher phototoxicity compared to free $AlPcS_4$. BIWA 4-

$AlPcS_4$ showed highest phototoxicity in all the five cell lines, exhibiting an IC_{50} as low as 0.06 nM as compared to $IC_{50} \geq 700$nM for the free PS. Interestingly, the effect of the other Mabs varied depending on the cell line but not on the internalizing efficiency of the particular Mab. Mab E48-$AlPcS_4$ conjugate was more active on 22A than on 431 cells, while Mab 425-$AlPcS_4$ conjugate had the opposite effect. After determination of Pc's cell binding and internalization, the authors suggested that the phototoxicity of these conjugates was more dependend on the overall cell binding than on their cellular internalization.

Overexpression of the low density lipoproteins (LDL) receptor has been reported for several tumors allowing the internalization of LDL proteins into the cell[95]. Therefore, Urizzi *et al*.[96] conjugated AlS_4Pc to LDL either via covalent linking of a bisulfonated substituent of $AlPcS_4$ through a 5-carbon spacer chain [($AlPcS_4A_2$): aluminium di-(6-carboxypentylaminosulfonyl)-tetrasulfophthalocyanine) or non-covalent linking to the phospholipidic region of LDL ($AlPcS_4(C_{12})$]. Loading ratios of 72:1 and 61:1 for $AlPcS_4A_2$-LDL and $AlPcS_4(C_{12})$-LDL, respectively, have been reported to be the most stable formulations.

These compounds were tested *in vitro* on EMT-6 and A549 cells. After 2 h of incubation with the conjugates or with free $AlPcS_4$, $AlPcS_4(C_{12})$-LDL displayed a 10-fold higher phototoxicity effect than $AlPcS_4A_2$-LDL. This has been ascribed to the increased aggregation tendency, higher scavenging of ROS products, and alteration of the conjugate interaction with cellular receptors when Pc was covalently coupled to the protein.

Interestingly, free $AlPcS_4$ and $AlPcS_4A_2$ were devoid of any photocytotoxic effects under the same conditions. A possible reason for this lack of photoxic activity could be the negative net charge of these Pcs, leading to a different cellular uptake and/or intracellular localization.

Further *in vivo* studies on mice bearing EMT-6 allografts were performed comparing free $AlPcS_4$ to $AlPcS_4(C_{12})$ and $AlPcS_4(C_{12})$-LDL conjugate. No difference in tumor response was reported for both conjugates. As compared to free $AlPcS_4$, 25 times lower drug doses could be used to induce similar responses. Moreover, the post-treatment oedema regressed within 3–4 days post-PDT. The similar phototoxic effect of free and $AlPcS_4(C_{12})$-LDL conjugate can presumably be attributed to binding of the free Pc to plasma proteins (*e.g.*, LDL) and redistribution post injection.

Overexpression of gastrin-releasing peptide-receptors (GRPR) have been associated with many cancerous conditions such as ovarian, breast, prostate and lung cancer[97]. Since bombesin is the amphibian homologue of the human gastrin releasing peptide[98] a recent study

reported an attempt to target human prostate tumor cells PC-3 by conjugating $AlPcS_4$ to bombesin.

However, due to the conjugation of bombesin to the $AlPcS_4$ (Figure 4), the binding affinity to GRPR was about 40 times lower for the conjugate as compared to bombesin, certainly resulting in a loss of specificity and a moderate phototoxicity[99]. Nevertheless, the photoactivity of the conjugate was 2.5 and 5 fold higher than $AlPcS_4A_1$ and the free tetrasulfonated aluminium phthalocyanine, respectively, *in vitro*.

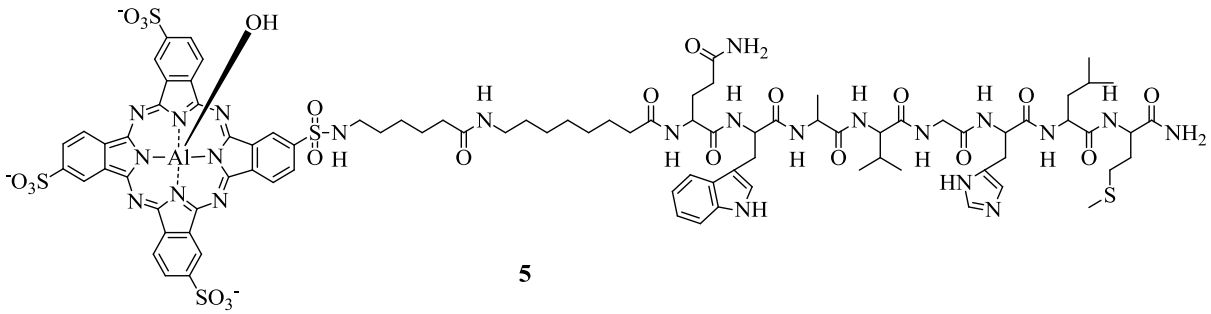

5

Figure 4. Chemical structure of the bombesin-$AlPcS_4$ conjugate **5** for the targeting of GRPR

2.1.5. AlPcS4-Formulation using Targeted Delivery Systems

Simple liposomes are usually unstable upon systemic administration and rapidly cleared from the body. However, the incorporation of PEG-derivatized phospholipids in the bilayer of liposomal membranes generally prolongs their circulation time. This property of PEGylated liposomes coupled to additional tumor targeting moiety such as transferrin was exploited by Gijsens *et al*. *in vitro*[100] and *in vivo*[101]. In HeLa cells, expressing approximatively 2 x 10^5 transferrin receptors per cell[102], transferrin conjugated PEG-Liposomes containing $AlPcS_4$ (Tf-Lip-$AlPcS_4$) were 10 times more efficient than free $AlPcS_4$ (IC_{50} of 0.63 µM *vs.* 6.3 µM, respectively) while non-Tf conjugated $AlPcS_4$ liposomes (Lip-$AlPcS_4$) were less potent than free PS. Indicating that non-targeted liposomes are only poorly taken up and additionally, show only limited release of their content into the cells[100].

Initially, the same tendencies were confirmed when these formulations were tested on AY-27 cells[101]. However, in a rat bladder model using the same cell line no or only moderate accumulation of all liposomal formulations was observed. However, pretreatment with a chondroitinase breaking the epithelial glycocalyx resulted in a selective retention of Tf-Lip-$AlPcS_4$. On the contrary, free $AlPcS_4$ was detectable with or without the enzymatic

pretreatment of the bladder but with a lower selectivity. The reported tumor-to-normal tissue ratio and tumor-to-submucosa/muscle ratio for Tf-Lip-$AlPcS_4$ were 18:1 and 78:1, respectively.

Qualls *et al.*[103] encapsulated $AlPcS_4$ into pH sensitive liposomes using 1,2-di-O-(Z—1′-hexadecenyl)-*sn*-glycero-3-phosphocholine (DPPlsC) an acid labile lipid. Moreover, folate-polyethyleneglycol 3350-distearoylphosphatidylethalonamine (Folate-PEG3350-DSPE) was incorporated for targeting of folate-receptors in order to promote the receptor-mediated Pc internalization. The liposomes were subsequently tested *in vitro* on folate receptor expressing human nasopharyngeal cancer cells. It was found that DPPIsC-folate liposomes were taken up faster and were photodynamically more active than the free $AlPcS_4$ confirming earlier studies with similar liposomes on colorectal carcinoma cells C170 cells by Morgan *et al.*[104]. Moreover, it was shown *in vitro* that the targeting moiety rather than the pH sensitivity of the delivery system dominated the photocytotoxicity of the PS[103].

2.1.6. AlClPc—SAR

Modulation of the axial substituents is another way to modulate the pharmacological, pharmaceutical as well as optical properties of Pcs. As confirmed by Chan *et al*., Ben Hur initially reported that a simple Pc carrying a chlorine as counterion (AlClPc, **6**, Figure 5) was photodynamically more active than its sulfonated counterparts[79,105]. In order to further improve these compounds systematic studies with different alterations of the axial substituents have been undertaken. Decreau *et al.*[106] reported increasing phototoxicity with increasing the hydrophobicity of AlClPc derivatives. Indeed, when incorporated into liposomal (Egg Yolk Lecithin based liposomes) or emulsion (Cremophor EL based emulsion) formulations, the hydrophobic aluminium Pc (AlPc) derivatives such as **7** and its cholesterol derivative **8** (Figure 5) were more phototoxic than **6**. After 1 h incubation of achromic M6 melanocytes with liposomal formulations of **6** or its derivatives the drug dose required to induce 50% of the cell death was 10^{-8}, 3 x 10^{-8} and 7 x 10^{-8} M for **8**, **7**, and **6**, respectively. This was further improved by a factor of approximatively 10 by using Cremophor EL based emulsions.

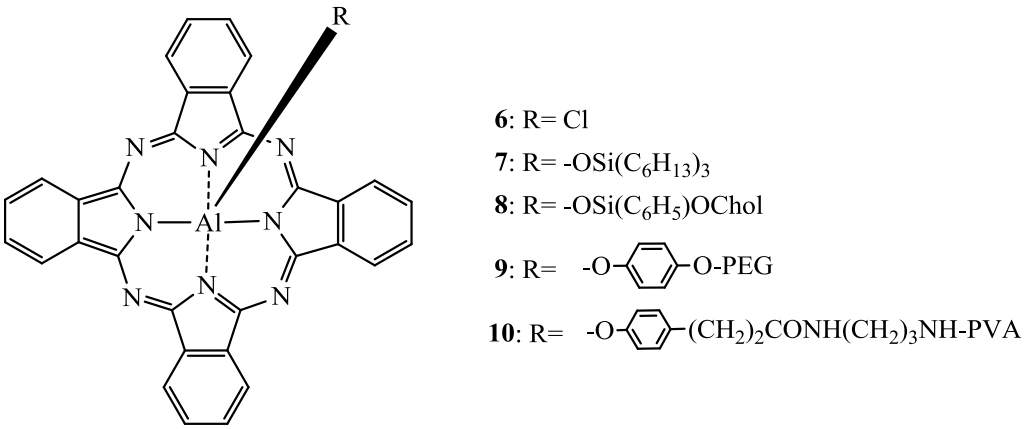

Figure 5. Chemical structure of AlPc **6–10**[106,107]

Brasseur *et al.*[107] conjugated polyethylene glycol [PEG; molecular weight (M.W.) of 2,000] or polyvinylalcohol (PVA; 13,000–23,000) axially to AlPc (Figure 5). The resulting steric hindrance combined with the increased water-solubility provided by the axial polymeric ligands, was expected to enhance the efficacy of such AlPc derivatives. *In vitro*, after 1 h of incubation, the hydrophobic **6** was 3 times more potent in EMT-6 cells to induce 90% of cell death than its axially derivatized counterparts. Interestingly, in *in vivo* experiments, **10** showed the longest half-life (6.8 h *vs.* 23 min for AlPc-PEG and 2.6 h for **6** in Cremophor EL), the lowest retention in the liver, spleen and lung and most importantly the highest tumor accumulation. Tumor-to-skin and a tumor-to-muscle ratios of 12 and 27 respectively after 24h post injection in EMT-6 tumor bearing mice have been reported whereas, **9** exhibited the lowest half-life and accumulation in tumor. Thus, the axial substitution of AlPc with PVA could exert the same efficiency as **6** formulated in Cremophor thereby avoiding potential risk factors such as anaphylactic reactions[108].

2.1.7. AlClPc-Formulation

Besides the use of Cremophor EL based emulsions, some efforts have been reported on the formulation of AlClPc (**6**) in suitable delivery vehicles aiming at improving the photodynamic outcome of AlClPc-based PDT such as polymeric pH-sensitive micelles.

Micelles are usually aimed at entrapping hydrophobic drugs in their lipophilic core mostly to enhance their bioavailability and to make them suitable for systemic administration. Furthermore, owing the Enhanced Permeability and Retention effect (EPR effect), micelles from 5 to 50–100 nm allows the preferential accumulation of drug into tumors[109,110]. Indeed, abnormalities at tumor sites *i.e.*, defective and leaky neovasculature, low lymphatic drainage

and limited venous return, enable drug accumulation and retention in tumors[111,112]. Moreover, pH-sensitive micelles are expected to enable specific tumor delivery of the therapeutic agent based on the physiological differences between healthy and cancerous tissues[113].

It was demonstrated *in vitro* that pH-sensitive Polymeric Micelles (PM) of N-isopropylacrylamide (NIPAM) copolymers loaded with **6** were photodynamically more active than **6** in a Cremophor formulation on EMT-6 cells[114]. Furthermore, the terminally alkylated NIPAM copolymers loaded with **6** were less efficient *in vitro* than its randomly alkylated counterpart.

In vivo, **6** encapsulated in PM exhibited a rapid clearance and a low accumulation compared to the Cremophor formulation. However, despite these unfavorable pharmacokinetic characteristics, **6** in PM showed a "similar phototoxic activity to that of the Cremophor formulation"[115].

Trials to decrease PM clearance and thus improve their phototoxicity by incorporating hydrophilic *N*-vinyl-2-pyrrolidone (VP) units into NIPAM copolymers failed; mainly due to increased accumulation in the lungs and unchanged uptake by tumor cells[116].

The intrinsic insolubility of AlClPc in aqueous media represents certainly a drawback if systemic administration of the drug is desired. However, in case of topical application, for the treatment of non-melanoma skin cancer the aggregation of the Pc can be circumvented by the use of pharmaceutically acceptable solvents that both enable the dissolution of the drug and additionally enhance the permeability of the skin such as DMSO[117]. In a study conducted by Kyriazi *et al*.[118], AlClPc was diluted in a mixture of DMSO, Tween 80 and water and tested on albino mice (SKH-HR1) and SKH-HR2 (with melanin) bearing UV-induced skin carcinomas. Irradiation was performed both on the tumor and also on the normal skin surrounding the tumor. Optimal tumor response in terms of "highest percentage of mice in complete remission" was obtained, with a light dose of 150 J/cm^2 and a fluence rate of 75W/cm^2. Furthermore, the formulation enabled a 40 times more selective uptake of the drug by the tumors compared to normal skin after 1 h post-administration. Interestingly, better therapeutic outcome was achieved when lower fluence rates were applied. This observation is in agreement with other studies conducted on mTHPC and 5-ALA photosensitisers and was related to the lower consumption of oxygen under these conditions[119,120].

2.2. Zinc Based Phthalocyanines

2.2.1. ZnPc—SAR

As mentionned in Section 2.1.1, providing permanent negative charges through sulfonation to Pcs increases their solubility in aqueous media. Wöhrle *et al*. reported[121] that amphiphilically sulfonated ZnPcs such as the mono- and disulfonated phthalocyanines are more potent and effective than their tri- and tetrasulfonated counterparts *in vivo*. Comparing Zn and Al substituted analogs, they found the following pattern of photodynamic efficacy: $AlPcS_2 \approx ZnPcS_1 > AlPcS_1 > AlPcS_3 \approx ZnPcS_2 > AlPcS_4 > ZnPcS_4$.

In 1997, Kudrevich *et al*. [122] conducted *in vitro* and *in vivo* experiments on Balb/c mice bearing EMT-6 tumors using a series of trisulfonated, amphiphilic water-soluble ZnPc derivatives (Figure 6).

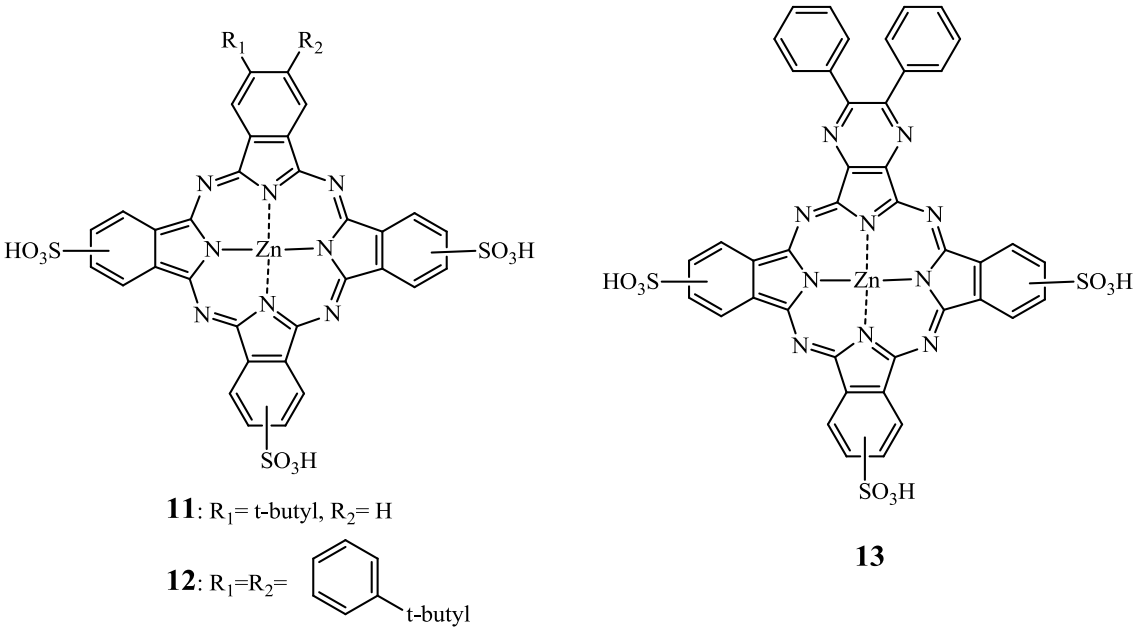

Figure 6. Structures of compounds **11**, **12** and **13**[122]

In vitro compounds **11** and **12** were two and more than five times more potent than the tri and tetrasulfonated zinc phthalocyanines, respectively, whereas compound **13**, exhibited the lowest phototoxicity probably due to its poor cellular uptake caused by the "bulky diphenylpyrazino substituent". *In vivo*, no tumor regression could be noticed with **13** and $ZnPcS_3$. However, in almost 90% of the mice treated with 5 μmol/kg of compounds **11**, **12**, and $ZnPcS_4$ no palpable tumors have been detected three weeks post-PDT. It was suggested that the amphiphilic character of **11** and **12** decreases the aggregation tendency, thus

increasing photoactivity and tumor uptake. Moreover, due to the higher conjugation extent, a bathochromic shift of the Q-band (*i.e.*, 706 nm) was induced.

Based on the experiments evaluating the impact of amphiphilicity on photodynamic activity with aluminium sulfonated phthalocyanines, there have been numerous attempts to increase the amphilic character of zinc sulfonated phthalocyanines. In one of their studies, Cauchon *et al.*[123] compared the photodynamic efficiency of different trisulfonated phthalocyanines bearing one alkyl chain containing between n = 2 and 16 carbon atoms ($ZnPcS_3(C_n)$).

In vitro studies revealed that $ZnPcS_3(C_9)$ exhibited the highest cellular uptake and photocytotoxic effect on EMT-6 cells, while the other hydrocarbon substituted phthalocyanines were less efficient. The structure-activity relationship to induce 90% cell death of these compounds followed a typical hyperbolic curve also observed for other homologous series of photosensitizers[124]. However, the most potent compound in this study was the disulfonated zinc phthalocyanine with two sulfonic groups positioned adjacently despite a lower cellular uptake which can be explained by different intracellular localization upon internalization.

In a series of different ZnPcs, disulfo-di-phthalimidomethyl zinc phthalocyanine ($ZnPcS_2P_2$ = **14**) (Figure 7) has been shown the highest photodynamic activity in Human myelogenous leukemia HL60 cells, K562, FGC85, SGC7901 and LCC carcinoma cell lines[125-127]. Moreover, when administered to mice bearing S180 and U14 solid tumors[126] in a Cremophor-based emulsion, the tumor weight in PDT treated animals decreased compared to the controls. The highest inhibitory rate was achieved with a drug dose of 2 mg/kg in both models. Moreover, no acute toxicity was reported after intravenous or intraperitoneal administration of **14** with drug dose up to 100 mg/kg[126]. The repeated-dose toxicity of this compound was assessed a few years later in healthy Wistar rats[128] using the same delivery system. Interestingly, an acute toxicity of **14** was found at a dose of approximatively 52mg/kg based on their investigations on mice[126] and on an "anticipated human clinical application" (data not disclosed).

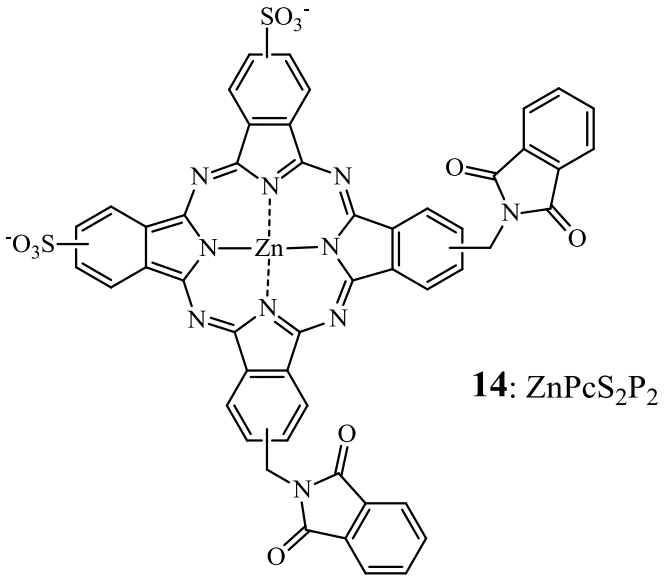

Figure 7. Chemical structure of phthalocyanine **14** *i.e.*, $ZnPcS_2P_2$

It was reported that a 10 times repeated administration of 4 mg/kg, which corresponds to 100 times that anticipated clinical "therapeutic" dose by the authors, induced notable hepatic and spleen damage.

Besides sulfonation, another means to enhance the solubility of Pcs in aqueous media and increase their amphiphilicity is hydroxylation. Boyle *et al.*[129] and Hu *et al.* [130], reported the synthesis and evaluation of several hydroxysubstituted zinc phthalocyanines.

When incorporated in Cremophor EL emulsions, all compounds showed strong photodynamic action both *in vitro* and *in vivo* except for the directly substituted tetrahydroxyphthalocyanine **15** (Figure 8) Indeed, Boyle *et al.*[129] showed that **15** was phototoxic *in vitro* on Chinese hamster lung fibroblasts V79; but failed *in vivo* on Balb/c mice bearing EMT-6 tumors, to induce any perceptible tumor response. Meanwhile, the tetra(3-hydroxypropyl) zinc phthalocyanine **16** (Figure 8) and tetra(6-hydroxyhexyl)zinc phthalocyanine **17** (Figure 8) induced tumor cure as measured by tumor necrosis within 48 h and no tumor regrowth up to 30 days at 0.5 μmol/kg and 1 μmol/kg (1.0 mg/kg), respectively, when applied intravenously. Compared to a mixture of mono, di, tri and tetrasulfonated ZnPcs, **16** and **17** were ten and five times more potent than ZnPcS. Furthermore, it seemed that the hydroxyderivatives function via vascular shutdown rather than direct cell killing as observed for the sulfonated zinc phthalocyanines.

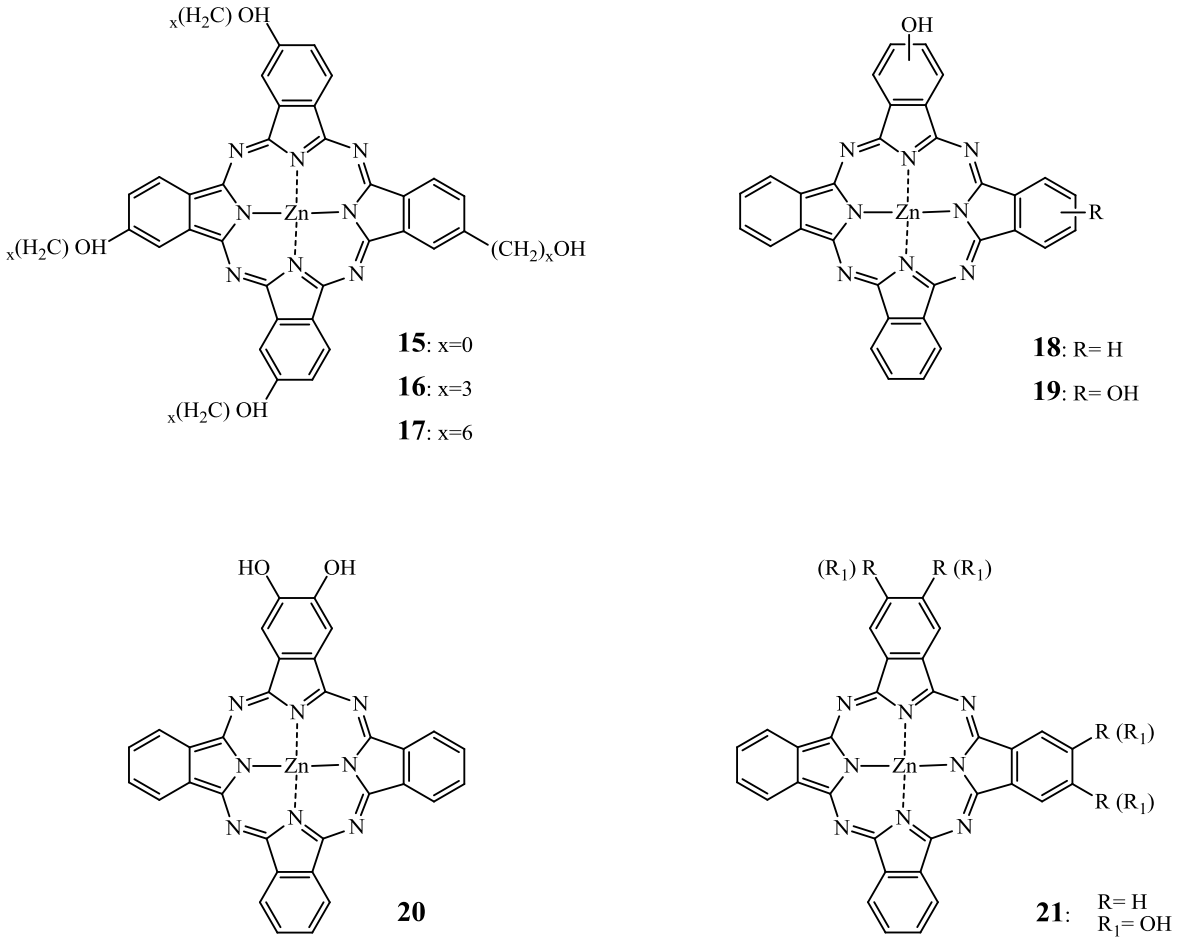

Figure 8. Chemical structure of hydroxylated phthalocyanines **15–21**

Moreover, Winkelman *et al.*[131] postulated that a critical distance of 1.2 nm is required between oxygen atoms of sulfonate, carboxyl or hydroxyl substituents and the core of phthalocyanines or porphyrins in order to present biological activity. This hypothesis could potentially explain the low photoactivity exhibited by **15** as well as the phototoxicity of the alkylhydroxy ZnPc derivatives.

A few years later, Hu *et al.*[130] tested mono-, di- and tri-substituted hydroxy ZnPcs derivatives **18–21** (Figure 8) formulated in Cremophor emulsions in EMT-6 tumor cells *in vitro* and *in vivo*. It was observed that the phototoxicity decreased with the introduction of hydroxyl groups (*i.e.*, **15** *vs.* **20**) and that adjacent positioning of the hydroxyl functions such as in **21** increased Pcs phototoxic effect.

A third possible chemical modulation of ZnPc consists in fluorination of the PS. Several articles report the synthesis and evaluation of this class of ZnPcs[132,133] (Figure 9). The main reasons being that fluorination increases the water solubility and triplet state quantum yield of the phthalocyanine while maintaining similar behavior in biological medias as hydrogen atoms[134].

The most extensive studies on fluorinated ZnPc in PDT have been performed by the van Lier group (using hexadecafluorinated zinc phthalocyanine ($ZnPcF_{16}$)(**25**, Figure 10)[135-138].

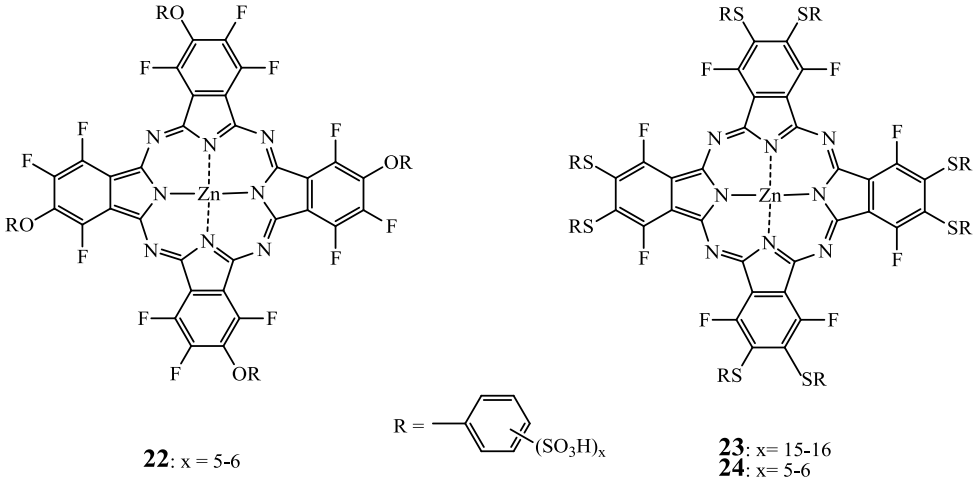

Figure 9. Structure of the fluorinated ZnPc **22**, **23** and **24**

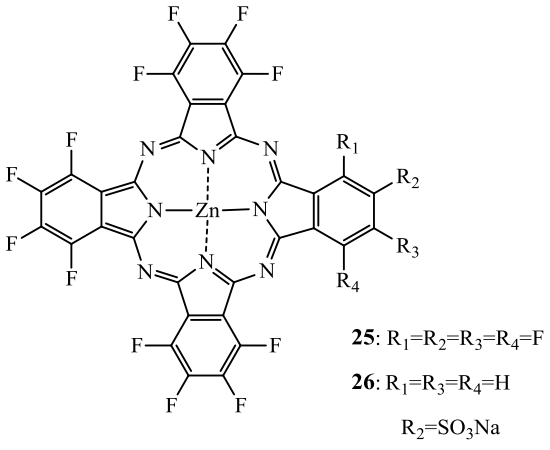

Figure 10. Structure of the zinc hexadecafluorinated Pc **25** and its monosulfonated analogue **26**

In their most recent publication on this subject, Allémann *et al*.[137] compared Cremophor based emulsion of compounds **25** and **26**. It is noteworthy to mention that Pc **26**, bears one sulfonated group to provide some amphiphilicity, thus, probably improving cell penetration. To BALB/c mice bearing EMT-6 tumor allografts, 1 μmol/kg of **25** or **26** were applied and their bioavailability as well as their PDT effect has been assessed. After one week, the area under the plasma concentration as a function of time of **25** and **26** were 237 and 183 nmol·h/g with half-lives of 9.25 and 12 h, respectively.

The highest PS tumor accumulation was recorded 24 h post-injection for both Pcs. However, **26** exhibited better tumor selectivity with reported tumor-to-muscle and tumor-to-skin ratios of approximatively 13 and 4 for **26** and, 7 and 2.5 for **25**, respectively. Strikingly, a 66% tumor response was recorded for **26** at 1 μmol/kg for a light dose of 100 J/cm^2 but was associated with 33% mortality. Hence, it was considered that the best PDT results (*i.e*., tumor response and animal viability) were obtained using 0.1 μmol/kg of **26** irradiated at 400 J/cm^2. As compared to previous results reported by Boyle *et al*.[138], **26** is twenty times more phototoxic than **25** while displaying equivalent tumor uptake. The impressive **26** phototoxicity observed was attributed to "extensive cellular damage". In tumor free rats, **26** formulated in Cremophor was devoid of any lethality after irradiation. Alterations of tumor surrounding tissues and extensive edema were reported, but were associated with rapid recovery[137]. A proposed way to avoid these collateral damages is to tune its biodistribution and elimination using different formulations forms, such as PEG-coated nanoparticles (NP). In Section 2.2.3 of this review, formulation of **25** in NP is further discussed.

Allémann *et al*.[137] also investigated the influence of incubation media on PDT efficiency of ZnPc *in vitro* by comparing 1-methyl-2-pyrrolidinone to pyridine. Dilution of Cremophor emulsion of ZnPc at 10 μM in 1-methyl-2-pyrrolidinone solution led to complete loss of *in vitro* PDT efficacy presumably due precipitation and aggregation as noticed by an altered absorption spectrum. This observation confirmed earlier *in vivo* studies by Boyle *et al*.[138] that obtained no significant tumor response in BALB/c mice bearing EMT-6 tumors when ZnPc was diluted in 1-methyl-2-pyrrolidinone. In the meantime, complete tumor ablation was achieved when pyridine was used to dilute ZnPc Cremophor-based emulsion at a drug dose of 2 μmol/kg. The authors assumed a possible "coordination of pyridine to the axial ligands of the central metal ion" resulting in an increase photodynamic activity.

Choi *et al*. and Liu *et al*. [139,140] reported recent *in vitro* investigation*s* on the influence of glycosylated ZnPc based on the strategy to concomitantly increase the water-solubility and

the selectivity of these compounds through targeting of glucose transporter[141,142]. In accordance with zinc sulfonated phthalocyanines, tetra-glycosylated ZnPc derivatives were substantially less photoactive than the mono-glycosylated and di-glucosylated ZnPcs derivatives *in vitro*[139,140]. Moreover, the α and β positioning of the glycose substituents seemed to influence the tendency to aggregate and consequently affects their phototoxicity. Indeed, α substitution appeared to prevent Pc aggregation as compared to the β positioned analogues. Promising phototoxicities in the nanomolar range were achieved in HT29 and HepG2 cells glucosylated di- α substituted ZnPc.

Ometto *et al*.[143] as well as Fabris *et al*.[144] have tested octapentyl (**27**) and octadecyl (**28**) substituted ZnPc (Figure 11). Administered intramuscularly to MS-2 fibrosarcoma bearing Balb/c mice in a Cremophor emulsion both compounds were highly selective for the tumor tissue. Limited skin photosensitization was confirmed with healthy Balb/c mice under the same experimental conditions. The strong binding of both compounds to LDL is presumably responsible for this selectivity[145]. Both **27** and **28** induced a shrinkage of the tumor volume after PDT[143,144]. However, both derivatives accumulated to a higher extend in the liver and spleen than in the tumor even one week post-PDT, presumably because the bile-gut is the primary elimination pathway characteristic for lipidic drug delivery systems[143,146].

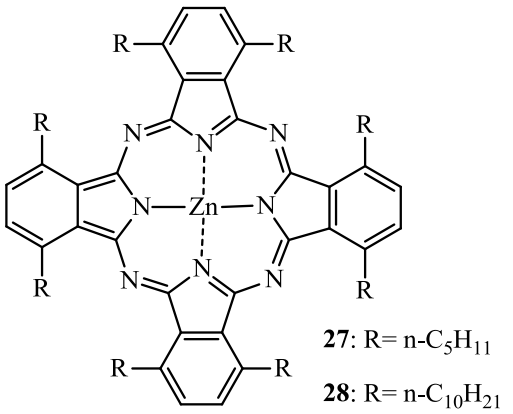

Figure 11. Chemical structure of octapentyl and octadecyl ZnPcs **27** and **28**

Liu *et al*. have achieved synthesis and *in vitro* evaluation of zinc octa[(biscarboxylate)-phenoxy]phthalocyanine and its sodium salts[147] (*i.e*, compounds **29** and **30**, see Figure 12).

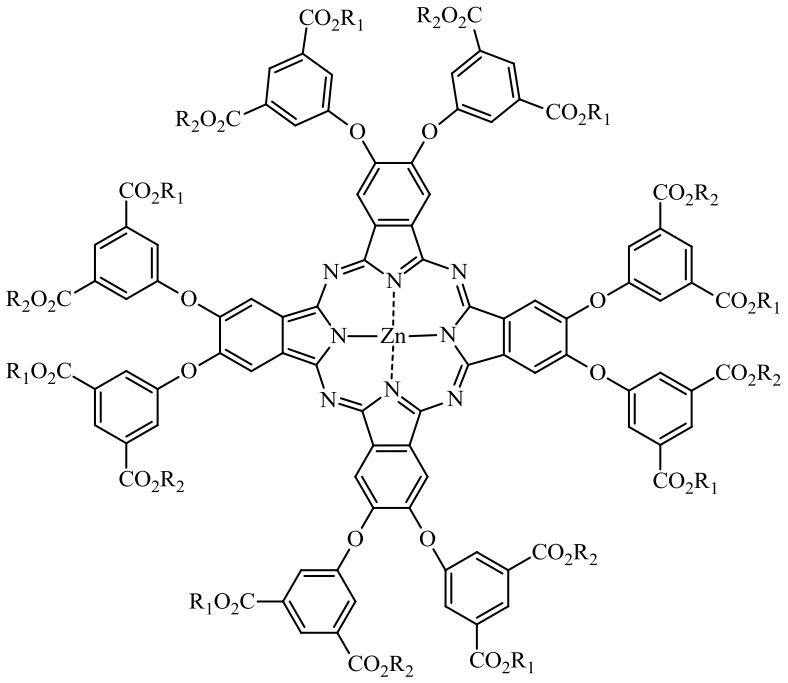

29: R_1=H/Na and R_2=H/Na
30: R_1=R_2=H

Figure 12. Chemical structure of phthalocyanines **29** and **30**

This structural extension with phenylcarboxylate groups resulted in a diminished stacking and aggregation tendency, due to possible non-planar orientation of this group as well as extended "inter-ring distance". However, at physiological pH, only **29** was water-soluble. The authors presented this aspect as the major drawback of **29** to HEp2 cell penetration, whereas the more hydrophobic **30** was taken up to a higher extent. However, cell penetration could have been also hampered by the presence of negative charges on **29** at physiological pH. Despite differences in cellular uptake both Pcs displayed similar but moderate phototoxicities. However, this low potential for photosensitization of biological materials can be efficiently used for fluorescence diagnostics. Very recently ZnPc similar to **29** zinc tetra[(monocarboxylate)phenoxy]phthalocyanine has been exploited for the use in PCR analysis[64]. This compound had similar but narrower absorption and emission bands in the NIR as compared to a conventional cyanine dye. Most importantly, the Pcs dyes were thermally and chemically stable and showed essentially no photobleaching.

The outstanding tendency of Pcs to form photoinactive aggregates can also be exploited for the design of "molecular beacons". These compounds are powerful tools for real time detection of RNA/DNA *in vitro* and *in vivo*. In molecular beacons, a quencher/donor pair is

positioned on the distal ends of a short, hairpin forming oligonucleotide. In absence of a complementary sequence the close proximity of the fluorophore and its corresponding quencher makes the molecular beacon optically silent. However, hybridization with the complementary sequence then restores the fluorescence of the reporter. Despite their high specificity the sensitivity of conventional molecular beacons is often compromised by a poor sensitivity provided by insufficient quenching. Futhermore, longer observation periods are often impeded by most fluorescent dyes' strong photobleaching. Therefore, in an earlier study the same group reported the use of a pair of Pc similar in structure to ZnPc in molecular beacons[148,149]. After optimization of the reaction conditions good yields for molecular beacons were achieved. However, since Pcs have long interaction ranges the authors had to use longer oligonucleotide sequences as complementary sequence to observe a fluorescence increase. A signal to background ration as high as 59 was reported. Furthermore, the perfect matched complementary sequence was five times more fluorescent than a single base mismatch. Therefore, water soluble Pcs can be efficiently employed as fluorescence reporters *in vitro* but their whole potential in this area remains to be demonstrated.

Lo and co-workers reported the photoactivity of monosubstituted ZnPc with a 1,3-bis(dimethyl-amino)-2-propoxy group at the α or β position (Figure 13), "and the corresponding di-*N*-methylated derivatives" on human colorectal carcinoma cells HT29[150]. The α and β positioning is an analogy to the α and β positions for sugar moieties. Indeed in sugars, α and β correspond to lower and upper position respectively of the hydroxylic group on the anomeric carbon (C1) of the cyclic sugar moiety, the cylcle defining the referential plane[151].

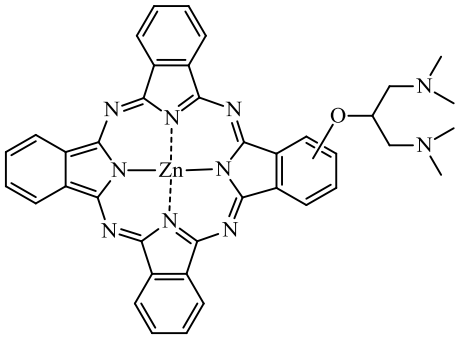

31 (α-substitution) and **32** (β-substitution)

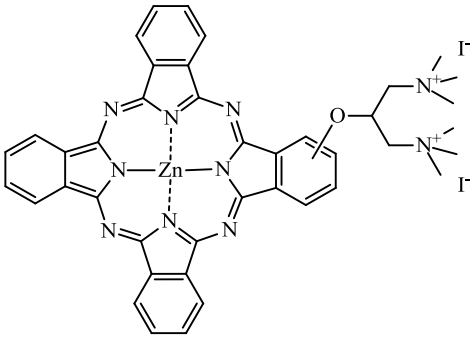

33 (α-substitution) and **34** (β-substitution)

Figure 13. Structure of compounds **31–34**

The absorption and fluorescence spectra showed a lower aggregation tendency for the β-substituted compounds as compared to their α-substituted analogues. Consequently, the IC_{50} of **32** and **34** were 0.15 and 0.08 μM, respectively, while **31** and **33** induced 50% of cell inactivation at doses of 0.48 and 0.64 μM, respectively.

Like AlPcs, PEGylated ZnPcs have also been designed aiming at increasing their water solubility[152]. Liu *et al*. have prepared a series of asymmetrically substituted ZnPcs using methylated polyethylene glycol. However, these compounds were essentially not water soluble. Therefore, just recently the synthesis of tetra and octa substituted PEGylated ZnPcs has been reported[153]. In these compounds the terminal methyl group of the tetraethylene glycol side chains has been omitted in order to provide a higher hydrophilicity through hydroxyl end groups. Despite these modifications, aggregation in water was still observed that could be circumvented by the addition of Triton-X100. The less aggregated compound that was non-peripherally substituted with polyethylene glycol showed a strong bathochromic shift of more than 20 nm. But *in vitro* evaluation showed an IC_{50} value that was in the order of two orders of magnitude higher than reported for the methylated counterparts. Recently, Ng and co-workers reported the synthesis and efficient photocytotoxic effect of several pegylated ZnPcs where IC_{50} values ranged from 0.25 to 3.72 μM on HT29 and HepG2 cells[154].

The net charge of pharmacological compounds is of importance with respect to the pharmacokinetic properties of a drug as well as in terms of uptake and intracellular localization. Several studies report the impact of the charge on Pc-mediated PDT. Banfi *et al*.[155] described the synthesis and *in vitro* assessment of some ZnPc derivatives on human colon adenocarcinoma cells HCT116. The most potent ZnPc derivatives among the synthesized series are shown in Figure 14.

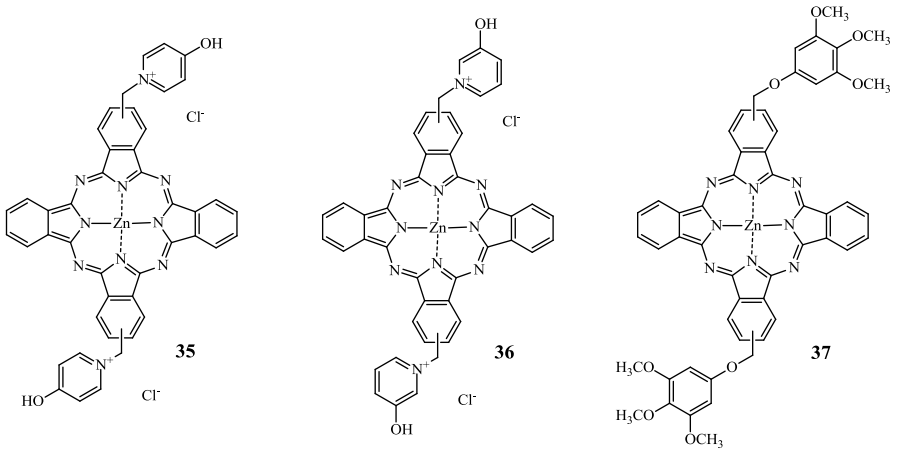

Figure 14. Structure of compounds **35**, **36** and **37**

Compound **35** was approximately five times more potent than compound **36** and approximately eight times more efficient than compound **37**.

Brown and coworkers[156,157] reported that the cationic pyridinium ZnPc **42** (see Figure 15) was more phototoxic to RIF-1 cells than the anionic tetraglycine analogue **39** or the neutral hydrophobic tetradioctylamine **43**[156]. *In vivo* all the tested compounds induced partial tumor regression, but only compound **42** led to complete remission, most presumably through vascular occlusion in the irradiated areas. This observation is in agreement with a study of Sibrian-Vazques *et al*. that showed that the cellular uptake of **44** was higher and faster than **46** (see Figure 16)[158].

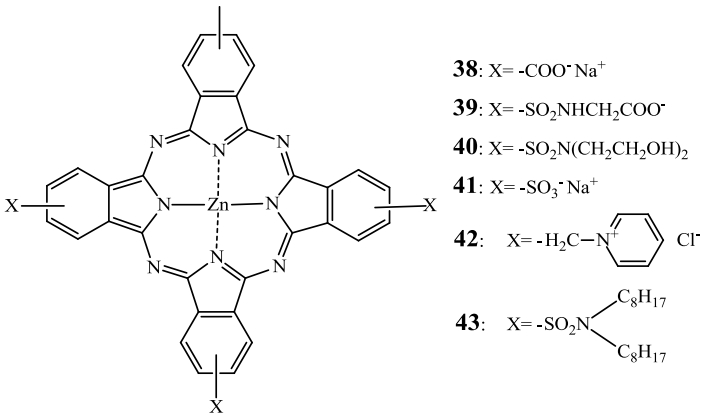

Figure 15. Chemical structure of phthalocyanines **38–43**

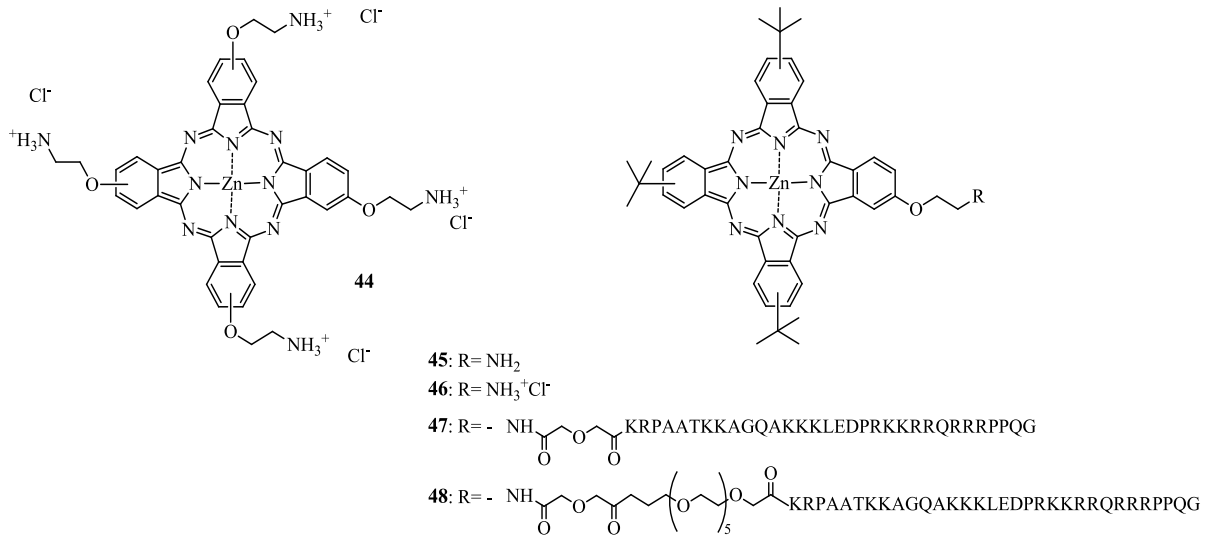

Figure 16. Chemical structure of compounds **44–48**

2.2.2. Tumor Targeting with Zinc Based Pc-Conjugates

In the same report the preparation and *in vitro* evaluation of zinc based phthalocyanines conjugates with cell-penetrating peptides (CPP) (see Figure 16) was described.

Conjugates **47** and **48** were taken up by HEp2 cells to a higher extent than the unconjugated ZnPc. The introduction of short polyethylene glycol linker between the ZnPc and CPP has been shown to further increase the uptake. At a light dose of approximately 1 J/cm^2, **47** and **48** were the most active compounds, with IC_{50} values of 1.44 μM, 1.87 μM, respectively. In contrast, **44** did not alter the cell viability at doses up to 10 μM.

2.2.3. Formulation of ZnPcs

Phototoxicity and fluorescence of Pcs is mostly hampered by their low water-solubility and tendency to aggregate. Their incorporation into suitable and biodegrable formulations is commonly accepted as a necessity in the development of new therapeutics. Indeed, development of drug delivery systems such as liposomes, micelles and nanoparticles could improve the unfavorable biodistribution of free Pcs (*i.e.*, improvement of PS pharmacokinetic properties, better targeting of diseased tissues due to size of the particles, association to serum proteins and specific activation of the PS through localized delivery of the PS) as well as avoidance of aggregation and loss of phototoxic activity/fluorescence which should result in a better therapeutic outcome (see following paragraphs).

Zinc based phthalocyanines have been mostly evaluated as liposomal formulations. Liposomes are phospholipids vesicles that present the advantage to entrap either hydrophilic drugs in the core of the phospholipid vesicle or hydrophobic drugs within the lipid membrane. Incorporation of drugs into liposomes results in passive targeting of tumors[159,160]. In studies reported in this review, only small unilamellar vesicles (*i.e.*, one phospholipid bilayer) were used.

Liposomal formulation of ZnPc showed photocytotoxic effect *in vitro* on a large variety of tumor cell lines[161-163]. The drug CGP55847 commercialized by CIBA has been the first Pc reaching clinical trials although no clinical results have been reported. Ben-Hur and Chan reported that the "early phase I/II clinical studies […] were discontinued but not for medical reasons"[164].

In vivo, ZnPc being incorporated in dipalmitoyl-phosphatidylcholine (DPPC) liposomes showed complete response at drug doses as low as 0.14 mg/kg in mice inoculated with MS-2

fibrosarcoma. At a slightly lower dose of 0.12 mg/kg (i.v.), ZnPc was found to be "associated exclusively with lipoprotein fraction", *i.e*., whether it was complexed with low density lipoproteins (LDL) or incorporated into liposomal structures, and 70% of the drug was cleared from the body within 12 h independently from its carrier system, while the remaining ZnPc was slowly eliminated. However, ZnPc associated with LDL presented a higher selectivity toward tumor than ZnPc liposomes with a tumor-to-liver ratio of 2.27 and 1.04 and a tumor-to-muscle ratio of 4.20 and 3.84 after 24 h post-injection, respectively. Nonetheless, the selectivity was somewhat limited by the redistribution of the photosensitizer among other lipoproteins, especially high density lipoproteins. As liposomal formulations of benzoporphyrin derivative, liposomal CGP55847 seems to be transferred to serum lipoproteins and more predominantly to low density lipoproteins[165-169] explaining the propensity of the PS to selectively accumulate in tumors[163,170]. Rodal *et al*. suggested that the observed internalization of ZnPc was not following the endocytotic pathway of LDL but rather occurred via diffusion through the cellular membrane after binding to the LDL receptor[161].

In vivo studies on different liposomal formulations consisting of a mixture 1-palmitoyl-2-oleoyl-sn-glycero-3-phosphocholine (POPC) and 1,2-dioleoyl-sn-glycero-3-phospho-L-serine (OOPS) revealed that intratumoral distribution pattern of ZnPc in C57BL/6 mice bearing Ehrlich carcinomas or B16 melanomas was a time dependent process[171]. In agreement with van Leengoed *et al*.[172], 3 h after intravenous injection of 0.5 mg/kg of ZnPc, the photosensitizer was present in and around the tumor vasculature but not 24 h post-injection. Indeed, using a dorsal skinfold chamber model, van Leengoed *et al*.[172], could detect vascular occlusion within five minutes after photoactivation which resolved 30 min after irradiation. Moreover, maximal vasculature damage and tumor-to-muscle ratio from 8:1 to 14:1 have been reported for this liposomal delivery system[173].

Nanoparticles are another type of drug delivery system that enables the incorporation of higher drug doses of hydrophobic drugs. Passive targeting of tumors is also achieved due to their size (*i.e*., below 1,000 nm, generally 200 nm) through EPR effect. A strategy to increase the circulation time of the nanoparticles as well as other drug delivery systems is the incorporation of PEG moieties on their surface. It is commonly accepted that PEGylation creates hydrophilic barrier that reduces the immunogenicity of the drug delivery system and lowers its clearance from the body[174-176].

Polylactic acid (PLA) based nanoparticular formulations of ZnPc were investigated by Allémann *et al.*[135,136]. The coating of nanoparticles with PEG moieties resulted in the decrease of the reticuloendothelial system and an increase in the PS tumor retention[135]. Incorporation of **25** (Figure 10) into PEG coated nanoparticles or using a Cremophor EL based emulsion increased the bioavailability as compared to uncoated-NP by a factor of four in BALB/c mice bearing EMT-6 tumors. The tumor-to-skin and tumor-to-muscle ratios for the PEG-NP and Cremophor based formulation were 2 to 21, respectively, with a maximum concentration in tumor 48 h post-injection[135]. However, the nanoparticular drug delivery system was nearly five times more efficient for PDT-mediated treatment of mice bearing EMT-6 tumors[136]. This is in agreement with a study reported by Fadel *et al.*[177] describing that tumor bearing animals treated with ZnPcs laden poly(lactic-coglycolic acid) nanoparticles showed the best PDT outcome, highest tumor growth delay and longest survival times as compared to mice treated with the free PS.

An interesting approach was recently described by Kataoka and co-workers[178-181] where dendrimer based zinc phthalocyanines showed promising results in PDT and PCI applications. Indeed, they could manage to prepare anionic dendrimer zinc phthalocyanine (DPc) incorporated into positively charged poly(ethylene glycol)-poly(L-lysine) (PEG-PLL) block copolymeric micelles referred to as polyion complex micelles (PIC)[180]. The substitution of large dendritic parts avoids the aggregation and increases their water solubility[181]. These micelles were tested both *in vitro* on human lung adenocarcinoma cells A549 and *in vivo* on (Balb/c nu/nu) mice bearing A549 tumors. It was shown that 7.6 times more of encapsulated DPc in micelles (DPc/m) was taken up and that these are 78 times more phototoxic *in vitro* than free DPc. In addition, subsequent *in vivo* studies confirmed the benefits of micelle encapsulation of DPc by delayed tumor growth and limited skin photosensitization.

Another interesting approach for drug delivery of hydrophobic PS is their conjugation to cyclodextrins. This strategy enables the water-solubilisation of lipophilic PS and thus its systemic administration at high concentrations. In one report, Baugh and al. proceeded to the conjugation of zinc based phthalocyanines to cyclodextrins. The double carbon bounding linkage between the dimers was cleaved, upon light activation and in presence of oxygen; resulting in the release of the Pc. Hence, this approach could be a promising systemic carrier of hydrophobic PS for photodynamic therapy[182,183].

Formulation of ZnPcs in gels or (micro)emulsions could be of interest in topical application. Indeed, several studies reported improved photophysical and aggregation properties of

ZnPcs[184,185] as well as successful delivery to the skin of sulfonated ZnPc either via simple skin penetration[184] or through iontophoresis[186].

2.3. Silicon Based Phthalocyanines: Pc 4 and its Analogues

2.3.1. SiPc-SAR

Several silicon based phthalocyanines (SiPc) mostly aiming at revealing the influence of axial ligands have been proposed and tested both *in vitro* and *in vivo*. Probably, the most famous representative of these compounds with some commercial value is "La Jolla Blue". Water-solubility of this dye absorbing at 680 nm as well as prevention of aggregation is provided by two axial polyethylene oxide moieties. Then, two peripherial carboxy groups at the macrocycle can be used for the coupling to biological molecules such as antibodies. This has been used for the design of an antibody for an FDA cleared *in vitro* immunofluorescence assay.

It has been shown by He *et al*.[187], that silicon based phthalocyanines with short aminosiloxy ligands [**49** (Pc 4) and **51**] are more phototoxic effect in Chinese hamster lung fibroblasts V79 and Murine leukemic lymphoblasts L5178Y-R as compared to compounds such as **50** and **52** with longer axial ligands (see Figure 17).

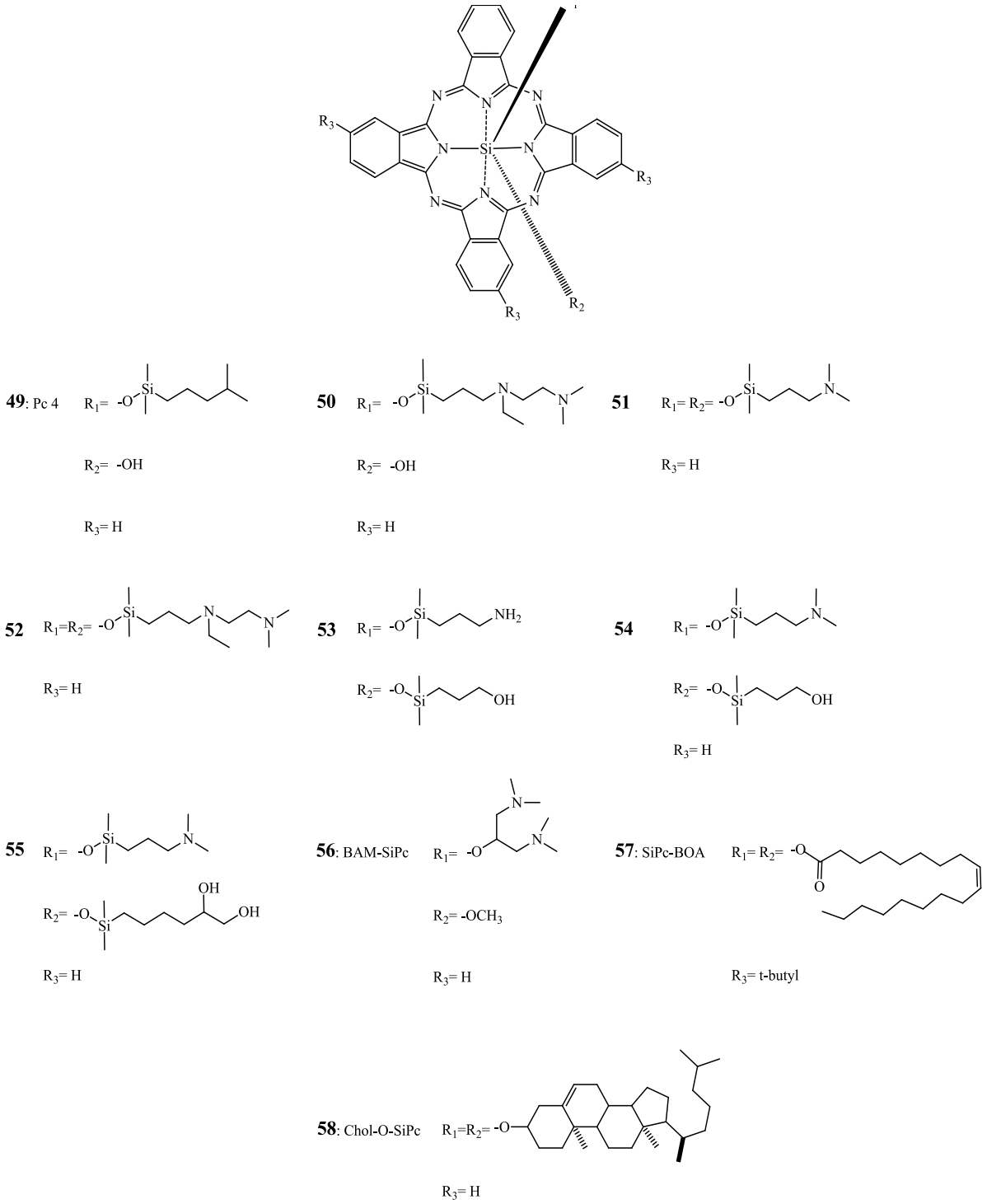

Figure 17. Chemical structure of Pc 4 (**49**) and derivatives **50–58**[187-194]

In another report[194], the PDT effects of these compounds *in vivo* on C3H/HeN mice bearing RIF-1 tumors were examined. The phthalocyanines were solubilized in a Cremophor EL emulsion and light was given 24 h post Pc injection. Except **52**, all axially substituted Si-Pc resulted in a complete remission. The authors suggested that **51**-mediated PDT may induce cellular destruction via a slower mechanism than Pc 4-mediated PDT.

In 2009, Rodriguez *et al*.[188], compared Pc 4 to compounds **51**, **53**, **54** and **55** on the human breast cancer cell line MCF-7c3. These analogues showed, among other features, higher cellular uptake and phototoxicity than Pc 4. Biaxial substitution reduced aggregation which, in turn, can explain their higher photodynamic efficiency. Furthermore, the presence of a hydroxyl group at one side seems to enhance the phototoxicity of the SiPcs. However, as shown by confocal microscopy, except for **51**, Pc 4 analogues seem to act through a different destructive pathway due to their principle association with lysosomes rather than with mitochondria/endoplasmic reticulum. Interestingly, when clonogenic assays were performed **51** and Pc 4 had a similar behavior. In contrast, **51** exhibited a 4-fold lower IC_{50} in comparison to Pc 4 (**49**) as demonstrated by means of a MTT test. Using bi-axially substituted polyamine SiPcs with fluorescence quantum yields in aqueous media of 0.12–0.21, IC_{50} ranging from 450 to 1 nM have been reported in HT29 cells by Ng and co-workers[195].

Moreover, the same group of research developed several SiPcs substituted axially with β-cyclodextrins[196-198]. They could reach a photocytotoxic effect on human colon adenocarcinoma and hepatocarcinoma cells (HT29 and HepG2 respectively) with reported IC_{50} ranging from 21 nM to 1.32 μM. In addition, early *in vivo* studies conducted by Lau *et al*.[197] show promising results as drug doses as low as 1 μmol/kg for a light dose of 30 J/cm^2 are efficient enough to suppress tumor growth in mice bearin HT29 xenografts.

Another promising approach used by the same group is the glucoconjugation of SiPcs[190,199]. In their report, Chan *et al*.[199] reported IC_{50} values as low as 6 nM on the same cell lines and could "retard tumor growth" in the same animal model.

Pc 4 has been developed at Case Western Reserve University at the beginning of the 90s. Since then Pc 4-mediated PDT has been reported effective *in vitro* against various tumor cell lines of different origin[187,200-205]. In experimental animal models for ovarian and colon cancer, no photodynamic effect was observed with doses of 0.4 mg/kg[202], whereas with doses of 0.6 or 1 mg/kg complete remission or at least significant tumor volume reduction occurred

between 3 to 7 days post-PDT. Furthermore, Pc 4-PDT was associated with a delay of tumor regrowth from 9 [203] up to 90 days[202].

A recent study conducted on immunideficient mice bearing papillomas[206] induced by the administration of cottontail rabbit papillomavirus led to the conclusion that Pc 4 at a dose of 1mg/kg and at a light dose of 150 J/cm^2 given 48 h administration resulted in complete remission in 87% of the cases with no observable re-growth during 79 days. In addition, it was suggested that the rapid destruction observed in Pc 4-mediated PDT could be explained by the mitochondrial/endoplasmic reticulum[188] localization of Pc 4 mainly leading to apoptosis and necrosis[207-209]. However in some cases vascular occlusion was also reported[188].

Moreover, Anderson *et al*.[210] demonstrated that Pc 4 exhibited less skin photosensititization as compared to Photofrin®. Topically applied, Oleinick and co-workers established that Pc 4 is "effectively delivered into the human skin"[211] and was consequently investigated clinically. In these trials, Pc 4-mediated PDT was reported to be well tolerated in patients and could have promising application in mycosis fungoides treatment[212].

Recently, Fong and coworkers reported the synthesis and characterization of several silicon-based phthalocyanines[189,213-217]. Out of this series, BAM-SiPc **56** (see Figure 17) having an IC_{50} as low as 0.015 μM on HepG2, Hep3B, HT29 and J744 was the most potent. However, this compound was phototoxic on normal liver cells (*i.e*., WRL-68 with IC_{50} of 0.035 microM under the same experimental conditions)[189,192,218]. In nude mice bearing hepatocarcinoma HepG2 and colorectal adenocarcinoma HT29 tumors the same compound showed remission/regression and tumor growth delay 15 days after PDT at a drug dose of 1μmol/kg[191].

Barge *et al*.[193] could also covalently link axial cholesterol moiety (Chol-O-SiPc) (Figure 17) and reported a seven fold higher potency of this derivative as compared to AlClPc (with IC_{50} of approximatively 8 nM) *in vitro*, on the pigmented melanoma cell lines M3Dau and SK-MEL-2.

2.3.2. SiPc Formulations

Pc 4 is the most extensively studied silicon-based phthalocyanine. Due to its insolubility in physiological media, Pc 4 tends to aggregate with subsequent loss of photodynamic activity and altered biodistribution. In order to avoid these issues, Pc 4 was incorporated in oil-based formulations, PEG-PCL (polyethylene glycol-block-poly-ε-caprolactone), micelles, and nanoparticles.

In a recent study Master *et al*.[219] were able to encapsulate with 70% efficiency Pc 4 in PEG-PCL micelles. The authors observed that in human breast cancer cells (MCF-7c3), Pc 4 delivered in PEG-PCL micelles seemed to colocalize with lysosomes and mitochondria, while Pc 4 in solution accumulated mainly in mitochondria and endoplasmic reticulum as well as in Golgi apparatus. However, no different photocytotoxic effect was observed for the two formulations.

Pc 4 was also encapsulated into silica and gold nanoparticles known for their biocompatibility and their stability[220]. Zhao *et al*.[221] showed that encapsulation into silica nanoparticles of 25–30 nm diameter lead to enhanced photodynamic activity *in vitro* as compared to the free Pc 4. Moreover, Pc 4 silica nanoparticles were found to be less sensitive to photobleaching. The reported IC_{50} values for the nanoparticluar delivery system were around 5 nM for A375 cells and 10 nM for B16F10.

An *in vivo* biodistribution study with Pc 4 adsorbed on PEG coated gold nanoparticles revealed that Pc 4 gold nanoparticles accumulated in the tumor faster than Pc 4 formulated in Cremophor EL. While the peak concentration in the tumors was only reached after 2 days using Cremophor the gold nanoparticles containing Pc 4 reached this peak within 2 h. It was also observed that the singlet oxygen yield of the two formulations was identical suggesting that the nanoparticles protect Pc 4 until its release in the target tissue[222].

Li *et al*. reported the synthesis and PDT effect of a neutral and lipophilic tetra-*t*-butyl silica phthalocyanine bisoleate referred to as SiPc-BOA (Figure 17)[223]. It was noticed that axial substitution of the oleate moieties decreased the propensity of the photosensistizer to aggregate and enabled its binding to the lipidic layer (*i.e*., LDL delivery system). Using this strategy, Li *et al*. increased the loading of the LDL nanovesicules with a molar ratio of 400 SiPc-BOA per one LDL[223]. These SiPcBOA laden nanoparticles were 10 times more effective than the free compound in HepG2 cells suggesting a LDL receptor-mediated photodynamic effect.

A multifunctional approach was proposed by Zheng *et al*.[224] through additional coupling of folic acid to lysine residues of the apolipoprotein B of the LDL part in SiPc-BOA-LDL conjugates. The validity of their hypothesis was tested in a system consisting of cells expressing the folate receptor (κB cells), those expressing the LDL receptor ($HepG_2$ cells), and cells that lack the folate receptor (HT1080, CHO cells). An interesting review of the aforementioned results could be found in the following book[225].

3. Applications of Pcs in Fluorescence Imaging

Most investigations on phthalocyanine dyes in biomedicine focus on their application in PDT for cancer. However, just recently research was also extended to parasite and bacterial disease treatment such as leishmaniosis[226-230]. Furthermore, in this context, an at least as important research area, *i.e.*, fluorescence imaging, is sometimes ignored. Fluorescence imaging allows the non-invasive detection of superficial disease in a preclinical or clinical setting. It is sensitive, can be perfomed in real time, and its resolution can be tuned to a molecular level. As few as a thousand cells can be detected by this methodology. Today, fluorescence imaging is successfully implemented in preclinical *in vitro* and *in vivo* research to specifically monitor the therapeutic outcome of new drugs in animals or to reveal disease mechanisms. Furthermore, it is used clinically for the detection of several diseases, including age-related macular degeneration[231] and cancer[232]. It has been shown to improve the detection rate of barely visible lesions, surgery and recurrence rate in malignant glioblastoma[233,234] and bladder cancer[235]. Despite the recent hype of fluorescent proteins introduced into molecular biology, exogenous fluorescent dyes[236,237] or exogenously-induced fluorescent dyes[238] still play an important role in this research area.

For optimal monitoring of diseases *in vivo* it will be advantageous that fluorescent dyes absorb and emit in the NIR region of the visble light spectrum in order to optimally penetrate into the tissue and induce only minimal autofluorescence upon excitation with light. Therefore, scientists have developed panoply of different NIR fluorescent dyes for the labeling of proteins, small bioactive peptides, or oligonucleotides[239]. Although there are many classes of NIR dyes including oxazines and rhodamines commercially available, the most commonly used belong to the class of cyanine dyes. One of these, indocyanine green, is approved for the detection of occult choroidal neovascularіuation secondary to age-related macular degeneration. Today these dyes cover an absorption spectrum ranging between 650 and 800 nm. As described above, phthalocyanine dyes can be fine-tuned to the desired absorption/emission wavelengths and can be made water-soluble[240]. Furthermore, they are chemically stable in most solvents and are not as prone to degradation in highly acidic/basic media. Some of these compounds can have a fluorescent quantum yield as high as 70% and are extremely photostable. And finally, compared to conventional cyanine dyes they have a long fluorescence lifetime and an extremely high extinction coefficient. Despite, these advantages there are only two compounds, La Jolla Blue® and IRDye 700DX®, belonging to this interesting class commercially available. Although these compounds have relatively high

fluorescence quatum yields, they can still be used as efficient photosensitizers, as demonstrated by, Mitsunaga *et al*.[58] by conjugation of IRDye 700DX® to monoclonal antibodies targeting epidermal growth factor receptors. Using these conjugates efficient killing of tumor cells was demonstrated *in vitro* and *in vivo* when NIR was used as light source.

Their tendency to aggregate seems to be ideally suited for a relatively new class of fluorescent reporters referred to as "smart probes"[241]. This approach has been pioneered by Ralph Weissleder's research group and is based on the selfquenching/dequenching paradigm[242]. In these compounds, typically several fluorescent dyes are coupled either directly or via chemically or enzymatically labile linker to a polymeric carrier. In their native state these reporters are optically silent due selfquenching of the fluorescent dyes. However, as soon as a chemical or enzymatic trigger results in the release of the fluorescent dye from its polymeric carrier this selfquenching is abrogated. Today, this methodology has been extensively used for the detection of proteolytic activity *in vivo*. One can deduce from the discussions on the photodynamic activity of aggregated Pc above, that these compounds can also be used in "smart probes" with a better selfquenching allowing the use of low molecular weight carriers with improved pharmacokinetics. Another phenomenon of aggregated Pc, will further favor their use in "smart probes". As the extinction coefficient of the Q-band undergoes significant reduction in the aggregated form, these fluorescence reporters not only show reduced fluorescence intensities in the non-activated form but also are less sensitive to excitation. Furthermore, due to their lipophilicity, once cleaved, Pc dyes will stay longer at the activation site due to reduced clearance. Currently, we are evaluating this approach for simultaneously treating and monitoring diseases with Pc-based polymeric photosensitizer prodrugs[243-245].

4. Conclusions

Throughout this review, it has been shown that phthalocyanines are promising photosensitizers for photodynamic therapy applications. Some of them are even currently used in PDT (*e.g.*, Photosens®) or tested in clinical trials (*e.g.*, Pc 4). At a chemical level, it is concluded that Pcs' mainly amphiphilic character leads to a higher efficiency *in vivo*. In addition, hampering their stacking via axial ligation and including positive charge(s) seems to influence their photocytotoxicity, by increasing their cellular uptake and internalization. It is also of major importance to consider their subsequent cellular (re)localization in order to understand and evaluate their photodynamic activity. Hence, by only considering their chemistry, phthalocyanines exhibit this flexibility, enabling further screening and

investigations, which rises hope for cancer treatment. Perspectives such as chemical coupling of two photosensitizers as well as screening of new phthalocyanines are currently examined and could be interesting prospects for PDT cancer treatment[246-249].

From a pharmaceutical point of view, suitable and optimal formulations of Pcs can increase dramatically the therapeutic efficacy. Suitable drug delivery systems can act as a solubilizing matrix for the PS as well as a shield and protection from degradation.

Acknowledgements

NL research is supported by the Swiss Science Foundation grants #205320-122144, #326030-117436, #CR32I3-129987, #205321-126834, #310030-119938, and #K-32K1-116460. TN and NL are grateful for the financial support of grant #IZLSZ2-123011 and Council for Scientific and Industrial Research in South Africa promoting the collaboration between South African and Swiss scientists.

References:

1. McKeown, N.B. The Synthesis of Symmetrical Phthalocyanines. In The Porphyrin Handbook; Kadish, K.M., Smith, K.M., Guilard, R., Eds.; Academic Press: San Diego, CA, USA, 2003; pp. 61-124.

2. Thomas, A.L. Phthalocyanine Research and Applications; CRC Press: Baton Rouge, FL, USA, 1990; p. 2.

3. McKeown, N.B. An Introduction to the Phthalocyanines. In Phthalocyanine Materials: Synthesis, Structure and Function; McKeown, N.B., Ed.; Cambridge University Press: Cambridge, UK, 1998; pp. 1-10.

4. Geng,Y.Y.; Gu, D.H.; Wu, Y.Q.; Gan,F.X. High speed recording property of phthalocyanine thin film for compact disc recordable. Proc. SPIE Int. Soc. Opt. Eng. 2003, 63, 63-66.

5. Petritsch, K.; Friend, R.H.; Lux, A.; Rozenberg, G.; Moratti, S.C.; Holmes, A.B. Liquid crystalline phthalocyanines in organic solar cells. Synth. Met. 1999, 102, 1776-1777.

6. Nyokong, T.; Vilakazi, S. Phthalocyanines and related complexes as electrocatalysts for the detection of nitric oxide. Talanta 2003, 61, 27-35.

7. Ali, H.; van Lier, J.E. Porphyrins and phthalocyanines as photosensitizers and radiosensitizers.
In Handbook of Porphyrin Science with Applications to Chemistry, Physics, Materials Science, Engineering, Biology and Medecine; Kadish, K.M., Smith, K.M., Guilard, R., Eds.; World Scientific: Singapore, 2010; pp. 1-119.

8. Alonso, C.; Boyle, R.W. Bioconjugates of porphyrins and related molecules for photodynamic Therapy. In Handbook of Porphyrin Science with Applications to Chemistry, Physics, Materials Science, Engineering, Biology and Medecine; Kadish, K.M., Smith, K.M., Guilard, R., Eds.; World Scientific: Singapore, 2010; pp. 121-190.

9. Ethirajan, M.; Patel, N.J.; Pandey, R.K. Porphyrin-based multifunctional agents for tumor-imaging and photodynamic therapy (PDT). In Handbook of Porphyrin Science with Applications to Chemistry, Physics, Materials Science, Engineering, Biology and Medecine; Kadish, K.M., Smith, K.M., Guilard, R., Eds.; World Scientific: Singapore, 2010; pp. 249-323.

10. Jux, N.; Röder, B. Targeting Strategies for Tetrapyrrole-Based Photodynamic Therapy. In Handbook of Porphyrin Science with Applications to Chemistry, Physics, Materials Science, Engineering, Biology and Medecine. Kadish, K.M., Smith, K.M., Guilard, R., Eds.; World Scientific: Singapore, 2010; pp. 325-401.

11. Nyokong, T.; Antunes, E. Photochemical and photophysical properties of metallophthalocyanines. In Handbook of Porphyrin Science with Applications to Chemistry, Physics, Materials Science, Engineering, Biology and Medecine; Kadish, K.M., Smith, K.M., Guilard, R., Eds; World Scientific: Singapore, 2010; pp. 247-349.

12. Fukuda, T.; Kobayashi, N. UV-visible absorption spectroscopic properties of phthalocyanines and related macrocycles. In Handbook of Porphyrin Science with Applications to Chemistry, Physics, Materials Science, Engineering, Biology and Medecine; Kadish, K.M., Smith, K.M., Guilard, R., Eds.; World Scientific: Singapore, 2010; pp. 1-645.

13. Dietze, A.; Peng, Q.; Selbo, P.K.; Kaalhus, O.; Muller, C.; Bown, S.; Berg, K. Enhanced photodynamic destruction of a transplantable fibrosarcoma using photochemical internalisation of gelonin. Br. J. Cancer 2005, 92, 2004-2009.

14. Selbo, P.K.; Sivam, G.; Fodstad, O.; Sandvig, K.; Berg, K. *In vivo* documentation of photochemical internalization, a novel approach to site specific cancer therapy. Int. J. Cancer 2001, 92, 761-766.

15. Adigbli, D.K.; Wilson, D.G.; Farooqui, N.; Sousi, E.; Risley, P.; Taylor, I.; Macrobert, A.J.; Loizidou, M. Photochemical internalisation of chemotherapy potentiates killing of multidrug-resistant breast and bladder cancer cells. Br. J. Cancer 2007, 97, 502-512.

16. Norum, O.J.; Selbo, P.K.; Weyergang, A.; Giercksky, K.E.; Berg, K. Photochemical internalization (PCI) in cancer therapy: From bench towards bedside medicine. J. Photochem. Photobiol. B 2009, 96, 83-92.

17. Norum, O.J.; Bruland, O.S.; Gorunova, L.; Berg, K. Photochemical internalization of bleomycin before external-beam radiotherapy improves locoregional control in a human sarcoma model.
Int. J. Radiat. Oncol. Biol. Phys. 2009, 75, 878-885.

18. Norum, O.J.; Giercksky, K.E.; Berg, K. Photochemical internalization as an adjunct to marginal surgery in a human sarcoma model. Photochem. Photobiol. Sci. 2009, 8, 758-762.

19. Prasmickaite, L.; Hogset, A.; Selbo, P.K.; Engesaeter, B.O.; Hellum, M.; Berg, K. Photochemical disruption of endocytic vesicles before delivery of drugs: A new strategy for cancer therapy. Br. J. Cancer 2002, 86, 652-657.

20. Hogset, A.; Prasmickaite, L.; Selbo, P.K.; Hellum, M.; Engesaeter, B.O.; Bonsted, A.; Berg, K. Photochemical internalisation in drug and gene delivery. Adv. Drug Deliv. Rev. 2004, 56, 95-115.

21. Ben-Hur, E.; Rosenthal, I. The phthalocyanines: A new class of mammalian cells photosensitizers with a potential for cancer phototherapy. Int. J. Radiat. Biol. Relat. Stud. Phys. Chem. Med. 1985, 47, 145-147.

22. Brasseur, N.; Ali, H.; Autenrieth, D.; Langlois, R.; van Lier, J.E. Biological activities of phthalocyanines-III. Photoinactivation of V-79 Chinese hamster cells by tetrasulfophthalocyanines. Photochem. Photobiol. 1985, 42, 515-521.

23. Ackroyd, R.; Kelty, C.; Brown, N.; Reed, M. The history of photodetection and photodynamic therapy. Photochem. Photobiol. 2001, 74, 656-669.

24. Dolmans, D.E.; Fukumura, D.; Jain, R.K. Photodynamic therapy for cancer. Nat. Rev. Cancer 2003, 3, 380-387.

25. Sharman, W.M.; Allen, C.M.; van Lier, J.E. Photodynamic therapeutics: Basic principles and clinical applications. Drug Discov. Today 1999, 4, 507-517.

26. Allen, C.M.; Langlois, R.; Sharman, W.M.; La, M.C.; van Lier, J.E. Photodynamic properties of amphiphilic derivatives of aluminum tetrasulfophthalocyanine. Photochem. Photobiol. 2002, 76, 208-216.

27. Brown, S.B.; Brown, J.E.; Vernon, D.I. Photosensitising drugs—Their potential in oncology. Expert Opin. Invest. Drugs 1999, 8, 1967-1979.

28. Allison, R.R. Photosenitizers in clinical PDT. Photodiag. Photod. Ther. 2004, 1, 27-42.

29. Lange, N. Controlled drug delivery in photodynamic therapy and fluorescence-based diagnosis of cancer. In Handbook of Biomedical Fluorescence; Mary-Ann, M., Brian, W.P., Eds.; CRC Press: Boca Raton, FL, USA, 2003; pp. 563-635.

30. Josefsen, L.B.; Boyle, R.W. Photodynamic therapy and the development of metal-based photosensitisers. Met. Based Drugs 2008, 2008, 1-24.

31. Ethirajan, M.; Saenz, C.; Gupta, A.; Dobhal, M.P.; Pandey, R.K. Photosensitizers for photodynamic therapy and imaging. In Advances in Photodynamic Therapy: Basic, Translational, and Clinical. Michael, R.H., Pawel, M., Eds.; Artech House: Boston, MA, 2008; pp. 13-39.

32. Stolik, S.; Delgado, J.A.; Perez, A.; Anasagasti, L. Measurement of the penetration depths of red and near infrared light in human "ex vivo" tissues. J. Photochem. Photobiol. B 2000, 57, 90-93.

33. Sevick-Muraca, E.M.; Godavarty, A.; Houston, J.P.; Thompson, A.B.; Roy, R. Near-infrared imaging with fluorescent contrast agents. In Handbook of Biomedical Fluorescence; Mycek, M.-A., Pogue, B.W., Eds.; CRC Press: Boca Raton, FL, USA, 2003; pp. 445-527.

34. MacDonald, I.J.; Dougherty, T.J. Basic principles of photodynamic therapy. J. Porphyr. Phthalocya. 2001, 5, 105-129.

35. Lang, K.; Mosinger, J.; Wagnerova, D.M. Photophysical properties of porphyrinoid sensitizers non-covalently bound to host molecules, models for photodynamic therapy. Coord. Chem. Rev. 2004, 248, 321-350.

36. Jori, G. Far-red-absorbing photosensitizers—Their use in the photodynamic therapy of tumors. J. Photochem. Photobiol. A 1992, 62, 371-378.

37. Haddad, R.; Blumenfeld, A.; Siegal, A.; Kaplan, O.; Cohen, M.; Skornick, Y.; Kashtan, H. *In vitro* and *in vivo* effects of photodynamic therapy on murine malignant melanoma. Ann. Surg. Oncol. 1998, 5, 241-247.

38. Boyle, R.W.; Dolphin, D. Structure and biodistribution relationships of photodynamic sensitizers. Photochem. Photobiol. 1996, 64, 469-485.

39. Bonnett, R. Photosensitizers of the porphyrin and phthalocyanine series for photodynamic therapy. Chem. Soc. Rev. 1995, 24, 19-33.

40. Brasseur, N.; Menard, I.; Forget, A.; El Jastimi, R.; Hamel, R.; Molfino, N.A.; van Lier, J.E. Eradication of multiple myeloma and breast cancer cells by TH9402-mediated photodynamic therapy: Implication for clinical ex vivo purging of autologous stem cell transplants. Photochem. Photobiol. 2000, 72, 780-787.

41. Brown, S.B.; Brown, E.A.; Walker, I. The present and future role of photodynamic therapy in cancer treatment. Lancet Oncol. 2004, 5, 497-508.

42. Ferreira, J.; Menezes, P.F.C.; Kurachi, C.; Sibata, C.H.; Allison, R.R.; Bagnato, V.S. Comparative study of photodegradation of three hematoporphyrin derivative: Photofrin (R), Photogem (R) and Photosan. Laser Phys. Lett. 2007, 4, 743-748.

43. Fickweiler, S.; Abels, C.; Karrer, S.; Baumler, W.; Landthaler, M.; Hofstadter, F.; Szeimies, R.M. Photosensitization of human skin cell lines by ATMPn (9-acetoxy-2,7,12,17-tetrakis-(beta-methoxyethyl)-porphycene) *in vitro*: Mechanism of action. J. Photochem. Photobiol. B 1999, 48, 27-35.

44. Jori, G. Tumour photosensitizers: Approaches to enhance the selectivity and efficiency of photodynamic therapy. J. Photochem. Photobiol. B 1996, 36, 87-93.

45. Karrer, S.; Abels, C.; Szeimies, R.M.; Baumler, W.; Dellian, M.; Hohenleutner, U.; Goetz, A.E.; Landthaler, M. Topical application of a first porphycene dye for photodynamic therapy—Penetration studies in human perilesional skin and basal cell carcinoma. Arch. Dermatol. Res. 1997, 289, 132-137.

46. Mathai, S.; Bird, D.K.; Stylli, S.S.; Smith, T.A.; Ghiggino, K.P. Two-photon absorption cross-sections and time-resolved fluorescence imaging using porphyrin photosensitisers. Photochem. Photobiol. Sci. 2007, 6, 1019-1026.

47. Mody, T.D. Pharmaceutical development and medical applications of porphyrin-type macrocycles. J. Porphyr. Phthalocya. 2000, 4, 362-367.

48. Nyman, E.S.; Hynninen, P.H. Research advances in the use of tetrapyrrolic photosensitizers for photodynamic therapy. J. Photochem. Photobiol. B 2004, 73, 1-28.

49. Ochsner, M. Light scattering of human skin: A comparison between zinc(II)-phthalocyanine and Photofrin II(R). J. Photochem. Photobiol. B 1996, 32, 3-9.

50. Palumbo, G. Photodynamic therapy and cancer: A brief sightseeing tour. Expert Opin. Drug Del 2007, 4, 131-148.

51. Rosenthal, M.A.; Kavar, B.; Hill, J.S.; Morgan, D.J.; Nation, R.L.; Stylli, S.S.; Basser, R.L.; Uren, S.; Geldard, H.; Green, M.D.; et al. Phase I and pharmacokinetic study of photodynamic therapy for high-grade gliomas using a novel boronated porphyrin. J. Clin. Oncol. 2001, 19, 519-524.

52. Usuda, J.; Kato, H.; Okunaka, T.; Furukawa, K.; Tsutsui, H.; Yamada, K.; Suga, Y.; Honda, H.; Nagatsuka, Y.; Ohira, T.; et al. Photodynamic therapy (PDT) for lung cancers. J. Thorac. Oncol. 2006, 1, 489-493.

53. Ogunsipe, A.; Nyokong, T. Photophysicochemical consequences of bovine serum albumin binding to non-transition metal phthalocyanine sulfonates. Photochem. Photobiol. Sci. 2005, 4, 510-516.

54. Huang, J.D.; Wang, S.; Lo, P.C.; Fong, W.P.; Ko, W.H.; Ng, D.K.P. Halogenated silicon(iv) phthalocyanines with axial poly(ethylene glycol) chains. Synthesis, spectroscopic properties, complexation with bovine serum albumin and *in vitro* photodynamic activities. New J. Chem. 2004, 28, 348-354.

55. Chen, X.L.; Li, D.H.; Zhu, Q.Z.; Yang, H.H.; Zheng, H.; Wang, Z.H., Xu, J.G. Determination of proteins at nanogram levels by a resonance light-scattering technique with tetra-substituted sulphonated aluminum phthalocyanine. Talanta 2001, 53, 1205-1210.

56. Vrouenraets, M.B.; Visser, G.W.; Stigter, M.; Oppelaar, H.; Snow, G.B.; van Dongen, G.A. Targeting of aluminum (III) phthalocyanine tetrasulfonate by use of internalizing monoclonal antibodies: Improved efficacy in photodynamic therapy. Cancer Res. 2001, 61, 1970-1975.

57. Peng, X.; Draney, D.R.; Volcheck, W.M.; Bashford, G.R.; Lamb, D.T.; Zhang, Y.; Johnson, C.M. Phthalocyanine dye as an extremely photostable and highly fluorescent near-infrared labeling reagent. Proc. SPIE Int. Soc. Opt. Eng. 2006, 6097, 60970E.

58. Mitsunaga, M.; Ogawa, M.; Kosaka, N.; Rosenblum, L.T.; Choyke, P.L.; Kobayashi, H. Cancer cell-selective *in vivo* near infrared photoimmunotherapy targeting specific membrane molecules. Nat. Med. 2011,17, 1685-91

59. Duan, W.; Smith, K.; Savoie, H.; Greenman, J.; Boyle, R.W. Near IR emitting isothiocyanato-substituted fluorophores: Their synthesis and bioconjugation to monoclonal antibodies. Org. Biomol. Chem. 2005, 3, 2384-2386.

60. Carcenac, M.; Dorvillius, M.; Garambois, V.; Glaussel, F.; Larroque, C.; Langlois, R.; Hynes, N.E.; van Lier, J.E.; Pelegrin, A. Internalisation enhances photo-induced cytotoxicity of monoclonal antibody-phthalocyanine conjugates. Br. J. Cancer 2001, 85, 1787-1793.

61. Devlin, R.; Studholme, R.M.; Dandliker, W.B.; Fahy, E.; Blumeyer, K.; Ghosh, S.S. Homogeneous detection of nucleic acids by transient-state polarized fluorescence. Clin. Chem. 1993, 39, 1939-1943.

62. Hammer, R.P.; Owens, C.V.; Hwang, S.H.; Sayes, C.M.; Soper, S.A. Asymmetrical, water-soluble phthalocyanine dyes for covalent labeling of oligonucleotides. Bioconjug. Chem. 2002, 13, 1244-1252.

63. Koval, V.V.; Chernonosov, A.A.; Abramova, T.V.; Ivanova, T.M.; Fedorova, O.S.; Derkacheva, V.M.; Lukyanets, E.A. Photosensitized and catalytic oxidation of DNA by metallophthalocyanine-oligonucleotide conjugates. Nucleos. Nucleot. Nucl. 2001, 20, 1259-1262.

64. Nesterova, I.V.; Verdree, V.T.; Pakhomov, S.; Strickler, K.L.; Allen, M.W.; Hammer, R.P.; Soper, S.A. Metallo-phthalocyanine near-IR fluorophores: oligonucleotide conjugates and their applications in PCR assays. Bioconjug. Chem. 2007, 18, 2159-2168.

65. Walker, G.T.; Fraiser, M.S.; Schram, J.L.; Little, M.C.; Nadeau, J.G.; Malinowski, D.P. Strand displacement amplification—An isothermal, *in vitro* DNA amplification technique. Nucleic Acids Res. 1992, 20, 1691-1696.

66. Rio, Y.; Rodriguez-Morgade, M.S.; Torres, T. Modulating the electronic properties of porphyrinoids: A voyage from the violet to the infrared regions of the electromagnetic spectrum. Org. Biomol. Chem. 2008, 6, 1877-1894.

67. Ali, H.; van Lier, J.E. Metal complexes as photo- and radiosensitizers. Chem. Rev. 1999, 99, 2379-2450.

68. Claessens, C.G.; Blau, W.J.; Cook, M.; Hanack, M.; Nolte, R.J.M.; Torres, T.; Whörle, D. Phthalocyanines and phthalocyanine analogues: The quest for applicable optical properties. Monatsh. Chem./Chem. Monthly 2001, 132, 3-11.

69. Nyokong, T.; Isago, H. The renaissance in optical spectroscopy of phthalocyanines and other tetraazaporphyrins. J. Porphyr. Phthalocya. 2004, 8, 1083-1090.

70. Foley, M.S.; Beeby, A.; Parker, A.W.; Bishop, S.M.; Phillips, D. Excited triplet state photophysics of the sulphonated aluminium phthalocyanines bound to human serum albumin. J. Photochem. Photobiol. B 1997, 38, 10-17.

71. Feofanov, A.; Grichine, A.; Karmakova, T.; Kazachkina, N.; Pecherskih, E.; Yakubovskaya, R.; Luk'yanets, E.; Derkacheva, V.; Egret-Charlier, M.; Vigny, P. Chelation with metal is not essential for antitumor photodynamic activity of sulfonated phthalocyanines. Photochem. Photobiol. 2002, 75, 527-533.

72. Karmakova, T.; Feofanov, A.; Nazarova, A.; Grichine, A.; Yakubovskaya, R.; Luk'yanets, E.; Maurizot, J.C.; Vigny, P. Distribution of metal-free sulfonated phthalocyanine in subcutaneously transplanted murine tumors. J. Photochem. Photobiol. B 2004, 75, 81-87.

73. Kolarova, H.; Nevrelova, P.; Bajgar, R.; Jirova, D.; Kejlova, K.; Strnad, M. *In vitro* photodynamic therapy on melanoma cell lines with phthalocyanine. Toxicol. *In vitro* 2007, 21, 249-253.

74. Ward, A.J.; Matthews, E.K. Cytotoxic, nuclear, and growth inhibitory effects of photodynamic drugs on pancreatic carcinoma cells. Cancer Lett. 1996, 102, 39-47.

75. Glassberg, E.; Lewandowski, L.; Lask, G.; Uitto, J. Laser-induced photodynamic therapy with aluminum phthalocyanine tetrasulfonate as the photosensitizer: differential phototoxicity in normal and malignant human cells *in vitro*. J. Invest. Dermatol. 1990, 94, 604-610.

76. Tralau, C.J.; Macrobert, A.J.; Coleridge-Smith, P.D.; Barr, H.; Bown, S.G. Photodynamic therapy with phthalocyanine sensitisation: Quantitative studies in a transplantable rat fibrosarcoma. Br. J. Cancer 1987, 55, 389-395.

77. Chan, W.S.; Marshall, J.F.; Svensen, R.; Bedwell, J.; Hart, I.R. Effect of sulfonation on the cell and tissue distribution of the photosensitizer aluminum phthalocyanine. Cancer Res. 1990, 50, 4533-4538.

78. Chan, W.S.; West, C.M.; Moore, J.V.; Hart, I.R. Photocytotoxic efficacy of sulphonated species of aluminium phthalocyanine against cell monolayers, multicellular spheroids and *in vivo* tumours. Br. J. Cancer 1991, 64, 827-832.

79. Chan, W.S.; Brasseur, N.; La, M.C.; Ouellet, R.; van Lier, J.E. Efficacy and mechanism of aluminium phthalocyanine and its sulphonated derivatives mediated photodynamic therapy on murine tumours. Eur. J. Cancer 1997, 33, 1855-1859.

80. Stylli, S.S.; Hill, J.; Sawyer, W.; Kaye, A. Aluminium phthalocyanine mediated photodynamic therapy in experimental malignant glioma. J. Clin. Neurosci. 1995, 2, 146-151.

81. Stylli, S.S.; Hill, J.S.; Sawyer, W.H.; Kaye, A.H. Phthalocyanine photosensitizers for the treatment of brain tumours. J. Clin. Neurosci. 1995, 2, 64-72.

82. Sandeman, D.R.; Bradford, R.; Buxton, P.; Bown, S.G.; Thomas, D.G. Selective necrosis of malignant gliomas in mice using photodynamic therapy. Br. J. Cancer 1987, 55, 647-649.

83. Peng, Q.; Moan, J. Correlation of distribution of sulphonated aluminium phthalocyanines with their photodynamic effect in tumour and skin of mice bearing CaD2 mammary carcinoma. Br. J. Cancer 1995, 72, 565-574.

84. Paquette, B.; Ali, H.; Langlois, R.; van Lier, J.E. Biological activities of phthalocyanines-VIII. Cellular distribution in V-79 Chinese hamster cells and phototoxicity of selectively sulfonated aluminum phthalocyanines. Photochem. Photobiol. 1988, 47, 215-220.

85. Mathews, M.S.; Chighvinadze, D.; Gach, H.M.; Uzal, F.A.; Madsen, S.J.; Hirschberg, H. Cerebral edema following photodynamic therapy using endogenous and exogenous photosensitizers in normal brain. Lasers Surg. Med. 2011, 43, 892-900.

86. Gupta, S.; Dwarakanath, B.S.; Chaudhury, N.K.; Mishra, A.K.; Muralidhar, K.; Jain, V. *In vitro* and *in vivo* targeted delivery of photosensitizers to the tumor cells for enhanced photodynamic effects. J. Cancer Res. Ther. 2011, 7, 314-324.

87. Lagoda, T.S.; Kaplan, M.A.; Krivosheev, I.; Zhavoronkov, L.P.; Bokova, M.B. The optimization of a plan for the photodynamic therapy of sarcoma M1 using photosens. Vopr.Onkol. 2000, 46, 327-331.

88. Budzinskaia, M.V.; Likhvantseva, V.G.; Shevxchik, S.A.; Loshchenov, V.B.; Kuz'min, S.G.; Vorozhtsov, G.N. Experimental assessment of the capacities of use of photosense. Communication 2. Photodynamic therapy for epibulbar and choroid tumors. Vestn. Oftalmol. 2005, 121, 17-19.

89. Likhvantseva, V.G.; Osipova, E.A.; Petrenko, M.A.; Merzliakova, O.I.; Kuz'min, S.G.; Vorozhtsov, G.N. Analysis of changes in the accumulation of the photosensitizer Photosens, its elimination kinetics and distribution in the tissues of the eye and eyelids in health and in some tumorous processes. Vestn.Oftalmol. 2008, 124, 38-44.

90. Apolikhin, O.I. Adjuvant photodynamic therapy (PDT) with photosensitizer photosens for superficial bladder cancer. Experimental investigations to treat prostate cancer by PDT with photosens. Soc. Photo-Opt. Instrum. 2007, 8. 45.

91. Trushina, O.I.; Novikova, E.G.; Sokolov, V.V.; Filonenko, E.V.; Chissov, V.I.; Vorozhtsov, G.N. Photodynamic therapy of virus-associated precancer and early stages cancer of cervix uteri. Photodiagn. Photodyn. Ther. 2008, 5, 256-259.

92. Carcenac, M.; Larroque, C.; Langlois, R.; van Lier, J.E.; Artus, J.C.; Pelegrin, A. Preparation, phototoxicity and biodistribution studies of anti-carcinoembryonic antigen monoclonal antibody-phthalocyanine conjugates. Photochem. Photobiol. 1999, 70, 930-936.

93. Vrouenraets, M.B.; Visser, G.W.; Stigter, M.; Oppelaar, H.; Snow, G.B.; van Dongen, G.A. Comparison of aluminium (III) phthalocyanine tetrasulfonate- and meta-tetrahydroxyphenylchlorin-monoclonal antibody conjugates for their efficacy in photodynamic therapy *in vitro*. Int. J. Cancer 2002, 98, 793-798.

94. Vrouenraets, M.B.; Visser, G.W.; Loup, C.; Meunier, B.; Stigter, M.; Oppelaar, H.; Stewart, F.A.; Snow, G.B.; van Dongen, G.A. Targeting of a hydrophilic photosensitizer by use of internalizing monoclonal antibodies: A new possibility for use in photodynamic therapy. Int. J. Cancer 2000, 88, 108-114.

95. Gueddari, N.; Favre, G.; Hachem, H.; Marek, E., Le, G.F.; Soula, G. Evidence for up-regulated low density lipoprotein receptor in human lung adenocarcinoma cell line A549. Biochimie 1993, 75, 811-819.

96. Urizzi, P.; Allen, C.M.; Langlois, R.; Ouellet, R.; La Madeleine, C.; van Lier, J.E. Low-density lipoprotein-bound aluminum sulfophthalocyanine: Targeting tumor cells for photodynamic therapy. J. Porphyr. Phthalocya. 2001, 5, 154-160.

97. Xiao, D.; Wang, J.; Hampton, L.L.; Weber, H.C. The human gastrin-releasing peptide receptor gene structure, its tissue expression and promoter. Gene 2001, 264, 95-103.

98. Yegen, B.C. Bombesin-like peptides: Candidates as diagnostic and therapeutic tools. Curr. Pharm. Des. 2003, 9, 1013-1022.

99. Dubuc, C.; Langlois, R.; Benard, F.; Cauchon, N.; Klarskov, K.; Tone, P.; van Lier, J.E. Targeting gastrin-releasing peptide receptors of prostate cancer cells for photodynamic therapy with a phthalocyanine-bombesin conjugate. Bioorg. Med. Chem. Lett. 2008, 18, 2424-2427.

100. Gijsens, A.; Derycke, A.; Missiaen, L.; De, V.D.; Huwyler, J.; Eberle, A.; De, W.P. Targeting of the photocytotoxic compound AlPcS4 to Hela cells by transferrin conjugated PEG-liposomes. Int. J. Cancer 2002, 101, 78-85.

101. Derycke, A.S.; Kamuhabwa, A.; Gijsens, A.; Roskams, T.; De, V.D.; Kasran, A.; Huwyler, J.; Missiaen, L.; de Witte, P.A. Transferrin-conjugated liposome targeting of photosensitizer AlPcS4 to rat bladder carcinoma cells. J. Natl. Cancer Inst. 2004, 96, 1620-1630.

102. Bridges, K.R.; Smith, B.R. Discordance between transferrin receptor expression and susceptibility to lysis by natural-killer cells. J. Clin. Invest. 1985, 76, 913-918.

103. Qualls, M.M.; Thompson, D.H. Chloroaluminum phthalocyanine tetrasulfonate delivered via acid-labile diplasmenylcholine-folate liposomes: Intracellular localization and synergistic phototoxicity. Int. J. Cancer 2001, 93, 384-392.

104. Morgan, J.; Gray, A.G.; Huehns, E.R. Specific targeting and toxicity of sulphonated aluminium phthalocyanine photosensitised liposomes directed to cells by monoclonal antibody *in vitro*. Br. J. Cancer 1989, 59, 366-370.

105. Ben-Hur, E.; Rosenthal, I. Photosensitization of Chinese hamster cells by water-soluble phthalocyanines. Photochem. Photobiol. 1986, 43, 615-619.

106. Decreau, R.; Richard, M.J.; Julliard, M. Photodynamic therapy against achromic M6 melanocytes: Phototoxicity of lipophilic axially substituted aluminum phthalocyanines and hexadecahalogenated zinc phthalocyanines. J. Porphyr. Phthalocya. 2001, 5, 390-396.

107. Brasseur, N.; Ouellet, R.; La, M.C.; van Lier, J.E. Water-soluble aluminium phthalocyanine-polymer conjugates for PDT: Photodynamic activities and pharmacokinetics in tumour-bearing mice. Br. J. Cancer 1999, 80, 1533-1541.

108. Dye, D.; Watkins, J. Suspected anaphylactic reaction to cremophor El. Brit. Med. J. 1980, 280, 1353.

109. Torchilin, V.P. Cell penetrating peptide-modified pharmaceutical nanocarriers for intracellular drug and gene delivery. Biopolymers 2008, 90, 604-610.

110. van Nostrum, C.F. Polymeric micelles to deliver photosensitizers for photodynamic therapy.
Adv. Drug Delivery Rev. 2004, 56, 9-16.

111. Iyer, A.K.; Khaled, G.; Fang, J.; Maeda, H. Exploiting the enhanced permeability and retention effect for tumor targeting. Drug Discov. Today 2006, 11, 812-818.

112. Matsumura, Y.; Maeda, H. A new concept for macromolecular therapeutics in cancer-chemotherapy—Mechanism of tumoritropic accumulation of proteins and the antitumor agent Smancs. Cancer Res. 1986, 46, 6387-6392.

113. Oerlemans, C.; Bult, W.; Bos, M.; Storm, G.; Nijsen, J.F.W.; Hennink, W.E. Polymeric micelles in anticancer therapy: Targeting, imaging and triggered release. Pharm. Res. 2010, 27, 2569-2589.

114. Taillefer, J.; Jones, M.C.; Brasseur, N.; van Lier, J.E.; Leroux, J.C. Preparation and characterization of pH-responsive polymeric micelles for the delivery of photosensitizing anticancer drugs. J. Pharm. Sci. 2000, 89, 52-62.

115. Taillefer, J.; Brasseur, N.; van Lier, J.E.; Lenaerts, V.; Le, G.D.; Leroux, J.C. In-vitro and in-vivo evaluation of pH-responsive polymeric micelles in a photodynamic cancer therapy model. J. Pharm. Pharmacol. 2001, 53, 155-166.

116. Le, G.D.; Taillefer, J.; van Lier, J.E.; Lenaerts, V.; Leroux, J.C. Optimizing pH-responsive polymeric micelles for drug delivery in a cancer photodynamic therapy model. J. Drug Target 2002, 10, 429-437.

117. Williams, A.C.; Barry, B.W. Penetration enhancers. Adv. Drug Delivery Rev. 2004, 56, 603-618.

118. Kyriazi, M.; Alexandratou, E.; Yova, D.; Rallis, M.; Trebst, T. Topical photodynamic therapy of murine non-melanoma skin carcinomas with aluminum phthalocyanine chloride and a diode laser: Pharmacokinetics, tumor response and cosmetic outcomes. Photodermatol. Photoimmunol. Photomed. 2008, 24, 87-94.

119. Robinson, D.J.; de Bruijn, H.S.; van der Veen, N.; Stringer, M.R.; Brown, S.B.; Star, W.M. Fluorescence photobleaching of ALA-induced protoporphyrin IX during photodynamic therapy of normal hairless mouse skin: The effect of light dose and irradiance and the resulting biological effect. Photochem. Photobiol. 1998, 67, 140-149.

120. Kruijt, B.; van der Ploeg-van den Heuvel; de Bruijn, H.S.; Sterenborg, H.J.; Amelink, A.; Robinson, D.J. Monitoring interstitial m-THPC-PDT *in vivo* using fluorescence and reflectance spectroscopy. Lasers Surg. Med. 2009, 41, 653-664.

121. Wohrle, D.; Hirth, A.; Bogdahn-Rai, T.; Schnurpfeil, G.; Shopova, M. Photodynamic therapy of cancer: second and third generations of photosensitizers. Russ. Chem. Bull. 1998, 47, 807-816.

122. Kudrevich, S.; Brasseur, N.; La, M.C.; Gilbert, S.; van Lier, J.E. Syntheses and photodynamic activities of novel trisulfonated zinc phthalocyanine derivatives. J. Med. Chem. 1997, 40, 3897-3904.

123. Cauchon, N.; Tian, H.; Langlois, R.; La, M.C.; Martin, S.; Ali, H.; Hunting, D.; van Lier, J.E. Structure-photodynamic activity relationships of substituted zinc trisulfophthalocyanines. Bioconjug. Chem. 2005, 16, 80-89.

124. Potter, W.R.; Henderson, B.W.; Bellnier, D.A.; Pandey, R.K.; Vaughan, L.A.; Weishaupt, K.R.; Dougherty, T.J. Parabolic quantitative structure-activity relationships and photodynamic therapy: Application of a three-compartment model with clearance to the *in vivo* quantitative structure-activity relationships of a congeneric series of pyropheophorbide derivatives used as photosensitizers for photodynamic therapy. Photochem. Photobiol. 1999, 70, 781-788.

125. Liu, E.S.; Dai, Z.F.; Huang, J.D.; Chen, N.S.; Huang, J.L.; Huang, Z.Q.; Sun, J.C. Syntheses of metal phthalocyanines and their photoinactivations on cancer cells. Acta Biochim. Bioph. Sin. 1998, 30, 31-34.

126. Huang, J.L.; Chen, N.S.; Huang, J.D.; Liu, E.S.; Xue, J.P.; Yang, S.L.; Huang, Z.Q.; Sun, J.C. Metal phthalocyanine as photosensitizer for photodynamic therapy (PDT)—Preparation, characterization and anticancer activities of an amphiphilic phthalocyanine ZnPcS2P2. Sci. China Ser. B 2001, 44, 113-122.

127. Huang, H.F.; Chen, Y.Z.; Wu, Y. Experimental studies of the effects of ZnPcS2P2-based-photodynamic therapy on bone marrow purging. Chin. Med. J. (Engl.) 2005, 118, 105-110.

128. Zhang, Z.; Jin, H.; Bao, J.; Fang, F.; Wei, J.; Wang, A. Intravenous repeated-dose toxicity study of ZnPcS2P2-based-photodynamic therapy in Wistar rats. Photochem. Photobiol. Sci. 2006, 5, 1006-1017.

129. Boyle, R.W.; Leznoff, C.C.; van Lier, J.E. Biological activities of phthalocyanines-XVI. Tetrahydroxy- and tetraalkylhydroxy zinc phthalocyanines. Effect of alkyl chain length on *in vitro* and *in vivo* photodynamic activities. Br. J. Cancer 1993, 67, 1177-1181.

130. Hu, M.; Brasseur, N.; Yildiz, S.Z.; van Lier, J.E.; Leznoff, C.C. Hydroxyphthalocyanines as potential photodynamic agents for cancer therapy. J. Med. Chem. 1998, 41, 1789-1802.

131. Winkelman, J.W.; Arad, D.; Kimel, S. Stereochemical factors in the transport and binding of photosensitizers in biological systems and in photodynamic therapy. J. Photochem. Photobiol. B 1993, 18, 181-189.

132. Fukushima, K.; Tabata, K.; Okura, I. Photochemical properties of water-soluble fluorinated zinc phthalocyanines and their photocytotoxicity against HeLa cells. J. Porphyr. Phthalocya. 1998, 2, 219-222.

133. Gao, L.; Qian, X.; Zhang, L.; Zhang, Y. Tetra-trifluoroethoxyl zinc phthalocyanine: potential photosensitizer for use in the photodynamic therapy of cancer. J. Photochem. Photobiol. B 2001, 65, 35-38.

134. O'Hagan, D.; Rzepa, H.S. Some influences of fluorine in bioorganic chemistry. Chem. Commun. 1997, 645-652.

135. Allemann, E.; Brasseur, N.; Benrezzak, O.; Rousseau, J.; Kudrevich, S.V.; Boyle, R.W.; Leroux, J.C.; Gurny, R.; van Lier, J.E. PEG-coated poly(lactic acid) nanoparticles for the delivery of hexadecafluoro zinc phthalocyanine to EMT-6 mouse mammary tumours. J. Pharm. Pharmacol. 1995, 47, 382-387.

136. Allemann, E.; Rousseau, J.; Brasseur, N.; Kudrevich, S.V.; Lewis, K.; van Lier, J.E. Photodynamic therapy of tumours with hexadecafluoro zinc phthalocynine formulated in PEG-coated poly(lactic acid) nanoparticles. Int. J. Cancer 1996, 66, 821-824.

137. Allemann, E.; Brasseur, N.; Kudrevich, S.V.; La, M.C.; van Lier, J.E. Photodynamic activities and biodistribution of fluorinated zinc phthalocyanine derivatives in the murine EMT-6 tumour model. Int. J. Cancer 1997, 72, 289-294.

138. Boyle, R.W.; Rousseau, J.; Kudrevich, S.V.; Obochi, M.; van Lier, J.E. Hexadecafluorinated zinc phthalocyanine: Photodynamic properties against the EMT-6 tumour in mice and pharmacokinetics using 65Zn as a radiotracer. Br.J. Cancer 1996, 73, 49-53.

139. Liu, J.Y.; Lo, P.C.; Fong, W.P.; Ng, D.K. Effects of the number and position of the substituents on the *in vitro* photodynamic activities of glucosylated zinc(II) phthalocyanines. Org. Biomol. Chem. 2009, 7, 1583-1591.

140. Choi, C.F.; Huang, J.D.; Lo, P.C.; Fong, W.P.; Ng, D.K. Glycosylated zinc(II) phthalocyanines as efficient photosensitisers for photodynamic therapy. Synthesis, photophysical properties and *in vitro* photodynamic activity. Org. Biomol. Chem. 2008, 6, 2173-2181.

141. Airley, R.E.; Mobasheri, A. Hypoxic regulation of glucose transport, anaerobic metabolism and angiogenesis in cancer: Novel pathways and targets for anticancer therapeutics. Chemotherapy 2007, 53, 233-256.

142. Medina, R.A.; Owen, G.I. Glucose transporters: expression, regulation and cancer. Biol. Res. 2002, 35, 9-26.

143. Ometto, C.; Fabris, C.; Milanesi, C.; Jori, G.; Cook, M.J.; Russell, D.A. Tumour-localising and photosensitizing properties of a novel zinc(II) octadecylphthalocyanine. Br. J. Cancer 1996, 74, 1891-1899.

144. Fabris, C.; Ometto, C.; Milanesi, C.; Jori, G.; Cook, M.J.; Russell, D.A. Tumour-localizing and tumour-photosensitizing properties of zinc(II)-octapentyl-phthalocyanine. J. Photochem. Photobiol. B 1997, 39, 279-284.

145. Jori, G.; Reddi, E. The role of lipoproteins in the delivery of tumour-targeting photosensitizers. Int. J. Biochem. 1993, 25, 1369-1375.

146. Polo, L.; Reddi, E.; Garbo, G.M.; Morgan, A.R.; Jori, G. The distribution of the tumour photosensitizers Zn(II)-phthalocyanine and Sn(IV)-etiopurpurin among rabbit plasma proteins. Cancer Lett. 1992, 66, 217-223.

147. Liu, W.; Jensen, T.J.; Fronczek, F.R.; Hammer, R.P.; Smith, K.M.; Vicente, M.G. Synthesis and cellular studies of nonaggregated water-soluble phthalocyanines. J. Med. Chem. 2005, 48, 1033-1041.

148. Nesterova, I.V.; Erdem, S.S.; Pakhomov, S.; Hammer, R.P.; Soper, S.A. Phthalocyanine dimerization-based molecular beacons using near-IR fluorescence. J. Am. Chem. Soc. 2009, 131, 2432-2433.

149. Tyagi, S.; Kramer, F.R. Molecular beacons: Probes that fluoresce upon hybridization. Nat. Biotechnol. 1996, 14, 303-308.

150. Lo, P.C.; Zhao, B.; Duan, W.; Fong, W.P.; Ko, W.H.; Ng, D.K. Synthesis and *in vitro* photodynamic activity of mono-substituted amphiphilic zinc(II) phthalocyanines. Bioorg. Med. Chem. Lett. 2007, 17, 1073-1077.

151. Jeremy M.Berg, John L.Tymoczko, and Lubert Stryer: Biochemistry. W. H. Freeman, 2002.

152. Liu, J.Y.; Jiang, X.J.; Fong, W.P.; Ng, D.K. Highly photocytotoxic 1,4-dipegylated zinc(II) phthalocyanines. Effects of the chain length on the *in vitro* photodynamic activities. Org. Biomol. Chem. 2008, 6, 4560-4566.

153. Tuncel, S.; Dumoulin, F.; Gailer, J.; Sooriyaarachchi, M.; Atilla, D.; Durmus, M.; Bouchu, D.; Savoie, H.; Boyle, R.W.; Ahsen, V. A set of highly water-soluble tetraethyleneglycol-substituted Zn(II) phthalocyanines: Synthesis, photochemical and photophysical properties, interaction with plasma proteins and *in vitro* phototoxicity. Dalton Trans. 2011, 40, 4067-4079.

154. Bai, M.; Lo, P.C.; Ye, J.; Wu, C.; Fong, W.P.; Ng, D.K. Facile synthesis of pegylated zinc(II) phthalocyanines via transesterification and their *in vitro* photodynamic activities. Org. Biomol. Chem. 2011, 9, 7028-7032.

155. Banfi, S.; Caruso, E.; Buccafurni, L.; Ravizza, R.; Gariboldi, M.; Monti, E. Zinc phthalocyanines-mediated photodynamic therapy induces cell death in adenocarcinoma cells. J. Organomet. Chem. 2007, 692, 1269-1276.

156. Ball, D.J.; Mayhew, S.; Wood, S.R.; Griffiths, J.; Vernon, D.I.; Brown, S.B. A comparative study of the cellular uptake and photodynamic efficacy of three novel zinc phthalocyanines of differing charge. Photochem. Photobiol. 1999, 69, 390-396.

157. Cruse-Sawyer, J.E.; Griffiths, J.; Dixon, B.; Brown, S.B. The photodynamic response of two rodent tumour models to four zinc (II)-substituted phthalocyanines. Br. J. Cancer 1998, 77, 965-972.

158. Sibrian-Vazquez, M.; Ortiz, J.; Nesterova, I.V.; Fernandez-Lazaro, F.; Sastre-Santos, A.; Soper, S.A.; Vicente, M.G. Synthesis and properties of cell-targeted Zn(II)-phthalocyanine-peptide conjugates. Bioconjug. Chem. 2007, 18, 410-420.

159. Torchilin, V.P. Targeted pharmaceutical nanocarriers for cancer therapy and Imaging. AAPS J. 2007, 9, E128-E147.

160. Liu, R.; Cannon, J.B.; Paspal, S.Y.L. Liposomes in solubilization. In Water-Insoluble Drug Formulation; Liu, R., Ed.; CRC Press: Boca Raton, FL, USA, 2008; pp. 375-409.

161. Rodal, G.H.; Rodal, S.K.; Moan, J.; Berg, K. Liposome-bound Zn (II)-phthalocyanine. Mechanisms for cellular uptake and photosensitization. J. Photochem. Photobiol. B 1998, 45, 150-159.

162. Valduga, G.; Reddi, E.; Garbisa, S.; Jori, G. Photosensitization of cells with different metastatic potentials by liposome-delivered Zn(II)-phthalocyanine. Int. J. Cancer 1998, 75, 412-417.

163. Milanesi, C.; Zhou, C.; Biolo, R.; Jori, G. Zn(II)-phthalocyanine as a photodynamic agent for tumours. II. Studies on the mechanism of photosensitised tumour necrosis. Br. J. Cancer 1990, 61, 846-850.

164. Ben-Hur, E.; Chan, W.S. Phthalocyanines in photobiology and their medical applications. In The Porphyrin Handbook; Kadish, K.M., Smith, K.M., Guilard, R., Eds; Academic Press: San Diego, CA, USA, 2003; pp. 1-35.

165. Allison, B.A.; Pritchard, P.H.; Richter, A.M.; Levy, J.G. The plasma distribution of benzoporphyrin derivative and the effects of plasma-lipoproteins on its biodistribution. Photochem. Photobiol. 1990, 52, 501-507.

166. Allison, B.A.; Pritchard, P.H.; Levy, J.G. Evidence for low-density-lipoprotein receptor-mediated uptake of benzoporphyrin derivative. Br. J. Cancer 1994, 69, 833-839.

167. Polo, L.; Bianco, G.; Reddi, E.; Jori, G. The effect of different liposomal formulations on the interaction of Zn(II)-phthalocyanine with isolated low and high density lipoproteins. Int. J. Biochem. Cell Biol. 1995, 27, 1249-1255.

168. Reddi, E.; Zhou, C.; Biolo, R.; Menegaldo, E.; Jori, G. Liposome- or LDL-administered Zn (II)-phthalocyanine as a photodynamic agent for tumours. I. Pharmacokinetic properties and phototherapeutic efficiency. Br. J. Cancer 1990, 61, 407-411.

169. Schmidt-Erfurth, U.; Michels, S.; Indorf, L.; Eggers, R.; Birngruber, R. Mechanism of photodynamic occlusion using liposomal Zn(II)-phtalocyanine. Curr. Eye Res. 2005, 30, 601-612.

170. Gal, D.; Macdonald, P.C.; Porter, J.C.; Simpson, E.R. Cholesterol-metabolism in cancer-cells in monolayer-culture. III. Low-density lipoprotein metabolism. Int. J. Cancer 1981, 28, 315-319.

171. Love, W.G.; Duk, S.; Biolo, R.; Jori, G.; Taylor, P.W. Liposome-mediated delivery of photosensitizers: Localization of zinc (II)-phthalocyanine within implanted tumors after intravenous administration. Photochem. Photobiol. 1996, 63, 656-661.

172. van Leengoed, H.L.; Cuomo, V.; Versteeg, A.A.; van der Veen, N.; Jori, G.; Star, W.M. *In vivo* fluorescence and photodynamic activity of zinc phthalocyanine administered in liposomes. Br. J. Cancer 1994, 69, 840-845.

173. Schieweck, K.; Capraro, H.G.; Isele, U.; van Hoogevest, P.; Ochsner, M.; Maurer, T.; Batt, E. CGP 55847, liposome-delivered zinc(II) phthalocyanine as phototherapeutic agent for tumours. Proc.SPIE Int.Soc.Opt.Eng. 1994, 2078, 107-118.

174. Gelperina, S.; Kisich, K.; Iseman, M.D.; Heifets, L. The potential advantages of nanoparticle drug delivery systems in chemotherapy of tuberculosis. Am. J. Respir.Crit. Care Med. 2005, 172, 1487-1490.

175. Betancourt, T.; Byrne, J.D.; Sunaryo, N.; Crowder, S.W.; Kadapakkam, M.; Patel, S.; Casciato, S.; Brannon-Peppas, L. PEGylation strategies for active targeting of PLA/PLGA nanoparticles. J. Biomed. Mater. Res. Part A 2009, 91A, 263-276.

176. Fattal, E.; Vauthier, C. Nanoparticles as Drug Delivery Systems. In Encyclopedia of Pharmaceutical Technology; Swarbrick, J., Boylan, J.C., Eds; Marcel Dekker, Inc.: New York, NY, USA, 2011; pp. 1864-1882.

177. Fadel, M.; Kassab, K.; Fadeel, D.A. Zinc phthalocyanine-loaded PLGA biodegradable nanoparticles for photodynamic therapy in tumor-bearing mice. Lasers Med. Sci. 2010, 25, 283-92.

178. Lu, H.L.; Syu, W.J.; Nishiyama, N.; Kataoka, K.; Lai, P.S. Dendrimer phthalocyanine-encapsulated polymeric micelle-mediated photochemical internalization extends the efficacy of photodynamic therapy and overcomes drug-resistance *in vivo*. J. Control. Release 2011, 155, 458-464.

179. Herlambang, S.; Kumagai, M.; Nomoto, T.; Horie, S.; Fukushima, S.; Oba, M.; Miyazaki, K.; Morimoto, Y.; Nishiyama, N.; Kataoka, K. Disulfide crosslinked polyion complex micelles encapsulating dendrimer phthalocyanine directed to improved efficiency of photodynamic therapy. J. Control. Release 2011, 155, 449-457.

180. Nishiyama, N.; Nakagishi, Y.; Morimoto, Y.; Lai, P.S.; Miyazaki, K.; Urano, K.; Horie, S.; Kumagai, M.; Fukushima, S.; Cheng, Y.; et al. Enhanced photodynamic cancer treatment by supramolecular nanocarriers charged with dendrimer phthalocyanine. J. Control. Release 2009, 133, 245-251.

181. Jang, W.D.; Nakagishi, Y.; Nishiyama, N.; Kawauchi, S.; Morimoto, Y.; Kikuchi, M.; Kataoka, K. Polyion complex micelles for photodynamic therapy: Incorporation of dendritic photosensitizer excitable at long wavelength relevant to improved tissue-penetrating property. J. Control. Release 2006, 113, 73-79.

182. Baugh, S.D.; Yang, Z.; Leung, D.K.; Wilson, D.M.; Breslow, R. Cyclodextrin dimers as cleavable carriers of photodynamic sensitizers. J. Am. Chem. Soc. 2001, 123, 12488-12494.

183. Ruebner, A.; Kirsch, D.; Andrees, S.; Decker, W.; Roeder, B.; Spengler, B.; Kaufmann, R.; Moser, J.G. Dimeric cyclodextrin carriers with high binding affinity to porphyrinoid photosensitizers. J. Inclus. Phenom. Mol. 1997, 27, 69-84.

184. Rossetti, F.C.; Lopes, L.B.; Carollo, A.R.; Thomazini, J.A.; Tedesco, A.C.; Bentley, M.V. A delivery system to avoid self-aggregation and to improve *in vitro* and *in vivo* skin delivery of a phthalocyanine derivative used in the photodynamic therapy. J. Control. Release 2011, 155, 400-408.

185. Rodriguez, M.E.; Diz, V.E.; Awruch, J.; Dicelio, L.E. Photophysics of zinc (II) phthalocyanine polymer and gel formulation. Photochem. Photobiol. 2010, 86, 513-519.

186. Souza, J.G.; Gelfuso, G.M.; Simao, P.S.; Borges, A.C.; Lopez, R.F. Iontophoretic transport of zinc phthalocyanine tetrasulfonic acid as a tool to improve drug topical delivery. Anti-Cancer Drugs 2011, 22, 783-793.

187. He, J.; Larkin, H.E.; Li, Y.S.; Rihter, D.; Zaidi, S.I.; Rodgers, M.A.; Mukhtar, H.; Kenney, M.E.; Oleinick, N.L. The synthesis, photophysical and photobiological properties and *in vitro* structure-activity relationships of a set of silicon phthalocyanine PDT photosensitizers. Photochem. Photobiol. 1997, 65, 581-586.

188. Rodriguez, M.E.; Zhang, P.; Azizuddin, K.; Delos Santos, G.B.; Chiu, S.M.; Xue, L.Y.; Berlin, J.C.; Peng, X.; Wu, H.; Lam, M.; et al. Structural factors and mechanisms underlying the improved photodynamic cell killing with silicon phthalocyanine photosensitizers directed to lysosomes versus mitochondria. Photochem. Photobiol. 2009, 85, 1189-1200.

189. Lo, P.C.; Huang, J.D.; Cheng, D.Y.; Chan, E.Y.; Fong, W.P.; Ko, W.H.; Ng, D.K. New amphiphilic silicon(IV) phthalocyanines as efficient photosensitizers for photodynamic therapy: Synthesis, photophysical properties, and *in vitro* photodynamic activities. Chemistry 2004, 10, 4831-4838.

190. Lo, P.C.; Chan, C.M.; Liu, J.Y.; Fong, W.P.; Ng, D.K. Highly photocytotoxic glucosylated silicon(IV) phthalocyanines. Effects of peripheral chloro substitution on the photophysical and photodynamic properties. J. Med. Chem. 2007, 50, 2100-2107.

191. Leung, S.C.H.; Lo, P.C.; Ng, D.K.P.; Liu, W.K.; Fung, K.P.; Fong, W.P. Photodynamic activity of BAM-SiPc, an unsymmetrical bisamino silicon(IV) phthalocyanine, in tumour-bearing nude mice. Br. J. Pharmacol. 2008, 154, 4-12.

192. Lai, J.C.; Lo, P.C.; Ng, D.K.; Ko, W.H.; Leung, S.C.; Fung, K.P.; Fong, W.P. BAM-SiPc, a novel agent for photodynamic therapy, induces apoptosis in human hepatocarcinoma HepG2 cells by a direct mitochondrial action. Cancer Biol. Ther. 2006, 5, 413-418.

193. Barge, J.; Decreau, R.; Julliard, M.; Hubaud, J.C.; Sabatier, A.S.; Grob, J.J.; Verrando, P. Killing efficacy of a new silicon phthalocyanine in human melanoma cells treated with photodynamic therapy by early activation of mitochondrion-mediated apoptosis. Exp. Dermatol. 2004, 13, 33-44.

194. Anderson, C.Y.; Freye, K.; Tubesing, K.A.; Li, Y.S.; Kenney, M.E.; Mukhtar, H.; Elmets, C.A. A comparative analysis of silicon phthalocyanine photosensitizers for *in vivo* photodynamic therapy of RIF-1 tumors in C3H mice. Photochem. Photobiol. 1998, 67, 332-336.

195. Jiang, X.J.; Yeung, S.L.; Lo, P.C.; Fong, W.P.; Ng, D.K. Phthalocyanine-polyamine conjugates as highly efficient photosensitizers for photodynamic therapy. J. Med. Chem. 2011, 54, 320-330.

196. Leng, X.; Choi, C.F.; Lo, P.C.; Ng, D.K. Assembling a mixed phthalocyanine-porphyrin array in aqueous media through host-guest interactions. Org. Lett. 2007, 9, 231-234.

197. Lau, J.T.; Lo, P.C.; Fong, W.P.; Ng, D.K. Preparation and photodynamic activities of silicon(IV) phthalocyanines substituted with permethylated beta-cyclodextrins. Chemistry 2011, 17, 7569-7577.

198. Lau, J.T.; Lo, P.C.; Tsang, Y.M.; Fong, W.P.; Ng, D.K. Unsymmetrical beta-cyclodextrin-conjugated silicon(IV) phthalocyanines as highly potent photosensitisers for photodynamic therapy. Chem. Commun. (Camb.) 2011, 47, 9657-9659.

199. Chan, C.M.; Lo, P.C.; Yeung, S.L.; Ng, D.K.; Fong, W.P. Photodynamic activity of a glucoconjugated silicon(IV) phthalocyanine on human colon adenocarcinoma. Cancer Biol. Ther. 2010, 10, 126-134.

200. Agarwal, M.L.; Clay, M.E.; Harvey, E.J.; Evans, H.H.; Antunez, A.R.; Oleinick, N.L. Photodynamic therapy induces rapid cell death by apoptosis in L5178Y mouse lymphoma cells. Cancer Res. 1991, 51, 5993-5996.

201. Ahmad, N.; Feyes, D.K.; Agarwal, R.; Mukhtar, H. Photodynamic therapy results in induction of WAF1/CIP1/P21 leading to cell cycle arrest and apoptosis. Proc. Natl. Acad. Sci. USA 1998, 95, 6977-6982.

202. Colussi, V.C.; Feyes, D.K.; Mulvihill, J.W.; Li, Y.S.; Kenney, M.E.; Elmets, C.A.; Oleinick, N.L.; Mukhtar, H. Phthalocyanine 4 (Pc4) photodynamic therapy of human OVCAR-3 tumor xenografts. Photochem. Photobiol. 1999, 69, 236-241.

203. Whitacre, C.M.; Feyes, D.K.; Satoh, T.; Grossmann, J.; Mulvihill, J.W.; Mukhtar, H.; Oleinick, N.L. Photodynamic therapy with the phthalocyanine photosensitizer Pc 4 of SW480 human colon cancer xenografts in athymic mice. Clin. Cancer Res. 2000, 6, 2021-2027.

204. Whitacre, C.M.; Satoh, T.H.; Xue, L.; Gordon, N.H.; Oleinick, N.L. Photodynamic therapy of human breast cancer xenografts lacking caspase-3. Cancer Lett. 2002, 179, 43-49.

205. Fei, B.; Wang, H.; Meyers, J.D.; Feyes, D.K.; Oleinick, N.L.; Duerk, J.L. High-field magnetic resonance imaging of the response of human prostate cancer to Pc 4-based photodynamic therapy in an animal model. Lasers Surg. Med. 2007, 39, 723-730.

206. Lee, R.G.; Vecchiotti, M.A.; Heaphy, J.; Panneerselvam, A.; Schluchter, M.D.; Oleinick, N.L.; Lavertu, P.; Alagramam, K.N.; Arnold, J.E.; Sprecher, R.C. Photodynamic therapy of cottontail rabbit papillomavirus-induced papillomas in a severe combined immunodeficient mouse xenograft system. Laryngoscope 2010, 120, 618-624.

207. Agarwal, R.; Korman, N.J.; Mohan, R.R.; Feyes, D.K.; Jawed, S.; Zaim, M.T.; Mukhtar, H. Apoptosis is an early event during phthalocyanine photodynamic therapy-induced ablation of chemically induced squamous papillomas in mouse skin. Photochem. Photobiol. 1996, 63, 547-552.

208. George, J.E., III; Ahmad, Y.; Varghai, D.; Li, X.; Berlin, J.; Jackowe, D.; Jungermann, M.; Wolfe, M.S.; Lilge, L.; Totonchi, A.; et al. Pc 4 photodynamic therapy of U87-derived human glioma in the nude rat. Lasers Surg. Med. 2005, 36, 383-389.

209. Oleinick, N.L.; Morris, R.L.; Belichenko, T. The role of apoptosis in response to photodynamic therapy: What, where, why, and how. Photochem. Photobiol. Sci. 2002, 1, 1-21.

210. Anderson, C.; Hrabovsky, S.; McKinley, Y.; Tubesing, K.; Tang, H.P.; Dunbar, R.; Mukhtar, H.; Elmets, C.A. Phthalocyanine photodynamic therapy: Disparate effects of pharmacologic inhibitors on cutaneous photosensitivity and on tumor regression. Photochem. Photobiol. 1997, 65, 895-901.

211. Lam, M.; Hsia, A.H.; Liu, Y.; Guo, M.; Swick, A.R.; Berlin, J.C.; McCormick, T.S.; Kenney, M.E.; Oleinick, N.L.; Cooper, K.D.; et al. Successful cutaneous delivery of the photosensitizer silicon phthalocyanine 4 for photodynamic therapy. Clin. Exp. Dermatol. 2011, 36, 645-651.

212. Baron, E.D.; Malbasa, C.L.; Santo-Domingo, D.; Fu, P.; Miller, J.D.; Hanneman, K.K.; Hsia, A.H.; Oleinick, N.L.; Colussi, V.C.; Cooper,K.D. Silicon phthalocyanine (Pc 4) photodynamic therapy is a safe modality for cutaneous neoplasms: Results of a phase 1 clinical trial. Lasers Surg. Med. 2010, 42, 728-735.

213. Choi, C.F.; Tsang, P.T.; Huang, J.D.; Chan, E.Y.; Ko, W.H.; Fong, W.P.; Ng, D.K. Synthesis and *in vitro* photodynamic activity of new hexadeca-carboxy phthalocyanines. Chem. Commun. (Camb.) 2004, 19, 2236-2237.

214. Huang, J.D.; Fong, W.P.; Chan, E.Y.M.; Choi, M.T.M.; Chan, W.K.; Chan, M.C.; Ng, K.P. Photodynamic activities of a dicationic silicon(IV) phthalocyanine and its bovine serum albumin conjugates. Tetrahedron Lett. 2003, 44, 8029-8032.

215. Huang, J.D.; Wang, S.Q.; Lo, P.C.; Fong, W.P.; Ko, W.H.; Ng, D.K.P. Halogenated silicon(IV) phthalocyanines with axial poly(ethylene glycol) chains. Synthesis, spectroscopic properties, complexation with bovine serum albumin and *in vitro* photodynamic activities. New J. Chem. 2004, 28, 348-354.

216. Lee, P.P.S.; Ngai, T.; Huang, J.D.; Wu, C.; Fong, W.P.; Ng, D.K.P. Synthesis, characterization, biodegradation, and *in vitro* photodynamic activities of silicon(IV) phthalocyanines conjugated axially with poly(epsilon-caprolactone). Macromolecules 2003, 36, 7527-7533.

217. Lee, P.P.S.; Lo, P.C.; Chan, E.Y.M.; Fong, W.P.; Ko, W.H.; Ng, D.K.P. Synthesis and *in vitro* photodynamic activity of novel galactose-containing phthalocyanines. Tetrahedron Lett. 2005, 46, 1551-1554.

218. Lo, P.C.; Leung, S.C.H.; Chan, E.Y.M.; Fong, W.P.; Ko, W.H.; Ng, D.K.P. Photodynamic effects of a novel series of silicon(IV) phthalocyanines against human colon adenocarcinoma cells. Photodiagn. Photodyn. Ther. 2007, 4, 117-123.

219. Master, A.M.; Rodriguez, M.E.; Kenney, M.E.; Oleinick, N.L.; Sen Gupta, A. Delivery of the photosensitizer Pc4 in PEG-PCL micelles for *in vitro* PDT studies. J. Pharm. Sci. 2010, 99, 2386-2398.

220. Roy, I.; Ohulchanskyy, T.Y.; Pudavar, H.E.; Bergey, E.J.; Oseroff, A.R.; Morgan, J.; Dougherty, T.J.; Prasad, P.N. Ceramic-based nanoparticles entrapping water-insoluble photosensitizing anticancer drugs: A novel drug-carrier system for photodynamic therapy. J. Am. Chem. Soc. 2003, 125, 7860-7865.

221. Zhao, B.Z.; Yin, J.J.; Bilski, P.J.; Chignell, C.F.; Roberts, J.E.; He, Y.Y. Enhanced photodynamic efficacy towards melanoma cells by encapsulation of Pc4 in silica nanoparticles. Toxicol. Appl. Pharm. 2009, 241, 163-172.

222. Cheng, Y.; Samia, A.C.; Meyers, J.D.; Panagopoulos, I.; Fei, B.W.; Burda, C. Highly efficient drug delivery with gold nanoparticle vectors for *in vivo* photodynamic therapy of cancer. J. Am. Chem. Soc. 2008, 130, 10643-10647.

223. Li, H.; Marotta, D.E.; Kim, S.; Busch, T.M.; Wileyto, E.P.; Zheng, G. High payload delivery of optical imaging and photodynamic therapy agents to tumors using phthalocyanine-reconstituted low-density lipoprotein nanoparticles. J. Biomed. Opt. 2005, 10, 41203.

224. Zheng, G.; Chen, J.; Li, H.; Glickson, J.D. Rerouting lipoprotein nanoparticles to selected alternate receptors for the targeted delivery of cancer diagnostic and therapeutic agents. P. Natl. Acad. Sci. USA 2005, 102, 17757-17762.

225. Juan, C.; Ian, R.C.; Gang, Z. Novel targeting and activation strategies for photodynamic therapy. In Proceedings of Light-activated Tissue Regeneration and Therapy Conference; Ronald, W., Darrell, B.T., Eds.; Springer: New York, NY, 2008; pp. 127-147.

226. Dutta, S.; Ongarora, B.G.; Li, H.; Vicente, M.G.; Kolli, B.K.; Chang, K.P. Intracellular targeting specificity of novel phthalocyanines assessed in a host-parasite model for developing potential photodynamic medicine. PLoS One 2011, 6, e20786.

227. Giuliani, F.; Martinelli, M.; Cocchi, A.; Arbia, D.; Fantetti, L.; Roncucci, G. *In vitro* resistance selection studies of RLP068/Cl, a new Zn(II) phthalocyanine suitable for antimicrobial photodynamic therapy. Antimicrob. Agents Chemother. 2010, 54, 637-642.

228. Mantareva, V.; Angelov, I.; Kussovski, V.; Dimitrov, R.; Lapok, L.; Wöhrle, D. Photodynamic efficacy of water-soluble Si(IV) and Ge(IV) phthalocyanines towards Candida albicans planktonic and biofilm cultures. Eur. J. Med. Chem. 2011, 46, 4430-4440.

229. Longo, J.P.; Leal, S.C.; Simioni, A.R.; de Fatima M.A.-S.; Tedesco, A.C.; Azevedo, R.B. Photodynamic therapy disinfection of carious tissue mediated by aluminum-chloride-phthalocyanine entrapped in cationic liposomes: an *in vitro* and clinical study. Lasers Med. Sci. 2011, Epub ahead of print.

230. Montanari, J.; Maidana, C.; Esteva, M.I.; Salomon, C.; Morilla, M.J.; Romero, E.L. Sunlight triggered photodynamic ultradeformable liposomes against Leishmania braziliensis are also leishmanicidal in the dark. J. Control. Release 2010, 147, 368-376.

231. van den,.B.H. Photodynamic therapy of age-related macular degeneration: History and principles. Semin. Ophthalmol. 2001, 16, 181-200.

232. Lange, N.; Jichlinski, P.; Zellweger, M.; Forrer, M.; Marti, A.; Guillou, L.; Kucera, P.; Wagnieres, G.; van den, B.H. Photodetection of early human bladder cancer based on the fluorescence of 5-aminolaevulinic acid hexylester-induced protoporphyrin IX: A pilot study. Br. J. Cancer 1999, 80, 185-193.

233. Stepp, H.; Beck, T.; Pongratz, T.; Meinel, T.; Kreth, F.W.; Tonn, J.C.; Stummer, W. ALA and malignant glioma: Fluorescence-guided resection and photodynamic treatment. J. Environ. Pathol. Toxicol.Oncol. 2007, 26, 157-164.

234. Stummer, W.; Novotny, A.; Stepp, H.; Goetz, C.; Bise, K.; Reulen, H.J. Fluorescence-guided resection of glioblastoma multiforme by using 5-aminolevulinic acid-induced porphyrins: A prospective study in 52 consecutive patients. J. Neurosurg. 2000, 93, 1003-1013.

PHTHALOCYANINES FOR POLYMERIC PHOTOSENSITIZER PRODRUGS

Nawal SEKKAT[1], Marino CAMPO[1], Nolwazi NOMBONA[2], Phindile KHOZA[2],

Tebello NYOKONG[2] and Norbert LANGE[*1]

[1]School of Pharmaceutical Sciences, University of Lausanne/Geneva, Geneva, 30, Quai Ernest Ansermet, Geneva CH-1211, Switzerland

[2]Department of Chemistry, Rhodes University, Grahamstown 6140, South Africa

*Corresponding author e-mail: norbert.lange@unige.ch

ABSTRACT

Phthalocyanines (Pcs) are promising photosensitizers for photodynamic therapy (PDT) and imaging applications. Due to their strong absorbance in the near-infrared region, Pcs are excellent candidates for deep tissue activation *in vivo*. However, they are associated with low water-solubility and strong tendency towards aggregation.

In this article, we report efficient synthesis of 10 chemically tunable Pcs bearing one functionalizable carboxylic moiety. Theses Pcs display distinct water-soluble properties and different phototoxic effects on the human prostate cancer cell line (PC-3 cell line).

This screening allowed identifying three promising Pc candidates for PDT and photodiagnosis of cancer. Further *in vitro* investigations on PC-3, A549 and, HT1080 cell lines, including cellular uptake and intracellular localization of the selected Pcs were established. In their free form, no Pc exhibited any significant phototoxic effect except a PEGylated and water-soluble Pc (Pc **(9)**). In HT1080, this Pc was able to achieve 90% of cell death at a concentration of 4µM and a light dose of 10J/cm^2. Complete cell destruction was observed for higher Pc doses, while being void of any dark toxicity. Furthermore, cellular accumulation of Pc **(9)** seemed to follow an energy dependent process in addition to passive diffusion. Its cellular internalization seemed to be in the form of endosomal/endolysosomal vacuoles established by means of confocal microscopy.

Finally, this study confirms the effectiveness of the Pc based polymeric approach *in vitro*. Hence, thanks to the carboxylic moiety introduced in these compounds further conjugation of the Pcs to a polymeric backbone (poly-L-lysine) was feasible and resulted in increased water-solubility and significant phototoxicity of two non-active Pcs in their free form.

KEY WORDS: Phthalocyanines, polymeric prodrugs, photodynamic therapy, photosensitizer, theranostics

1. Introduction

Photodynamic therapy (PDT) is based on the interaction of three non-toxic compounds: light, oxygen and photosensitizer (PS) which combined result in cell death and selective tumor destruction[1].

Selectivity is achieved by **1)** a selective or increased accumulation of the PS in the diseased tissue [2-4], **2)** a controlled light activation of the PS and **3)** a consecutive production of reactive oxygen species which have a short lifetime (< 0.04 μs) and, thus, a narrow range of action (< 0.02 μm) hence, enabling a localized cell destruction[5-7]. Depending on the PS's cellular and intracellular localization/relocalization, PDT exhibits direct and indirect cell killing, vascular occlusion, release of cytokines and the response of the immune system[8-10]. However, conventional photosensitizers are associated with lack of selectivity towards diseased tissues leading to increased side-effects such as skin photosensitivity and reduced efficacy due to unsuitable pharmacokinetic/pharmacodynamics (PK/PD). One way to overcome this drawback is the macromolecular prodrug approach introduced by Ringsdorf[11], further developed for anticancer agent by Duncan's et al [12-17]and other groups for PDT and imaging[18-28].

In polymeric photosensitizer prodrugs (PPP) multiple copies of a photosensitizer (PS) are tethered either directly or via a peptide linker to a polymeric carrier. Due to the strong interactions of the PS moieties in close proximity on the carrier, no photoactivity can be observed upon irradiation with light. However, upon proteolytic digestion of the polymeric carrier or the peptidic linker, photoactivity is restored.

As a 2nd generation of photosensitizers, phthalocyanines (Pcs) fulfill one the most fundamental requirement for photodiagnosis and photodynamic therapy. Indeed, they exhibit suitable fluorescence quantum yields for fluorescence imaging purposes. Furthermore, their absorbance in the spectral range of daylight is weak thus minimizing the risk of skin photosensitivity. In addition, photosensitizers with the highest absorbance between 600 and 800 nm are the ideal candidates because of optimal light penetration into tissues[29-34]. In this regard, phthalocyanines are promising candidates for PDT treatment. Moreover, their "flexible chemistry" allows a modulation of their properties amongst them their pharmacokinetic and optical properties as well as their solubility, resulting in the optimization of their PDT efficiency[35-38].

Since phthalocyanines are well known to form strong non-photoactive aggregates, we hypothesized that these compounds are ideal candidate PS for PPPs. One requirement for the selective coupling of the PS to the polymeric carrier is the presence of only one chemical handle within the phthalocyanine skeleton while all other peripheric positions can be used to fine tune absorption, stacking and photodynamic properties. A direct consequence of this A_3B configuration is the apparent split of the Q-band when in solution which disappears when aggregates are formed.

The purpose of this study is the screening and the evaluation of potentially active phthalocyanines (Pcs) for PPP-mediated PDT of tumors. Therefore, *in vitro* studies on PC-3 (human prostate adenocarcinoma), HT1080 (human fibrosarcoma) and A549 (human lung carcinoma) cell lines were performed with and without light irradiation at different Pcs concentrations and phototoxicity of two phthalocyanine-polymer based conjugates were evaluated on PC-3 cells.

2. Materials and Methods

2.1. Chemicals

Anhydrous forms of dimethylsulfoxide (DMSO), N,N-diisoproprylethylamine (DIPEA), O-(7-aza-benzotriazol-1-yl)-N,N,N,N-tetramethyluronium hexafluorophosphate (HATU), Poly-L-lysine hydrobromide (115DPVIS-57DPMALLS-24000MWVIS-12000MWMALLS) were purchased from Sigma-Aldrich (Buchs, Switzerland). Methoxy PEG Succinimidyl Carboxymethyl Ester (mPEG-SPA) of 20 kDa was obtained from Nektar (San Carlos, USA). Acetonitrile (ACN) was bought from Biosolve BV (Valkenswaard, Netherlands) and trifluoroacetic acid (TFA) was purchased from Acros Organics (Geel, Belgium). Trypsin 0.25%-EDTA solution, Nutrient Mixture Kaighn's Modification (F-12K) with L-Glutamine, Dulbecco's phosphate buffer saline (DPBS) solution without calcium and magnesium, Dulbecco's Modified Eagle Medium (DMEM+ GlutaMAX-I) containing Pyruvate and 1g/L D-Glucose, Penicillin 10 000 units/mL and Streptomycin 10 000 µg/mL solution were provided by Life Technologies Corporation (Paisley, UK). DMSO of analytical grade was obtained from Fisher Scientific UK Limited (Loughborough, Leicestershire, UK). Fetal Bovine Serum (FBS) was acquired from PAA Laboratories GmbH (Pasching, Austria), Triton X-100 from Applichem. (ITW Company, Germany), NaOH from Reactolab S.A. (Servion, Switzerland) and 3-(4,5-Dimethylthiazol-2-yl)-2,5-diphenyl-2H-tetrazolium bromide

(Thiazolyl Blue Tetrazolium Bromide) used in the MTT assay was obtained from Sigma-Aldrich Company (St. Louis, MO, USA).

2.2. Phthalocyanines structures

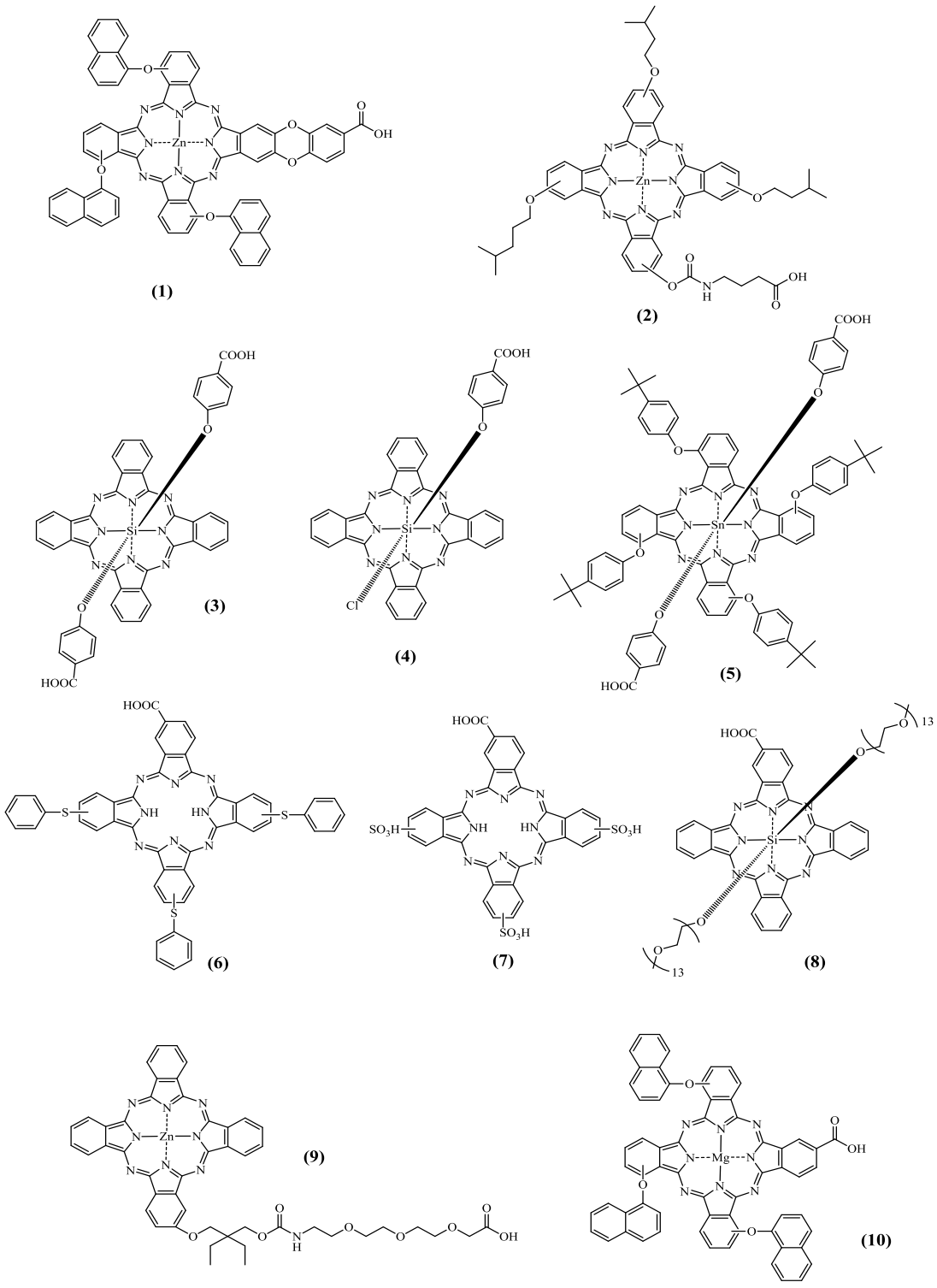

Figure 1. Chemical structures of investigated phthalocyanines

Table 1. Maximal Excitation and Emission Wavelengths of Pc's tested in the study

Compound	Excitation Wavelength $\lambda_{exc, max}$ [nm]	Emission Wavelength $\lambda_{em, max}$ [nm]
(1)	690	715
(2)	680	710
(3)	660	680
(4)	660	680
(5)	720	750
(6)	680	720
(7)	670	700
(8)	680	710
(9)	650	680
(10)	680	700

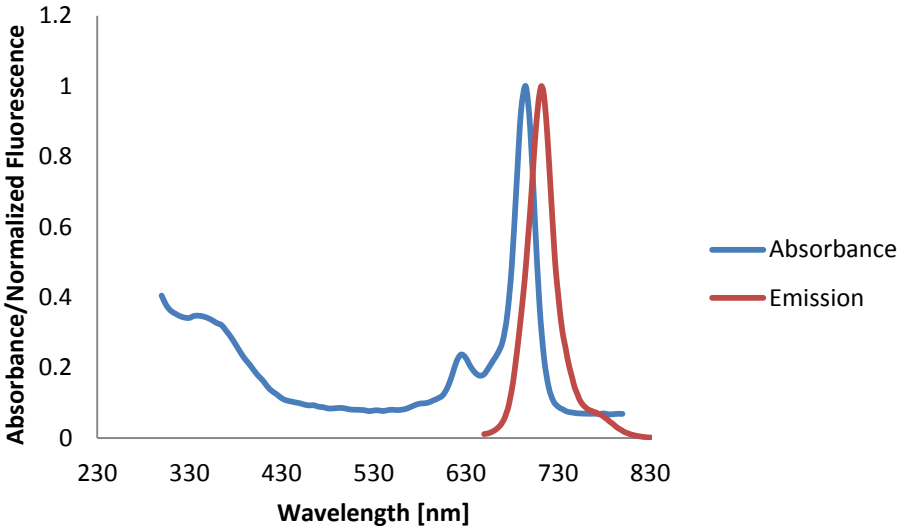

Figure 2. Typical absorption and emission spectrum of phthalocyanines, here Pc **(1)**, in DMSO.

2.3. Phthalocyanines synthesis

Phthalocyanines were synthesized as reported before[39].

2.4. Phthalocyanine Pc (1) and Pc (10) conjugates synthesis

To a solution of poly-L-lysine HBr (25kDa, DP=118.5 (PLL)) (3 mg, $1.4*10^{-5}$ moles) in anhydrous DMSO was added DIPEA (3 equiv. based on the number of ε-NH_2 on PLL) and

mPEG-SPA of 20kDa (2.9 mg, Nektar) to reach an average loading of 1%. The reaction was allowed to proceed for 8 hours and subsequently, Pc **(1)** was added in order to reach an average loading of 10% (1.8mg). 1.5 equiv of HATU (1.3mg) were added in regard to the carboxylic acid moiety on Pc. Finally, after 24 hours, nicotinic acid-NHS ester was added to reach a 25% loading on PLL[26]. The reaction was stirred overnight and quenched by addition of water/TFA mixture to pH=3. After filtration, the solution was purified by Size-Exclusion Chromatography using sephacryl^{TM} S-100 (Amersham Biosciences, Otelfingen, Switzerland) column and water/acetonitrile/TFA (70/30/0.025%) as eluent. The product of interest was collected, lyophilized and resulted in a green product that was kept at -20°C in the dark. Pc **(10)** conjugate was synthesized as reported before[39].

2.5. Cell Culture

PC-3 as well as A549 cells (ATCC, Manassas, VA) were maintained as monolyaers in F-12K medium supplemented with 10% fetal bovine serum (FBS) and 100µL/mL streptomycin and 100IE/mL penicillin in a humidified incubator containing 5% CO_2. HT1080 cells were grown as monolayers using Dulbecco's Modified Eagle Medium (1g/L D-Glucose and with Pyruvate) supplemented with 10%FBS and containing the same amounts of antibiotics as previously described. Cells were trypsinized using 0.25% Trypsin-EDTA solution.

2.6. Photocytotoxicity of photosensitizers-Screening

The photocytotoxicity of the different phthalocyanines (Pcs) was first assessed on human prostate cancer PC-3 cell line using the Thiazolyl Blue Tetrazolium Bromide assay (MTT assay). Cells were seeded in 96-well plates as aliquots of 100 µL containing 1.8 x 10^4 cells and allowed to grow to 70% confluence. Pcs were brought to the targeted concentrations, *i.e.*, 1, 2, 6 and 10µM by dissolving the corresponding volume of the Pcs stock solution in DMSO in the fresh complete medium. The amount of DMSO for all solutions was adjusted to the highest amount of DMSO of the most concentrated PS solution and did not exceed 2% of the total volume. Cells were incubated with these solutions for 2 hours then rinced twice with 200µL PBS followed by the addition of 100 µL of fresh medium. Cells were subsequently, either kept in the dark (plate control) or irradiated with a light dose of 10 J/cm^2 (PCI light, PCI Biotech, Oslo, Norway). 50 µL of fresh medium was added after irradiation and cells survival assay was performed 24 hours after irradiation by means of the MTT assay as described by

Gabriel et al. [25]. Positive and negative controls were treated with complete medium or 0.1% Triton in NaOH 5M, respectively. Percentage cell survival was calculated with respect to control samples, as follows:

[A (test-conc.) - A (100% dead)] / [A (100% viable) – A (100% dead)]*100. All conditions were tested in sextuplicates.

2.7. Dark and Photocytotoxicity of Pc (9) on PC3, A549 and HT1080

Similarly to the cell test of **(7)**, **(8)** and **(9)** on PC-3 cells, phototoxicity of Pc **(9)** was performed on human prostate cancer PC-3, A549 and HT1080 cell lines using an MTT assay. Cells were seeded in 96-well plates as aliquots of 100 µL containing 1.5 x 10^4 and 1.2 x 10^4 cells respectively, and allowed to grow to 70-80% confluence. Pcs were brought to the desired concentrations, *i.e.*, 0.5, 1, 2, 3, 4, 5, 6, 8 and 10µM by dissolving the corresponding volume of the Pc stock solution in DMSO in the fresh complete medium. Cells were treated and analysed as described above.

2.8. Photosensitizers Cellular Uptake in PC-3, A549 and HT1080

The three different cell lines were seeded in 96-well plates and incubated with 5µM of PS (here **(7)**, **(8)** and **(9)**) in complete medium during one hour at 37 or 6°C. After washing with PBS, cells were lysed using 100 µL of a solution of 1M NaOH and 0.5% Triton and 100 µL of milliQ water was added to enable solubilisation of PS. A Safire (Tecan, Switzerland) was used for fluorescence measurements using an excitation wavelength of 610 nm and an emission wavelength of 680 nm. Fluorescence recorded (Fl_x) was normalized as a function of the fluorescence obtained at 680 nm for equimolar and equiabsorbant Pc samples at 610 nm (Fl_{x0}) (Normalized fluorescence = Fl_x/ Fl_{x0}). Data were obtained in triplicates.

2.9. Intracellular Fate of Pc (9) in PC-3 cells - Confocal Microscopy

PC-3 cells were seeded at a concentration of 6x10^4 cells per well and allowed to attach during 2 days. Cells were then co-incubated with 120nM of Lysotracker® Green and the 20 µM of probes during 2 hours. Cells were then washed with HBSS and HBSS with BSA 1% and subsequently fixed using paraformaldehyde solution at 4%. After fixation, cells were rinsed 3 times using HBSS and once with water and were finally mounted using Vectashield® mounting medium containing DAPI. Cells were then imaged by confocal fluorescence

microscopy using Zeiss Axiovert 710 microscope (Carl Zeiss, Jena, Germany).

2.10. Dark and Photocytotoxicity of Pc (1) and Pc (10) conjugates on PC-3 cells

As described before, PC-3 cells were grown at 70-80% confluence in 96-well plates. Cells were then exposed to the polymeric prodrugs to desired concentrations of Pcs based on the loading of the conjugates (*i.e.* equivalent Pcs). Desired concentrations *i.e.* 1, 3, 6 and 10µM were achieved by dissolving the corresponding volume of the conjugates-Pc stock solution in fresh complete medium. Cells were incubated either with Pc or with Pc based conjugates for two different incubation times (2 and 8 hours of incubation). Cellular toxicity of these compounds was investigated under dark and light exposition condition for a light dose of 10J/cm^2. Cellular survival was estimated by performing an MTT assay as described before.

3. Results

3.1. Dark and Photocytotoxicity of Pcs on cells

Phthalocyanines for PDT are supposed to be non-toxic without exposition to light but when activated by light, cell eradication should be achieved. No significant phototoxicity was observed for compounds **(1)** to **(8).** At the highest concentrations a slight cytotoxicity was noticed for compound **(6)** (see supplementary informations).

Figure 3 represents the cell survival as a function of Pc **(9)** concentration in the dark and exposed to light (to a light dose of 10J/cm^2). Due to the cellular tests variability, Pcs inducing more than 20% of cell death when irradiated were considered as potentially phototoxic.

Compound **(9)**, did not show any significant dark toxicity over the entire range of concentration. However, as compared to the dark conditions, phototoxicity was observed at concentration as low as 1 µM and a light dose of 10J/cm^2. From our library only Pc **(9)** shows the expected phototoxicity, we pursued characterizing this compound in other human cell lines.

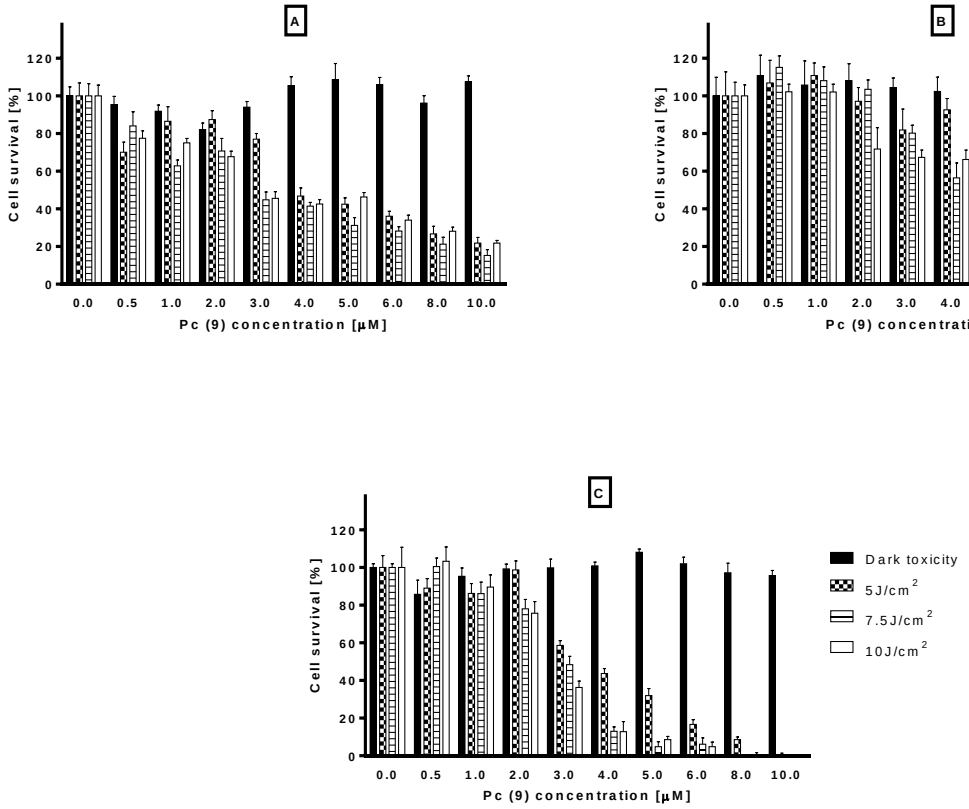

Figure 3. Pc **(9)** dark and light toxicity at light doses of 5, 7.5 and 10 J/cm^2 on **(A)**, PC-3, **(B)**, A549 and **(C)**, HT1080 cell lines.

Figure 3 shows compound **(9)** dark and light cytotoxicity on PC-3, A549 and HT1080 cells as a function of light and drug dose. In PC-3 cells, a light and PS dose dependent photocytotoxicity can be observed. Concentrations higher than 1 and 2 µM led to a significant decrease of cell survival. At 3 µM for light doses of 7.5 and 10J/cm^2 approximately 50% of cell destruction is achieved. At PS concentration higher than 4 µM, no significant difference between the light doses can be observed.

As for PC-3 cells, also in A549 and HT1080 cells, no dark toxicity can be seen, using Pc **(9)**. Phototoxic effects are visible at a concentration of 2 µM for a light dose of 10J/cm^2. Interestingly, equivalent cell death is achieved at both 5 µM for a light dose of 10J/cm^2 and 10µM at a light dose of 5 J/cm^2. At 10 µM, no more A549 cells survived for light doses of 7.5 and 10 J/cm^2.

The highest sensitivity to PDT was observed in HT1080. In this cell line, 90% of cell death can already be achieved at concentration and light doses as low as 4 µM for 7.5 and 10J/cm^2.

3.2. Cellular uptake of Pc (7), (8) and (9) on A549, HT1080 and PC-3 cell lines

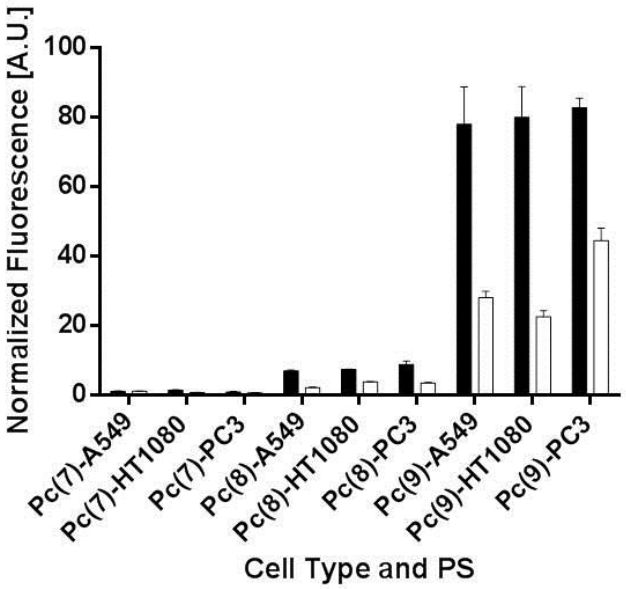

Figure 4. Cellular uptake of Pc **(7)**, **(8)** and **(9)** by A549, HT1080 and PC-3 cells at two different temperatures *i.e.* 37 (■) and 6°C (□).

The potential cellular uptake of water soluble Pcs **(7)** and **(8)** was compared to the one of Pc**(9)** at different temperatures as shown in Figure 7. While high amounts of Pc **(9)** were taken up by all three cell lines, only low amounts of Pc **(7)** and Pc **(8)** shows were taken up at both temperatures, presumably explaining the low phototoxicity of these compounds. However, a significantly lower uptake was recorded when cells are incubated at 6°C with Pcs **(9)** and **(8)** as compared to the 37°C condition, suggesting an energy dependent uptake involving endocytosis. Furthermore, the total uptake was independent on the respective cell line.

When looking at the uptake of the same Pc by the different cells, all cells took up each Pc to a same extent. However when comparing the phototoxic effect of these Pcs on the same cells, the difference of phototoxic effect could probably be due to the cell susceptibility towards the Pcs rather than linked to the ability of the Pc to be taken up.

Finally, one can establish a parallel between cellular uptake and cell phototoxicity. Hence, Pc**(7)**'s lack of phototoxic effect is probably due to a hampered cellular uptake resulting in loss of efficient *in vitro* killing. Pc **(9)**, on the other hand, exhibits cellular toxicity that correlates with efficient cellular uptake, suggesting that Pc **(9)** reaches target organelles in cells through endocytosis at a fast pace (in less than 2 hours). Finally, although Pc **(8)** is taken

up to a relatively high extent as compared to all Pcs tested, did not exhibit any cellular toxic effect suggesting a potential promising application in tumor imaging rather than PDT-mediated tumor treatment.

3.3. Intracellular Fate of Pc (9) in PC-3 cells - Confocal Microscopy

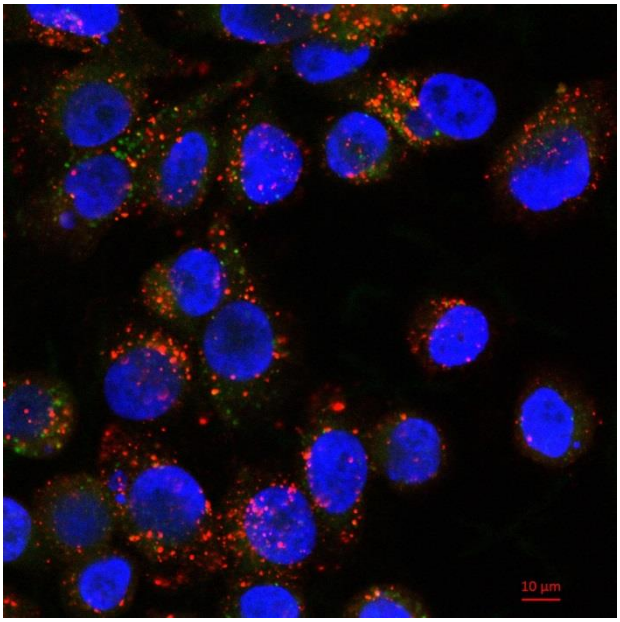

Figure 5. Intracellular localization pattern of Pc **(9)** in PC-3 cells. The nuclei are stained in blue using DAPI, PS is depicted in red, while green marks lysomomal structures revealed by means of Lysotracker Green®.

Two hours after incubation, Pc **(9)** seems to be localized in vacuolar structures distinct from the lysosomes as shown in Figure 5. Based on the intracellular uptake, Pc **(9)** internalization is expected to follow an endolysosomal pathway which is confirmed by confocal microscopy. However, low/no colocalisation with lysosomal structures could be observed under these conditions suggesting that either the incubation time was not long enough for the Pc to reach lysosomes or that there could be a lysosomal escape of the Pc and formation of vacuolar structures.

3.4. Dark and Photocytotoxicity of Pc (1) and Pc (10) conjugates on PC-3 cells

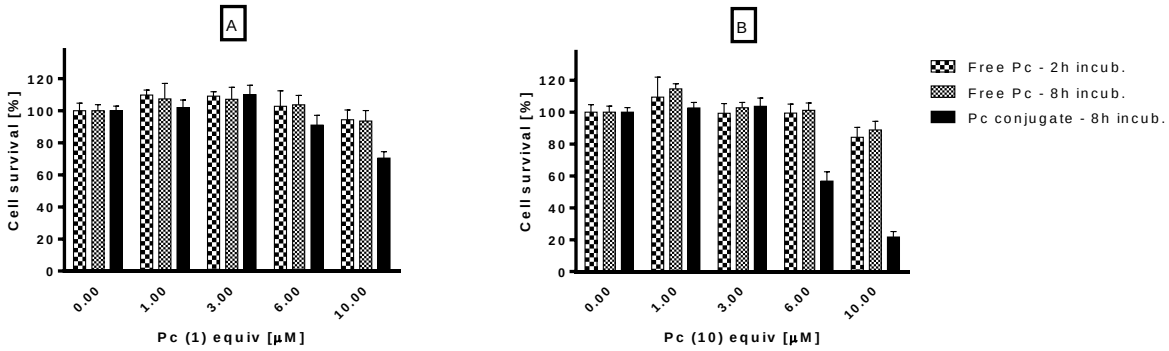

Figure 6. Photoxicity of Pc **(1) (A)** and Pc **(10) (B)** and their respective Pc-conjugates at a light dose of 10 J/cm^2 on PC-3 cells.

Phototoxicity of Pc **(1)** and Pc **(10)** and their corresponding polymeric conjugates is presented in Figure 6A and 6B, respectively. No dark toxicity was observed for all Pc and Pc conjugates studied after 2 or 8 hours of incubation (data not shown). Moreover, while no photoxic effect was observed in PC-3 cells after irradiation at 10J/cm^2 for the free Pcs, their respective conjugate counterparts exhibited noticeable phototoxic effect by provoking approximately 40% and 80% of cell death for conjugate Pc **(1)** and conjugate Pc **(10)** respectively, at the highest drug dose of 10 µM (expressed as equivalent of PS on conjugates) at 10J/cm^2. By increasing the water solubility of these Pcs by PLL conjugation, we were able to improve its PDT outcome and phototoxicity while maintaining its harmlessness under dark conditions. Hence, these preliminary results constitute a proof-of-principle in the promising approach that is the polymeric prodrug Pc approach.

4. Discussion

We and others have reported the application of polymeric photosensitizer prodrugs for both for imaging and PDT of cancer and inflammatory diseases[18-28,40-42]. The most recent approach consists in three parts where a polymeric backbone has the chemical versatility to enable coupling of a targeting moiety (*e.g.* protease cleavable peptide) and active drug (*e.g.* PS).

The aim of this study was to identify potentially photoactive PS for subsequent development into prostate cancer probes and active molecules for PDT and fluorescence imaging.

All evaluated Pcs investigated in this study should in principle show significant photocytotoxicities. Indeed, it is reported that even though metallation of Pcs with diamagnetic metal ions such as tin and zinc is associated with high triplet state yield, longer triplet state lifetimes and subsequently high singlet oxygen yields[38,43-46], paramagnetic metal ions such as silicon and non metallated Pcs can be highly photodynamically active as shown by the investigation in clinical trials of Pc 4 (a silicon based Pc)[47], and by Feofanov *et al*[48] and Karmakova *et al*[49] on other Pcs. In the pool of phthalocyanines tested, only Pc **(9)** exhibited significant light toxicity under our conditions. This may be explained by the propensity of Pcs to form aggregates especially in aqueous cell medium especially for compounds **(1)** and **(6)**. Indeed, aggregation of Pcs lowers dramatically their singlet oxygen quantum yield, rendering them inefficient as photosensitizers for PDT[36]. In order to decrease their potential stacking, axial ligation of substituants to the central metal ion was adopted for Pcs **(3)**, **(4)** and **(5)**. In order to further decrease the aggregation potential of insoluble Pcs[50], addition of 20% of FBS was tested. However, cytotoxic effects were observed which were attributed to the amount of FBS itself (data not shown). Therefore, FBS was maintained at 10% for all *in vitro* investigations.

Furthermore, we investigated water-soluble Pc (compounds **(7)**, **(8)** and **(9)**). The water solubility is supposed to prevent Pc's loss of activity due to PS aggregation. One way of reducing the propensity of Pcs towards aggregation is the introduction of polar groups such as –OH, -COOH and -SO_3H at their periphery[51-54]. By varying the number of sulfonated groups coupled to the Pc, one can modify the Pc towards an amphiphilic (*e.g.*disulfonation) and even a hydrophilic character (tetrasulfonation), **Pc (7)** falls into this chemical approach.

Another approach is the coupling of molecules with one or more PEG entities. Besides increased water solubility, the PEGylation of Pc **(8)** and Pc **(9)** was aiming at longer circulation time in the body, thus, presumably resulting in higher accumulation in tumors [55-59]. During the past decades, several studies reported synthesis and evaluation of PEGylated Pc with relatively successful effect *in vitro* and *in vivo*[60-65].

In this article, we report synthesis and *in vitro* evaluation of two PEGylated Pcs. Indeed, Pc**(8)** combines axial ligation and PEGylation strategy whilst Pc **(9)** is peripherally PEGylated.

Significant PDT efficacy was observed only for Pc **(9)** on A549, HT1080 and PC-3. Cell death was achieved at drug doses as low as 2 μM and a light dose of 10J/cm^2. Moreover,

complete destruction of tumor cells was achieved at 10 μM in the case of A549 and HT1080 for the same light dose. Similarly, Ng and co-workers[64,65] reported IC_{50} values (drug dose responsible for 50% of cell death) on human colorectal adenocarcinoma HT29 and on human hepatocarcinoma HepG2 cells ranging from 0.02 to 3.72 μM. However, these Pcs had to be formulated in Cremophor EL emulsions due to solubility issues. In 2011, Tuncel *et al*[61] were able to achieve *in vitro* phototoxicity of water-soluble PEGylated Zinc Phthalocyanine on HT29 cells without incorporation into a Cremophor EL formulation. However, phototoxic effect was approximately two orders of magnitude lower than the one reported by Ng *et al*. with the lowest IC_{50} reported of 85 μM for a light dose of approximately 4 J/cm^2. In the present study, IC_{50} of Pc **(9)** for a light dose of 5 J/cm^2 was about 4 μM.

Pc **(9)** efficiency as phototosensitizer may be due to its amphiphilic character as compared to the hydrophilic **(7)**. Amphiphilicity of a PS is considered to be advantageous for both cellular uptake and accumulation of the phototoxic agent[33,51,54,66-70].

Based on Figure 7, Pc **(9)**'s efficacy is associated with an effective cellular uptake. It was observed that the internalization of Pc **(9)** was lower at 6°C, suggesting that the Pcs diffusion through the cell membrane implicates an energy dependent process. Based on confocal fluorescence microscopy, Pc **(9)** seems to accumulate in endosomal vacuoles distinct from lysomes after 2 hours of incubation. Since Pc **(9)** exhibits significant phototoxic effects after the same incubation time, one might suggest that this phenomenon lies in the targeting of other organelles or disruption of cytoplasm. Finally, since PEGylation is known to increase the body-residence time and stability *in vivo*, these promising *in vitro* results suggest that Pc **(9)** could be of great value for *in vivo* PDT treatment of cancer.

As shown by Figure 7, Pc **(7)** inefficacy is due to a very low cellular uptake rather than aggregation in aqueous media. Its hydrophilic character seems to hamper its diffusion through cellular membrane *in vitro* which results in lower cellular uptake, accumulation and PDT effect. This is not surprising since it was reported earlier by Chan *et al*.[51,68,69] and by Wöhrle *et al*.[54] that the tetra- and tri-sulfonated Pcs had a lower efficacy than their less sulfonated homologues, *in vitro*. *In vivo* however, Chan *et al*. reported that $AlPcS_2$ was more potent than $AlPcS_3$ and $AlPcS_4$, despite its lower accumulation in tumor xenografts. This discrepancies were attributed to differences in pharmacokinetics and biodistribution of these compounds[51,68,69,71]. Hence, tetrasulfonated Pcs seem to provoke indirect tumor destruction by

affecting tumor nutrient and oxygen supply leading to tumor starvation through vascular damage. Based on our observations, it will be interesting to evaluate the efficacy of this compound *in vivo*. More interestingly, the possibility to link this compound via its carboxylic function to polymers and targeting moieties such as in the polymeric prodrug approach could be beneficial to its PDT effect *in vitro* as well as *in vivo* as illustrated by the case of $AlPcS_4$ enhanced PDT effect when coupled to tumor targeting and amphiphilic moieties[72-79]. However, the PPP approach would add a beneficial enhancement in Pc's pharmacokinetic features and selectivity in order to increase its tumor uptake and accumulation as well as its photodynamic efficacy.

Finally, although Pc **(8)** did not exhibit any cell phototoxicity as shown by Figure 7, this Pc accumulated in the three cell types tested to a higher extent at 37°C as shown by Figure 4. Hence, as for Pc **(9)**, its uptake seems to follow also an energy dependent pathway. This result suggests that this specific compound could be of major interest for tumor imaging since it accumulates in tumor cells, with no phototoxicity at the doses tested. Hence, polymer labeling with Pc **(8)** could be beneficial for *in vivo* tumor imaging and tracking as well as for treatment through fluorescence tumor guided resection without toxic effect.

Finally, based on the illustrative examples of Pc **(1)** and Pc **(10)** conjugates, phototoxicity is achievable also for Pcs that did not exhibit any phototoxic effect on their own. This effect is based on the improved water solubility of the Pc conjugates as compared to the Pcs alone. Hence, proof of principle of the Pc based polymeric prodrug approach was obtained and addition of targeting moieties may further improve therapeutical outcome of PDT-mediated cancer treatment.

5. Conclusions

Several Pcs were prepared and their phototoxic activity was investigated for further development into photosensitizer protease based polymeric prodrugs. Among the Pcs synthesised and tested, only one Pc **(9)** has shown a significant phototoxic activity towards tumourous cells, hence suggesting promising application of this Pc for PDT-mediated tumor ablation. Two other interesting Pcs were identified, *i.e.* Pc **(7)** and Pc **(8)** for potential tumor fluorescence imaging. These encouraging results are of major value for further investigation of these Pc in the protease based prodrug approach and efforts should be put on the

development of such probes for tumor targeting and destruction *in vitro* and *in vivo*. Other applications for chemical coupling of Pcs to DNA, peptides, polymers and other structures and biomaterials could be envisaged for imaging and therapeutic outcome. Finally, proof-of-principle of this concept was illustrated with two inefficient Pcs on their own at the drug and light doses applied in this study but that exhibited significant phototoxic effect when conjugated to water soluble polymer and moieties for similar drug and light doses.

Acknowledgements

This work has been supported in part by the SNF grants 205320_13830, CR32I3_129987, CR32I3_147018, 31003A_149962, CR32I3_150271, and 205321_126834.

Supplementary material

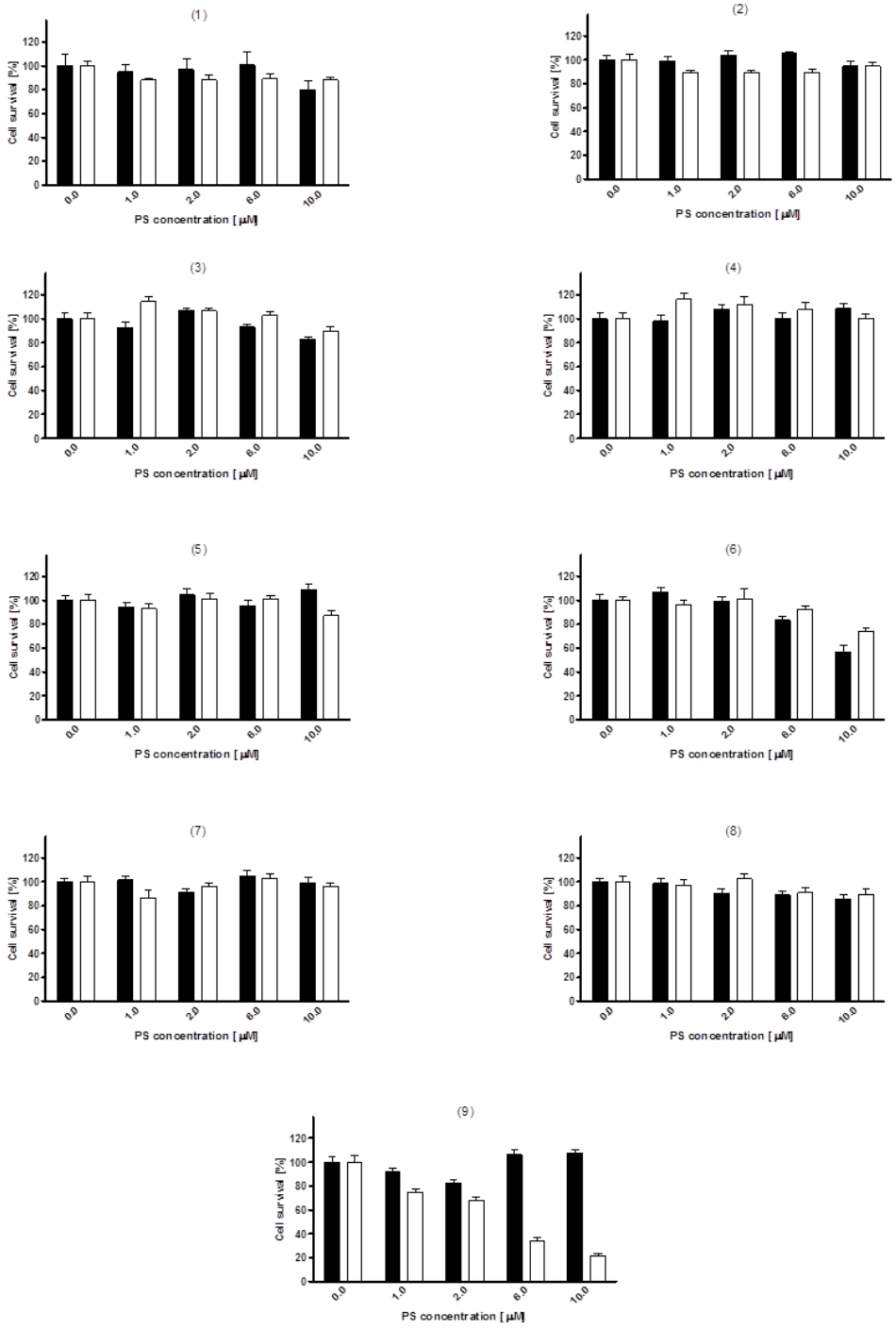

Figure 7. Phthalocyanines **(1)** to **(9)** dark (■) and light (□) toxicity at a light dose of 10 J/cm^2 on PC-3 cell line.

References:

1. Sharman WM, Allen CM, van Lier JE: Photodynamic therapeutics: basic principles and clinical applications. Drug Discovery Today 4:507-517, 1999

2. Maeda H, Takeshita J, Kimura M: Improvement of pharmacological properties of protein drugs by tailoring with synthetic polymers. Journal of Bioactive and Biocompatible Polymers 3:27-43, 1988

3. Maeda H, Takeshita J, Kanamaru R: Lipophilic Derivative of Neocarzinostatin - a Polymer Conjugation of an Anti-Tumor Protein Antibiotic. International Journal of Peptide and Protein Research 14:81-87, 1979

4. Maeda H, Matsumura Y, Kato H: Purification and identification of [hydroxyprolyl3] bradykinin in ascitic fluid from a patient with gastric cancer. Journal of Biological Chemistry 31:16051-16054, 1988

5. Kvam E, Stokke T, Moan J: The Lengths of DNA Fragments Light-Induced in the Presence of a Photosensitizer Localized at the Nuclear-Membrane of Human-Cells. Biochimica Et Biophysica Acta 1049:33-37, 1990

6. Moan J, Berg K: The Photodegradation of Porphyrins in Cells Can Be Used to Estimate the Lifetime of Singlet Oxygen. Photochemistry and Photobiology 53:549-553, 1991

7. Weishaupt KR, Gomer CJ, Dougherty TJ: Identification of Singlet Oxygen as Cytotoxic Agent in Photo-Inactivation of a Murine Tumor. Cancer Research 36:2326-2329, 1976

8. Ackroyd R, Kelty C, Brown N, et al: The history of photodetection and photodynamic therapy. Photochem Photobiol 74:656-69, 2001

9. Dolmans DEJGJ, Fukumura D, Jain RK: Photodynamic therapy for cancer. Nature Reviews Cancer 3:380-387, 2003

10. Sekkat N, van den Bergh H, Nyokong T, et al: Like a bolt from the blue: phthalocyanines in biomedical optics. Molecules 17:98-144, 2012

11. Ringsdorf H: Structure and Properties of Pharmacologically Active Polymers. Journal of Polymer Science Part C-Polymer Symposium:135-153, 1975

12. Kopecek J: Targetable polymeric anticancer drugs. Temporal control of drug activity. Ann N Y Acad Sci 618:335-44, 1991

13. Duncan R, Seymour LW, Ohare KB, et al: Preclinical Evaluation of Polymer-Bound Doxorubicin. Journal of Controlled Release 19:331-346, 1992

14. Duncan R, Kopeckovarejmanova P, Strohalm J, et al: Anticancer Agents Coupled to N-(2-Hydroxypropyl)Methacrylamide Copolymers .1. Evaluation of Daunomycin and Puromycin Conjugates Invitro. British Journal of Cancer 55:165-174, 1987

15. Duncan R, Kopeckova P, Strohalm J, et al: Anticancer Agents Coupled to N-(2-Hydroxypropyl)Methacrylamide Copolymers .2. Evaluation of Daunomycin Conjugates Invivo against L1210 Leukemia. British Journal of Cancer 57:147-156, 1988

16. Duncan R, Kopecek J: Soluble Synthetic-Polymers as Potential-Drug Carriers. Advances in Polymer Science 57:51-101, 1984

17. Duncan R, Hume IC, Kopeckova P, et al: Anticancer Agents Coupled to N-(2-Hydroxypropyl)Methacrylamide Copolymers .3. Evaluation of Adriamycin Conjugates against Mouse Leukemia-L1210 Invivo. Journal of Controlled Release 10:51-63, 1989

18. Zuluaga MF, Sekkat N, Gabriel D, et al: Selective Photodetection and Photodynamic Therapy for Prostate Cancer through Targeting of Proteolytic Activity. Molecular Cancer Therapeutics 12:306-313, 2013

19. Tung CH, Bredow S, Mahmood U, et al: Preparation of a cathepsin D sensitive near-infrared fluorescence probe for imaging. Bioconjug Chem 10:892-6, 1999

20. Tijerina M, Fowers KD, Kopeckova P, et al: Chronic exposure of human ovarian carcinoma cells to free or HPMA copolymer-bound mesochlorin e(6) does not induce P-glycoprotein-mediated multidrug resistance. Biomaterials 21:2203-2210, 2000

21. Soukos NS, Hamblin MR, Hasan T: The effect of charge on cellular uptake and phototoxicity of polylysine chlorin(e6) conjugates. Photochemistry and Photobiology 65:723-729, 1997

22. Renno RZ, Terada Y, Haddadin MJ, et al: Selective photodynamic therapy by targeted verteporfin delivery to experimental choroidal neovascularization mediated by a homing peptide to vascular endothelial growth factor receptor-2. Archives of Ophthalmology 122:1002-1011, 2004

23. Peterson CM, Lu JM, Sun YR, et al: Combination chemotherapy and photodynamic therapy with N-(2-hydroxypropyl)methacrylamide copolymer-bound anticancer drugs inhibit human ovarian carcinoma heterotransplanted in nude mice. Cancer Research 56:3980-3985, 1996

24. Gabriel D, Zuluaga MF, Martinez MN, et al: Urokinase-plasminogen-activator sensitive polymeric photosensitizer prodrugs: design, synthesis and *in vitro* evaluation. Journal of Drug Delivery Science and Technology 19:15-24, 2009

25. Gabriel D, Campo MA, Gurny R, et al: Tailoring protease-sensitive photodynamic agents to specific disease-associated enzymes. Bioconjugate Chemistry 18:1070-1077, 2007

26. Campo MA, Gabriel D, Kucera P, et al: Polymeric photosensitizer prodrugs for photodynamic therapy. Photochemistry and Photobiology 83:958-965, 2007

27. Bremer C, Bredow S, Mahmood U, et al: Optical imaging of matrix metalloproteinase-2 activity in tumors: Feasibility study in a mouse model. Radiology 221:523-529, 2001

28. Brasseur N, Ouellet R, La Madeleine C, et al: Water-soluble aluminium phthalocyanine-polymer conjugates for PDT: photodynamic activities and pharmacokinetics in tumour-bearing mice. British Journal of Cancer 80:1533-1541, 1999

29. Stolik S, Delgado JA, Perez A, et al: Measurement of the penetration depths of red and near infrared light in human "ex vivo" tissues. J Photochem Photobiol B 57:90-3, 2000

30. Lang K, Mosinger J, Wagnerova DM: Photophysical properties of porphyrinoid sensitizers non-covalently bound to host molecules; models for photodynamic therapy. Coordination Chemistry Reviews 248:321-350, 2004

31. Jori G: Far-Red-Absorbing Photosensitizers - Their Use in the Photodynamic Therapy of Tumors. Journal of Photochemistry and Photobiology a-Chemistry 62:371-378, 1992

32. Haddad R, Blumenfeld A, Siegal A, et al: *In vitro* and *in vivo* effects of photodynamic therapy on murine malignant melanoma. Annals of Surgical Oncology 5:241-247, 1998

33. Boyle RW, Dolphin D: Structure and biodistribution relationships of photodynamic sensitizers. Photochemistry and Photobiology 64:469-85, 1996

34. Bonnett R, White RD, Winfield UJ, et al: Hydroporphyrins of the meso-tetra(hydroxyphenyl)porphyrin series as tumour photosensitizers. Biochem J 261:277-80, 1989

35. Rio Y, Salome Rodriguez-Morgade M, Torres T: Modulating the electronic properties of porphyrinoids: a voyage from the violet to the infrared regions of the electromagnetic spectrum. Org Biomol Chem 6:1877-94, 2008

36. Ethirajan M, Saenz C, Gupta A, et al: Advances in Photodynamic Therapy: Basic, Translational, and Clinical (ed Artech House: Boston, MA, USA), 2008 pp. 13-39

37. Claessens CG, Blau WJ, Cook M, et al: Phthalocyanines and phthalocyanine analogues: The quest for applicable optical properties. Monatshefte Fur Chemie 132:3-11, 2001

38. Ali H, van Lier JE: Metal complexes as photo- and radiosensitizers. Chem Rev 99:2379-450, 1999

39. Nombona N, Antunes E, Nyokong T: The synthesis and fluorescence behaviour of phthalocyanines unsymmetrically substituted with naphthol and carboxy groups. Dyes and Pigments 86:68-73, 2010

40. Mahmood U, Tung CH, Bogdanov A, Jr., et al: Near-infrared optical imaging of protease activity for tumor detection. Radiology 213:866-70, 1999

41. Krinick NL, Sun Y, Joyner D, et al: A polymeric drug delivery system for the simultaneous delivery of drugs activatable by enzymes and/or light. J Biomater Sci Polym Ed 5:303-24, 1994

42. Weissleder R, Tung CH, Mahmood U, et al: *In vivo* imaging of tumors with protease-activated near-infrared fluorescent probes. Nat Biotechnol 17:375-8, 1999

43. Nyman ES, Hynninen PH: Research advances in the use of tetrapyrrolic photosensitizers for photodynamic therapy. J Photochem Photobiol B 73:1-28, 2004

44. Josefsen LB, Boyle RW: Photodynamic therapy and the development of metal-based photosensitisers. Met Based Drugs 2008:276109, 2008

45. Foley MS, Beeby A, Parker AW, et al: Excited triplet state photophysics of the sulphonated aluminium phthalocyanines bound to human serum albumin. J Photochem Photobiol B 38:10-7, 1997

46. Allen CM, Sharman WM, Van Lier JE: Current status of phthalocyanines in the photodynamic therapy of cancer. Journal of Porphyrins and Phthalocyanines 5:161-169, 2001

47. Baron ED, Malbasa CL, Santo-Domingo D, et al: Silicon Phthalocyanine (Pc 4) Photodynamic Therapy Is a Safe Modality for Cutaneous Neoplasms: Results of a Phase 1 Clinical Trial. Lasers in Surgery and Medicine 42:728-735, 2010

48. Feofanov A, Grichine A, Karmakova T, et al: Chelation with metal is not essential for antitumor photodynamic activity of sulfonated phthalocyanines. Photochemistry and Photobiology 75:527-533, 2002

49. Karmakova T, Feofanov A, Nazarova A, et al: Distribution of metal-free sulfonated phthalocyanine in subcutaneously transplanted murine tumors. Journal of Photochemistry and Photobiology B-Biology 75:81-87, 2004

50. Ogunsipe A, Nyokong T: Photophysicochemical consequences of bovine serum albumin binding to non-transition metal phthalocyanine sulfonates. Photochemical & Photobiological Sciences 4:510-516, 2005

51. Chan WS, Marshall JF, Svensen R, et al: Effect of Sulfonation on the Cell and Tissue Distribution of the Photosensitizer Aluminum Phthalocyanine. Cancer Research 50:4533-4538, 1990

52. Zhao JF, Wang J, Chen JY, et al: Gallium Phthalocyanine Photosensitizers: Carboxylation Enhances the Cellular Uptake and Improves the Photodynamic Therapy of Cancers. Anti-Cancer Agents in Medicinal Chemistry 12:604-610, 2012

53. Hu M, Brasseur N, Yildiz SZ, et al: Hydroxyphthalocyanines as potential photodynamic agents for cancer therapy. Journal of Medicinal Chemistry 41:1789-1802, 1998

54. Wohrle D, Hirth A, Bogdahn-Rai T, et al: Photodynamic therapy of cancer: second and third generations of photosensitizers. Russian Chemical Bulletin 47:807-816, 1998

55. Veronese FM, Pasut G: PEGylation, successful approach to drug delivery. Drug Discov Today 10:1451-8, 2005

56. Veronese FM: Peptide and protein PEGylation: a review of problems and solutions. Biomaterials 22:405-17, 2001

57. Molineux G: Pegylation: engineering improved pharmaceuticals for enhanced therapy. Cancer Treat Rev 28 Suppl A:13-6, 2002

58. Abuchowski A, van Es T, Palczuk NC, et al: Alteration of immunological properties of bovine serum albumin by covalent attachment of polyethylene glycol. J Biol Chem 252:3578-81, 1977

59. Abuchowski A, Mccoy JR, Palczuk NC, et al: Effect of Covalent Attachment of Polyethylene-Glycol on Immunogenicity and Circulating Life of Bovine Liver Catalase. Journal of Biological Chemistry 252:3582-3586, 1977

60. Zhao B, Duan W, Lo PC, et al: Mono-PEGylated zinc(II) phthalocyanines: preparation, nanoparticle formation, and *in vitro* photodynamic activity. Chem Asian J 8:55-9, 2013

61. Tuncel S, Dumoulin F, Gailer J, et al: A set of highly water-soluble tetraethyleneglycol-substituted Zn(II) phthalocyanines: synthesis, photochemical and photophysical properties, interaction with plasma proteins and *in vitro* phototoxicity. Dalton Trans 40:4067-79, 2011

62. Mewis RE, Savoie H, Archibald SJ, et al: Synthesis and phototoxicity of polyethylene glycol (PEG) substituted metal-free and metallo-porphyrins: effect of PEG chain length, coordinated metal, and axial ligand. Photodiagnosis Photodyn Ther 6:200-6, 2009

63. Lv F, Cao B, Cui Y, et al: Zinc phthalocyanine labelled polyethylene glycol: preparation, characterization, interaction with bovine serum albumin and near infrared fluorescence imaging *in vivo*. Molecules 17:6348-61, 2012

64. Liu JY, Jiang XJ, Fong WP, et al: Highly photocytotoxic 1,4-dipegylated zinc(II) phthalocyanines. Effects of the chain length on the *in vitro* photodynamic activities. Org Biomol Chem 6:4560-6, 2008

65. Bai M, Lo PC, Ye J, et al: Facile synthesis of pegylated zinc(II) phthalocyanines via transesterification and their *in vitro* photodynamic activities. Org Biomol Chem 9:7028-32, 2011

66. Paquette B, Ali H, Langlois R, et al: Biological-Activities of Phthalocyanines .8. Cellular-Distribution in V-79 Chinese-Hamster Cells and Phototoxicity of Selectively Sulfonated Aluminum Phthalocyanines. Photochemistry and Photobiology 47:215-220, 1988

67. Kudrevich S, Brasseur N, LaMadeleine C, et al: Syntheses and photodynamic activities of novel trisulfonated zinc phthalocyanine derivatives. Journal of Medicinal Chemistry 40:3897-3904, 1997

68. Chan WS, West CML, Moore JV, et al: Photocytotoxic Efficacy of Sulfonated Species of Aluminum Phthalocyanine against Cell Monolayers, Multicellular Spheroids and Invivo Tumors. British Journal of Cancer 64:827-832, 1991

69. Chan WS, Brasseur N, LaMadeleine C, et al: Efficacy and mechanism of aluminium phthalocyanine and its sulphonated derivatives mediated photodynamic therapy on murine tumours. European Journal of Cancer 33:1855-1859, 1997

70. Cauchon N, Tian HJ, Langlois J, et al: Structure-photodynamic activity relationships of substituted zinc trisulfophthalocyanines. Bioconjugate Chemistry 16:80-89, 2005

71. Peng Q, Moan J: Correlation of Distribution of Sulfonated Aluminum Phthalocyanines with Their Photodynamic Effect in Tumor and Skin of Mice Bearing Cad2 Mammary-Carcinoma. British Journal of Cancer 72:565-574, 1995

72. Vrouenraets MB, Visser GWM, Stigter M, et al: Targeting of aluminum (III) phthalocyanine tetrasulfonate by use of internalizing monoclonal antibodies: Improved efficacy in photodynamic therapy. Cancer Research 61:1970-1975, 2001

73. Vrouenraets MB, Visser GWM, Loup C, et al: Targeting of a hydrophilic photosensitizer by use of internalizing monoclonal antibodies: A new possibility for use in photodynamic therapy. International Journal of Cancer 88:108-114, 2000

74. Vrouenraets MB, Visser GW, Stigter M, et al: Comparison of aluminium (III) phthalocyanine tetrasulfonate- and meta-tetrahydroxyphenylchlorin-monoclonal antibody conjugates for their efficacy in photodynamic therapy *in vitro*. Int J Cancer 98:793-8, 2002

75. Urizzi P, Allen CM, Langlois R, et al: Low-density lipoprotein-bound aluminum sulfophthalocyanine: targeting tumor cells for photodynamic therapy. Journal of Porphyrins and Phthalocyanines 5:154-160, 2001

76. Dubuc C, Langlois R, Benard F, et al: Targeting gastrin-releasing peptide receptors of prostate cancer cells for photodynamic therapy with a phthalocyanine-bombesin conjugate. Bioorganic & Medicinal Chemistry Letters 18:2424-2427, 2008

77. Carcenac M, Larroque C, Langlois R, et al: Preparation, phototoxicity and biodistribution studies of anti-carcinoembryonic antigen monoclonal antibody-phthalocyanine conjugates. Photochemistry and Photobiology 70:930-936, 1999

78. Carcenac M, Dorvillius M, Garambois V, et al: Internalisation enhances photo-induced cytotoxicity of monoclonal antibody-phthalocyanine conjugates. British Journal of Cancer 85:1787-1793, 2001

79. Allen CM, Langlois R, Sharman WM, et al: Photodynamic properties of amphiphilic derivatives of aluminum tetrasulfophthalocyanine. Photochemistry and Photobiology 76:208-216, 2002

SELECTIVE PHOTODETECTION AND PHOTODYNAMIC THERAPY FOR PROSTATE CANCER THROUGH TARGETING OF PROTEOLYTIC ACTIVITY

Maria-Fernanda ZULUAGA[1], Nawal SEKKAT[1], Doris GABRIEL[1],

Hubert VAN DEN BERGH[2] and Norbert LANGE[1]

[1]School of Pharmaceutical Sciences, University of Lausanne/Geneva, Geneva, 30, Quai Ernest Ansermet, Geneva CH-1211, Switzerland

[2]Laboratory of Photomedicine, Swiss Federal Institute of Technology (EPFL), Lausanne, CH-1015 Switzerland

*Corresponding author e-mail: norbert.lange@unige.ch

ABSTRACT

Published in Molecular Cancer Therapeutics 12*(3)*, 306-313, *2013*

Frequent side effects of radical treatment modalities and the availability of novel diagnostics have raised the interest in focal therapies for localized prostate cancer. To improve the selectivity and therapeutic efficacy of such therapies, we developed a minimally invasive procedure, based on a novel polymeric photosensitizer prodrug sensitive to urokinase-like plasminogen activator (uPA). The compound is inactive in its prodrug form and accumulates passively at the tumor site by the enhanced permeability and retention effect. There, the prodrug is selectively converted to its photoactive form by uPA which is over-expressed by prostate cancer cells. Irradiation of the activated photosensitizer exerts a tumor-selective phototoxic effect.

The prodrug alone (8 μM) showed no toxic effect on PC-3 cells, but upon irradiation the cell viability was reduced by 90%. *In vivo*, after systemic administration of the prodrug, PC-3 xenografts became selectively fluorescent. This is indicative of the prodrug accumulation in the tumor and selective local enzymatic activation. Qualitative analysis of the activated compound confirmed that the enzymatic cleavage occurred selectively in the tumor, with only trace amounts in the neighboring skin or muscle.

Subsequent photodynamic therapy studies demonstrated complete tumor eradication of animals treated with light (150 J/cm^2 at 665 nm) 16 hours after the injection of the prodrug (7.5 mg/kg). These promising results evidence the excellent selectivity of our prodrug with the potential to be used for both, imaging and therapy of localized prostate cancer.

KEY WORDS: Polymeric prodrugs; protease-sensitive prodrugs; photodynamic therapy; urokinase-like plasminogen activator; prostate cancer.

1. Introduction

Prostate cancer (PCa) is the most prevalent cancer in the male population[1]. The gold standard for the treatment of localized disease is radical prostatectomy or radiation therapy. A minority of low risk patients can be kept under active surveillance, but this often only delays the final treatment[2]. The excellent results obtained in the radical treatment come at the cost of frequent side effects (mainly sexual or urinary dysfunction) and their long-lasting impact on the quality of life. Mapping biopsies and imaging with endo-rectal coil MRI have laid the foundation for local therapies, which might cause fewer side effects.

Current options for localized therapy include brachytherapy, cryotherapy, high intensity focused ultrasound, laser ablation, and photodynamic therapy (PDT)[3].

The latter requires three main elements: a photosensitizer (PS), light and oxygen. After administration, the PS accumulates to some extent in the target tissue and subsequently can be selectively activated by light to produce reactive oxygen species. With recent progress in light delivery and dosimetry, the use of PDT is no longer restricted to the skin. Fairly superficial lesions in hollow organs can be treated[4,5] and PCa is also open to PDT if one inserts optical devices into the lesions.

HpD, a hematoporphyrin derivative, which is a complex mixture of porphyrins was among the first PSs assessed clinically. This was followed by the use of a somewhat purified mixture called Photofrin® that was used to treat PCa[6]. Subsequently, small prospective clinical trials using Foscan®[7] and 5-aminolevulinic acid[8], have been reported. Despite promising PDT responses, one observed prolonged skin sensitization in the case of Foscan® and occasional extra-prostatic tissue injury. This encouraged further research efforts which aimed mainly at improving PDT selectivity and reducing side effects. In this context, LuTex® and Tookad® specifically targeting the vasculature combined with local light delivery to the prostate were evaluated[9]. Trials for the treatment of primary and recurrent PCa using these agents showed good tolerability. However, some patients did not respond to the treatment or presented urinary and rectal damage[10-13]. Even with the improved formulation of Tookad®, insufficient therapeutic responses and collateral damage have been reported recently (Emberton, IPA congress, Innsbruck, 2011).

Therefore, improvements in the tumor selective delivery of PS are needed to avoid collateral damage of the urethra, rectum and urinary sphincter[14]. With this goal in mind, we have developed polymeric protease-sensitive photosensitizer prodrugs (PPPs) following a triple

targeting strategy: 1) Selective delivery of the PPP into tumor tissue is promoted by the polymeric carrier through the enhanced permeability and retention effect[15]. In its prodrug form photoactivity is impeded through efficient intramolecular quenching between closely positioned PS molecules on the polymeric carrier. 2) Proteolytic activation occurs via cleavage of the peptide linkers by urokinase-like plasminogen activator (uPA), which is over-expressed by PCa cells[16]. Release from the polymeric backbone thus reestablishes the PS's photoactivity selectively in the target tissue. 3) Local irradiation further increases selectivity and induces toxic radicals.

In a previous study, we have reported on a prodrug candidate (uPA-PPP-4) capable of accumulating in PCa tumors and being activated by upregulated urokinase-like plasminogen activator (uPA)[17]. The present report investigates the therapeutic potential of this prodrug by evaluating its phototoxic effect *in vitro* in PC-3 and luciferase-transfected PC-3M-luc-C6 cancer cells as well as *in vivo* in a PCa xenograft-model.

2. Materials and Methods

2.1. Compounds

uPA-PPP-4 (Figure 1) consisted of multiple copies of the photosensitizer pheophorbide a (Pb*a*) attached to a poly-L-lysine backbone via GSGRSAG peptide sequence. It was synthesized and characterized as described previously[17,18] as well as in more detail in Supplementary Materials and Methods. The purity of the prodrug was confirmed by RP-HPLC, with monitoring at 280, 330 and 450 nm. A prodrug mass of approximately 108 kDa was confirmed by SEC-MALLS-RI-UV using a column Waters Ultrahydrogel linear (column temperature: 35.0 ± 0.2°C; mobile phase: 0.15 M acetic acid, 0.1 M sodium acetate, 0.05% NaN_3 at a pH of 4.0; flux: 0.4 mL/min). This system contains a pump: Waters Alliance HPLC system (Milford, MA), and three detectors: a Schambeck RI detector (Bad Honnef, Germany), a light-scattering detector Wyatt MiniDawn (Dernbach, Germany), and a UV-VIS detector Waters Lambda-Max (Milford, MA).

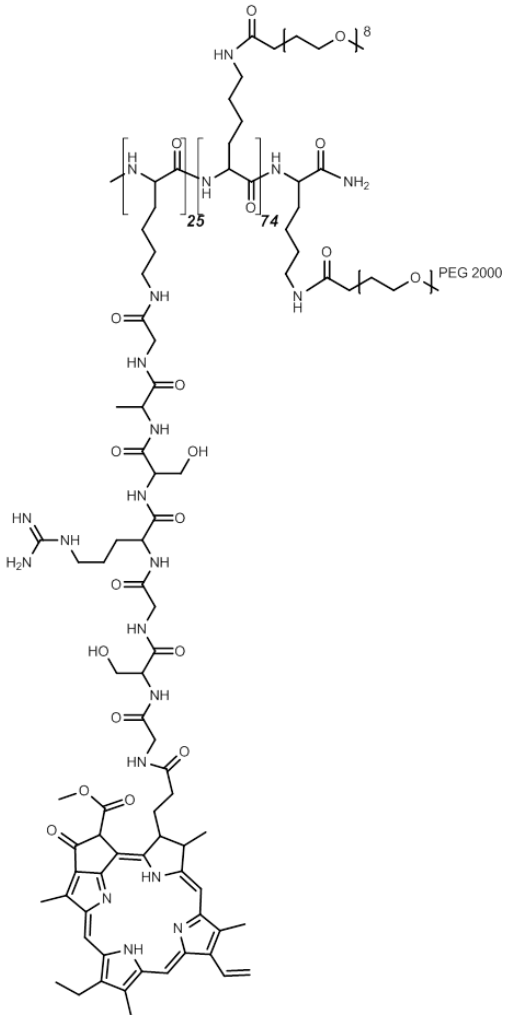

Figure 1. Schematic representation of the macromolecular prodrug uPA-PPP-4. The prodrug is synthesized with an average loading of 30% Pb*a*-peptides per polymer chain. The polymeric backbone is modified with a single high molecular weight mPEG (20kDa) and the remaining ε-lysine residues are capped with $mPEO_8$.

2.2. Cell culture

PC-3 cells (ATCC, Manassas, VA) from human PCa origin were cultured in F-12 growth medium supplemented with 10% FBS. Luciferase-transfected PC-3M-luc-C6 cells, a kind gift of Caliper LifeSciences (Hopkinton, MA), were maintained in MEM/EMBSS with 10% FBS, non-essential amino acids, L-glutamine, sodium pyruvate, and MEM vitamin solution. Both cell lines were grown as monolayers at 37°C in a humidified incubator containing 5% CO_2. The cells were harvested using TrypLE Express, and passaged every 4 to 5 days. Cell lines used in this study were not authenticated.

2.3. *In vitro* PDT

Phototoxicity was tested on PC-3 and luciferase-transfected PC-3M-luc-C6 cells. Aliquots of 1.2 x 10^4 and 1.0 x 10^4 cells, respectively, in 100 µL complete medium were seeded in 96-well plates and cultured for 12 hours to 70% confluence. Cells were given fresh complete medium containing uPA-PPP-4 at final concentrations of 0.5, 1.0, 2.0, 4.0 and 8.0 µM Pb*a* equivalents for 6 hours. Cells were washed twice with sterile HBSS and fresh medium was added. Plates were either placed on a light table equipped with OSRAM L 18W/67 Blue light tubes (PCI Biotech, Oslo, Norway) or kept in the dark. The radiation intensity was 7.5 mW/cm^2. Cells were irradiated at light doses of 2.5, 5.0 and 10 J/cm^2. Cell viability was measured using a mitochondrial MTT assay 24 hours after irradiation. First, cells were washed once with 200µL HBSS and 50 µL MTT (1mg/mL) in complete medium was added into each well. After 3hours, DMSO (200 µL) was added to dissolve formed violet formazan crystals. After brief agitation on a microplate shaker, the absorption at 525 nm was measured with a plate reader (Saphire, Tecan, Switzerland). Positive and negative controls were treated with complete medium or 0.1% Triton in NaOH 5M, respectively. Percentage cell survival was calculated with respect to control samples, as follows: [A (test-conc.) - A (100% dead)] / [A (100% viable) – A (100% dead)]*100. All conditions were tested in sextuplicates.

2.4. Prostate cancer model

Female swiss Nu/Nu mice (5 to 6 weeks, 17 to 22 g) were supplied by Charles River Laboratories (L'Arbresle, France). The mice were maintained with *ad libitum* access to sterile food and acidified water in a light cycled room acclimatized at 22 ± 2°C under pathogen free conditions. All experimental procedures on animals were performed in compliance with the Swiss Federal Law on the Protection of the Animals, according to a protocol approved by the local veterinary authorities. To induce xenografts, 1.5 x 10^6 cells were injected subcutaneously into the dorsal region of mice. Tumors of approximately 200 mm^3 in size were formed within 3 weeks after inoculation.

2.5. *In vivo* PDT

PC-3M-luc-C6 xenograft bearing mice (n=7) were injected retro-orbitally with uPA-PPP-4 (7.5 mg Pb*a* equivalents /kg) when tumors had an estimated volume of 200 mm^3 (3-4 weeks after inoculation). Tumors were irradiated with a light dose of 150 J/cm^2 at 665 ± 5 nm

(Ceralas I 670, Biolitec; Jena, Germany) 16 hours after conjugate administration. The radiation intensity was 70 mW/cm^2. Animals were maintained under 1–2% isoflurane inhalation during irradiation. Two other groups of animals received drug alone (n=4) and light alone (n=4). PDT effects were followed up to 90 days by bioluminescence imaging of animals using an IVIS 200 small-animal imaging system (Caliper Life Sciences Inc., Hopkinton, MA). 10 to 15 minutes before *in vivo* bioluminescence imaging, animals received an intra-peritoneal injection of D-luciferin (150mg/kg in DPBS). Mice were sacrificed when tumors reached volumes bigger than 1000 mm^3 or at the end of the study (90 days after treatment). Data were analyzed with Living Image 3.0 software (Caliper Life Sciences Inc.).

2.6. Qualitative analysis of prodrug cleavage products

Cleavage products were qualitatively analyzed in tumor, skin and muscle homogenates of the corresponding tissues 16 hours after systemic administration of uPA-PPP-4 (7.5 mg Pb*a* equivalents/kg). Briefly, frozen tissues were weighed and homogenized with a solution containing a protease-inhibitor cocktail (5 µL per 100 mg tissue) and acetonitrile:water (1:1; 1 mL per 100 mg tissue) by means of a tissue homogenizer (Eurostar digital IKA; Werke, Staufen, DE). The suspensions were sonicated (15 min at 14 kHz) and centrifuged (15 min at 1450 rpm). The supernatant was collected and extraction was repeated twice as described. Collected supernatants were lyophilized and subsequently reconstituted in acetonitril:water (1:1; 1 mL/100 mg tissue). Samples were sonicated (5 min, 14 kHz), filtered and subjected to analytical HPLC (LaChroma, Merck, Darmstadt, Germany) with a fluorescence detector (λ_{ex}=405 nm, λ_{em}=670nm). Separation was performed on a C18 column (Nucleodur gravity 3µ CC 125/4; Macherey-Nagel) using a 0.01%TFA/water/acetonitrile gradient.

2.7. Statistical analysis

Mean ± SD values were used for expression of data. Statistical analyses of data were done using Student's t test. Differences of $P < 0.05$ were considered statistically significant.

3. Results

The phototoxic effect induced by uPA-PPP-4 was investigated in the uPA-overexpressing PCa cells PC-3[19,20] and its luciferase mutant PC-3M-luc-C6 cells. The latter was chosen for the subsequent quantitative assessment of PDT studies *in vivo*. The effect of PDT on cells

treated with prodrug (0.5, 1.0, 2.0, 4.0 and 8.0 µM Pb*a* equivalents), either irradiated with a light dose of 2.5, 5.0 and 10 J/cm^2 or kept in the dark is summarized in Figure 2.

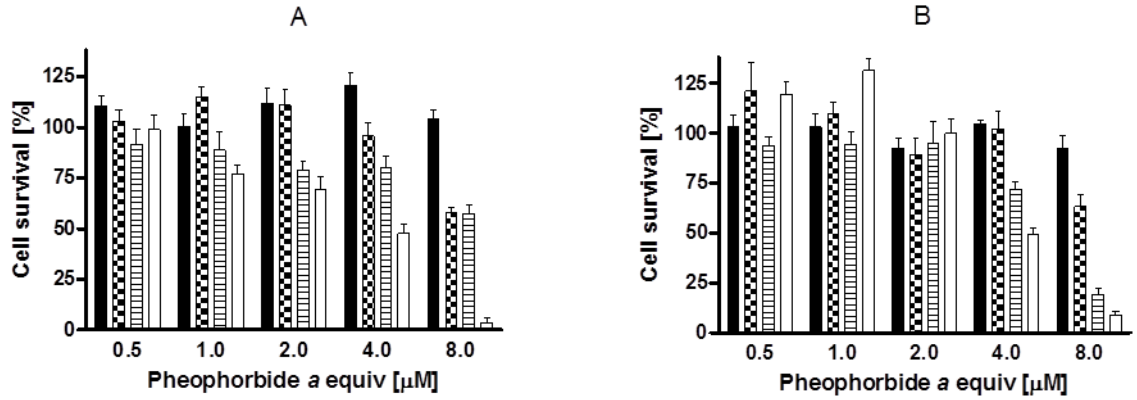

Figure 2. Light and drug dose-dependent phototoxicity induced by uPA-PPP-4 in (A) PC-3 and (B) PC-3M-luc-C6 cells. After incubation with the prodrug for 6 hours, cells were kept in the (■) dark or irradiated at (▪▫) 2.5 J/cm^2, (≡) 5 J/cm^2 or (□) 10 J/cm^2.

Both cell lines display a light and drug dose-dependent cell survival. uPA-PPP-4 alone presented little to no toxic effects as shown by cell survival percentages around 100% for all prodrug concentrations. Phototoxic effects were particularly evident at PS dose of 4.0 µM or higher. In PC-3 cells at 8 µM of Pb*a* equivalents approximately 50% of cells survived irradiation with 2.5 or 5 J/cm^2 of light, while at a dose of 10 J/cm^2 only 5% of cells remained viable. In PC3-3M-luc-C6 cells similar dose-response curves were observed. Cell survival after treatment with 4.0 and 8.0 µM of Pb*a* equivalents at all light doses were not statistically different between PC-3 and PC3-3M-luc-C6 cells (P values > 0.05) except for the condition 8 µM-5 J/cm^2 (P=2.11 x 10^{-5}).

We have used PC-3M-luc-C6 as basis for our experimental animal model for PCa, since they allow non-invasive monitoring of tumor growth through bioluminescence in a quantitative manner[21]. In this study, bioluminescence was used to assess the photodynamic efficacy of uPA-PPP-4 on tumors. Using whole body fluorescence imaging we found that tumors became selectively fluorescent 16 hours after prodrug administration[17]. Figure 3 illustrates the typical colocalization of fluorescence (rainbow-color scale) and bioluminescence (yellowhot-color scale) signals at this time point. Therefore, we selected this condition as drug-light interval in further PDT studies.

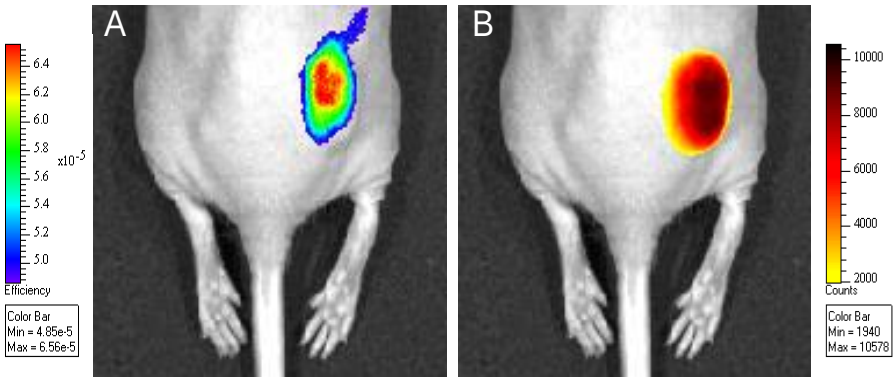

Figure 3. A, tumor fluorescence intensity 16 hours after retro-orbital administration of 2 mg/Kg of uPA-PPP-4 (as Pb*a* equivalents). **B**, bioluminescence of luciferase-expressing PC-3M-luc-C6 tumor 15 minutes after intra-peritoneal injection of D-luciferin.

HPLC analysis of tissue extracts confirmed the presence of the expected photoactive Pb*a*-GSGR fragment inside tumors (see Figure 4). Concentration of this compound in tumor was 27 times higher than in the skin. Some smaller fragments with longer retention times presumably due to further proteolytic processing were also found in the tumor and also to a much smaller extend in the skin. In contrast, no photoactive fragments were found in muscle.

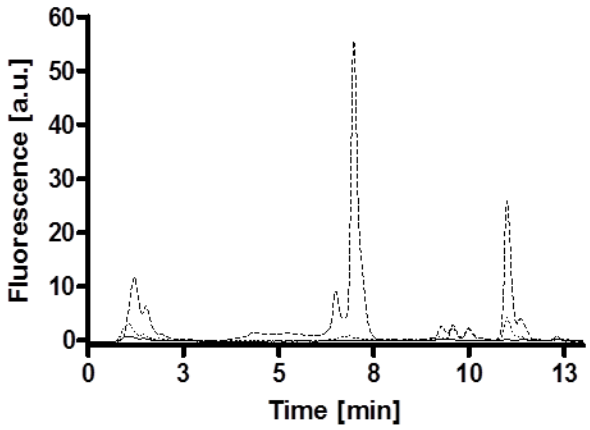

Figure 4. Analytical HPLC analysis of tumor (– –), skin (---), and muscle (—) extracts. In tumor a major peak was found at 7.5 minutes, corresponding to the cleaved Pb*a*-peptidyl-fragment. The small peaks at 6.3 and 10 minutes are other minor cleavage Pb*a* peptidyl-fragments. The same compounds were detected in skin in trace amounts. In muscle, no cleavage products were detected at all. Chromatograms show representative traces of mouse tissues 16 hours after retroorbital injection of uPA-PPP-4 (7.5 mg Pb*a* equivalents /kg).

For PDT, 7.5 mg Pb*a* equivalents per kg of prodrug was given to the mice via retroorbital injection and 16 hours later, tumors were irradiated with 150 J/cm^2 at 665 ± 5 nm. The radiation intensity was 70 mW/cm^2. Animals receiving the drug alone or irradiated with light alone were used as controls. Figure 5A shows a sequence of images before and after PDT taken on one mouse which ended up with complete remission. Bioluminescent images taken 15 minutes after administration of D-luciferin were used to quantify PCa cells. On the average a tumor volume of 200 mm^3 corresponds to 2.5 x 10^7 photon s^{-1}. Macroscopically, one day after treatment a local inflammatory response was visible. Inflammation developed into necrosis that appeared as a dark crust on the skin by day 3 and this was succeeded by healing and complete elimination of the tumor as confirmed with the bioluminescence image. The absence of a bioluminescent signal, which persisted over 90 days, indicated complete destruction of the tumor associated cells. Figure 5B summarizes the ROI analysis of sequences of images obtained for the three treatment regimes (PDT, drug alone and light alone) until day 15 after treatment. Mice receiving both light and drug showed a three log reduction of tumor bioluminescence already the day after treatment. In this group the mean bioluminescent signal remained below the initial value for at least 30 days (See Supplementary Material Figure 7). In contrast to PDT, light alone showed a slight reduction on tumor bioluminescence (P = 0.002). No reduction in bioluminescence was observed for animals receiving prodrug alone (P = 0.001). In both control groups, we observed a 4-fold increase in tumor bioluminescence until day 15 after treatment, day at which the animals were euthanized. No significant difference between control groups could be established (P = 0.6).

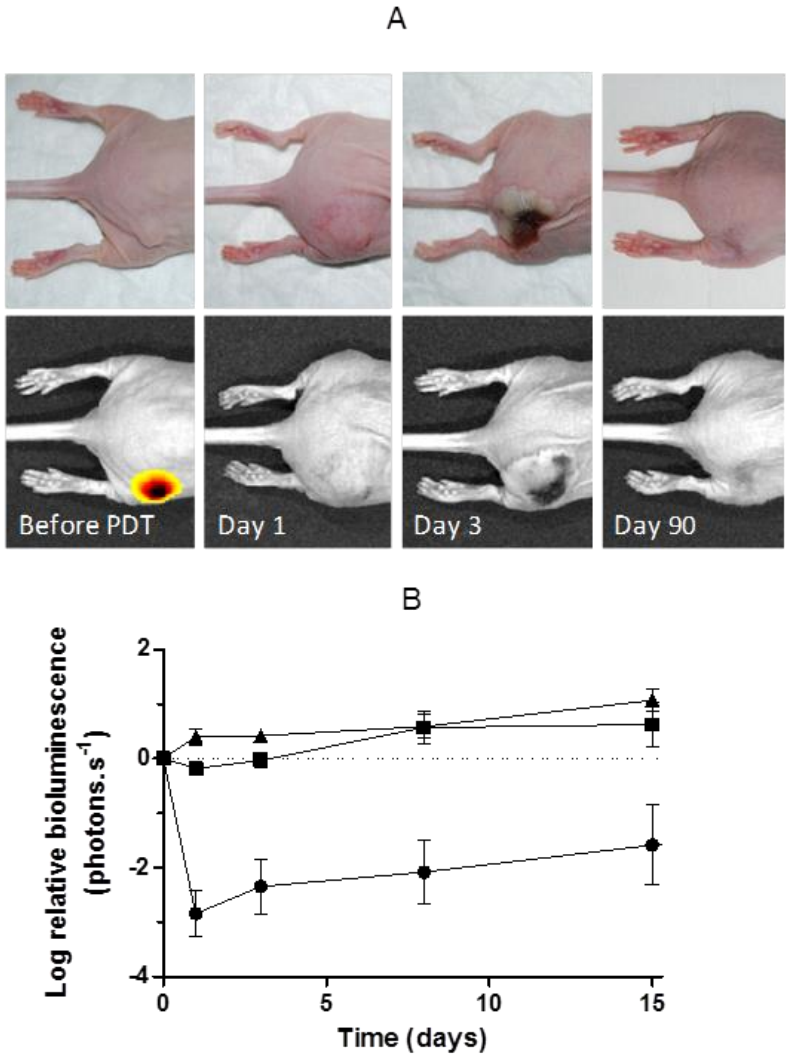

Figure 5. Treatment response was evaluated in terms of the remaining bioluminescence. **A**, *in vivo* imaging of a PC-3M-luc-C6 tumor-bearing mouse receiving PDT. The animal was administered with 7.5 mg Pb*a* equivalents/kg of the prodrug and 16 hours after, the tumor was irradiated with a light dose of 150 J/cm^2 at 665 ± 5 nm. The radiation intensity was 70mW/cm^2. Images were taken 15 minutes after peritoneal injection of d-luciferin. The intensity of the signal is correlated to cell density. The sequence on the top corresponds to the white-light images, from left to right: before, day 1, 3, and 90 after PDT. The sequence on the bottom corresponds to bioluminescent images, which confirmed total eradication of tumor cells. **B**, relative bioluminescence of PDT (•; n = 7), drug alone (▲; n = 4) and light alone (▪; n=4) groups. Tumor growth was monitored weekly by *in vivo* bioluminescence imaging. Images were taken 15 minutes after peritoneal injection of d-luciferin. Because control mice had to be sacrificed 15 days after PDT, comparison was done only for this period.

The survival of mice treated with PDT, prodrug alone, and light alone is presented in Figure 6.

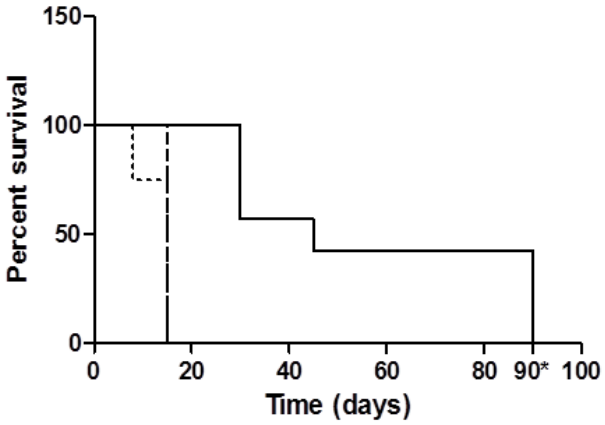

Figure 6. Survival curves in PCa xenografted mice after PDT (—) as compared to control groups of light alone (– –) or drug alone (---). Animals receiving PDT were treated with 7.5mg Pba equivalents /kg of the prodrug. 16 hours after administration, tumors were irradiated with a light dose of 150 J/cm^2 at 665 ± 5 nm. The radiation intensity was 70mW/cm^2. * The study was concluded after 90 days.

Animals treated with either prodrug alone or light alone had to be sacrificed before or on day 15 after treatment because of high tumor burden. The PDT survival curve was significantly different from these two groups (P = 0.001). Four animals which presented partial response to PDT were sacrificed on day 30 or 45 after treatment (57% survival). Complete remission to PDT treatment was observed in the 3 remaining mice (43% survival), which were sacrificed at the end of the study (90 days).

4. Discussion

Today, uPA is recognized as one of the key players in tumor progression in a wide panel of pathologies. Therefore, it has been identified as a target to specifically release cytotoxic agents. The first uPA sensitive prodrug was reported by Chung and Kratz[22]. It consisted of an albumin-bound doxorubicin containing a uPA substrate. This compound was stable in human plasma and the maximum tolerated dose was 4.5-folds the dose of free doxorubicin as determined in a single nude mouse experiment. Subsequently, other uPA-sensitive prodrugs of TNF[23] and anthrax toxin[24] containing motifs recognized by uPA have been evaluated, providing *in vivo* evidence of potent antitumor effects. Recently, a doxorubicin analogue was

used for the development of an uPA-sensitive prodrug platform[25]. The evaluation of one of these prodrugs in a variety of cancer cells lines showed a powerful inhibition of cell growth when activated *in vitro*.

The first polymeric photosensitizer prodrugs were developed by Choi *et al*.[26] for a more selective PDT. In this first generation PPP, multiple copies of the photosensitizer are tethered to a protease-sensitive polymeric backbone[26,27]. A major drawback of these compounds is their limited selectivity, since all proteases recognizing a Lys-Lys motif are able to activate them. To circumvent this problem a second generation PPPs have been developed introducing a small peptide linker between the PS and the polymeric backbone[18]. In this new design the linker-sequence is constructed according to the specific cleavage requirements of proteolytic enzymes of the target site.

Due to the known overexpression of uPA in PCa[16,28], we began to explore the potential of uPA-sensitive PPPs for a selective PDT of PCa. Upon the known uPA-sensitive substrates we have chosen the GSGRSAG peptide sequence for our PPPs[29]. These have been characterized and optimized in our lab in the last years[17,30].

We have demonstrated the selective cleavage of uPA-PPPs by uPA in the test tube and in the PCa cell lines DU145 and PC-3 overexpressing this protease[30]. We further demonstrated a selective accumulation/activation in a PCa-xenograft model[17]. In the present study, we combined enzymatic prodrug activation with light irradiation to obtain a phototoxic therapeutic effect. Because we have mostly used the wild type line PC-3 for *in vitro* optimization but intended to monitor PDT effects *in vivo,* we first investigated prodrug phototoxicity with a luciferase transfected mutant, PC-3M-luc-C6. Both cell lines were susceptible to PDT with uPA-PPP-4 and no dark toxicity was observed at the applied conditions.

Using *in vivo* fluorescence imaging, we observed a highly selective tumor fluorescence 16hours after prodrug administration. According to a previous study comparing the tumor fluorescence after administration of the prodrug and its analogous non-cleavable conjugate, this selective signal is mainly due to the site-specific proteolytic activation[17].

We further looked into the prodrug selectivity by analysis of various tissue samples for cleavage fragments. HPLC analysis of tumor tissue revealed a major peak corresponding to the Pb*a*-GRGS fragment, whereas neighboring skin contained only insignificant amounts of the cleavage product. In previous studies using orthotopic PCa models, PS (BPDMA) content

in tissues in close proximity to the prostate including nerve, rectum, and lymph node were found to be similar to those found in skin[31]. However, comparison of the PS distribution between orthotopic and subcutaneous tumors has shown significant differences[32], and therefore, the prodrug accumulation/activation in prostate surrounding tissues will need to be addressed by performing studies in an orthotopic model.

In vivo, uPA-PPP-4 produced a strong photodynamic effect after irradiation of fluorescent PC-3M-luc-C6 tumors. Bioluminescence images show a drastic reduction of tumor cells in all animals included in the PDT group. 3 animals were completely cured from PCa after PDT (43% cure rate). In these animals the total bioluminescence was reduced by three orders of magnitude as compared to the pretreatment images. Only few PCa cells remained after treatment in 4 animals. However, tumor growth was delayed and tumors reached original volumes only 15 days after treatment or later. The phototoxic effect induced by prodrug alone and by light alone was negligible.

Successful eradication of PCa bulky tumors has been also achieved with a single session of the "vascular" PDT agent, Tookad®[33]. Tookad® is so far, one of the most studied PS in the treatment of PCa and currently under clinical investigation for recurrent PCa[13]. In the present *in vivo* studies, our prodrug has shown results that indicate that more satisfactory outcomes of PDT can be expected in the future, thus overcoming some of Tookad®'s limitations. In the case of Tookad® collateral damage to the urinary and rectal function has been observed in the clinical trials[12,13].

In the present study, bioluminescence imaging helped to evaluate the tumor progression non-invasively. Furthermore, the ratio between the photon counts before PDT and 1 day after was indicative for the therapeutic outcome. This is in accordance with Fleshker *et al*.[34] who evaluated bioluminescence imaging in the treatment of breast cancer with WST11 after "vascular" PDT. We found that an average reduction of more than 3-log values was necessary to cure the animals. Thus, bioluminescence imaging can also help to improve the cure rate and adapt photodynamic treatment regimes.

To further improve the therapeutic outcome, repetitive PDT can be envisaged to address the occasional partial response. This concept of repetitive PDT has been already studied in spheroids models*, in vivo* and in the clinic mostly for the treatment of brain cancer[35-39]. According to these studies, the use of multiple sessions enhanced elimination of deep tumor cells infiltrating the surrounding brain. Combination treatments might also help to improve

PDT efficacy. It is now widely accepted that stress induced through photodynamic insult in certain cases initiates signaling pathways, leading to VEGF increase in PCa cells[40], which in turn contributes to tumor survival and regrowth. In this context, PDT in combination with anti-angiogenic agents for PCa might result in an increased anticancer response.

5. Conclusions

We developed a uPA-sensitive prodrug that is not toxic to PCa cells but efficiently inactivates cells *in vitro* after enzymatic activation and exposure to light. Activation of the prodrug occurs selectively in the tumors and is correlated with uPA overexpression. *In vivo* PDT can completely eliminate PCa xenografts as demonstrated by bioluminescence imaging. More research in orthotropic PCa models is envisioned to confirm the potential advantages of our strategy over other current PDT approaches.

Acknowledgements

NL is grateful for the financial support from the Swiss National Science Foundations through the grants 205320-122144, 205321_126834, K-32K1-116460, IZLSZ2_123011, and Diabetes.

Supplementary material

Chemicals

Anhydrous forms of dichloromethane (DCM), dimethylformamide (DMF), dimethylsulfoxide (DMSO), acetonitrile (ACN), diethylether and trifluoroacetic acid (TFA) were purchased from Acros Organics (Geel, Belgium). HGly-2-chlorotrityl resin (1.1 mmol/g), Boc-glycine, Fmoc-glycine, Fmoc-alanine, triphenylisopropylsilane, *N*,*N*-diisopropylethylamine (DIPEA), piperidine, picrylsulfonic acid aqueous solution (1 M), sodium iodide and ethanol were obtained from Fluka (Buchs, Switzerland). The L-aminoacids Fmoc(tBu)-serine, Fmoc(Pbf)-arginine, as well as O-(7-azabenzotriazol-1-yl)-*N*,*N*,*N*,*N*-tetramethyluronium hexafluorophosphate (HATU) were purchased from Genscript (Piscataway, USA). Poly-L-lysine HBr (PL; 18 kDa) were provided by Sigma-Aldrich (Buchs, Switzerland). Pheophorbide *a* (Pb*a*) was purchased from Frontier Scientific (Carnforth, UK). mPEG-SPA (20 kDa) was purchased from Nektar (San Carlos, USA). $mPEO_8$-NHS, were provided by ThermoFisher Scientific (Erembodegem, Belgium).

Synthesis of prodrug

uPA-PPP was synthesized in three steps. The L-configured peptide GSGRSAG containing the reported urokinase minimal substrate was synthesized using standard Fmoc chemistry. Subsequently, NHS-activated pheophorbide a (Pb*a*) was coupled to the N-terminus of the peptide and the corresponding Pb*a*-peptide conjugate was purified by preparative RP-HPLC (Waters Delta 600 HPLC) on a C8, Nucleosil 300-10 column (Macherey–Nagel) using a 0.01%TFA/water/acetonitrile gradient and molecular mass was analyzed by ESI-MS, with a Finnigan MAT SSQ 7000 (Thermo Electron Co. Waltham, MA).

Pb*a*-peptide was then loaded on PL (25 units per 100 free epsilon-NH_2 groups of the PL). For this propose, Pb*a*-peptide (3.06 mg, 3.1×10^{-6}mol), PL 18 kDa (2.00 mg, 0.11×10^{-6}mol, 1.1×10^{-5}mol of $-NH_2$ functions), and HATU (1.36 mg, 4.03×10^{-6}mol, 1.3 equivalents based on Pb*a*-peptides to be activated) were dissolved in DMSO (0.65 mL) and, DIPEA (3.7 mg, 3.3×10^{-5} mol, 3 equivalents of free -NH_2 functions of PL) was added to the stirred solution. The reaction was carried out in the dark under argon for 4 hours at room temperature. Complete loading of the Pb*a*-peptide on PL was confirmed by analytical RP-HPLC.

The polymeric carrier was further modified by the covalent coupling with high molecular weight *methoxypoly*(ethylene glycol) (mPEG) chains and secondly, by capping the remaining epsilon-lysine residues with methyl octa-ethylene oxide ($mPEO_8$). For this propose, mPEG-SPA 20 kDa (1.91/3.83 mg, 9.56/19.1 x 10^{-8}mol 1.1 equivalents based on the number of -NH_2 of PL in 0.2 mL DMSO) was added to the PL-Pb*a*-peptide solution under stirring and at 19 C°. The reaction was kept in the dark and left to proceed overnight at room temperature. Then, $mPEO_8$-NHS (3.61mg, 7.01 x x 10^{-6}mol; 0.1 mL in DMSO) was added. The reaction was kept in the dark and left to proceed overnight at room temperature. The crude product was purified by size exclusion chromatography using a sephacryl™ S-100 (Amersham Biosciences, Otelfingen, Switzerland) column and a mixture of acetonitrile/water/TFA (30:70:0.0025) as eluent. The fractions containing the product were pooled, lyophilized and stored light-protected at -20 °C until use.

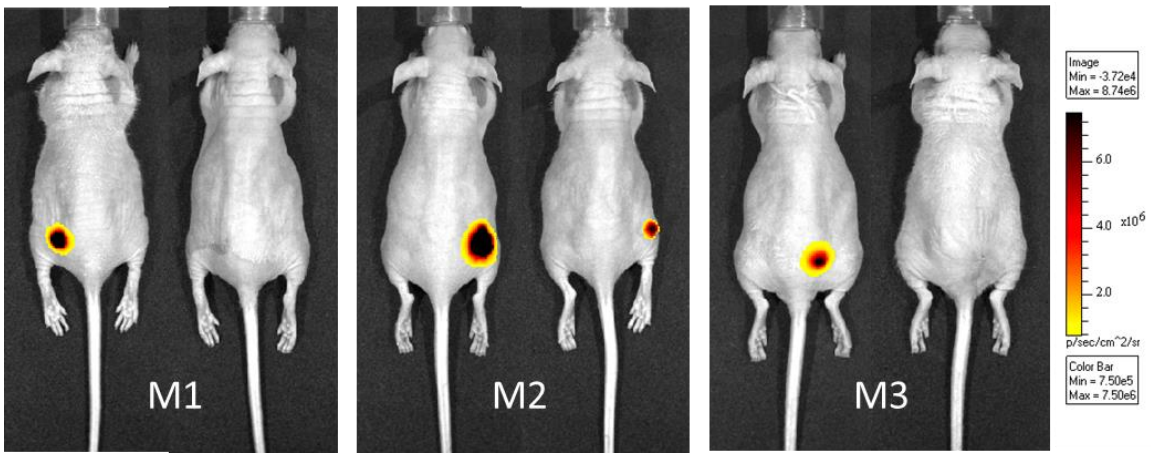

Figure 7. Bioluminescence imaging of three PCa-xenografted-mice before and 30 days after PDT. Animals bearing subcutaneous prostate tumors were treated with 7.5 mg/kg of uPA-PPP as Pb*a* equivalents and 16 hours after injection, tumors were irradiated with 150J/cm^2 at 665 ± 5 nm. Images were taken 15 min after intra-peritoneal injection of D-luciferin.

References

1. Jemal A, Bray F, Center MM, Ferlay J, Ward E, Forman D. Global cancer statistics. CA Cancer J Clin 2011;61:69-90.

2. Ahmed HU, Pendse D, Illing R, Allen C, van der Meulen JH, Emberton M. Will focal therapy become a standard of care for men with localized prostate cancer? Nat Clin Pract Oncol 2007;4:632-42.

3. Ahmed HU, Moore C, Emberton M. Minimally-invasive technologies in uro-oncology: The role of cryotherapy, hifu and photodynamic therapy in whole gland and focal therapy of localised prostate cancer. Surg Oncol 2009;18:219-32.

4. Pinthus JH, Bogaards A, Weersink R, Wilson BC, Trachtenberg J. Photodynamic therapy for urological malignancies: Past to current approaches. J Urol 2006;175:1201-7.

5. Moore CM, Hoh IM, Bown SG, Emberton M. Does photodynamic therapy have the necessary attributes to become a future treatment for organ-confined prostate cancer? Brit J Urol Int 2005;96:754-8.

6. Windahl T, Andersson SO, Lofgren L. Photodynamic therapy of localised prostatic cancer. Lancet 1990;336:1139.

7. Moore CM, Nathan TR, Lees WR, Mosse CA, Freeman A, Emberton M, et al. Photodynamic therapy using meso tetra hydroxy phenyl chlorin (mthpc) in early prostate cancer. Lasers Surg Med 2006;38:356-63.

8. Zaak D, Sroka R, Höppner M, Khoder W, Reich O, Tritschler S, et al. Photodynamic therapy by means of 5-ala induced ppix in human prostate cancer - preliminary results. Med Laser Appl 2003;18:91-95.

9. Lepor H. Vascular targeted photodynamic therapy for localized prostate cancer. Rev Urol 2008;10:254-61.

10. Verigos K, Stripp DCH, Mick R, Zhu TC, Whittington R, Smith D, et al. Updated results of a phase i trial of motexafin lutetium-mediated interstitial photodynamic therapy in patients with locally recurrent prostate cancer. J Environ Pathol Toxicol Oncol 2006;25:373-88.

11. Patel H, Mick R, Finlay J, Zhu TC, Rickter E, Cengel KA, et al. Motexafin lutetium-photodynamic therapy of prostate cancer: Short- and long-term effects on prostate-specific antigen. Clin Cancer Res 2008;14:4869-76.

12. Trachtenberg J, Bogaards A, Weersink RA, Haider MA, Evans A, McCluskey SA, et al. Vascular targeted photodynamic therapy with palladium-bacteriopheophorbide photosensitizer for recurrent prostate cancer following definitive radiation therapy: Assessment of safety and treatment response. J Urol 2007;178:1974-9; discussion 79.

13. Trachtenberg J, Weersink RA, Davidson SR, Haider MA, Bogaards A, Gertner MR, et al. Vascular-targeted photodynamic therapy (padoporfin, wst09) for recurrent prostate cancer after failure of external beam radiotherapy: A study of escalating light doses. Brit J Urol Int 2008;102:556-62.

14. Arumainayagam N, Moore CM, Ahmed HU, Emberton M. Photodynamic therapy for focal ablation of the prostate. World J Urol 2010;28:571-6.

15. Maeda H, Wu J, Sawa T, Matsumura Y, Hori K. Tumor vascular permeability and the epr effect in macromolecular therapeutics: A review. J Control Release 2000;65:271-84.

16. Cozzi PJ, Wang J, Delprado W, Madigan MC, Fairy S, Russell PJ, et al. Evaluation of urokinase plasminogen activator and its receptor in different grades of human prostate cancer. Hum Pathol 2006;37:1442-51.

17. Zuluaga MF, Gabriel D, Lange N. Enhanced prostate cancer targeting by modified protease sensitive photosensitizer prodrugs. Mol Pharm 2012;9:1570-9.

18. Gabriel D, Campo MA, Gurny R, Lange N. Tailoring protease-sensitive photodynamic agents to specific disease-associated enzymes. Bioconjug Chem 2007;18:1070-7.

19. Sehgal I, Forbes K, Webb MA. Reduced secretion of mmps, plasminogen activators and timps from prostate cancer cells derived by repeated metastasis. Anticancer Res 2003;23:39-42.

20. Forbes K, Gillette K, Kelley LA, Sehgal I. Increased levels of urokinase plasminogen activator receptor in prostate cancer cells derived from repeated metastasis. World J Urol 2004;22:67-71.

21. Jenkins DE, Yu SF, Hornig YS, Purchio T, Contag PR. *In vivo* monitoring of tumor relapse and metastasis using bioluminescent pc-3m-luc-c6 cells in murine models of human prostate cancer. Clin Exp Metastasis 2003;20:745-56.

22. Chung DE, Kratz F. Development of a novel albumin-binding prodrug that is cleaved by urokinase-type-plasminogen activator (upa). Bioorg Med Chem Lett 2006;16:5157-63.

23. Gerspach J, Nemeth J, Munkel S, Wajant H, Pfizenmaier K. Target-selective activation of a tnf prodrug by urokinase-type plasminogen activator (upa) mediated proteolytic processing at the cell surface. Cancer Immunol Immunother 2006;55:1590-600.

24. Rono B, Romer J, Liu SH, Bugge TH, Leppla SH, Kristiansen PEG. Antitumor efficacy of a urokinase activation-dependent anthrax toxin. Mol Cancer Ther 2006;5:89-96.

25. Barthel BL, Rudnicki DL, Kirby TP, Colvin SM, Burkhart DJ, Koch TH. Synthesis and biological characterization of protease-activated prodrugs of doxazolidine. J Med Chem 2012;55:6595-607.

26. Choi Y, Weissleder R, Tung CH. Selective antitumor effect of novel protease-mediated photodynamic agent. Cancer Res 2006;66:7225-9.

27. Campo MA, Gabriel D, Kucera P, Gurny R, Lange N. Polymeric photosensitizer prodrugs for photodynamic therapy. Photochem Photobiol 2007;83:958-65.

28. Shariat SF, Roehrborn CG, McConnell JD, Park S, Alam N, Wheeler TM, et al. Association of the circulating levels of the urokinase system of plasminogen activation with the presence of prostate cancer and invasion, progression, and metastasis. J Clin Oncol 2007;25:349-55.

29. Ke SH, Coombs GS, Tachias K, Navre M, Corey DR, Madison EL. Distinguishing the specificities of closely related proteases. Role of p3 in substrate and inhibitor discrimination between tissue-type plasminogen activator and urokinase. J Biol Chem 1997;272:16603-9.

30. Gabriel D, Zuluaga MF, Martinez MN, Campo MA, Lange N. Urokinase-plasminogen-activator sensitive polymeric photosensitizer prodrugs: Design, synthesis and *in vitro* evaluation. J Drug Deliv Sci Tec 2009;19:15-24.

31. Momma T, Hamblin MR, Wu HC, Hasan T. Photodynamic therapy of orthotopic prostate cancer with benzoporphyrin derivative: Local control and distant metastasis. Cancer Res 1998;58:5425-31.

32. Chen B, Pogue BW, Zhou X, O'Hara JA, Solban N, Demidenko E, et al. Effect of tumor host microenvironment on photodynamic therapy in a rat prostate tumor model. Clin Cancer Res 2005;11:720-7.

33. Koudinova NV, Pinthus JH, Brandis A, Brenner O, Bendel P, Ramon J, et al. Photodynamic therapy with pd-bacteriopheophorbide (tookad): Successful *in vivo* treatment of human prostatic small cell carcinoma xenografts. Int J Cancer 2003;104:782-9.

34. Fleshker S, Preise D, Kalchenko V, Scherz A, Salomon Y. Prompt assessment of wst11-vtp outcome using luciferase transfected tumors enables second treatment and increase in overall therapeutic rate. Photochem Photobiol 2008;84:1231-7.

35. Madsen SJ, Sun CH, Tromberg BJ, Hirschberg H. Repetitive 5-aminolevulinic acid-mediated photodynamic therapy on human glioma spheroids. J Neurooncol 2003;62:243-50.

36. Bogaards A, Varma A, Zhang K, Zach D, Bisland SK, Moriyama EH, et al. Fluorescence image-guided brain tumour resection with adjuvant metronomic photodynamic therapy: Pre-clinical model and technology development. Photochem Photobiol Sci 2005;4:438-42.

37. Hirschberg H, Sorensen DR, Angell-Petersen E, Peng Q, Tromberg B, Sun CH, et al. Repetitive photodynamic therapy of malignant brain tumors. J Environ Pathol Toxicol Oncol 2006;25:261-79.

38. Zilidis G, Aziz F, Telara S, Eljamel MS. Fluorescence image-guided surgery and repetitive photodynamic therapy in brain metastatic malignant melanoma. Photodiagnosis Photodyn Ther 2008;5:264-6.

39. Mathews MS, Angell-Petersen E, Sanchez R, Sun CH, Vo V, Hirschberg H, et al. The effects of ultra low fluence rate single and repetitive photodynamic therapy on glioma spheroids. Lasers Surg Med 2009;41:578-84.

40. Solban N, Selbo PK, Sinha AK, Chang SK, Hasan T. Mechanistic investigation and implications of photodynamic therapy induction of vascular endothelial growth factor in prostate cancer. Cancer Res 2006;66:5633-40.

PEPTIDIC SCAFFOLDS FOR TARGETED DELIVERY OF PROTEASE-SENSITIVE PHOTOSENSITIZER PRODRUGS IN PHOTODYNAMIC THERAPY

Nawal SEKKAT[1], Andrej BABIC[1] and Norbert LANGE[1]

[1]School of Pharmaceutical Sciences, University of Lausanne/Geneva, Geneva, 30, Quai Ernest Ansermet, Geneva CH-1211, Switzerland

*Corresponding author e-mail: norbert.lange@unige.ch

ABSTRACT

Recently, photosensitizer (PS) based protease-sensitive prodrugs have been successfully tested *in vitro* and in experimental animal models for photodynamic therapy (PDT) and fluorescence imaging of cancer. Until today, two main strategies have been followed for this purpose. The first is based on the coupling of a pair of PS or PS/quencher on each extremity of a protease-sensitive peptide linker. The second approach consists of the grafting of multiple copies of a photosensitizer (PS) on a polymeric carrier directly or through a protease-sensitive peptide linker. Due to energy transfer, such prodrugs exhibit no or only low native fluorescence and reactive oxygen species (ROS) production upon excitation with light. Following proteolytic cleavage, release of the PS occurs and fluorescence signal amplification and ROS production can be observed. Although the use of a polymeric carrier results in high quenching efficiencies, this approach is mainly limited by batch-to-batch variability of the polymeric carrier and the unknown exact chemical nature, due to the statistical approach of compound preparation. In this study, a novel approach is presented where a defined cyclopeptidic scaffold is used as a versatile drug delivery system for the PS pheophorbide-a. Fluorescence quenching, selective proteolytic activation, water-solubility and phototoxic efficacy on cancer cell lines have been studied. These properties have been modulated and optimized through the tuning and variation of **1)** the number and **2)** nature of the pheophorphide-protease-sensitive peptides used (urokinase plasminogen like activator (uPA) or matrix metalloproteinase-2 (MMP-2) sensitive peptides) and **3)** the grafting of PEG moieties of two different molecular weights (5 and 20kDa).

The highest phototoxic effect was obtained for conjugates bearing PEG (20kDa) and multiple copies of pheophorbide-MMP-2 sensitive peptides. Significant cell destruction (50%) was observed for these conjugates at low drug doses of 100 nM under a light dose of 10 J/cm^2. These conjugates presented the appreciable advantage of remaining non-toxic in the dark on PC-3 and HT1080 cell lines at doses as high as 10 μM, demonstrating a great opportunity for *in vivo* PDT-application of this approach.

KEY WORDS: Photodynamic therapy, Regioselectively Addressable Functionalized Templates, urokinase plasminogen activator, matrix metalloproteinases, drug delivery, targeting, peptidic scaffolds, oligomeric prodrugs, protease-sensitive prodrugs, cancer, photosensitizers

1. Introduction

Photodynamic therapy (PDT) is a non-invasive technique for the treatment of several diseases such as microbial infections[1], rheumatoid arthritis[2], age-related macular degeneration[3], and cancer[4]. PDT is based on the combined effect of three non-toxic components: a photosensitizer (PS), light, and oxygen. Hence, PDT relies on the PS activation by light, which subsequently results in cellular damage and destruction through formation of reactive oxygen species (ROS). To improve pharmacokinetic and pharmacodynamics properties of conventional PS and reduce the sides effects associated with this treatment, we and others[5-15] have developed a protease sensitive PS delivery system. The approach named polymeric photosensitizer prodrugs (PPPs) was adapted from the concept and precursory work of Ringsdorf[16], Duncan[17] and Kopecek[18]. A polymeric backbone bears several moieties of PS-protease cleavable peptides. Due to the close proximity of the PS moieties in which efficient energy transfer occurs, the prodrug is optically "silent" in its native configuration. Upon proteolytic cleavage, PS are released and photoactivity with respect to fluorescence emission and ROS formation is restored [19]. Although proteases are essential enzymes capable of cleaving peptidic bonds and are involved in many non-pathological conditions such as coagulation, wound healing and digestion, their overexpression and dysfunction is known to be associated with cancer.

Proteases such as urokinase-like plasminogen activator (uPA) and matrix metalloproteinases were reported to be up-regulated in breast, ovarian, colorectal, bladder, and prostate cancers[20-33]. Taking advantage of these pathological features is one way of improving selective delivery of the PS. The PPP approach using polymeric carriers, although being successfully assessed in PDT treatment *in vitro* and *in vivo* of prostate cancer [8,9,15] and many others [5,34-38] , have some drawbacks with respect to potential clinical use. First, batch-to-batch variations and high polydispersity of the polymer carrier might impede the transfer to clinical practice. Furthermore, the exact position as well as exact number of PS per polymeric carrier is unknown due to the statistical nature of PPP synthesis. In this paper, we propose an alternative cyclopeptidic carrier system for the protease-mediated delivery of quenched PS prodrugs. Since the pioneering work of Mutter *et al.*[39] regioselectively addressable functionalized templates (RAFT) cyclopeptidic structures have been envisioned as promising scaffolds. Their high stability toward hydrolysis and enzymatic degradation combined with their defined and modulable structure that enables orthogonal and versatile chemical

functionalization of a wide range of chemicals makes them highly valuable tools for drug delivery. Recently, Dumy and co-workers have reported the successful synthesis and evaluation of RAFT systems for the study of integrins and imaging of tumors[40-50]. Although very promising results were reported for the use of these templates as drug delivery systems no evaluation of the RAFTs as protease sensitive drug delivery system has been reported so far.

In this study, we report the development and evaluation of RAFT for protease-mediated drug delivery for PDT of cancer using pheophorbide a as PS. As illustrated by Figure 1, these "oligomeric" prodrugs are expected to give low native fluorescence due to efficient energy transfer as a function of PS loading on the RAFT. However, upon proteolytic cleavage, these will give rise to increased fluorescence and ROS production leading to Photodetection (PD)/PDT effect.

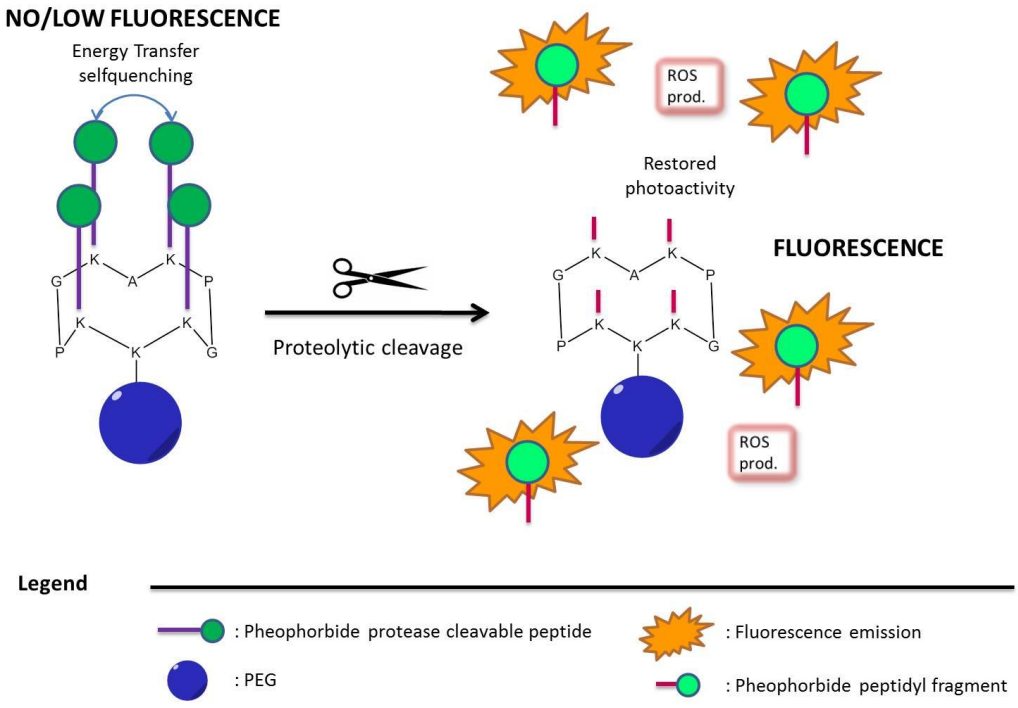

Figure 1. Schematic illustration of Peptide Based RAFT-Prodrugs Principle

Figure 1 represents schematically the principle behind the prodrug design approach used in this study. Before proteolytic cleavage, the prodrug is "silent" due to energy transfer between the closely positioned photosensitizer (PS) moieties (here pheophorbide a) on RAFT. With increasing number of PS moieties attached to RAFT, this quenching is expected to increase.

When the prodrug reaches the target tissue, peptidyl-pheophorbide fragments are released upon enzymatic cleavage. This release enables imaging and destruction of the diseased tissue by fluorescence emission of the PS and reactive oxygen species production.

This study investigates the influence of the PS loading on RAFT for suitable quenching/activation properties. Furthermore, the influence of PEGylation and the influence of the PEG molecular weight with respect to synthetic yield, water solubility, and PDT efficacy were evaluated. Finally, two proteases uPA and matrix metalloproteinase-2 (MMP-2) were targeted using uPA/MMP-2 sensitive peptide linkers and are expected to bring selectivity toward tumors. The evaluation of these prodrugs was performed *in vitro* using two cancer cells lines *i.e.* human prostate cancer cell line PC-3 and human fibrosarcoma HT1080 cell line.

2. Materials and Methods

2.1. Chemicals

Anhydrous forms of dimethylsulfoxide (DMSO), dichloromethane (DCM), methanol (MeOH) and ethyl acetate (EtAc), N-(3-dimethylaminopropyl)-N'-ethyl-carbodiimide hydrochloride (EDC), N-hydroxysuccinimide (NHS), N,N-diisoproprylethylamine (DIPEA), O-(7-aza-benzotriazol-1-yl)-N,N,N,N-tetramethyluronium hexafluorophosphate (HATU), piperidine, 1M picrylsulfonic acid and triisopropylsilane, HGly-2-chlorotrityl resin (1.1mmol/g), Fmoc-Gly-OH, Fmoc-Val-OH, Fmoc-Pro-OH, Fmoc-Leu-OH and Boc-Glycine were purchased from Sigma-Aldrich (Buchs, Switzerland). Pheophorbide a was purchased from Frontier Scientific (Logan, UT). Methoxy PEG Succinimidyl Carboxymethyl Ester (mPEG-SPA) of 5 and 20 kDa were obtained from Nektar (San Carlos, USA) and JenKem Technology (Texas, USA) respectively. Acetonitrile (ACN) and Methanol HPLC grade were bought from Biosolve BV (Valkenswaard, Netherlands) and trifluoroacetic acid (TFA) was purchased from Acros Organics (Geel, Belgium). Urokinase peptide (GSGRSAG) and cyclic peptide scaffolds were purchased from CASLO **(**CASLO Aps (Lyngby, Denmark))**.**

2.2. Cell Culture Chemicals

The following chemicals were used for the cell culture Trypsin 0.25%-EDTA solution, Nutrient Mixture Kaighn's Modification (F-12K) with L-Glutamine, Dulbecco's phosphate buffer saline (DPBS) solution without calcium and magnesium, Dulbecco's Modified Eagle

Medium (DMEM+ GlutaMAX-I) containing Pyruvate and 1g/L D-Glucose, Penicillin 10'000 units/mL and Streptomycin 10 000 µg/mL solution and 0.25% trypsine-EDTA solution (1x) were provided by Life Technologies Corporation (Paisley, UK). DMSO as well as ethanol of analytical grade were purchased from Fisher Scientific (Leicestershire, UK). Fetal Bovine Serum (FBS) (PAA Laboratories GmbH (Pasching, Austria)), Triton X-100 of Applichem. (ITW Company, Germany), sodium hydroxide (NaOH) of Reactolab S.A. (Servion, Switzerland), and 3-(4,5-Dimethylthiazol-2-yl)-2,5-diphenyl-2H-tetrazolium bromide **(**Thiazolyl Blue Tetrazolium Bromide**)** (Sigma-Aldrich Company (St. Louis, MO, USA)) were used for the cellular assays. Urokinase (high molecular weight, human urine) was obtained from Calbiochem/VWR (Zug, Switzerland).

2.3. Cell Culture

PC-3 cells (ATCC, Manassas, VA) were maintained in monolayers in F-12K medium supplemented with 10% fetal bovine serum (FBS) and 100µL/mL streptomycin and 100IE/mL penicillin in a humidified incubator containing 5% CO_2. HT1080 cells were grown in monolayers using Dulbecco's Modified Eagle Medium (1g/L D-Glucose and with Pyruvate) supplemented with 10% FBS and containing the same amounts of antibiotics as previously described. Cells were trypsinized using 0.25% Trypsin-EDTA solution.

2.4. RAFT-Prodrugs Synthesis

Figure 2 illustrates the chemical pathway synthesis of the RAFT conjugate.

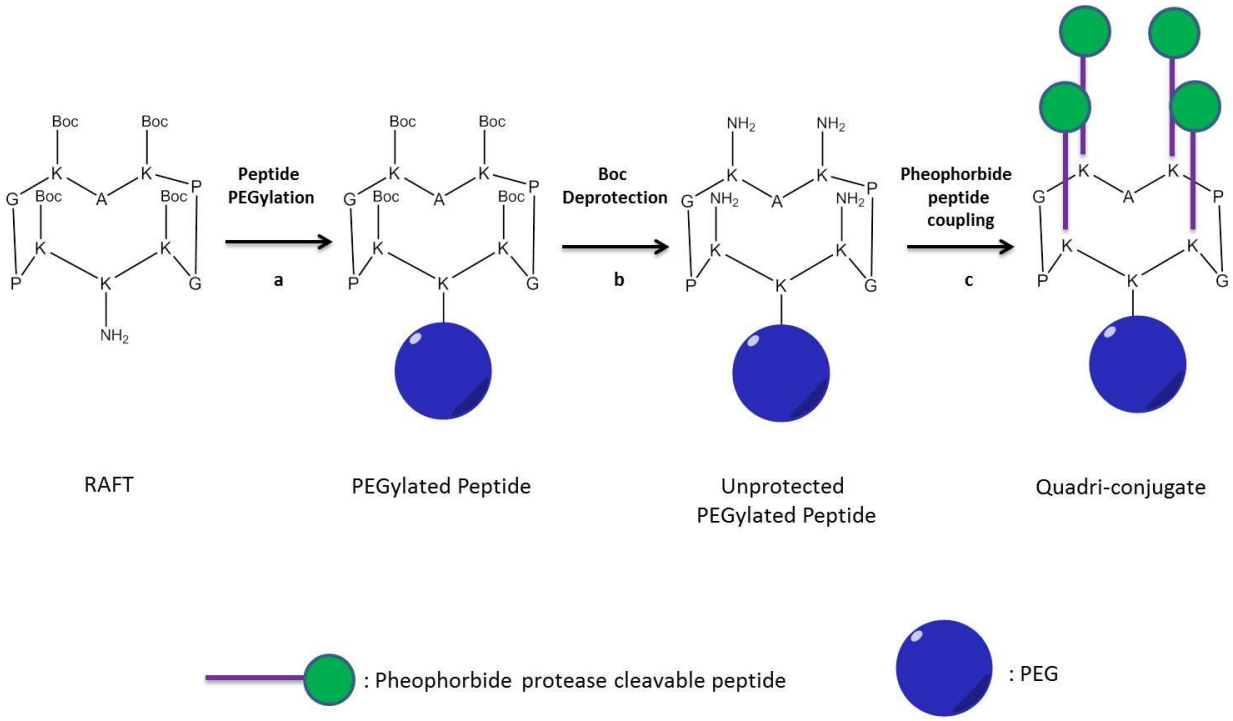

Figure 2. Schematic view of the conjugates synthesis exemplified by the tetra-conjugate synthesis. (a) DMSO, PEG-SPA, overnight under argon at RT, dialysis; (b) 50% DCM, TFA, 1h, evaporation; (c) DMSO, HATU, DIPEA, Pheophorbide-peptide, overnight under argon at 50°C, dialysis, filtration and size exclusion purification.

2.5. Synthesis of MMP2-cleavable peptide (GPLGVG)

Synthesis of MMP-2 cleavable peptide was performed using a standard Fmoc strategy [51] on HGly-2-chlorotrityl resin 200-400 mesh (1.1mmol/g, 0.355g, 0.39 mmol). ESI-MS: 499.3 $([M+H])^+$ =499.3 calculated for $C_{22}H_{39}N_6O_7^+$ and substrate selectivity towards MMP-2 was reported earlier by Lee *et al*.[52].

2.6. Synthesis of pheophorbide NHS ester

Synthesis of Pheophorbide a-NHS ester was performed as described previously[7].

2.7. Synthesis of pheophorbide peptide cleavable peptides

To a solution of the corresponding peptide (urokinase or MMP-2 cleavable peptide) (30mg, 1mL) in DMSO was added pheophorbide a-NHS ester in DMSO (0.8 equiv., 1mL). The base

(DIPEA, 20 equiv.) was added drop wise and the reaction was allowed to proceed overnight under argon. The reaction was then quenched by addition of a mixture of 50% water/50% acetonitrile/0.1% TFA (2.5mL) to reach pH 3. The solution was then filtrated and pheophorbide peptide was purified by preparative RP-HPLC (Waters Delta 600 HPLC) using a C18 column (Nucleodur 250x21, 5µm column from Macherey-Nagel) at a flow rate of 10mL/min using a gradient water-0.1% TFA/ acetonitrile gradient. Purification was monitored through absorbance (UV/VIS) at 280 and 400nm and products of interest were collected, lyophilized and obtained as green solids that were stored at -20°C and kept in the dark. ESI-MS: 1165.5 $([M+H])^+$ =1165.6 calculated for $C_{56}H_{73}N_{14}O_{14}^+$ obtained for L and D-urokinase pheophorbide peptides and 1074.3 $([M+H])^+$ =1074.25 calculated for $C_{59}H_{73}N_{10}O_{11}^+$ for MMP-2- pheophorbide peptide.

2.8. Synthesis of PEGylated cyclopeptide

To a solution of the corresponding cyclic peptide (see Table 1) carrying one unprotected lysine residue on the lower face of the scaffold (5mg) in 1mL DMSO was added a solution of PEG-SPA (0.5 equiv. based on free NH_2 functions on the cyclic peptides) of 20kDa or 5kDa. DIPEA (30 equiv. based on free NH_2 functions on the cyclic peptides) was added drop wise and the reaction proceed overnight under argon. Dialysis was performed in water for purification of the corresponding PEGylated cyclopeptides using dialysis membranes of 1000 and 6-8000 g/mol (Spectra/Por® Dialysis Membrane, SpectrumLabs Inc.). The products were then lyophilized and obtained as white solids. MALDI: **See Table 2.** Purity was confirmed by RP-HPLC using linear gradient of water-0.1% TFA/ acetonitrile and UV and Light-Scattering Detector (see Figure 9 in supplementary material).

2.9. Synthesis of PEGylated cyclopeptide pheophorbide peptide

Boc protections on PEGylated cyclopeptides were first removed by dissolving the products in a 2mL mixture of DCM/TFA (50/50). After 1h agitation, DCM and TFA were removed by high vacuum evaporation and after 3 successive cycles of co-evaporation using methanol and ethyl acetate alternatively. The remaining product was solubilized in 1mL DMSO and the corresponding pheophorbide peptide (7 equiv. based on the deprotected lysines corresponding to free NH_2 functions on the cyclic peptides, 500µL) and HATU (3 equiv. based on pheophorbide-peptide to be activated, 200µL) were added. DIPEA (30 equiv. based on the number of NH_2 functions on the PEGylated cyclopeptides) was added drop wise and the

mixture stirred under argon overnight in an oil bath set to 50°C. Completion of the reaction was monitored by RP-HPLC and established as the amount of pheophorbide peptide and reaction time where the peak corresponding to pheophorbide peptide did not decrease any-more. The reaction was then quenched by adding a water/acetonitrile/TFA mixture (70/30/0.025%) (4 mL). The resulting solution was dialysed as described above (Mw cut-off= 1000 or 6-8000 g/mol). After dialysis, the solution was concentrated by high vacuum evaporation and solubilized in water (3.5mL). After, filtration, the solution was purified by size exclusion chromatography (SEC) using a sephacryl TM S-100 (Amersham Biosciences, Otelfingen, Switzerland) column and water/acetonitrile/TFA mixture (70/30/0.025%) as eluent. The fraction containing the corresponding product of interest was lyophilized and obtained as a green solid that was stored at -20°C away from light exposition. MALDI: **See Table 2**.

2.10. Compounds structures, denomination and characteristics

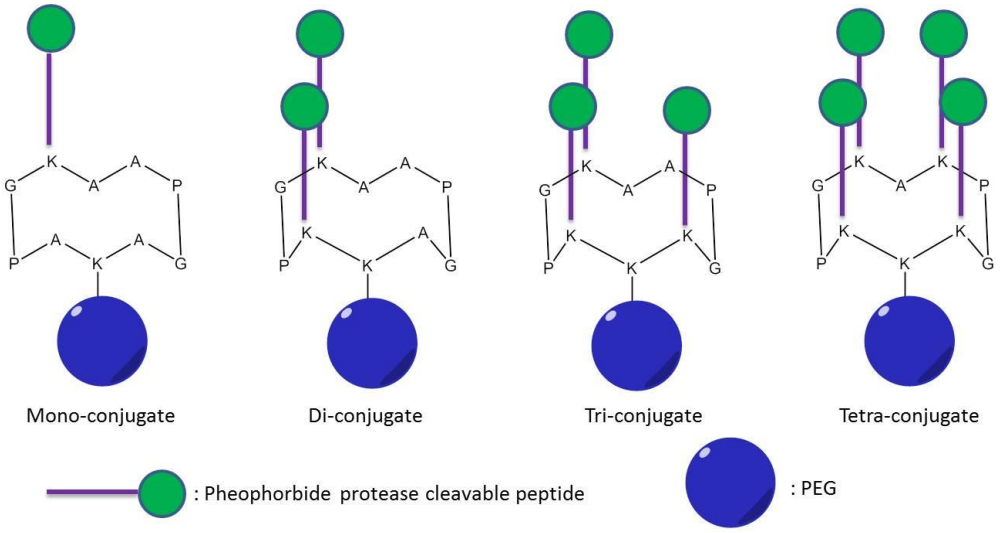

Figure 3. Schematic illustration of Peptide Based RAFT –Prodrugs Design

Figure 3 shows the schematic representation of mono, di, tri and tetra substituted conjugates synthesized in this study. First, cyclic peptides listed in Table 1 are PEGylated. Subsequently one, two, three or four pheophorbide peptide protease cleavable moieties were attached to the respective carriers. Table 2 lists the conjugates synthesized in this study as well as their characteristics and yield of reactions.

2.11. *In vial* uPA cleavage of L and D configured conjugates

Conjugate-PBS solutions of 5 μM with respect to pheophorbide a content were incubated at 37°C in the dark with or without urokinase for 1 hour. Activation of the conjugates by the release of peptidyl fragment pheophorbide a-Gly-Ser-Gly-Arg was monitored by analytical RP-HPLC using a nucleodur C18 gravity 3μ CC 125/4 column from Macherey-Nagel and using a 0.1% TFA water/acetonitrile gradient. Fluorescence was measured using the Safire under the same conditions as described above.

2.12. Fluorescence measurements of intact conjugates

Fluorescence intensity of conjugates-PBS solutions of 5μM with respect to pheophorbide a was measured at 37°C by the Safire using an excitation wavelength of 400nm and emission wavelength of 670nm.

2.13. *In vitro* activation on PC-3 cells

PC-3 cell suspension (100μL) containing 1.8 x 10^4 cells were seeded in 96-well plates and allowed to attach overnight. Subsequent washing with 200 μL PBS was performed and cells were incubated with solutions of 1μM corresponding conjugates in F12K medium containing 10%FBS. Fluorescence was measured as described previously. The increase in fluorescence emission was calculated by subtraction of the fluorescence intensity Ft_0 immediately after incubation start, from the value Ft_x obtained at time x and divided by Ft_0. All conditions were tested in sextuplicate and are expressed as mean value +/- S.D.

2.14. Dark and light toxicity on PC-3 and HT1080 cells

Phototoxicity of the conjugates was performed in the cancer cell lines PC-3 and HT1080 of human prostate and fibrosarcoma origin, respectively , using 3-(4,5-Dimethylthiazol-2-yl)-2,5-diphenyl-2H-tetrazolium bromide assay (MTT assay). Cells were seeded in 96-well plates as aliquots of 100 μL containing 1.8 x 10^4 cells and 1.2 x 10^4 cells, respectively, and allowed to grow to 70-80% confluence. Cells were incubated with prodrug containing solutions for 8 hours then rinsed twice with 200 μL PBS followed by addition of 100 μL of fresh medium. Cells were subsequently, kept in the dark (plate control) or irradiated with light doses of 10 or 20J/cm^2 (PCI light, PCI Biotech, Oslo Norway) 50 μL of fresh medium was added after irradiation and an MTT assay (cells survival assay) was performed 24 hours after irradiation according to the provider's instructions. Percentage cell survival was calculated with respect

to control samples, as follows: [A (test-conc.) - A (100% dead)] / [A (100% viable) – A (100% dead)]*100. All conditions were tested in sextuplicates.

3. Results and Discussion

3.1. Denomination and synthesis of conjugates

Table 1 and Table 2 summarize the terms of the conjugates prepared for this paper. It lists their characteristics as well as the yields obtained for each compound. Due to thorough purification steps in order to limit the amount of conjugate mixtures, yields are lower with increasing PS units. *In vitro* characterization and evaluation of such conjugates is presented below.

Table 1. PEGylated Peptides Denomination, Characteristics and Yields

Compounds	Protease Cleavable Peptide	Expected Molecular Weight	Molecular Weight Found [a)]	Yield
PEG-SPA	N.A.	5 or 20kDa	5687Da±858 or 21.6±1.2kDa	-
Peptide-1 K(Boc)-AAPGAK(mPEG)APG	N.A.	5949Da or 20.7kDa	6430Da±530 or 22.0±0.2 kDa	85%
Peptide-2 K(Boc)AAPGAK(mPEG)K(Boc)PG	N.A.	6106Da or 20.9kDa	6633±572 or 22.0±0.2 kDa	85%
Peptide-3 K(Boc)AAPGK(Boc)K(mPEG)K(Boc)PG	N.A.	6263Da or 21.0kDa	6791±486.or 22.0±0.2 kDa	85%
Peptide-4 K(Boc)AK(Boc)PGK(Boc)K(mPEG)K(Boc)PG	N.A.	6420Da or 21.2kDa	6947Da±600 or 22.0±0.2 kDa	85%

a) Higher molecular weight corresponds to a cyclic scaffold linked to 20kDa mPEG residue and lower molecular weight to cyclic scaffolds linked to 5kDa mPEG.

Table 2. Conjugates Denomination, Characteristics and Yields

Conjugate*	Protease Cleavable Peptide	PEG molecular weight	Expected Molecular Weight	Molecular Weight Found	Yield
PheoLX	uPA-cleavable peptide in L-configuration	20kDa	PheoL1 21.9kDa PheoL2 23.2kDa PheoL3 24.5kDa PheoL4 25.8kDa	PheoL1 23.6±0.8kDa PheoL2 25.0±1.2kDa PheoL3 25.6±1.3kDa PheoL4 26.7±1.5kDa	70% 65% 60% 35%
PheoDX	uPA-cleavable peptide in D-configuration	20kDa	PheoD1 21.9kDa PheoD2 23.2kDa PheoD3 24.5kDa PheoD4 25.8kDa	PheoD1 23.0±0.7kDa PheoD2 24.2±0.9kDa PheoD3 24.8±1.0kDa PheoD4 25.2±1.2 kDa	70% 65% 60% 35%
PheoSX	uPA-cleavable peptide in L-configuration	5kDa	PheoS1 7280Da PheoS2 8560Da PheoS3 9840Da PheoS4 11120Da	PheoS1 7280±833Da PheoS2 8666±900Da PheoS3 9464±1250Da PheoS4 11661±1420Da	50% 35% 24% 20%
MPheoX	MMP-cleavable peptide in L-configuration	20kDa	MPheo1 21.9kDa MPheo2 23.3kDa MPheo3 24.6kDa MPheo4 25.9kDa	MPheo1 23.8±0.9kDa MPheo2 24.6±0.5kDa MPheo3 25.2±0.5kDa MPheo4 25.5±1.2kDa	53% 36% 30% 20%

* $_X$ indicates the number of Pheophorbide protease cleavable peptide(s) grafted on RAFT.

3.2. *In vial* experiments and quenching

The quenching factors of each conjugate tested are represented in Table 3

Table 3. Quenching factors of all Pheo-conjugates

Conjugate	Quenching factor Fo/Fl
PheoL$_1$	1
PheoL2	2.79 ± 0.04
PheoL3	10.76 ± 0.17
PheoL4	28.26 ± 0.69
PheoD1	1
PheoD2	2.56 ± 0.04
PheoD3	10.94 ± 0.10
PheoD4	30.62 ± 1.29
PheoS1	1
PheoS2	115.25 ± 6.65
PheoS3	213.59 ± 15.10
PheoS4	264.66 ± 22.92
MPheo1	1
MPheo2	4.68 ± 0.08
MPheo3	15.81 ± 0.10
MPheo4	25.63 ± 0.65

The conjugates containing only one pheophorbide peptide residue are considered as unquenched standard, and their fluorescence is compared to their homologues carrying multiple pheophorbide peptides copies. With increasing number of copies on the cyclopeptidic carrier in all conjugates the quenching factor increases. Furthermore, independently of the peptide sequence or the configuration all high molecular weight conjugates carrying the same number of pheophorbide a-peptide motifs show similar quenching factors. Most importantly, by reducing the molecular weight of PEG, the highest quenching factors were recorded as shown by PheoS conjugates similar to those previously reported with a poly-L-lysine carrier[7-9,15]. This indicates that the PEG chains can interact with the exciton formation of the pheophorbide moieties.

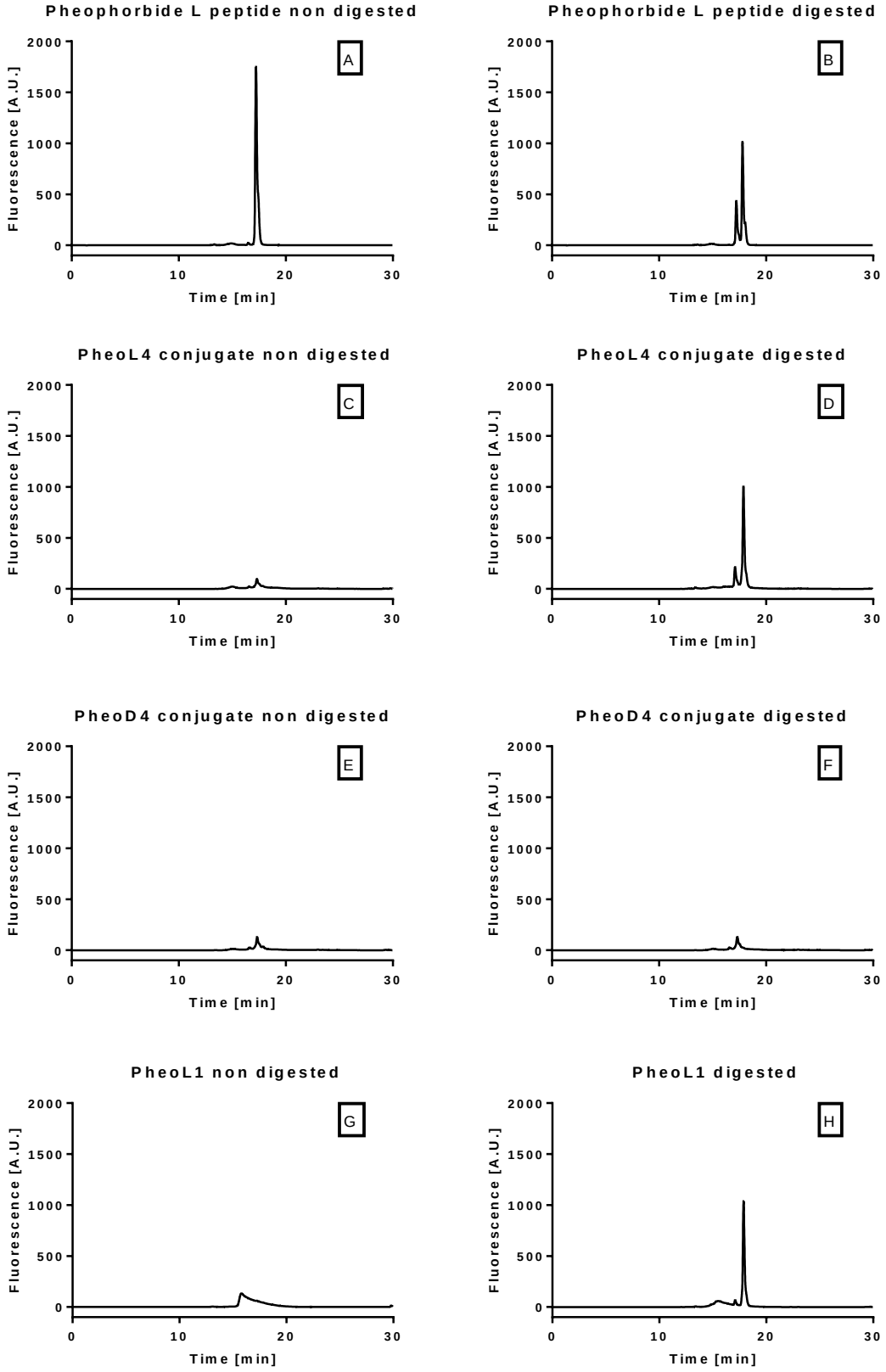

Figure 4. Analytical HPLC trace of the undigested (**A, C, E** and **G**) and digested (**B, D,F** and **H**) uPA cleavable pheophorbide peptide, PheoL4 and PheoD4 and PheoL1 conjugates. Digestion has been achieved by co-incubation during 1h of the peptide or conjugate with uPA.

Figure 4 presents the RP-HPLC patterns obtained for pheophorbide urokinase cleavable peptide, for the PheoL4 conjugate and PheoD4 conjugate (negative control) in presence or absence of urokinase. These traces are representative of the behavior of all other conjugates.

In presence of urokinase, proteolytic cleavage transcribes into the release of pheophorbide peptidyl fragment (Pheo-G-S-G-R) as shown by elution of a new peak at RT of 17.8 min distinct from the phephorbide peptide (RT=17 min) (Figure 4B and D). When co-incubated with negative controls D-conjugates no appearance of a second peak could be observed.

These results confirm the selective recognition and cleavage of the L-pheophorbide peptide conjugates by uPA at the expected site. Moreover, all conjugates exhibited reduced fluorescence as compared to equivalent pheophorbide dose as shown by Figure 4C and E, confirming the effective "silencing" and quenching of the drug.

3.3. *In vitro* activation

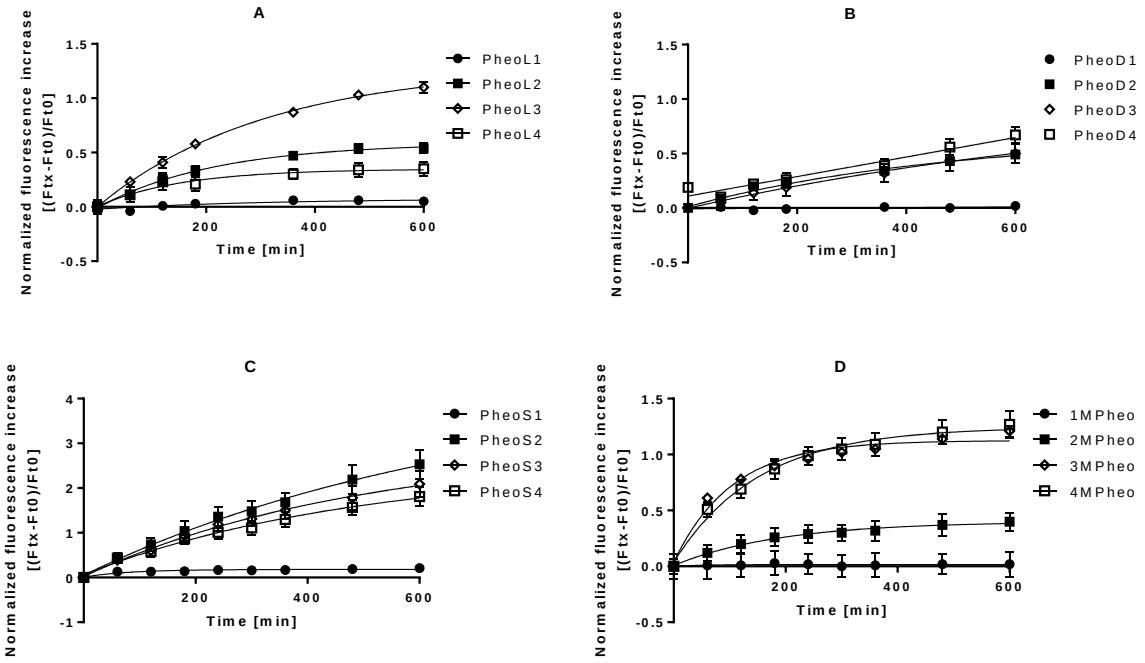

Figure 5. Activation *in vitro* of conjugates Pheo in L-configuration (A), Pheo D-configuration (B), PheoS conjugates (C) and MPheo conjugates (D) at concentration of 1 μM pheophorbide equivalent with (●) mono-conjugate, di-conjugate (■), tri-conjugate (◊) and tetra-conjugate (□) on PC-3 cells.

As shown by Figure 5A, in compounds pegylated with high molecular PEG PheoL2 and PheoL3 are more efficiently activated *in vitro* as compared to the tetra-substituted counterpart. No significant activation was observed for the monosubstituted conjugates. The activation is

time-dependent and seems to reach a plateau after 480 min of incubation. Surprisingly, also the PheoD conjugates are also activated in PC-3 cells but to a lesser extent. However, it cannot be excluded that other peptidases digest the remaining AAPGA motif on the cyclopeptidic scaffold. Based on expasy cutter peptide, proteinase K and thermolysin are two potential enzymes capable of cleaving this motif. However, since proteinase K is an endopeptidase and thermolysin is expressed only in bacteria, it is more likely that the PheoD conjugate cleavage is mostly due to other peptidases or may involve other cleavage sites at the Lysine residues of the RAFT.

In contrast, conjugates carrying a lower molecular weight PEG chain, seem to be less resistant to proteolytic activation (see Figure 5C). Fluorescence increase can still be observed after 10 hours. Again, the bisubstituted PheoS2 is more efficiently activated when compared to PheoS3 and PheoS4 conjugates.

Finally, also MMP sensitive conjugates show fluorescence increase in PC-3 cells. Beyond these compounds 3MPheo and 4MPheo show a 1.3-time increase over a time period of 4hours while 2MPheo showed an intermediate activation and 1MPheo almost no activation over time. The activation plateau of these conjugates is reached after about 4 hours of incubation.

3.4. *In vitro* PDT

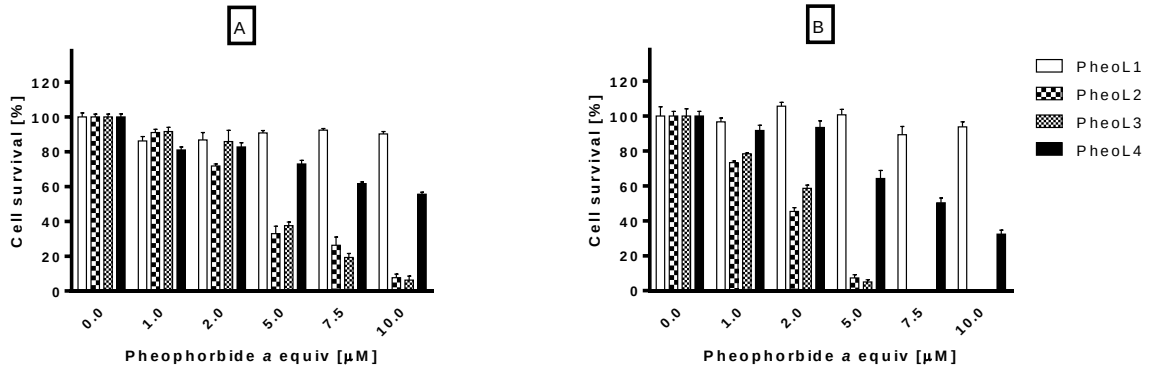

Figure 6. Cellular phototoxicity of PheoL conjugates 1, 2, 3 and 4 after 8 hours of incubation on PC-3 cells. Cells were exposed either to a light dose of 10 J/cm^2 (A) or 20 J/cm^2 (B).

Figure 6 presents the phototoxicity of PheoL conjugates on PC-3 cells exposed to a light dose of either 10 J/cm^2 or 20 J/cm^2. The phototoxic effect of the conjugates is concentration and light dose dependent (see also Table 4 for IC_{50} values of all compounds in PC-3 cells). No

dark toxicity was observed for all conjugates at concentrations as high as 30μM (Data not shown). As expected from the *in vitro* activation, out of the four conjugates tested, PheoL2 and PheoL3 are the most potent ones. Significant cell death is observed with these two conjugates at a drug dose of 5μM and light dose of 10J/cm^2 or even 2μM for a light dose of 20J/cm^2. Complete eradication of PC-3 cells was achieved at a concentration of 7.5 μM for both conjugates at a light dose of 20 J/cm^2. In contrast, PheoL4 achieves less than 50% of cell death only when using a drug dose of 10μM and a light dose of 10J/cm^2. A light dose of 20J/cm^2 reduced this IC_{50} to 7.0μM. PheoL1, on the other hand, did not exhibit any significant phototoxic effect.

Table 4. IC_{50} of all RAFT conjugates with respect to the cell type and light doses cells were exposed to. The values reported are the graphical extrapolation of the non-linear regression based on MTT results presented in Figures 6 to 8.

IC_{50}	Cell type & Light Dose	
	PC-3 cells - 10J/cm^2	***PC-3 cells - 20J/cm^2***
PheoL1	N.A.	N.A.
PheoL2	3.8 μM	1.8 μM
PheoL3	4.4 μM	2.3 μM
PheoL4	N.A.	7.0 μM
PheoS1	N.A.	N.A.
PheoS2	0.8 μM	0.2 μM
PheoS3	2.0 μM	1.4 μM
PheoS4	4.1 μM	1.7 μM
	PC-3 cells - 10J/cm^2	***HT1080 cells - 10J/cm^2***
MPheo1	N.A.	N.A.
MPheo2	250 nM	165 nM
MPheo3	288 nM	135 nM
MPheo4	227 nM	112 nM

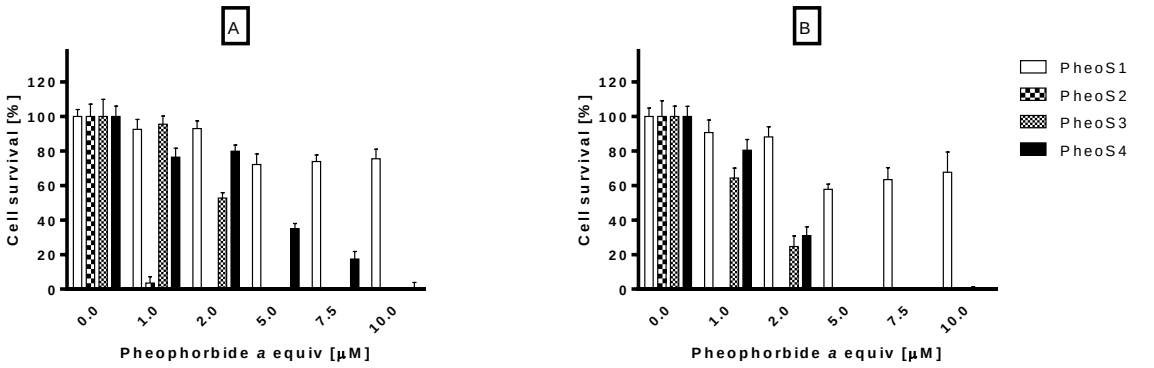

Figure 7. Cellular phototoxicity of PheoS conjugates 1, 2, 3 and 4 after 8 hours of incubation on PC-3 cells. Cells were exposed either to a light dose of 10 (**A**) or 20 J/cm^2 (**B**).

Figure 7 represents cell survival of PC-3 cells when exposed to the low molecular weight compounds (*i.e.* PheoS conjugates) and light doses of either 10 or 20 J/cm^2. Similarly to PheoL conjugates, no dark toxicity is observed for all the conjugates tested. Complete cell death is achieved when using PheoS2 at a drug dose as low as 2µM for a light dose of 10J/cm^2. PheoS3 has completely destroyed cells at a drug dose of 5µM while PheoS4 requires a drug dose of 10µM for a light dose of 10 J/cm^2 for a complete cell death. Meanwhile, PheoS1 exhibits cell phototoxicity only at the light doses of 20 J/cm^2 for a drug dose of 5µM, suggesting that this conjugate is the least potent one.

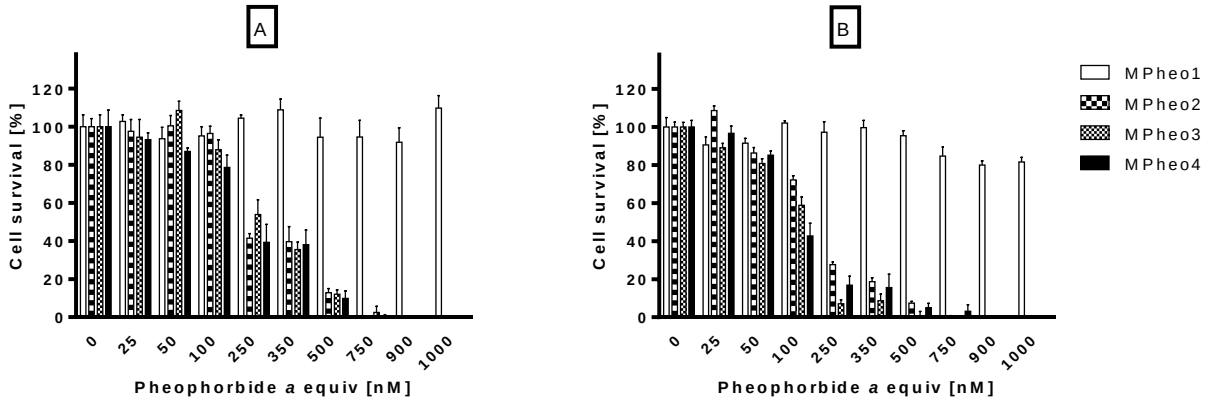

Figure 8. Cellular phototoxicity on PC-3 cells (**A**) and HT1080 cells (**B**) of MPheo conjugates 1, 2, 3 and 4 after 8 hours of incubation. Cells were exposed to a light dose of 10J/cm^2.

Finally, Figure 8 shows the cellular phototoxicity of the MPheo conjugates towards PC-3 and HT1080 cell lines, cells that are known to overexpress MMP proteases[6,53-55]. While no dark toxicity is noticed for cells exposed to MPheo conjugates only a complete cellular destruction is achieved at a drug dose as low as 900 nM for conjugates 2, 3 and 4MPheo for a light dose of 10J/cm^2. Moreover, these three conjugates exhibit a similar phototoxicity pattern with IC_{50} values situated between 100 and 300nM. Finally, MPheo1 conjugate did not exhibit any phototoxic effect toward PC-3 cells for a drug dose as high as 10 μM (Data not shown).

While monoconjugate pheophorbide peptide conjugates had no to low phototoxic effects, conjugates bearing two or more pheophorbide peptides moieties exhibited significant photocytoxicity. Low molecular weight PEGylated compounds displayed higher phototoxicities than their corresponding high molecular weight compounds. Cellular activation of PheoS conjugates and different cellular uptake, may explain this observation.

By reducing the molecular weight of the PEG used, the quenching factor of the conjugates could be significantly increased as reported in Table 3 and as noted on previous studies on polymeric prodrugs. Hence, when using a polymeric scaffold, Lange and coworkers [7-9,15], reported quenching factors of 131,7 and 145.8 for polymeric prodrug containing only pheophorbide peptide moieties of respectively 18 and 24 units/polylysine chain (1st generation conjugates) while PEGylation and addition of other solubilizing moieties lead for similar number of PS units/polylysine to reduced quenching factors *e.g.* to 84.6 for the conjugate bearing 18 units/polylysine chain.

Moreover, Zuluaga *et al*,[9,15] proved that with of fluorescence quenching factor of 61 ± 3, good contrast could be obtained *in vivo* and efficient PDT treatment of PC-3 xenografts on mice could be achieved. Hence, balance should be found between good quenching factor, water-solubility and ROS generation to achieve efficient imaging and therapeutic treatment.

Although, the size of the conjugates reported in this study and the size and molecular weight of the polymeric prodrugs differ one may compare the quenching factors obtained for RAFT-conjugates with PPP conjugates. For example, PheoS conjugate's quenching factors are similar to the ones obtained for 1rst generation PPPs using 18units/polymer. The RAFT conjugates, however, present the advantages of having a more defined structure as compared to PPPs, use less PS units and maintain complete water-solubility of such construct.

Low molecular weight prodrug may also be detrimental for *in vivo* applications, due to a reduced circulation time and an increased elimination time of the conjugates. Indeed, in order

to be efficient PDT agents, the conjugates should be presented to tumor cells and its environment for a sufficient time to allow the cleavage and release of PS in sufficient amounts. PEGylation with higher molecular weight PEGs is known[56,57] to increase the circulation time in the body, hence enhancing its tumor accumulation and biodistribution, as well as reducing its elimination. Although less efficiently quenched than the PheoS conjugates, PheoL and MPheo conjugates can be expected to be more active *in vivo*.

Interestingly, MPheo2, 3 and 4 exhibited similar phototoxic effect despite different activation profiles. Finally, MPheo conjugates exhibited surprising phototoxic effects at drug doses as low as 100 to 300nM *in vitro* in PC-3 cells. These prodrugs combine the advantage of no dark toxicity, high photocytotoxicity for moderate light doses of 10J/cm^2, but also rapid activation. Reduced elimination *in vivo* can be expected due to the conjugation of PEG 20kDa. These are very promising results which are confirming the significant potential of these prodrugs as efficient PDT agents for an *in vivo* treatment of prostate cancer and fibrosarcoma.

4. Conclusions

In this study, the synthesis of new water-soluble and potentially active prodrugs for PDT treatment of cancer was described. The photosensitizer prodrug demonstrated an *in vitro* activation and a phototoxicity targeting cancers associated with uPA and MMPs up-regulated activity such as prostate cancer. Without light irradiation, no phototoxic effect was observed. Upon light activation and proteolytic cleavage, the release of peptidyl-photoactive fragments of PS resulted in cell phototoxic effect. Moreover, high quenching factors and efficiencies were achieved by conjugates containing PEG of 5kDa when compared to conjugates that had a PEG of 20kDa. This study confirmed that the peptide sequence is of major importance for the specificity and selectivity towards tumor cells resulting in improved PDT-efficacy as shown by PheoL, PheoD and MPheo conjugates. *In vivo* and clinical potentials of the prodrugs reported in this study have to be further evaluated in order to confirm these promising results.

Acknowledgements

This work has been supported in part by the SNF grants 205320_13830, CR32I3_129987, CR32I3_147018, 31003A_149962, CR32I3_150271, and 205321_126834. The authors would like to thank Dr Doris Gabriel and Dr Maria Fernanda Zuluaga Estrada for their advices and support.

Supplementary material

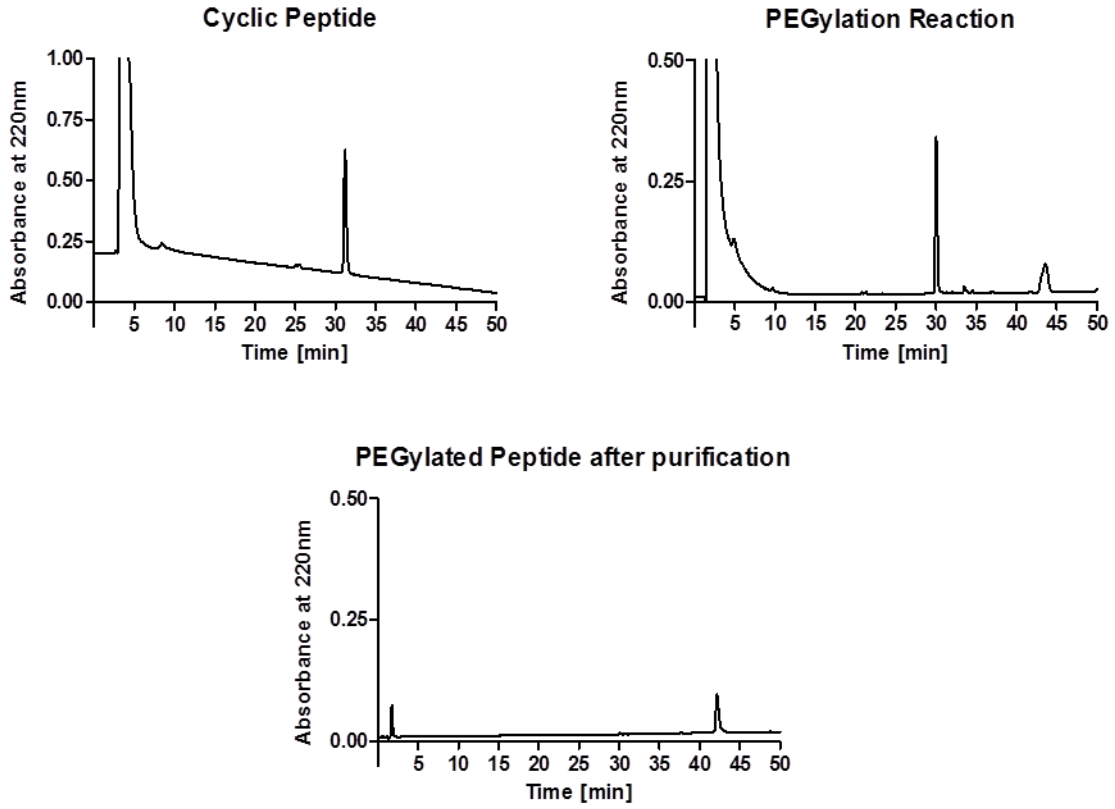

Figure 9. RP-HPLC chromatograms of one cyclic peptide, the reaction mixture after 24h and PEGylated peptide after purification.

Figure 9 represents the RP-HPLC patterns obtained for one cyclic peptide (RAFT) as well as the one of the reaction mixture and the resulting purified product.

The first peak observed either corresponds to the peak of DMSO or the injection peak (Retention Time (RT) < 5 min). RAFT is eluting at 30 min and the novel product appears when the reaction occurs at higher retention time (*i.e.* 42 min). After purification, no more RAFT is present and only the PEGylated cyclic peptide is detectable. These chromatograms are representative of all peptides and PEGylated peptides reported in this study.

References:

1. Jori G, Fabris C, Soncin M, et al: Photodynamic therapy in the treatment of microbial infections: basic principles and perspective applications. Lasers Surg Med 38:468-81, 2006

2. Hendrich C, Siebert WE: Photodynamic therapy for rheumatoid arthritis? Lasers Surg Med 21:359-64, 1997

3. Schmidt-Erfurth U, Hasan T: Mechanisms of action of photodynamic therapy with verteporfin for the treatment of age-related macular degeneration. Surv Ophthalmol 45:195-214, 2000

4. Brown SB, Brown EA, Walker I: The present and future role of photodynamic therapy in cancer treatment. Lancet Oncol 5:497-508, 2004

5. Brasseur N, Ouellet R, La Madeleine C, et al: Water-soluble aluminium phthalocyanine-polymer conjugates for PDT: photodynamic activities and pharmacokinetics in tumour-bearing mice. British Journal of Cancer 80:1533-1541, 1999

6. Bremer C, Bredow S, Mahmood U, et al: Optical imaging of matrix metalloproteinase-2 activity in tumors: Feasibility study in a mouse model. Radiology 221:523-529, 2001

7. Campo MA, Gabriel D, Kucera P, et al: Polymeric photosensitizer prodrugs for photodynamic therapy. Photochem Photobiol 83:958-65, 2007

8. Gabriel D, Campo MA, Gurny R, et al: Tailoring protease-sensitive photodynamic agents to specific disease-associated enzymes. Bioconjug Chem 18:1070-7, 2007

9. Gabriel D, Zuluaga MF, Martinez MN, et al: Urokinase-plasminogen-activator sensitive polymeric photosensitizer prodrugs: design, synthesis and *in vitro* evaluation. Journal of Drug Delivery Science and Technology 19:15-24, 2009

10. Peterson CM, Lu JM, Sun Y, et al: Combination chemotherapy and photodynamic therapy with N-(2-hydroxypropyl) methacrylamide copolymer-bound anticancer drugs inhibit human ovarian carcinoma heterotransplanted in nude mice. Cancer Res 56:3980-5, 1996

11. Renno RZ, Terada Y, Haddadin MJ, et al: Selective photodynamic therapy by targeted verteporfin delivery to experimental choroidal neovascularization mediated by a homing peptide to vascular endothelial growth factor receptor-2. Arch Ophthalmol 122:1002-11, 2004

12. Soukos NS, Hamblin MR, Hasan T: The effect of charge on cellular uptake and phototoxicity of polylysine chlorin(e6) conjugates. Photochem Photobiol 65:723-9, 1997

13. Tijerina M, Fowers KD, Kopeckova P, et al: Chronic exposure of human ovarian carcinoma cells to free or HPMA copolymer-bound mesochlorin e6 does not induce P-glycoprotein-mediated multidrug resistance. Biomaterials 21:2203-10, 2000

14. Tung CH, Bredow S, Mahmood U, et al: Preparation of a cathepsin D sensitive near-infrared fluorescence probe for imaging. Bioconjug Chem 10:892-6, 1999

15. Zuluaga MF, Sekkat N, Gabriel D, et al: Selective photodetection and photodynamic therapy for prostate cancer through targeting of proteolytic activity. Mol Cancer Ther 12:306-13, 2013

16. Ringsdorf H: Structure and Properties of Pharmacologically Active Polymers. Journal of Polymer Science Part C-Polymer Symposium:135-153, 1975

17. Duncan R, Kopecek J: Soluble Synthetic-Polymers as Potential-Drug Carriers. Advances in Polymer Science 57:51-101, 1984

18. Kopecek J: Targetable Polymeric Anticancer Drugs - Temporal Control of Drug Activity. Annals of the New York Academy of Sciences 618:335-344, 1991

19. Dolmans DEJGJ, Fukumura D, Jain RK: Photodynamic therapy for cancer. Nature Reviews Cancer 3:380-387, 2003

20. Cozzi PJ, Wang J, Delprado W, et al: Evaluation of urokinase plasminogen activator and its receptor in different grades of human prostate cancer. Hum Pathol 37:1442-51, 2006

21. Garzetti GG, Ciavattini A, Lucarini G, et al: Tissue and serum metalloproteinase (MMP-2) expression in advanced ovarian serous cystoadenocarcinomas: Clinical and prognostic implications. Anticancer Research 15:2799-2804, 1995

22. Gohji K, Fujimoto N, Hara I, et al: Serum matrix metalloproteinase-2 and its density in men with prostate cancer as a new predictor of disease extension. International Journal of Cancer 79:96-101, 1998

23. Han B, Nakamura M, Mori I, et al: Urokinase-type plasminogen activator system and breast cancer (Review). Oncology Reports 14:105-112, 2005

24. Harbeck N, Kates RE, Gauger K, et al: Urokinase-type plasminogen activator (uPA) and its inhibitor PAI-I: novel tumor-derived factors with a high prognostic and predictive impact in breast cancer. Thromb Haemost 91:450-6, 2004

25. Hasui Y, Marutsuka K, Suzumiya J, et al: The content of urokinase-type plasminogen activator antigen as a prognostic factor in urinary bladder cancer. Int J Cancer 50:871-3, 1992

26. Kim TD, Song KS, Li G, et al: Activity and expression of urokinase-type plasminogen activator and matrix metalloproteinases in human colorectal cancer. Bmc Cancer 6, 2006

27. Konecny G, Untch M, Pihan A, et al: Association of urokinase-type plasminogen activator and its inhibitor with disease progression and prognosis in ovarian cancer. Clin Cancer Res 7:1743-9, 2001

28. Kuhn W, Schmalfeldt B, Reuning U, et al: Prognostic significance of urokinase (uPA) and its inhibitor PAI-1 for survival in advanced ovarian carcinoma stage FIGO IIIc. Br J Cancer 79:1746-51, 1999

29. Pesta M, Holubec L, Topolcan O, et al: Quantitative estimation of matrix metalloproteinases 2 and 7 (MMP-2, MMP-7) and tissue inhibitors of matrix metalloproteinases 1 and 2 (TIMP-1, TIMP-2) in colorectal carcinoma tissue samples. Anticancer Research 25:3387-3391, 2005

30. Schmalfeldt B, Prechtel D, Harting K, et al: Increased expression of matrix metalloproteinases (MMP)-2, MMP-9, and the urokinase-type plasminogen activator is associated with progression from benign to advanced ovarian cancer. Clinical Cancer Research 7:2396-2404, 2001

31. Shariat SF, Monoski MA, Andrews B, et al: Association of plasma urokinase-type plasminogen activator and its receptor with clinical outcome in patients undergoing radical cystectomy for transitional cell carcinoma of the bladder. Urology 61:1053-8, 2003

32. Somiari SB, Somiari RI, Heckman CM, et al: Circulating MMP2 and MMP9 in breast cancer - Potential role in classification of patients into low risk, high risk, benign disease and breast cancer categories. International Journal of Cancer 119:1403-1411, 2006

33. van der Burg ME, Henzen-Logmans SC, Berns EM, et al: Expression of urokinase-type plasminogen activator (uPA) and its inhibitor PAI-1 in benign, borderline, malignant primary and metastatic ovarian tumors. Int J Cancer 69:475-9, 1996

34. Choi Y, Weissleder R, Tung CH: Selective antitumor effect of novel protease-mediated photodynamic agent. Cancer Research 66:7225-7229, 2006

35. Choi Y, Weissleder R, Tung CH: Protease-mediated phototoxicity of a polylysine-chlorin(e6) conjugate. Chemmedchem 1:698-+, 2006

36. Hamblin MR, Miller JL, Rizvi I, et al: Pegylation of charged polymer-photosensitiser conjugates: effects on photodynamic efficacy. British Journal of Cancer 89:937-943, 2003

37. Hamblin MR, Miller JL, Rizvi I, et al: Pegylation of a chlorin(e6) polymer conjugate increases tumor targeting of photosensitizer. Cancer Research 61:7155-7162, 2001

38. Krinick NL, Sun Y, Joyner D, et al: A Polymeric Drug-Delivery System for the Simultaneous Delivery of Drugs Activatable by Enzymes and or Light. Journal of Biomaterials Science-Polymer Edition 5:303-324, 1994

39. Mutter M, Altmann KH, Tuchscherer G, et al: Strategies for the Denovo Design of Proteins. Tetrahedron 44:771-785, 1988

40. Boturyn D, Coll JL, Garanger E, et al: Template assembled cyclopeptides as multimeric system for integrin targeting and endocytosis. Journal of the American Chemical Society 126:5730-5739, 2004

41. Boturyn D, Defrancq E, Dolphin GT, et al: RAFT nano-constructs: surfing to biological applications. Journal of Peptide Science 14:224-240, 2008

42. Dufort S, Sancey L, Hurbin A, et al: Targeted delivery of a proapoptotic peptide to tumors *in vivo*. Journal of Drug Targeting 19:582-588, 2011

43. Garanger E, Boturyn D, Coll JL, et al: Multivalent RGD synthetic peptides as potent alpha(V)beta(3) integrin ligands. Organic & Biomolecular Chemistry 4:1958-1965, 2006

44. Jin ZH, Josserand V, Foillard S, et al: *In vivo* optical imaging of integrin alpha(v)-beta(3) in mice using multivalent or monovalent cRGD targeting vectors. Molecular Cancer 6, 2007

45. Jin ZH, Josserand V, Razkin J, et al: Noninvasive optical imaging of ovarian metastases using Cy5-labeled RAFT-c(-RGDfK-)(4). Molecular Imaging 5:188-197, 2006

46. Jin ZH, Razkin J, Josserand V, et al: *In vivo* noninvasive optical imaging of receptor-mediated RGD internalization using self-quenched Cy5-labeled RAFT-c(-RGDfK-) (4). Molecular Imaging 6:43-55, 2007

47. Razkin J, Josserand V, Boturyn D, et al: Activatable fluorescent probes for tumour-targeting imaging in live mice. Chemmedchem 1:1069-+, 2006

48. Texier I, Razkin J, Josserand V, et al: Activatable probes for non-invasive small animal fluorescence imaging. Nuclear Instruments & Methods in Physics Research Section a-Accelerators Spectrometers Detectors and Associated Equipment 571:165-168, 2007

49. Wenk CHF, Josserand V, Dumy P, et al: Integrin and matrix metalloprotease dual-targeting with an MMP substrate-RGD conjugate. Organic & Biomolecular Chemistry 11:448-452, 2013

50. Wenk CHF, Keramidas M, Josserand V, et al: Near-infrared guided surgery of cancer in cats and dogs: from models to clinical cases. Bulletin Du Cancer 97:S22-S23, 2010

51. Chan WC: Fmoc Solid Phase Peptide Synthesis: A practical approach. Oxford, UK, Oxford Univ Press, 2000

52. Lee GY, Park K, Kim SY, et al: MMPs-specific PEGylated peptide-DOX conjugate micelles that can contain free doxorubicin. Eur J Pharm Biopharm 67:646-54, 2007

53. Vijayababu MR, Arunkumar A, Kanagaraj P, et al: Quercetin downregulates matrix metalloproteinases 2 and 9 proteins expression in prostate cancer cells (PC-3). Mol Cell Biochem 287:109-16, 2006

54. Wilson MJ, Sinha AA: Plasminogen activator and metalloprotease activities of Du-145, PC-3, and 1-LN-PC-3-1A human prostate tumors grown in nude mice: correlation with tumor invasive behavior. Cell Mol Biol Res 39:751-60, 1993

55. Wilson MJ, Sinha AA: Human prostate tumor angiogenesis in nude mice: metalloprotease and plasminogen activator activities during tumor growth and neovascularization of subcutaneously injected matrigel impregnated with human prostate tumor cells. Anat Rec 249:63-73, 1997

56. Banerjee SS, Aher N, Patil R, et al: Poly(ethylene glycol)-Prodrug Conjugates: Concept, Design, and Applications. J Drug Deliv 2012:103973, 2012

57. Veronese FM, Pasut G: PEGylation, successful approach to drug delivery. Drug Discov Today 10:1451-8, 2005

IN VITRO EVALUATION OF NOVEL FAR-RED FLUORESCENT PROBES

Nawal SEKKAT[1], Arnaud CHEVALIER[2,3], Anthony ROMIEU[2,3,4]

Pierre-Yves RENARD[2,3,4] and Norbert LANGE*[1]

[1]School of Pharmaceutical Sciences, University of Lausanne/Geneva, Geneva, 30, Quai Ernest Ansermet, Geneva CH-1211, Switzerland

[2]Université de Rouen Laboratory COBRA UMR 6014 & FR 3038, IRCOF, rue Lucien Tesnière, 76821 Mont-Saint-Aignan, France

[3] CNRS Délégation Normandie, 14, rue Alfred Kastler, 14052 Caen Cedex, France

[4] INSA Rouen, Avenue de l'Université, 76800 St Etienne du Rouvray, France

*Corresponding author e-mail: norbert.lange@unige.ch

ABSTRACT

The non-invasive detection of disease at early stages is of major importance for improved patient management. Therefore, much effort is currently undertaken to develop novel imaging probes and techniques. Since increased proteases expression is associated with numerous pathologies such as cancer, protease targeting and sensing has been suggested as a promising tool for new reporters. Activatable fluorescent probes known as "molecular beacons" represent one class of such compounds. The aim in fluorescence detection using these probes is to increase the signal-to-noise ratio by lowering the background fluorescence and favor the selective activation of the probe by specific, disease related proteases. An *in vitro* evaluation of 5 protease sensitive near-infrared fluorescently quenched probes was performed in this study. In these probes, a fluorophore (Cy5 or Texas Red) and a Black-Hole Quencher (BHQ-3) are attached to a protease sensitive peptide linker (urokinase-like plasminogen activator or cathepsin B sensitive peptide) resulting in efficient quenching ((>99%) in the native configuration. Here, we show that our "molecular beacons" display an increase of their low native fluorescent emission upon proteolytic cleavage of the peptide *in vial* and *in vitro,* with an almost 20 times increase in fluorescence for one of the tested probes when incubated with human prostate cancer cell line (PC-3) while the control probes remained uncleaved and hence, silent. Both activation and intracellular localization of the probes were assessed in PC-3 cells. The promising results obtained suggest a high potential for medical application in *e.g. in vivo* detection and imaging of protease related diseases such as prostate cancer. Furthermore, using this approach, new methods for the testing of protease sensitive prodrugs can be envisioned.

KEY WORDS: FRET, urokinase-like plasminogen activator, cathepsin, near-infrared probes, molecular beacons, quenching, fluorescence imaging

1. Introduction

Due to its high sensitivity, fluorescence is one of the most powerful tools for bioimaging for both *in vitro* and *in vivo* monitoring. The expanding interest in fluorescence imaging resides in the development and optimization of time and spatial resolution achieved over the past decades. Thus, significant progress in clinically relevant applications such as early detection of diseases and the improvement of patient treatments and prognosis has been made. Three of the major drawbacks of conventional fluorescent probes are the lack of selectivity, often a low signal-to-noise ratio and mostly for *in vivo* applications, unfavorable spectral properties of the designed probes. With the emergence of near-infrared fluorophores deeper light penetration into tissues is feasible and more body sites can be imaged. Moreover, by the association of the fluorophore to a targeting moiety, one can improve the selectivity towards diseased tissues[1-4]. Abundant expression of proteases has been proposed as biomarkers for several diseases including rheumatoid arthritis and cancer[5-11]. This hallmark can be exploited to increase the selectivity of the probes towards the diseased tissue. Finally, increasing the signal amplification by lowering the native fluorescence of the probes can be achieved by the development of "fluorescent activatable prodrugs".

One of the approaches currently explored consists in the design and synthesis of "fluorescent activatable prodrugs" which are "silent" in their native state but, when in presence with the target protease give rise to an increased fluorescent signal. The activatable probe principle resides on the fact that, when a photon is absorbed by a fluorophore, the dye becomes excited electronically. The energy absorbed can be either 1) transferred radiatively to the lowest excited state of the fluorophore, which results in fluorescence or 2) transferred non-radiatively between a donor (the fluorophore) and an acceptor (fluorophore or quencher), which hampers the photon emission. Due to the close proximity of the donor and acceptor in the native state, a transfer of energy occurs and is referred to as Förster Resonnance Energy Transfer (FRET)[12,13]. The selectivity of the probes can be achieved by the fluorophore (donor) coupling to a protease specific peptidic bond. On the other hand, "silencing" is obtained by coupling on the other side of the peptide, another fluorophore or quencher (acceptor). This approach is known as the "molecular beacons" approach[4,14-17]. Zheng and coworkers were the pioneers for such approach and could obtain specific targeting of several proteases with similar quenching efficiencies among them caspase-3[17,18], MMPs[16,19] and fibroblast

activating protein (FAP) [14] which resulted after proteolytic cleavage respectively in a 8 fold, 12 fold and 200 times increase in fluorescence.

In this study, an *in vitro* evaluation of five quenched probes (AC226, AC203, AC560, AC594, AC595) designed as molecular beacons was performed. Two different fluorophores (Cy5 and Texas Red (TR)) and two protease cleavable peptide linkers sensitive to urokinase like plasminogen activator (uPA) and cathepsin B were tested. Both proteases are known to be associated with development, progression, and invasion of cancer such as prostate, colorectal, ovarian, breast and bladder cancer[20-27].

2. Materials and Methods

2.1. Chemicals

Trypsin 0.25%-EDTA solution, Nutrient Mixture Kaighn's Modification (F-12K) with L-Glutamine, Hank's Balanced Salt Solution with calcium and magnesium, Penicillin 10 000 units/mL and Streptomycin 10 000 µg/mL solution were provided by Life Technologies Corporation (Paisley, UK). DMSO and ethanol of analytical grades were obtained from Fisher Scientific UK Limited (Loughborough, Leicestershire, UK). Fetal Bovine Serum (FBS) was acquired from PAA Laboratories GmbH (Pasching, Austria), Triton X-100 from Applichem. (ITW Company, Germany) and NaOH from Reactolab S.A. (Servion, Switzerland). Albumine from Bovine Serum (BSA) essentially globulin free, Cathepsin B from bovine spleen, amiloride hydrochloride and p-aminobezamidine dihydrochloride were purchased from Sigma-Aldrich Chemie GmbH (Germany). Vectashield® Mounting Medium for Fluorescence with DAPI was obtained from Vector Laboratories, Inc. (Burlingame, California, USA) and Lysotracker® Green DND-26 from Invitrogen Molecular Probes™ (Eugene, Oregon, USA).

2.2. AC Structures

AC203 uPA detection

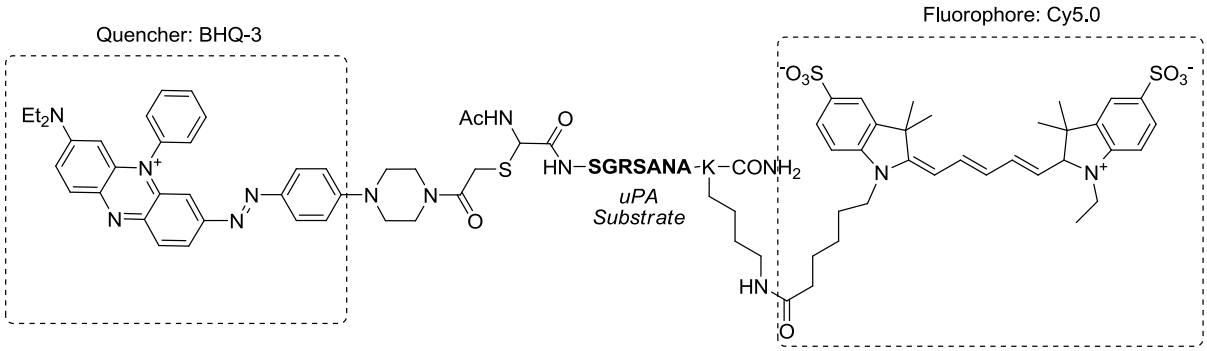

AC226 uPA detection

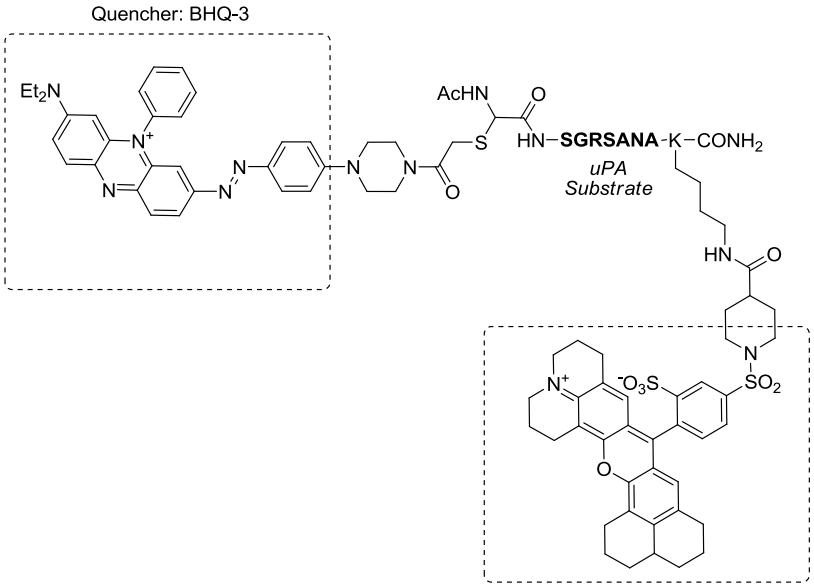

AC594 Cathepsin B detection

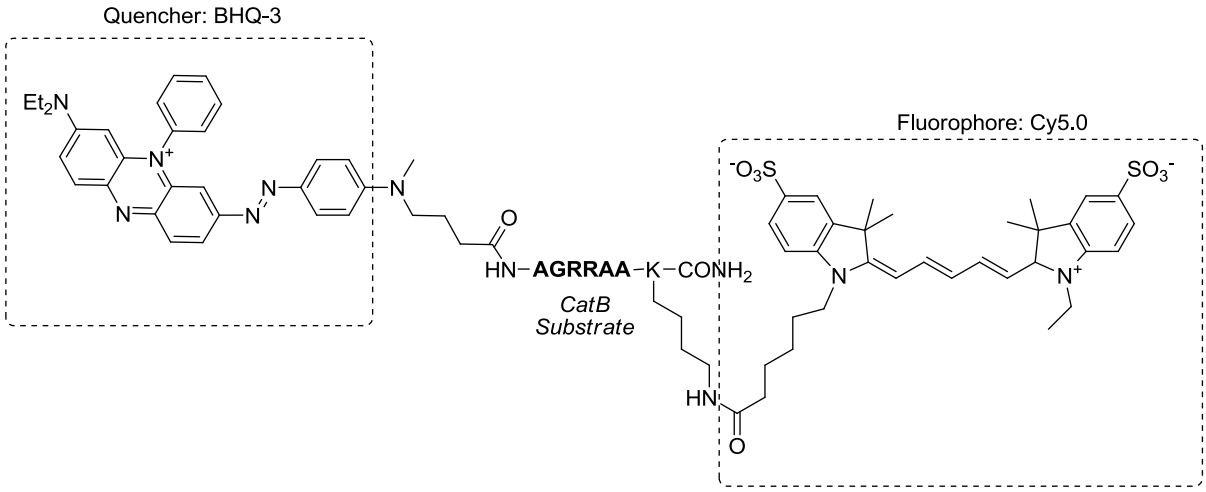

AC560 uPA detection

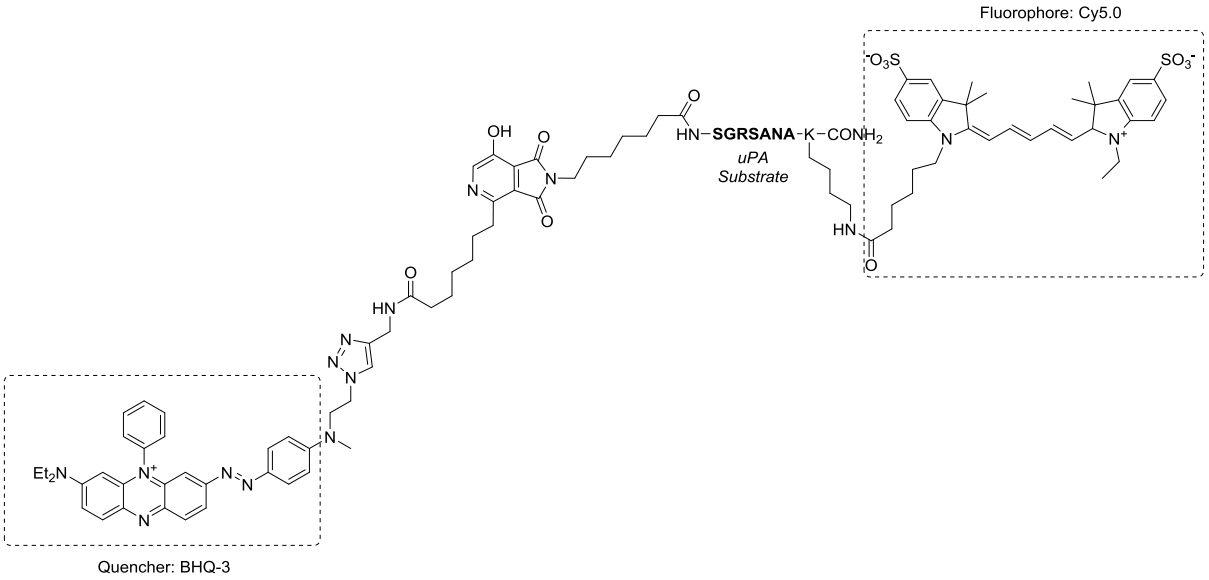

AC595 uPA detection (negative control)

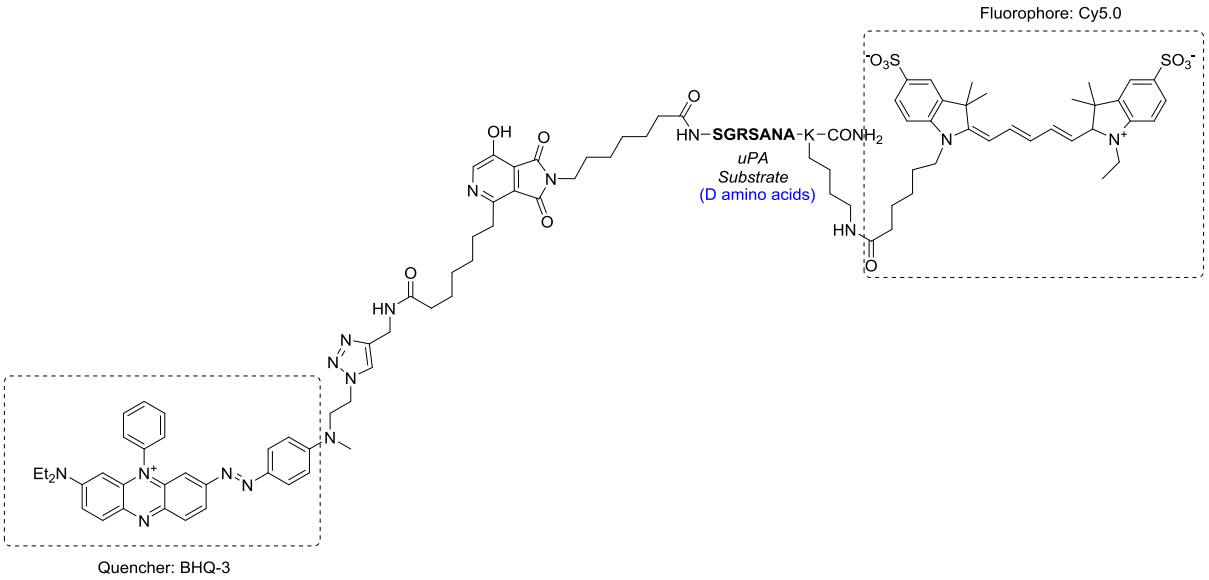

2.3. Cell Culture

PC-3 cells (ATCC, Manassas, VA) were maintained as monolayers in F-12K medium supplemented with 10% fetal bovine serum (FBS), 100µL/mL streptomycin and 100IE/mL penicillin in a humidified incubator containing 5% CO_2. Cells were trypsinized using 0.25% Trypsin-EDTA solution. Probes as well as amiloride and p-aminobenzamidine stock solutions were diluted in milliQ water.

2.4. Probes *in vitro* activation on PC-3 cells

PC-3 cell suspension (100µL) containing 1.8 x 10^4 cells were seeded in 96-well plates and allowed to attach overnight. Subsequent washing with 200µL PBS was performed and cells were incubated with solutions of 1µM corresponding conjugates in F12K medium containing 10% FBS. Additionally, cells were separately co-incubated with either 250µM amiloride and 1µM probe or 250µM p-aminobenzamidine and 1µM probe. Fluorescence was measured using a Safire microplate reader (Tecan, Switzerland). For probe AC226, an excitation wavelength (λ_{exc}) of 580nm and an emission wavelength (λ_{em}) of 608nm were used. For probes AC203, AC560, AC594 and AC595, λ_{exc}=650nm and λ_{em}=670nm was applied. The increase in fluorescence emission was calculated by substraction of the fluorescence intensity Ft_0 immediately after incubation start, from the value Ft_x obtained at time x and divided by Ft_0. All conditions were tested in sextuplicate and are expressed as mean value +/- S.D.

2.5. *In vial* activation of AC594

PBS buffered solution of AC594 was treated with or without cathepsin B (100µL, 2u) for a final probe concentration of 3 µM. Samples were incubated at 37°C and fluorescence was measured using Safire as described above. The quenching efficiency was calculated as the following:

100 x (1- (Fl_{max}/Ft_0)), where Fl_{max} corresponds to the fluorescence of the activated probes after 1 min and Ft_0, corresponds to the fluorescence of the non-digested probe.

2.6. Intracellular fate of the probes in cells - Confocal Microscopy

PC-3 cells were seeded at a concentration of 6x10^4 cells per well and allowed to attach over two days. Cells were co-incubated with 120nM of Lysotracker® Green and the 20µM of probes during 2 hours. Then, the cells were washed with HBSS and HBSS with BSA 1% and subsequently fixed using paraformaldehyde solution at 4%. After fixation, cells were rinsed 3 times using HBSS and once with water and were finally mounted using Vectashield® mounting medium containing DAPI. Thereafter, the cells were imaged by confocal fluorescence microscopy using Zeiss Axiovert 710 microscope (Carl Zeiss, Jena, Germany).

3. Results and Discussion

3.1. *In vial* activation of AC594

Table 1. Excitation and Emission Wavelength of fluorogenic probes AC203, AC226, AC560, AC594 and AC595 as well as their quenching efficiency.

Probes	λ_{exc} [nm]	λ_{em} [nm]	Initial Fluorescence Ft_0	Quenching Efficiency	Reference
AC226 (TR)	580	608	1166 ± 48	98.9%	[28]
AC203 (CY5)	650	670	210 ± 8	98.8%	[28]
AC560	650	670	219 ± 4	95.0%	[28]
AC594*	650	670	109 ± 5	99.3%	
AC595	650	670	227 ± 13	N.A.	

*the proteolytic cleavage of AC594 was performed using Cathepsin B.

In Table 1, the excitation and emission wavelengths of all probes are listed as well as their quenching efficiency, which was calculated as a function of their proteolytic cleavage by their corresponding target protease. Since AC595 probe was not cleaved by urokinase, no quenching efficiency could be calculated. All probes tested in this study and by Chevalier *et al*.[28] exhibited high quenching efficiencies with fluorescence increase after proteolytic cleavage of 83 to 153 folds as compared to non-digested probes over time. Interestingly, using the polymeric prodrug approach Gabriel *et al*.[29] and Zuluaga *et al*.[30] were able to achieve quenching efficiencies ranging from 95% to 99%, only by varying the number of photosensitizer units per polymer with the highest reported activation of 22 times *in vial* while a signal fluorescence increase of approximately 40 to 60 fold was reported by Weissleder's group of research[31,32] when using cathepsin D sensitive polymeric Cy5.5 probe and a 9-fold increase when using Cy5.5 polymeric Cathepsin K targeting probe[33] *in vial*.

3.2. Probes *in vitro* activation on PC-3 cells

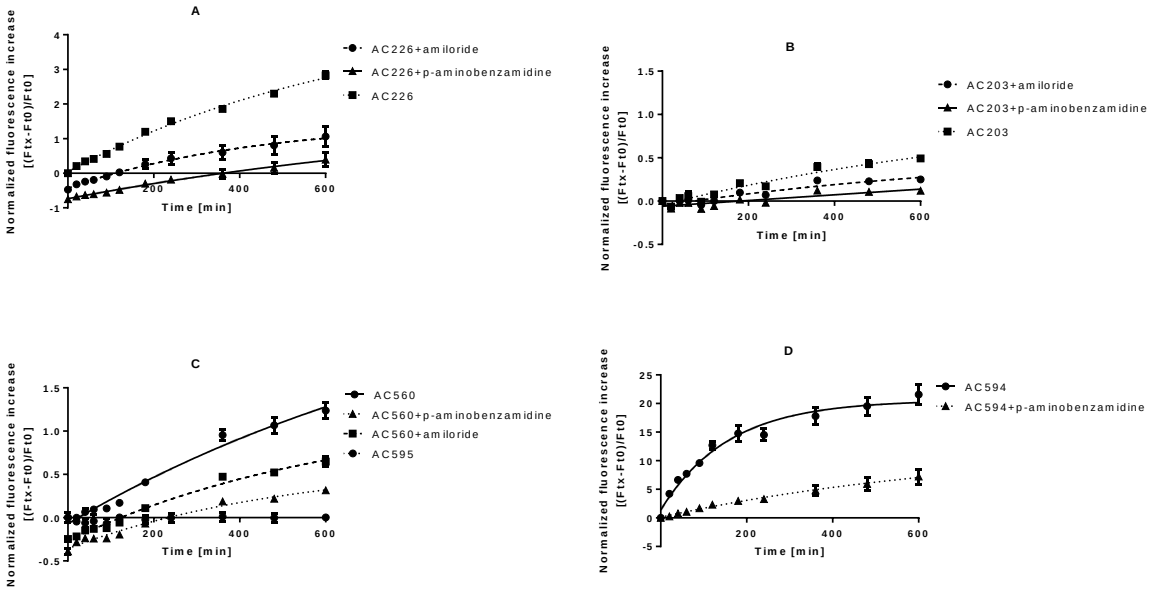

Figure 1. PC-3 cellular activation of probes AC226 **(A)**, AC203 **(B)**, AC560 and AC595 **(C)**, and AC594 **(D)** over time as compared to their activation in presence of two protease inhibitors, amiloride and p-aminobenzamidine.

Figure 1 shows the *in vitro* activation of all probes in PC-3 cells as a function of time and allows the comparison of their activation in presence or in absence of two different protease inhibitors i.e. amiloride and p-aminobenzamidine. All probes displayed an increase of fluorescence over time, hence confirming their activation in PC-3 cells. The cathepsin B probe, AC594, was the most rapidly and the most highly activated probe and reached a plateau after 400 minutes of incubation. The highest fluorescence increase of approximately 20 times was achieved by this probe over time after 600 minutes while AC226 exhibited an intermediate activation followed by AC560 and lastly AC203.

Table 2 provides an overview of the percentage inhibition of PC-3 cellular activation of the probes.

Table 2. Percentage inhibition of PC3 cellular activation of the probes after 10h of incubation

Probes	Fluorescence increase $(Ft_x-Ft_o)/Ft_o$	Inhibition using amiloride	Inhibition using p-aminobenzamidine
AC226	2.825 ± 0.102	62 ± 12 %	86 ± 8 %
AC203	0.492 ± 0.030	73 ± 8 %	100 ± 15 %
AC560	1.237 ± 0.089	48 ± 7 %	74± 3 %
AC594	21.551 ± 1.715	N.A.	66 ± 8 %
AC595	0.002 ± 0.032	N.A.	N.A.

When cells were co-incubated with the probes and the broad spectrum serine protease inhibitor p-aminobenzamidine, their activation was significantly reduced after 10 hours of incubation, *i.e.*, between approximately 70 and 100% inhibition was observed. The specific uPA-inhibitor amiloride also inhibited the activation of the L-aminoacid uPA probes by approximately 50 to 70%. Therefore, it seems that cellular activation of the probes is dependent on uPA cleavage but also involves other proteases produced by PC-3 cells.

The only difference between AC203 and AC560 is the length of the linker while maintaining the uPA sensitive peptidic sequence intact and the pair of FRET donor/acceptor. The shorter linker used in AC203 resulted in a higher fluorescence quenching although the initial fluorescence of these two probes were similar. *In vitro*, AC560 was activated almost twice as much as AC203, suggesting that a longer linker may facilitate the accessibility of the proteases to the cleavable site and leads to a higher propensity towards proteolytic activation.

Although the peptidic sequence is maintained for all these three probes, different *in vitro* behavior and activation are recorded, suggesting that fluorophore selection may influence proteolytic recognition, accessibility and cleavage. As expected, no fluorescence increase was observed using the negative control AC595, which consists in the corresponding D-amino acids in the peptidic linker. Interestingly, Romieu and coworkers[28,34-36], reported the synthesis

and evaluation of protease sensitive probes notably using the molecular beacon approach[28,34]. When using, caspase-3 sensitive probes using two NIR cyanines as FRET pair a 2 to 8 fold increase in fluorescence of their NIR dyes was reported when in presence of the protease[34].

3.3. Intracellular fate of PS in cells - Confocal Microscopy

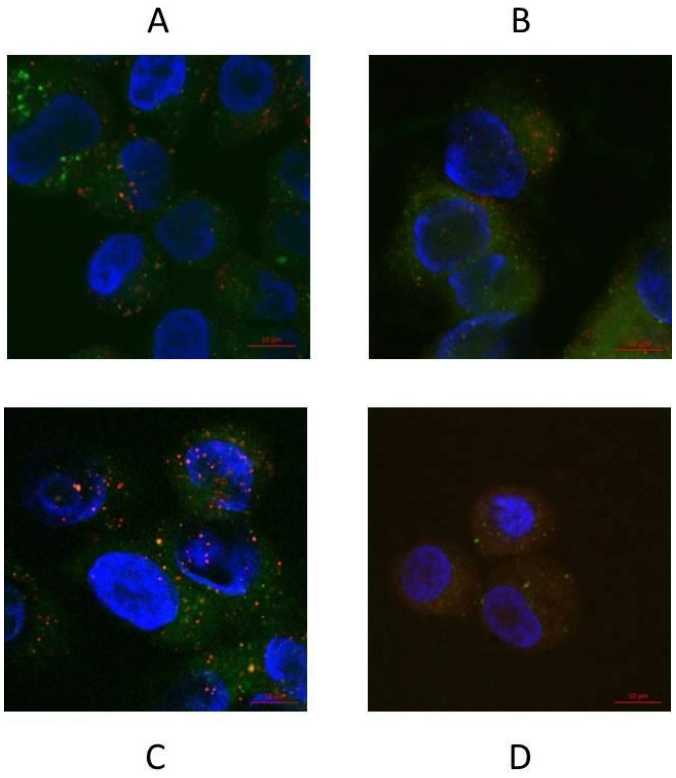

Figure 2. Intracellular localization of probes AC203 **(A)**, AC560 **(B)** , AC594 **(C)** and AC226 **(D)** (in red) after 2 hours of incubation. Lysotracker green® (in green) is used to mark lysosomes and DAPI (in blue) was used as a marker for nuclei.

Figure 2 presents the intracellular localization of all probes assessed after 2 hours of incubation. All probes, except AC595 (negative control) showed strong fluorescence. Intracellular accumulation was observed as a form of vacuolar structures. This confirms that the cellular uptake is dependent on the peptidic sequence used and its recognition by target proteases in this case, hence giving specificity of these probes towards protease expressing cells. Similar vacuolar localization was observed using polymeric prodrugs[29]. Furthermore probe AC594 which targets cathepsin B showed a good co-localization with stained lysosomes. These observations are in accordance with cathepsin B intracellular localization since it is known to participate in the early and late stages of endolysosomal breakdown of proteins and have higher concentration of cathepsin B is found in early endosomes and less in

lysosomes[37]. Interestingly, AC226 showed vacuolar but also cytoplasmic localization that was not present for the other probes tested. This observation suggests a fast cellular uptake of this probe as compared to the other probes tested. However, all probes studied in this paper exhibited good cellular activation and uptake with high specificity toward PC-3 cells giving hope for the *in vivo* diagnosis of prostate cancer.

4. Conclusions

The high quenching efficiency of the probes as well as their cellular activation and accumulation with high specificity towards PC-3 cells is of great opportunity for the *in vivo* diagnosis of prostate cancer and many other protease-related tumors. Tuning these probes for other target proteases can be easily achieved by varying the protease cleavable peptidic sequence and may open new horizons in *in vivo* imaging of cancer and other overexpressing protease diseases such as rheumatoid arthritis, Alzheimer's disease, stroke and atherosclerosis[38].

Acknowledgements

This work has been supported in part by the SNF grants 205320_13830, CR32I3_129987, CR32I3_147018, 31003A_149962, CR32I3_150271, and 205321_12683

References:

1. Celli JP, Spring BQ, Rizvi I, et al: Imaging and photodynamic therapy: mechanisms, monitoring, and optimization. Chem Rev 110:2795-838, 2010

2. Gabriel D, Zuluaga MF, Lange N: On the cutting edge: protease-sensitive prodrugs for the delivery of photoactive compounds. Photochem Photobiol Sci 10:689-703, 2011

3. Law B, Tung CH: Proteolysis: a biological process adapted in drug delivery, therapy, and imaging. Bioconjug Chem 20:1683-95, 2009

4. Lovell JF, Liu TW, Chen J, et al: Activatable photosensitizers for imaging and therapy. Chem Rev 110:2839-57, 2010

5. Hanahan D, Weinberg RA: The hallmarks of cancer. Cell 100:57-70, 2000

6. Hanahan D, Weinberg RA: Hallmarks of cancer: the next generation. Cell 144:646-74, 2011

7. Lee M, Fridman R, Mobashery S: Extracellular proteases as targets for treatment of cancer metastases. Chem Soc Rev 33:401-9, 2004

8. Lopez-Otin C, Bond JS: Proteases: multifunctional enzymes in life and disease. J Biol Chem 283:30433-7, 2008

9. Morris R, Winyard PG, Blake DR, et al: Thrombin in inflammation and healing: relevance to rheumatoid arthritis. Ann Rheum Dis 53:72-9, 1994

10. Nakano S, Ikata T, Kinoshita I, et al: Characteristics of the protease activity in synovial fluid from patients with rheumatoid arthritis and osteoarthritis. Clin Exp Rheumatol 17:161-70, 1999

11. So AK, Varisco PA, Kemkes-Matthes B, et al: Arthritis is linked to local and systemic activation of coagulation and fibrinolysis pathways. J Thromb Haemost 1:2510-5, 2003

12. Lee S, Park K, Kim K, et al: Activatable imaging probes with amplified fluorescent signals. Chem Commun (Camb):4250-60, 2008

13. Sekar RB, Periasamy A: Fluorescence resonance energy transfer (FRET) microscopy imaging of live cell protein localizations. J Cell Biol 160:629-33, 2003

14. Lo PC, Chen J, Stefflova K, et al: Photodynamic molecular beacon triggered by fibroblast activation protein on cancer-associated fibroblasts for diagnosis and treatment of epithelial cancers. J Med Chem 52:358-68, 2009

15. Lovell JF, Chen J, Huynh E, et al: Facile synthesis of advanced photodynamic molecular beacon architectures. Bioconjug Chem 21:1023-5, 2010

16. Zheng G, Chen J, Stefflova K, et al: Photodynamic molecular beacon as an activatable photosensitizer based on protease-controlled singlet oxygen quenching and activation. Proc Natl Acad Sci U S A 104:8989-94, 2007

17. Chen J, Stefflova K, Niedre MJ, et al: Protease-triggered photosensitizing beacon based on singlet oxygen quenching and activation. Journal of the American Chemical Society 126:11450-11451, 2004

18. Stefflova K, Chen J, Marotta D, et al: Photodynamic therapy agent with a built-in apoptosis sensor for evaluating its own therapeutic outcome in situ. Journal of Medicinal Chemistry 49:3850-3856, 2006

19. Liu TW, Akens MK, Chen J, et al: Imaging of Specific Activation of Photodynamic Molecular Beacons in Breast Cancer Vertebral Metastases. Bioconjugate Chemistry 22:1021-1030, 2011

20. Andreasen PA, Kjoller L, Christensen L, et al: The urokinase-type plasminogen activator system in cancer metastasis: a review. Int J Cancer 72:1-22, 1997

21. Cozzi PJ, Wang J, Delprado W, et al: Evaluation of urokinase plasminogen activator and its receptor in different grades of human prostate cancer. Hum Pathol 37:1442-51, 2006

22. Kim TD, Song KS, Li G, et al: Activity and expression of urokinase-type plasminogen activator and matrix metalloproteinases in human colorectal cancer. BMC Cancer 6:211, 2006

23. Konecny G, Untch M, Pihan A, et al: Association of urokinase-type plasminogen activator and its inhibitor with disease progression and prognosis in ovarian cancer. Clin Cancer Res 7:1743-9, 2001

24. Lah TT, Kokalj-Kunovar M, Drobnic-Kosorok M, et al: Cystatins and cathepsins in breast carcinoma. Biol Chem Hoppe Seyler 373:595-604, 1992

25. Sidenius N, Blasi F: The urokinase plasminogen activator system in cancer: recent advances and implication for prognosis and therapy. Cancer Metastasis Rev 22:205-22, 2003

26. Staack A, Tolic D, Kristiansen G, et al: Expression of cathepsins B, H, and L and their inhibitors as markers of transitional cell carcinoma of the bladder. Urology 63:1089-94, 2004

27. van der Burg ME, Henzen-Logmans SC, Berns EM, et al: Expression of urokinase-type plasminogen activator (uPA) and its inhibitor PAI-1 in benign, borderline, malignant primary and metastatic ovarian tumors. Int J Cancer 69:475-9, 1996

28. Chevalier A, Massif C, Renard PY, et al: Bioconjugatable azo-based dark-quencher dyes: synthesis and application to protease-activatable far-red fluorescent probes. Chemistry 19:1686-99, 2013

29. Gabriel D, Zuluaga MF, Martinez MN, et al: Urokinase-plasminogen-activator sensitive polymeric photosensitizer prodrugs: design, synthesis and *in vitro* evaluation. Journal of Drug Delivery Science and Technology 19:15-24, 2009

30. Zuluaga MF, Gabriel D, Lange N: Enhanced Prostate Cancer Targeting by Modified Protease Sensitive Photosensitizer Prodrugs. Molecular Pharmaceutics 9:1570-1579, 2012

31. Bogdanov AA, Lin CP, Simonova M, et al: Cellular activation of the self-quenched fluorescent reporter probe in tumor microenvironment. Neoplasia 4:228-236, 2002

32. Tung CH, Mahmood U, Bredow S, et al: *In vivo* imaging of proteolytic enzyme activity using a novel molecular reporter. Cancer Research 60:4953-4958, 2000

33. Jaffer FA, Kim DE, Quinti L, et al: Optical visualization of cathepsin K activity in atherosclerosis with a novel, protease-activatable fluorescence sensor. Circulation 115:2292-2298, 2007

34. Bouteiller C, Clave G, Bernardin A, et al: Novel water-soluble near-infrared cyanine dyes: Synthesis, spectral properties, and use in the preparation of internally quenched fluorescent probes. Bioconjugate Chemistry 18:1303-1317, 2007

35. Meyer Y, Richard JA, Delest B, et al: A comparative study of the self-immolation of para-aminobenzylalcohol and hemithioaminal-based linkers in the context of protease-sensitive fluorogenic probes. Organic & Biomolecular Chemistry 8:1777-1780, 2010

36. Richard JA, Meyer Y, Jolivel V, et al: Latent fluorophores based on a self-immolative linker strategy and suitable for protease sensing. Bioconjugate Chemistry 19:1707-1718, 2008

37. Guha S, Padh H: Cathepsins: fundamental effectors of endolysosomal proteolysis. Indian J Biochem Biophys 45:75-90, 2008

38. Choi KY, Swierczewska M, Lee S, et al: Protease-activated drug development. Theranostics 2:156-78, 2012

SUMMARY, CONCLUSIONS & PERSPECTIVES

Photodynamic Therapy (PDT) is considered a selective and a site targeted treatment modality as compared to radiotherapy and chemotherapy for cancer.

The selectivity is attributed to the PS accumulation in the tumor, its localised activation by light and the subsequent confined formation of the cytotoxic of reactive oxygen species. Despite its promise, clinical applications of PDT remain somehow limited, partially because of the yet-to-be improved light delivery systems and accessibility of the treatment site. Furthermore, the poor PS bioavailability and selectivity of PS for reduced side-effects and drug doses administered need to be optimized. Hence, investigation of new near-infrared PS suitable for deep light penetration and to reach tissues as well as pharmaceutical improvements of PS-selective and controlled delivery in the tumors has been addressed in this thesis through the different protease-prodrug approaches offering great opportunity for tumor fluorescent detection, monitoring and treatment.

Phthalocyanines are potent and promising photosensitizer (PS) class notably because of their good spectral properties mainly their high fluorescence and oxygen quantum yields and high absorbance in the near-infrared region as reviewed in **Chapter I**. Improvement of their phototoxic effect can be obtained by increasing their water-solubility and by reducing their tendency to aggregate. This can be achieved by chemical tuning of their tetrapyrrolic ring but also through their pharmaceutical formulation in suitable drug delivery systems. Polymeric prodrug approach is a way of PS efficient delivery and accumulation in the diseased tissue resulting in increased PS phototoxic effect and subsequently improved therapeutical PDT outcome. Hence, as shown in **Chapter II**, *in vitro* identification of hit compounds as well as the grafting of multiple PS moieties on water-soluble polymers is beneficial for phototoxic effect *in vitro* on cancer cell lines with amphiphilic Pc **(9)** inducing 90% of cellular death at a drug dose of 4 μM on HT1080 cells at a light dose of 10J/cm^2 and complete cellular destruction at higher drug doses. Moreover, free Pcs void of any phototoxic effect exhibited

improved cellular toxicity when formulated into polymeric PS prodrugs and up to 80% cell death could be observed on PC-3 cells using 10 μM of Pc **(10)**-conjugate for a light dose of 10J/cm^2. These results held promise for further *in vivo* experiments and evaluations. The selectivity and phototoxic effect of PS and PS-polymeric prodrug conjugates can further be improved by the introduction of a targeting part *e.g.* protease-sensitive peptide with the molecular beacon and the protease-polymeric prodrug approach respectively. Furthermore, approaches such as RAFT prodrugs with and without a targeting moiety can be envisioned for tuning of pharmacokinetic/pharmacodynamic (PK/PD) properties of PS and for more defined, controlled and spatially arranged chemical structures which renders this perspective suitable for fundamental understanding of prodrug-tumor interaction(s), for pharmaceutical production and for FDA approval.

A simple and defined way of PS selective delivery is the use of the molecular beacon approach explained and investigated *in vitro* in **Chapter V**. The approach reported in this thesis is the thethering of a fluorophore and a black hole quencher (BHQ-3) to a protease-cleavable peptide. High quenching efficiencies and high fluorescence signal amplification upon proteolytic cleavage could be observed making the intracellular visualization of such probes possible *in vitro* with good selectivity and resolution. Further *in vivo* evaluation of these probes has still to be conducted in order to define their PK features. Hence, molecular beacons can suffer from reduced circulation time in the body after systemic administration and high elimination rates as compared to polymeric prodrugs, resulting in suboptimal therapeutic outcome. The modulation of the drug dose and the treatment/imaging modality through PK/PD studies can bring great improvements to this approach and its application for *in vivo* monitoring and imaging of tumors. This approach can be easily transferred to the imaging of other protease related diseases as well as to their treatment using PDT by the modification of the targeting moiety (*i.e.* peptide sensitive peptide) and by using suitable PS respectively.

Since PK feature is a key aspect for *in vivo* application of the protease prodrug approach, we focused our efforts in the synthesis, *in vitro* and *in vivo* evaluation of other types of drug delivery systems with the aim of prolonging their circulation time in the body and their selectivity towards targeted diseased tissues (*i.e.* tumors). Two approaches, the protease

polymeric prodrug approach and the protease-RAFT prodrug approach have been investigated in this thesis.

Although polymeric prodrug approach suffers mainly from polydispersity of the polymeric backbone carrying multiple copies of PS or PS-protease-sensitive peptide moieties, **Chapter III** gives substantial elements in favor to such an approach for efficient fluorescence tumor imaging and PDT mediated tumor destruction with high resolution due to high signal amplification and high signal-to-noise ratio, high selectivity towards diseased tissue, low side-effects related to therapy and positive long term effect with reduced recurrence of tumors and prolonged life span *in vivo* as shown by the experiment conducted in **Chapter III** where 3 out of 7 animals submitted to PPP conjugate based PDT completely responded to the treatment with no resurgence of tumors after completion of the study (*i.e.* 90 days) while the rest of the group exhibited partial PDT response with prolonged life span of 15 days as compared to control groups. However, random distribution of PS/PS-peptide moieties on the polymeric backbone as well as batch-to-batch variability associated with the design of such prodrugs renders this approach difficultly manageable in large scale production especially in terms of reproducibility, hence making its routine use in clinics complicated.

A more recently applied approach for tumor imaging with more spatially and chemically defined structures than polymeric prodrugs is the Regioselectively Addressable Functionalised Templates (RAFT) approach. A peptidic cyclic scaffold defines a plane and gives the ability to use biorthogonal chemistry with distinct grafting of the two sides of this plane using different amino-acid chemical protection such as Boc, Alloc and Fmoc. Each side of the plane can bear on one side a reporter moiety and on the other side a targeting moiety as Dumy and co-workers described. As shown in **Chapter IV** we have instead prepared protease sensitive photosensitizer prodrugs based on a similar scaffold carrying a water-solubilizing moiety (*i.e.* PEG) and one to several PS-peptide moieties. PEG is known to reduce the drug immunogenicity and increase the circulation time in the body. On the other side of the plane defined by RAFT, one to four PS linked to protease-sensitive peptides were grafted. Increase in the number of PS-peptides moieties resulted in increased self-quenching. Among all the conjugates tested, the highest quenching efficiency was achieved by the tetravalent conjugates and more specifically to the PheoS4 conjugate. The discrepancy observed between quenching

efficiencies of PheoS4, PheoL4 and PheoM4 is probably due to the steric hindrance of the PEG bore by the conjugates and higher molecular weight PEGs resulted in lower quenching effect. However, the high quenching efficiency of PheoS4 was detrimental to its cellular activation and resulted in overall moderated phototoxic effect. Hence, balance between quenching efficiency, cellular uptake and accumulation, and cellular activation should be aimed at in order to reach the highest PDT effect.

The highest phototoxic effects were observed for MMP-2 sensitive prodrug (PheoM conjugates) resulting in complete cellular death of PC-3 and HT1080 cells at a light dose of $10J/cm^2$ and drug doses as low as 750 nM.

Major efforts should be undertaken for further improvement of this concept. Hence, the first proof-of-principle of the PS-RAFT constructs has been given through this study. However, further improvements in terms of chemical synthesis and purity of PS-RAFT conjugates have to be implemented and are currently under investigation. Nonetheless, the promising *in vitro* results obtained as well as good reproducibility of the conjugates and their distinct *in vitro* behavior held great promises for their *in vivo* application and therapeutical outcome using PDT.

Finally, because of their versatility, extension of these RAFT prodrugs to other PS such as Pcs and to other diseases associated with overexpressed proteases could be successfully achieved and RAFT based PDT successful clinical application is within reach.

FRENCH SUMMARY - RÉSUMÉ

La Thérapie Photodynamique (*Photodynamic Therapy: PDT* en anglais) est une modalité de traitement local innovante basée sur l'action conjuguée de trois éléments non-toxiques en soi mais toxiques une fois combinés à savoir, un photosensibilisateur (PS), la lumière et l'oxygène.

L'activation locale du PS par la lumière à une longueur d'onde appropriée conduit d'une part à l'émission de fluorescence par le PS et d'autre part à la formation d'espèces hautement réactives et cytotoxiques de l'oxygène plus connues sous le nom de radicaux libres dérivés de l'oxygène (*Reactive Oxygen Species (ROS)* en anglais). La fluorescence émise par le PS permet alors à la fois la détection ainsi que l'imagerie du tissu malade tandis que la production locale de ROS en permet la destruction confinée et sélective.

Dans le cadre de la lutte contre le cancer, la PDT tire avantage des caractéristiques physiopathologiques spécifiques aux tissus tumoraux. Ainsi, et en comparaison aux tissus sains, la vascularisation du tissu cancéreux présente des fenestrations permettant le passage facilité du PS dans la tumeur. De plus, l'élimination du PS du tissu tumoral est ralentie du fait d'un drainage lymphatique réduit. Ces caractéristiques tumorales, décrites pour la première fois par Maeda *et al*. et connu de nos jours sous le nom de *Enhanced Permeability and Retention Effect (EPR effect)*, sont ainsi responsables d'une accumulation prononcée du PS au sein de la tumeur.

A cette distribution préférentielle du PS dans la tumeur, s'ajoute l'activation ciblée du PS par l'application localisée et contrôlée de la lumière entraînant une production confinée de ROS. Ces espèces toxiques formées ont un champ d'action (10-55nm) ainsi qu'un temps de vie limités (10-320 nanosecondes) ce qui amenuise les risques de dommages collatéraux au niveau des tissus sains environnants la tumeur. La PDT présente donc l'avantage sur les autres

thérapies conventionnelles du cancer (*i.e.* chimiothérapie systémique, radiothérapie) d'avoir un effet antitumoral sélectif et ciblé et par conséquent présente moins d'effets secondaires.

La principale limitation actuelle de la PDT est la photosensibilisation de la peau des patients traités. Ceci est dû à une exposition incontrôlée et non désirée du patient à la lumière (notamment une exposition au soleil) du fait d'une accumulation partielle du PS dans les tissus sains au temps de l'exposition. Plusieurs approches thérapeutiques permettent de réduire cet effet secondaire notamment la synthèse de nouveaux PS aux propriétés optiques et physiques perfectionnées, l'optimisation de l'intervalle d'exposition au PS et à la lumière, l'évitement et la protection contre une exposition non-désirée à la lumière mais surtout l'optimisation de la sélectivité du PS. Ce dernier point peut être amélioré de façon significative par le développement pharmaceutique du PS. C'est sur ce dernier point que l'essentiel de cette thèse est consacré.

En effet, outre la synthèse de nouvelles molécules faisant partie de la classe des Phthalocyanines (Pc) et l'identification *in vitro* de candidats prometteurs au sein de cette classe pour la PDT du cancer notamment de la prostate, le développement d'approches multidisciplinaires chimiques et pharmaceutiques dans le transport et la libération sélective du PS au tumeur a fait l'objet de constants efforts et optimisations dans le cadre de cette thèse.

L'approche appliquée dans cette thèse est l'approche de la prodrogue susceptible d'être activée sélectivement au sein de la tumeur et de libérer le PS localement par clivage protéolytique (protease sensitive prodrug approach).

Cette stratégie se base sur une propriété pathophysiologique associée à la formation, au développement, à la progression et à la métastase des tumeurs à savoir la dérégulation et la surexpression dans certains cas de l'expression de protéases. La Protease-Sensitive-Prodrug Approach repose sur le clivage d'un lien peptidique reconnu et permettant le ciblage spécifique des protéases surexprimées au niveau tumoral. Du fait de cette surexpression, l'activation de la prodrogue se fait majoritairement au sein de la tumeur et permet la libération ciblée du PS qui est par la suite activé sélectivement par irradiation lumineuse localisée au niveau de la tumeur.

Dans le cadre de ce travail, l'évaluation de 3 systèmes de livraison (*drug delivery systems* en anglais) ciblée et sélective du PS a été réalisée à savoir, **1)** l'approche des liens peptidiques "silencieux" ou "quenchés" dénommée **Molecular Beacon**, **2)** l'approche polymérique (avec

ou sans ciblage peptidique) désignée sous le terme de **Polymeric Protease Sensitive Prodrugs (PPP)** et **3)** l'approche peptidique cyclique connue sous le nom de **Regioselectively Adressable Functionnalised Templates** (**RAFT**).

Dans un premier temps, l'évaluation de l'approche de la prodrogue polymérique a été évaluée. Cette approche repose sur le chargement sur un squelette polymérique de poly-L-Lysine de plusieurs entités de PS (ici, le Pheophorbide a) couplées à un lien peptidique susceptible d'être clivé par l'activateur du plasminogène de type urokinase, une protéase connue pour être surexprimée dans le cancer de la prostate notamment. Après optimisation du chargement (loading), du nombre de PS-peptides sur le polymère et la vérification du clivage sélectif de ce lien par la protéase ciblée, une évaluation *in vivo* de l'efficacité d'une telle drogue a été établie dans le cadre de la PDT. Ainsi, l'administration 7.5 mg de Pheophorbide a (PS) sous la forme de prodogue optimisée (uPA-PPP-4) à des souris portant des xenografts de cancer de la prostate (issu de la lignée cellulaire PC-3) et l'irradiation des tumeurs à une dose lumineuse de 150J/cm^{2}a permis la guérison complètede 3 souris sur 7 ainsi que la rémission partielle des 4 autres souris prolongeant de ce fait leur espérance de vie de 15 jours comparé aux groupes contrôles.

In vitro sur les cellules de cancer de la prostate humaines (PC-3), l'approche polymérique de la formulation de PS a permis d'obtenir un effet phototoxique significatif (jusqu'à 80% de mort cellulaire pour une dose de 10J/cm^2 et 10 μM de PS) pour des phthalocyanines qui, sans formulation, ne présentaient aucune efficacité.

Ces observations démontrent clairement le bénéfice thérapeutique d'une telle approche, que ce soit au niveau cellulaire ou clinique. Cependant cette approche reste limitée du fait de la polydispersité du polymère utilisé, de la distribution aléatoire des PS-peptides sur le polymère et de la variabilité inter-lots associée à la synthèse de ce type de prodrogues.

C'est donc dans le but de répondre à ces limitations que les approches de liens peptidiques "silencieux" ou "quenchés" (Molecular Beacons) et d'échafaudages peptidiques (Regioselectively Adressable Functionnalized Templates-RAFT) de structures définies ont été instaurées, synthétisées et évaluées.

Le principe reste le même à savoir que la prodrogue présente une fluorescence basse voire nulle (état silencieux). Cet état "quenché" est principalement dû au transfert d'énergie non-

radiatif ayant lieu entre un donneur et un accepteur d'énergie situés à proximité l'un de l'autre. Cet effet est dépendant de la distance qui sépare le donneur et l'accepteur d'énergie. Ainsi, dans le cas où cette distance s'accroît, l'effet de quenching diminue jusqu'à s'annuler. Dans le cas de la prodrogue, une fois en présence de la protéase ciblée, la prodrogue est activée, la distance entre PSs ou entre fluorophores augmente ce qui conduit à l'augmentation de fluorescence de la sonde et à la production de ROS nécessaires à l'effet toxique de la PDT. Ainsi la détection tumorale, de même que sa destruction sélective peuvent être accomplis avec une haute résolution du fait d'une amplification de signal significative au sein du tissu malade et d'un ratio signal/bruit de la prodrogue élevé.

L'approche la plus simple est celle du molecular beacon où le donneur est lié à l'accepteur à travers un lien peptidique reconnu spécifiquement par la protéase ciblée. Dans le cadre de cette thèse, le donneur utilisé est un fluorophore (Cy5 ou Texas Red) tandis que l'accepteur est un Black Hole Quencher (BHQ-3). L'utilisation de lien peptidiques adaptés ont permis une activation sélective et significative des sondes utilisées et ont finalement résulté en l'imagerie réussie de ces drogues au niveau cellulaire avec une haute résolution. Cette étude montre le potentiel non négligeable d'une telle approche dans le cadre de l'imagerie et de la compréhension moléculaire du cancer. De telles sondes restent cependant à évaluer au niveau *in vivo* et clinique. Le potentiel de ces sondes au niveau médical réside dans la versatilité de leur conception grâce à la modulation du lien peptidique qui permet la variation de la cible et de la maladie étudiée.

Enfin, l'approche la plus innovante exposée dans cette thèse est l'utilisation de RAFT dans la PDT. En effet, ces échafaudages peptidiques permettent d'allier les avantages des deux approches citées précédemment tout en en évitant les inconvénients. Cette stratégie permet d'avoir une structure définie, modulable et reproductible comparée à l'approche polymérique mais permet également d'obtenir une pharmacocinétique (PK) du PS plus favorable que dans le cas des molecular beacons. A cela s'ajoute la propriété du RAFT en lui-même qui définit un plan sur lequel il est possible de fixer différentes entités de part et d'autre de ce plan. Ainsi, dans l'étude qui est reportée dans cette thèse, la partie supérieure de ce plan est constituée de la partie PS-peptide soit la partie responsable du ciblage et de l'effet photocytotoxique. La partie inférieure, quant à elle, contient l'entité PEG (d'un poids

moléculaire variable) permettant de moduler la PK de la prodrogue. Il a, ainsi, été démontré *in vitro* que de tels concepts étaient non seulement applicables mais aussi hautement efficaces. L'équilibre à trouver entre le quenching, l'activation cellulaire et l'accumulation intracellulaire de la drogue est d'une importance capitale pour assurer l'effet thérapeutique optimal de cette approche appliquée à la PDT. Enfin, l'optimisation du lien peptidique de ciblage des protéases permet l'amélioration de l'effet de la drogue. L'évaluation *in vivo* de ces prodrogues reste à établir de même qu'une optimisation de leur synthèse et purification.

Cependant, le succès de cette approche *in vitro* notamment pour les prodrogues MPheo (qui induisent une mort cellulaire de 50% à une dose de PS aussi basse que 100 nM et une destruction complète à 750 nM pour une dose de lumière de 10 J/cm^2 sur les lignées cellulaires PC-3 (cancer de la prostate) et HT1080 (fibrosarcome)), ouvrent la perspective d'une application médicale prometteuse de ces prodrogues dans le traitement du cancer par la PDT mais également d'autres pathologies et modalités de traitements.